UNIVERSITY OF PARMA

PhD in Biotechnology

(XXIX cycle)

Protein corona and nanomaterials: from molecular adsorption to physiological complexity

PhD Coordinator:
Prof. Nelson Marmiroli

PhD Tutor:
Prof. Roberta Ruotolo

PhD student: Graziella Pira

SUMMARY

Abstract

Nanotechnology is an emerging branch of applied science and technology for designing tools and devices of size 1-100 nm. Engineered nanomaterials (ENMs) have been widely used in several fields from medical to electronics and possess unique chemical, biological and physical properties (e.g., thermal and optical properties, solubility, fluorescence, electrical parameters) as compared to their bulk material. The increasing interest for these advanced technologies has led to great excitement about potential benefits, but little is known about the potential effects of ENM exposure on environment and human health. Due to their nano-size and large surface-to-mass ratio, ENMs may interact with several biomolecules, mainly proteins, upon contact with biological fluids forming the so-called "protein corona". Toxicity and biocompatibility of these materials may depend predominantly on the formation of protein corona, which influence also cell interactions, localization and bioactivity of ENMs.

The aim of this PhD thesis is to study the interactions of cadmium sulfide quantum dots (CdS QDs) and amorphous silica nanoparticles (SiO_2 NPs) with different biological systems: yeast cells (*Saccharomyces cerevisiae*), human cell lines (Caco-2) and human plasma. We employed a proteomics-based approach coupled with MS analysis to determine the identities of proteins that associate to form the hard corona of these NPs for understanding the properties of ENMs that govern their interactions with proteins in biological environments.

We observed that proteins involved in specific cellular pathways, as protein synthesis, are more prone to bind on NPs. Electrostatic and/or hydrophobic interactions are critical in the formation of the protein corona. Most of the identified proteins contains long disordered regions that provide flexibility to protein structure, a property that promotes their adsorption.

We also focused on the possible toxicological implications of the CdS QD-corona formation in yeast, studying effects at transcriptomic, proteomic and phenotypic levels. Our results demonstrated that CdS QDs cause a general transcriptional up-regulation of genes coding for yeast corona proteins; this effect could represent a cellular mechanism in response to "physical sequestration" of the corona proteins adsorbed on CdS QD surface. Yeast mutant strains deleted in genes coding for corona proteins showed a tolerant phenotype also in presence of concentrations of CdS QDs that suppress the viability of the wild-type strain. Tolerant phenotype of these mutants suggest that the formation of protein corona may mediate the cytotoxicity of CdS QDs in yeast. Finally, using an *in vitro* enzymatic activity assay, we observed that adsorption onto CdS QD surface results in a dose-dependent inhibition of the activity of the GAPDH, a protein strongly associated to these ENMs. These results demonstrate that the characterization of the protein corona would be a relevant approach to predict potential toxicological effects of the ENMs.

INTRODUCTION

1. NANOTECHNOLOGY

The term "Nanotechnology" embraces many different fields and specialties, including engineering, chemistry, electronics, and medicine, among others, but all are concerned with bringing existing technologies down to a very small scale, measured in nanometers (*American Heritage Dictionary, 2010*). The birth of the concept of Nanotechnology is usually linked to a speech by Richard Feynman at the December 1959 meeting of the American Physical Society (*Feynman, 1959*). In general, the size of the **nanomaterials** (NMs) spans the range between 1 and 100 nm in at least one dimension (*BSI PD, 2007*; Fig. 1). Thus, the sizes of NMs are comparable to those of viruses, with maximum dimensions of 10 to 100 nm, or biological macromolecules, as DNA or proteins. **Nanoparticles** (NPs) are defined as NMs with all three external dimensions in the nanoscale.

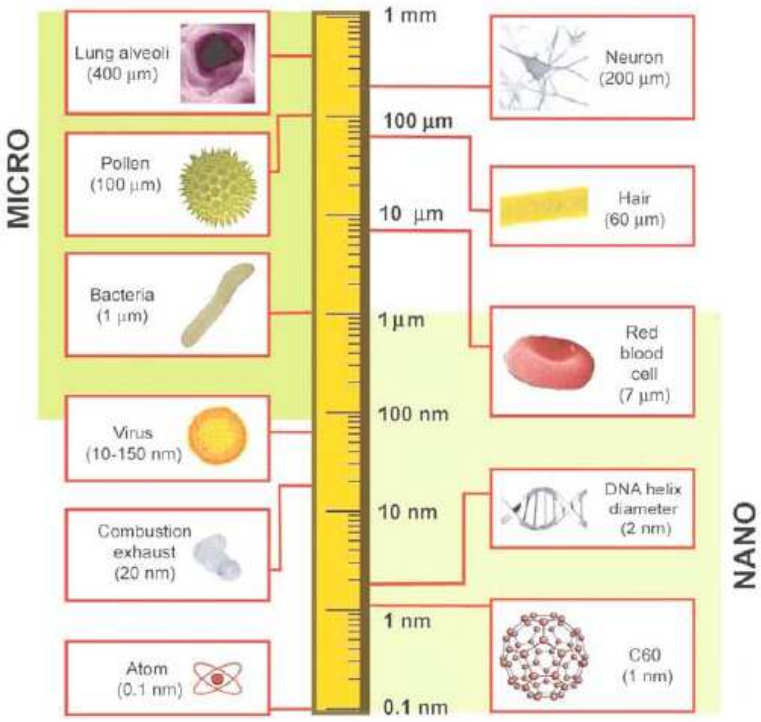

Figure 1. *Size of nanomaterials compared to biological components and definition of 'nano' and 'micro' sizes (Biointerphases, 2007).*

Naturally occurring NMs are abundant in nature and can be produced in many natural processes, including photochemical reactions, volcanic eruptions, forest fires, simple erosion, or by plants and animals (*Klaine et al., 2008*). Moreover, many important functions of living organisms take place at the nanoscale. For example, in the human body, a typical protein such as hemoglobin, which carries oxygen through the bloodstream, is 5 nm in diameter (*National Nanomaterial Initiative, 2010*). Though we usually associate air pollution with human activities (e.g., car emissions, industrial activities, and charcoal burning), natural events such as dust storms, volcanic eruptions and forest fires can produce vast quantities of nanoparticulate matter that can profoundly affects air quality. These large-scale phenomena are visible from satellites and produce airborne particles of dust and soot ranging from the micro- to nanoscales. These small particles suspended in the atmosphere, known as "aerosols", can affect the entire planet's energy balance because they absorb radiation from the sun and scatter it back to space (*Houghton, 2005*). The aerosols generated by human activities are estimated to be only about 10% of the total, the remaining 90% having a natural origin (*Taylor, 2002*).

Synthetic (or anthropogenic) nanomaterials (NMs) fall into two general categories: "incidental" and **"engineered" nanoparticles** (ENMs). Incidental NMs are the byproducts of human activities, generally have poorly controlled sizes and shapes, and may be made of a hodge-podge of different elements. Many of the processes that generate incidental nanoparticles are common every day activities: running diesel engines, large-scale mining, and even starting a fire.
ENMs have been specifically designed and deliberately synthesized by human beings. Growing numbers of nanotoxicologists recognize that the emerging definition of ENMs as measuring 100 nm in one dimension or less (*Kittelson, 2001*; *Borm et al., 2006*) is inadequate and suggest 200 nm as a more correct upper boundary to differentiate the nanosized from the microscaled materials (*Van Broekhuizen et al., 2012*).
Due to their small size, ENMs exhibit unique properties that are often different from their "bulk counterparts" (namely larger sized particles with the same chemical composition): very large surface-area-to-mass-ratio that causes high reactivity and affects thermal, mechanical, optical, electric and magnetic properties; quantum effects, particularly for ENMs at sizes of less than 10 nm, resulting in constrained bonds which are more likely to be disrupted (*Roduner, 2006*). The discovery of these properties and recent advances in synthesis and characterization tools of the ENMs, has led to widespread interest in their potential commercial and industrial applications (*ISO, 2008; Roduner E. 2006*).

1.1 ENM classification

The range of parameters that has to be assessed to characterize these materials is large: dimensionality, morphology, composition and agglomeration, which is the tendency of the ENMs to clump together and form larger combined particles (Fig. 2).

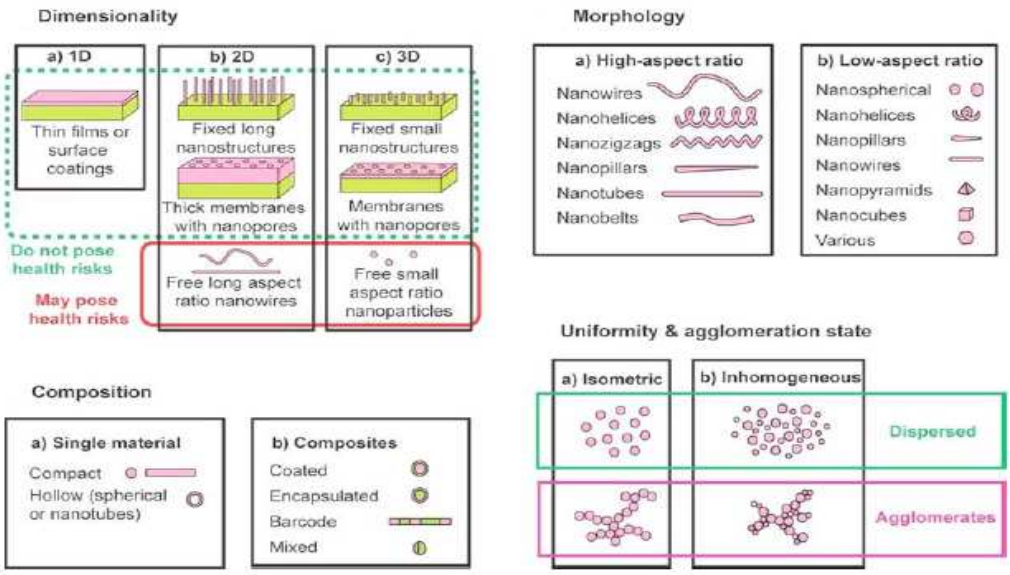

Figure 2. *Classification of nanostructured materials from the point of view of nanostructure dimensions, morphology, composition, uniformity and agglomeration state.*

1.1.1 *ENM dimensionality*

Regarding their dimension, ENMs are classified in 1D, 2D and 3D nanostructured materials (*ISO, 2008*). 1D ENMs are materials with one dimension in the nanometer scale and are typically thin films or surface coatings. Thin films have been developed and used for decades in various fields, such as electronics, chemistry, and engineering.

2D ENMs are materials with two dimensions in the nanometer scale. These include 2D nanostructured films, with nanostructures firmly attached to a substrate, or nanopore filters used for small particle separation and filtration. Free particles with a large aspect ratio, but dimensions in the nanoscale range, are also considered 2D nanomaterials. Asbestos fibers are an example of 2D nanoparticles.

Finally, materials that are nano-scaled in all three dimensions are considered 3D ENMs. These include thin films deposited under conditions that generate atomic-scale porosity, colloids, and free NPs with various morphologies (*Robbie et al., 2007*).

1.1.2 *ENM morphology*

A general classification for morphology exists between high- and low-aspect ratio particles. High aspect ratio ENMs include: nanotubes and nanowires, with various shapes, such as helices, zigzags, belts; nanowires with diameter that varies with length. Small-aspect ratio morphologies include spherical, oval, cubic, prism, helical, or pillar NPs (Fig. 2).

1.1.3 *ENM uniformity and agglomeration*

Based on their chemistry and electro-magnetic properties, ENMs can exist as dispersed aerosols, suspensions/colloids, or in an agglomerate state. For example, magnetic NPs tend to cluster, forming an agglomerate state, unless their surfaces are coated with a non-magnetic material. In an agglomerate state, NPs may behave as larger particles, depending on the size of the agglomerate (*Biointerphases, 2007*).

1.1.4 *ENM composition*

ENMs can be composed of a single constituent material or be a composite of several materials. Single constituent ENMs are carbon-based ENM, metal-based ENMs (e.g. metal oxide NPs) and dendrimers. The composites are ENMs with a heterogeneous composition.

Carbon-based ENMs, including carbon nanotubes, graphene, fullerenes, nanofibers and nanodiamonds, are potential candidates for various applications (Fig. 3). Carbon nanotubes (CNTs) have a cylindrical carbon structure and possess a wide range of electrical and optical properties (*Saito et al., 1998*). CNTs are manufactured as single wall carbon nanotubes (SWCNT) or multiwall carbon nanotubes (MWCNT). Due to the diverse array of their useful properties, CNTs have been explored for use in many industrial applications (*Baughman et al., 2002*); their measured rigidity and flexibility are greater than that of some commercially available high-strength materials (e.g., high tensile steel, carbon fibers, and Kevlar®).

Graphene is a one atom thick planar sheet of carbon atoms densely packed in a honeycomb crystal lattice and it is the basic structural building block of CNTs and fullerenes. Graphene and CNTs possess similar electrical, optical, and thermal properties, but the two-dimensional atomic sheet structure of graphene gives unique electronic characteristics (*Geim et al., 2007*).

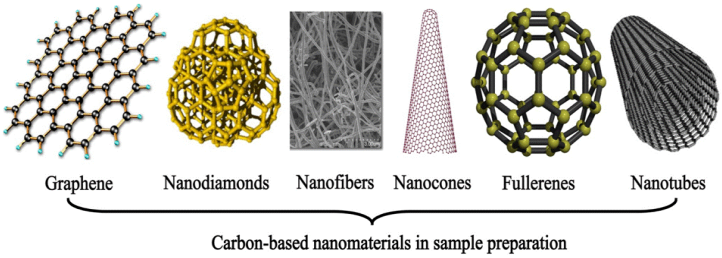

Fig. 3 *Carbon-based ENMs (Zhang et al., 2013).*

Fullerene, also commonly known as the "buckyball", is made up of sixty sp2 hybridized carbons (C60) in a rigid spherical (soccer ball) shape. The popularity of C60 has somewhat diminished in recent years with the rise of more scalable and practical carbon based NMs such as CNTs and graphene. However, its uniform size and shape as well as availability for chemical modification led many scientists to develop C60 derivatives for therapeutic purposes (*Jensen A .W. et al., 1996*). The most fascinating and highly promising aspect of C60 is its anti-human immunodeficiency virus (HIV) activity; Schinazi et al. (*1993*) first discovered a group of water-soluble C60 derivatives that, due to their unique molecular structure and hydrophobicity, inhibit HIV protease activity by binding to its active site.

Nanodiamonds (NDs) are synthesized by high energy treatment of graphite, most commonly via detonation, and are ENMs smaller than 10 nm diameter. They have similar physical properties as bulk diamond, such as fluorescence and photoluminescence, as well as biocompatibility. In recent years, NDs have also generated interest in the field of biomedical engineering, in drug delivery and tissue labeling (*Mochalin et al., 2012*), for example, Lien et al. (*2012*) recently used fluorescent and magnetic NDs for cell labelling.

Metal-based ENMs play a very important role in many areas of chemistry, physics and material science (*Noguera, 1996*; *Kung, 1989*; *Henrich et al., 1994*; *Wells, 1987*; *Rodríguez et al., 2007*; *Fernández-García et al., 2004*). Metal oxide NPs (Fig. 4), expecially silica (SiO_2), titania (TiO_2), alumina (Al_2O_3), iron oxide (Fe_3O_4, Fe_2O_3) NPs, nanoscale zero-valent metal (e.g. iron NPs) or Quantum Dots (QDs) at present occupy the first position in terms of economic importance within the range of inorganic NPs. Mixed oxides, such indium-tin oxide (ITO) and antimony-tin oxide (ATO), silicates (aluminum and zirconium silicates) and titanates (e.g. barium titanate) are also of increasing importance (Fig. 4).

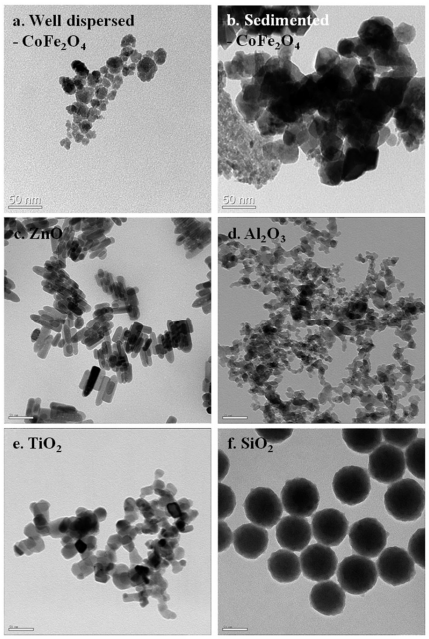

Fig. 4 *(**a**) Well-dispersed $CoFe_2O_4$ (20.4 ± 10.3 nm), (**b**) Sedimented $CoFe_2O_4$ (48.3 ± 9.7 nm), (**c**) ZnO nanorods (width: 16.2 ± 1.3 nm, length: 50.8 ± 11.8 nm), (**d**) Al_2O_3 (15.6 ± 5.4 nm), (**e**) TiO_2 (26.5 ± 6.7 nm), (**f**) SiO_2 (72.9 ± 4.0 nm) (Jeong et al., 2016).*

Main application fields of metal oxide NPs are electronics, pharmacy/medicine, cosmetics (NP-based sunscreens) as well as chemistry and catalysis. In technological applications, these NPs are used in the fabrication of microelectronic circuits, sensors, piezoelectric devices, fuel cells, coatings for the passivation of surfaces against corrosion, and as catalysts (*Gleiter, 1999*; *Valden et al., 1998*; *Rodriguez et al., 2002*). Applications of NPs in medicine are, for instance, markers for biological screening tests (e.g. gold or semiconductor NPs), contrast agents for magnetic resonance imaging (MRI) as well as antimicrobic coatings and composite materials for medical devices (*Salata, 2004*).

Dendrimers are small (2-10 nm diameter), monodispersed, regularly hyperbranched, flexible macromolecules with a large number of peripheral functional groups (*Lee et al., 2005a*; *Svenson et al., 2005b*) (Fig. 5). Currently, a fundamental limitation is the high cost of production of these compounds. A lot of attention is paid to the research on the use of these polymers in medicine, chemistry, genetic engineering and environmental protection (*Kubiak, 2014*).

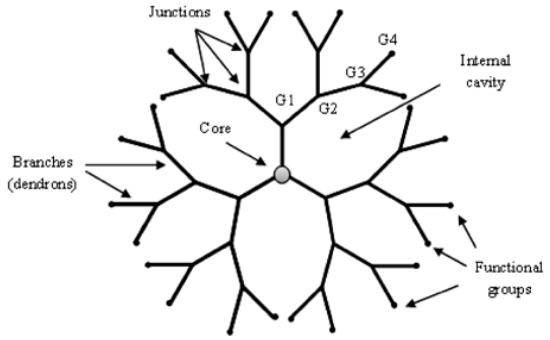

Fig. 5 *Schematic description of dendrimer structure (Kubiak M. 2016).*

Polymer nanocomposites are the result of the combination of polymers and inorganic/organic fillers at the nanometer scale, offering a multitude of desirable (and tailorable) properties, such as high strength, stiffness, dimensional and thermal stability (Table 1). Nanocomposites promise new applications in many fields, such as mechanically-reinforced lightweight components, non-linear optics, battery cathodes and ionics, nanowires, sensors and other systems. Such mechanical property improvements have resulted in major interest in nanocomposite materials in numerous automotive and general/industrial applications. Furthermore, nanocomposites are very interesting for biomedical technologies, such as tissue engineering, bone replacement/repair, dental applications, and controlled drug delivery.

Table 1. *Characteristics of nano-composites (Demetrakakes, 2002)*

Improved properties	**Disadvantages**
Mechanical properties (tensile strength, stiffness, toughness)	Viscosity increase (limits process ability)
Gas barrier	Dispersion difficulties
Synergistic flame retardant additive	Optical issues
Dimensional stability	Sedimentation
Thermal expansion	Black color when different carbon containing nanoparticles are used
Thermal conductivity	
Ablation resistance	
Chemical resistance	
Reinforcement	

1.2 *Applications of ENMs*

The unique properties make the ENMs promising in a wide range of fields, from medical applications to environmental sciences: in fabrics and their treatments, filtration, dental materials, surface disinfectants, diesel and fuel additives, hazardous chemical neutralizers, automotive components, electronics, scientific instruments, sports equipment, flat panel displays, drug delivery systems, and pharmaceutics (Fig. 6).

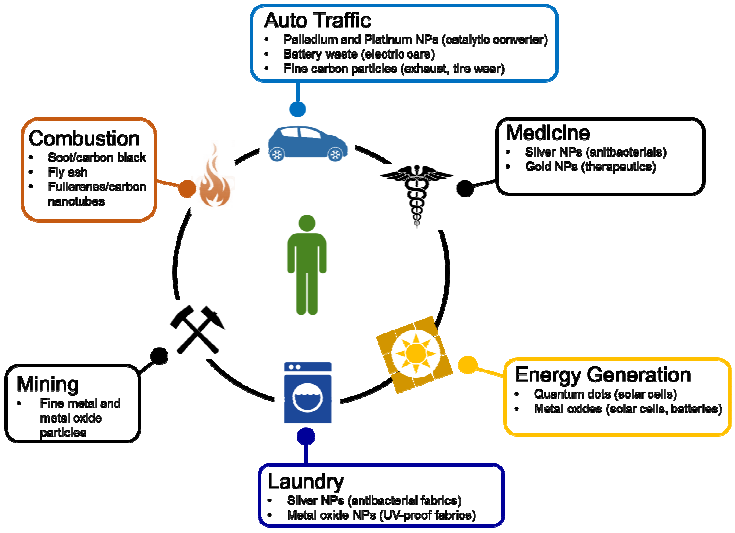

Fig. 6 *Applications of ENMs.*

Several studies have revealed enormous prospects for the progress of nanotechnology in both life sciences and information technology (*Donaldson et al., 2004*). In electronics, many of the current microelectronics applications are already at a nanoscale (*Thompson et al., 2006*). For instance, the use of nanocrystalline materials for TV monitor can greatly enhance resolution and may significantly reduce costs. Also, flat-panel displays constructed with ENMs may possess much higher brightness and contrast than conventional displays owing to the enhanced electrical and optical properties of the new materials. New ENMs show promising properties as anode and cathode materials in lithium-ion batteries, having higher capacity and better cycle life than their larger-particle equivalents (*Liu et al., 2006*).

In biomedical applications, nanofiber scaffolds can be used to regenerate central nervous system cells and possible other organs. Experiments performed on a hamster with severed optic tract demonstrated the regeneration of axonal tissue initiated by a peptide nanofibers scaffold (*Behnke et al., 2006*).

Certain nanopowders possess antimicrobial properties (*Bosi et al., 2003* ; *Koper et al., 2002*); when these powders contact cells of *Escherichia coli* or other bacteria species and viruses, over 90% are killed within a few minutes. Due to their antimicrobial effect, silver and titanium dioxide NPs (<100 nm diameter) are assessed as coatings for surgical masks (*Li et al., 2006*). Nanotubes can act as channels for highly selective transport of molecules and ions inside the cell (*Jirage et al., 1997*).

The ability of ENMs to target and penetrate specific organs and cells contributes to their toxicity; however, this ability may be exploited in nanomedicine: e.g., nanospheres composed of biodegradable polymers can incorporated drugs, allowing the timed release of the drug as the polymer degrades (*Uhrich et al., 1999*). When ENMs are set to degrade in an acid microenvironment, such as tumor cells or around inflammation sites, this allows site-specific or targeted drug delivery.

Surface-functionalization of the ENMs can be used to permeate cell membranes (*Maïté et al., 2000*) and improve applications in the field of medical imaging; e.g., superparamagnetic magnetite particles coated with dextran are used as image-enhancement agents in magnetic resonance imaging (*Harisinghani et al., 2003*). CNTs are ideal probe tips for scanning microscopy due to their small diameter (which maximizes resolution), high aspect ratio, and stiffness. Furthermore, CNTs have been used as probe tips for atomic force microscopy (AFM) imaging of antibodies, DNA, etc. (*Hafner et al., 2001*). Fluorescent QDs coated with selected molecules can be used to allow intracellular processes to be observed directly. In addition, nanospheres carriers for vaccines are in development (*Matsusaki et al., 2005*).

In the field of pollution remediation, the potential of ENMs to react with pollutants in the air, soil, and water and transform them into harmless compounds is currently being researched. Nanotechnology could be applied at both ends of the environmental spectrum, to clean up existing pollution and to decrease or prevent its generation. Due to their enhanced chemical activity, ENMs can be used as catalysts to react with toxic gases (such as carbon monoxide and nitrogen oxide) in automobile catalytic converters and power generation equipment. This could prevent gaseous environmental pollution arising from burning gasoline and coal (*Hogan, 2004*).

In cosmetics, titanium dioxide and zinc oxide become transparent to visible light when formed at the nanoscale, however are able to absorb and reflect UV light, being currently used in sunscreens and in the cosmetic industry.

2. Nanotoxicology

A new research field of toxicology, namely "nanotoxicology", was defined to address gaps in knowledge and also to assess the problems likely to be caused by ENMs (*Pardridge, 2012*). More specifically, nanotoxicology aims to understand the principles and mechanisms of interactions at the nano–bio interface and also to determine the relationship between ENMs physicochemical properties and the associate toxicological profiles (*Salvati et al., 2011*). Nanotoxicology encompasses the physicochemical determinants, routes of exposure, biodistribution, molecular determinants, genotoxicity, and regulatory aspects (*Donaldson et al., 2004*; *Lewinski et al., 2008*) (Fig. 8). Toxicity of ENMs has been studied in different biological systems, in cell systems, as bacteria, yeast, human cell lines (e.g. macrophages; *Sohaebuddin et al., 2010*), or different organisms, which include plants (*Marmiroli et al. 2015 and 2016*), rodents, aquatic species, such as zebrafish (*Gonzalez et al., 2008*), catfish (*Wang et al., 2011*) or algae (*Wang et al., 2011*).

Several studies suggested that ENMs could easily enter into the human body (*Milic et al., 2014*; *Oberdorster et al., 2005*). The tiny size of ENMs allows them to pass more easily through cell membranes and other biological barriers and cause cellular dysfunction (*Nel et al., 2006*).
The understanding of the cellular uptake mechanisms of ENMs is important to determine their intracellular fate and biological response (*Jiang. et al., 2008*).

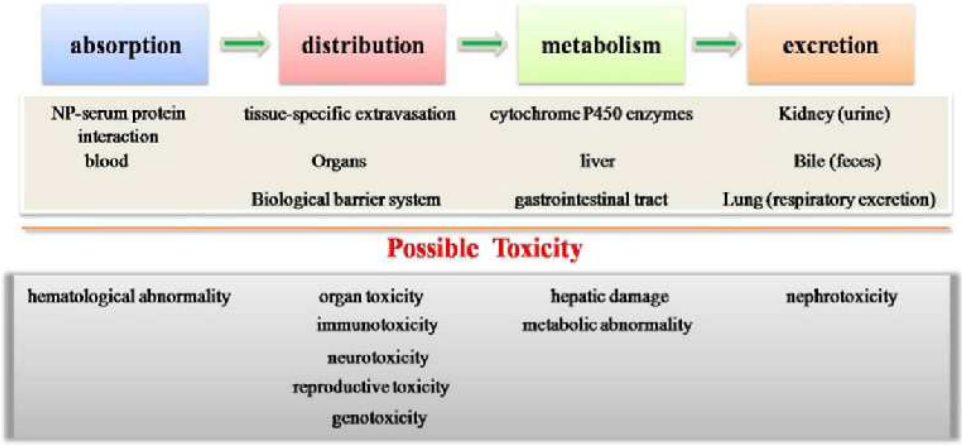

Fig. 7 *An illustrative scheme for the pharmacokinetics of ENMs in vivo and possible mechanisms of toxicity. After delivered into the body, ENMs can be absorbed and ENM–serum protein interactions frequently occur into the bloodstream. Then, they spread into tissues and organs via tissue-specific extravasation from the bloodstream. ENMs may be metabolized in the liver by cytochrome P450-dependent enzymes or by metabolic process early in the gastrointestinal tract. Finally, ENMs can be removed from the body via the kidney (urine) or bile (feces). At each step of this process, ENM toxicity may arise: alteration of metabolic processes, hematological abnormality, organ toxicity and immunotoxicity arise from the long-term retention of ENMs in the liver, lung, spleen and kidney. Moreover, ENMs may cross the biological barrier system (blood–brain barrier, placental barrier) and cause neurotoxicity or reproductive toxicity. Genotoxicity may also appear (Li et al., 2014).*

2.1 *Nanotoxicity: physical and chemical properties of NPs*

Physicochemical characteristics of the materials are very important with respect to the observed biological effects: it is believed that the most important parameters in determining the adverse health effects of nanoparticles are dose, dimension, and durability (the three D's) (*Oberdörster, 2002*). However, recent studies show different correlations between various physico-chemical properties of nanoparticles and the associated health effects, raising some uncertainties as

to which are the most important parameters in deciding their toxicity: mass, number, size (surface area and size distribution), shape, bulk or surface chemistry (surface reactivity, surface groups, inorganic or organic coatings etc.), solubility and aggregation (*Nel et al., 2006*) (Fig. 8). Therefore, a detailed and comprehensive physicochemical characterization of the test NMs is stated as the first step before any toxicological screening (*Boverhof et al., 2010*).

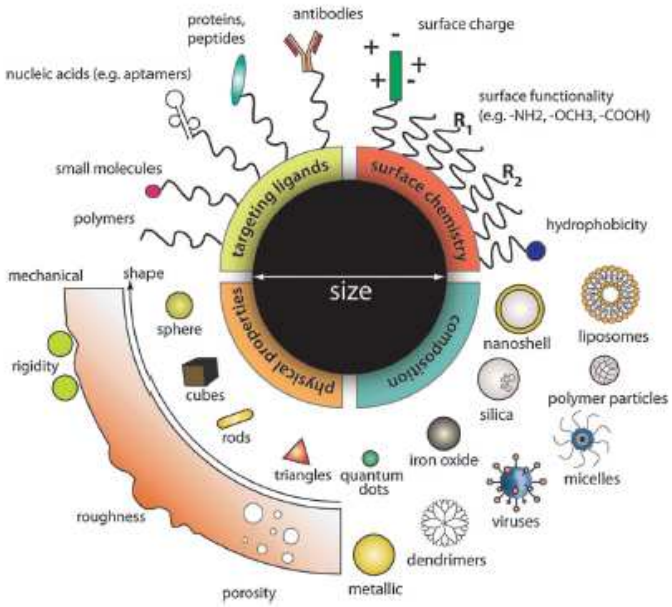

Fig. 8 *Designing ENMs for intracellular applications. ENMs can be modularly assembled from different materials composition with different physical and chemical properties and functionalized with a myriad of ligands for biological targeting. Such flexibility in design freedom enables researchers to tailor ENM for specific intracellular applications as contrast agents, drug delivery vehicles, and therapeutics (Chou et al., 2010).*

2.2 *Cellular uptake of ENMs*

The intracellular milieu is physically segregated from the environment by the plasma membrane, an elastic lipid bilayer embedded with domains of lipids, carbohydrates and proteins. The membrane regulates the transport of molecules into the cells, thereby representing a universal barrier protecting fragile intracellular structures from extracellular materials. In nature, polar or charged biomolecules, such as amino acids, nucleosides, or glucose, are transported across the lipid bilayer through specialized membrane-transport protein channels (active transport systems) (*Alberts et al., 2002*). ENM internalization depends on their size, for example, environmental particles (2.5-10 μm diameter) were found to collect in large cytoplasmic vacuoles, while smaller NPs (<100 nm) localize in organelles, such as mitochondria, leading to disruption of mitochondrial architecture. Therefore, ENMs interact with cell membrane, cytoskeleton and nucleus, leading to conformational changes of macromolecules like DNA and proteins, deformation of cellular membrane, as well as reorganization of the cytoskeleton at a subcellular level, changing the cell elasticity, morphology, adhesion, motility, and cell invasion processes.

Experimental studies revealed that most ENMs are incorporated into the cell via different endocytic pathways comprising phagocytosis ("cell-eating") and pinocytosis ("cell-drinking") or directly by "adhesive interactions" (*Yameen et al., 2014*). Furthermore, pinocytosis pathway can be

divided into clathrin-mediated endocytosis (CME) or caveolae-mediated endocytosis (CvME) (*Lühmann et al., 2008*; *Mailänder et al., 2009*) (Fig. 9 and 10)

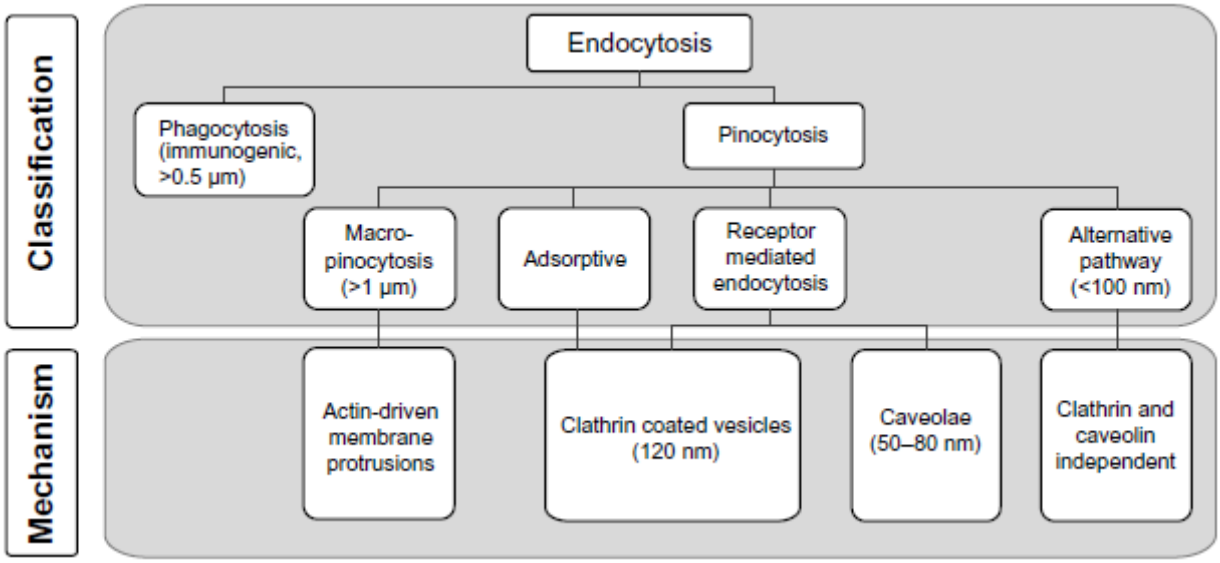

Fig. 9 *Different pathways of ENM cellular uptake (Kettiger et al., 2013).*

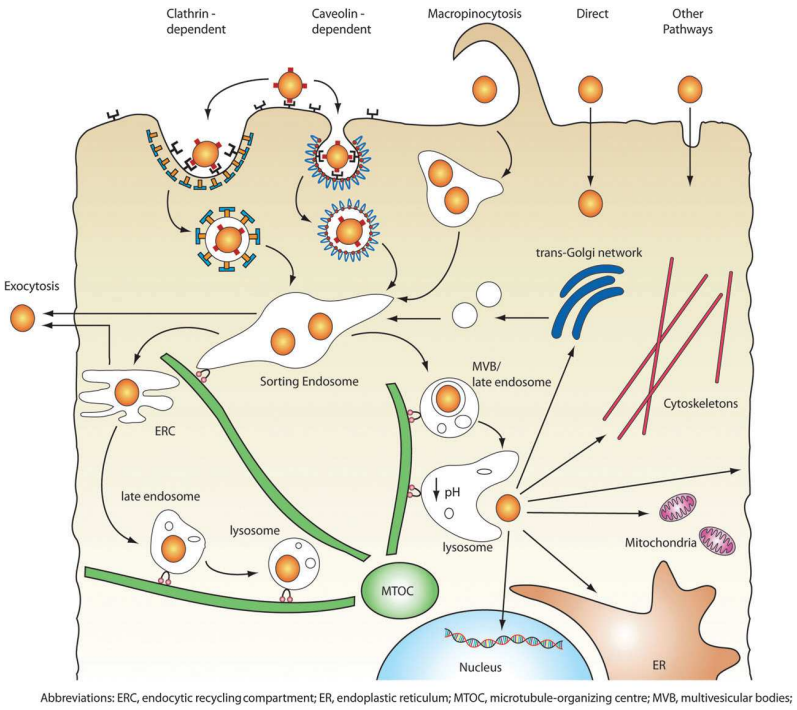

Fig. 10 *Intracellular transport of ENMs. After internalization via one or more of the endocytic pathways, ENMs are trafficked along the endo-lysosomal network within vesicles with the help of motor proteins and cytoskeletal structures. Vesicles can transport their contents into sorting endosomes, or excrete/recycle them back to the cell surface by fusing with the plasma membrane. Alternatively, endosomes can mature into lysosomes via luminal acidification and recruitment of degradative enzymes, which target the vesicle contents for degradation. In order to access cytoplasmic or nuclear targets, nanoparticles must be capable of escaping from the endo-lysosomal network as well as traverse through the crowded cytoplasm (Chou et al., 2010).*

2.3 *Characteristics of NPs influencing cellular uptake*

Research has shown that different physicochemical properties of ENMs result in different cellular uptake. Currently, it has been described that several factors play a critical role in toxicity; such as (i) size and surface; (ii) concentration, crystallinity, and mechanical strength, (iii) chemical attributes, the development of hydrophilic polymer functionalization(*Li et al., 2014*).
Over physicochemical properties of the ENMs, the cell-NP interactions are modulated by cell-specific parameters such as cell type or cell cycle phase (*Mahmoudi et al., 2012*), but also on the experimental conditions (buffer or medium supplemented with human serum). Specific cell types may interact with identical ENMs differently (*Iversen et al., 2011*; *Dos Santos et al., 2011*).

An additional factor is protein binding: once they have entered a biological milieu, NPs will inevitably come into contact with a huge variety of biomolecules including proteins, sugars and lipids that are dissolved in body fluids, such as the interstitial fluid between cells, lymph or blood. These biomolecules immediately coat the NP surfaces and form the so-called protein corona (*Röcker et al., 2009*; *Maffre et al., 2011*). Protein adsorption onto the surface of an NP changes properties such as size or surface charge dramatically (*Jansch et al., 2012*; *Monopoli et al., 2012*) and confers a new biological identity to the NP, which may completely modify the subsequent cellular and tissue responses, e.g., the distribution to various organs, tissues, and cells.

The state of dispersion and the variable size and shape of NPs induces different uptake mechanisms for the same material. These interactions are a function of the intrinsic physicochemical properties of NPs: they possess extremely high surface area to volume ratio which renders them highly reactive. High reactivity potentially could lead to toxicity due to harmful interactions of NPs with biological systems and the environment (*Oberdorster et al., 2005b*).

2.4 *Intracellular fate*

Once in the cytosol, NPs may induce different effects such as oxidative stress (*AshaRani et al., 2009*), genotoxicity, alterations on the normal cell cycle and inflammation. But NPs determine also alterations with cell membrane as a result of the interaction, such as deformation and reconstruction and distruption of cytoskeleton.

2.4.1 *Deformation of Cellular Membrane*

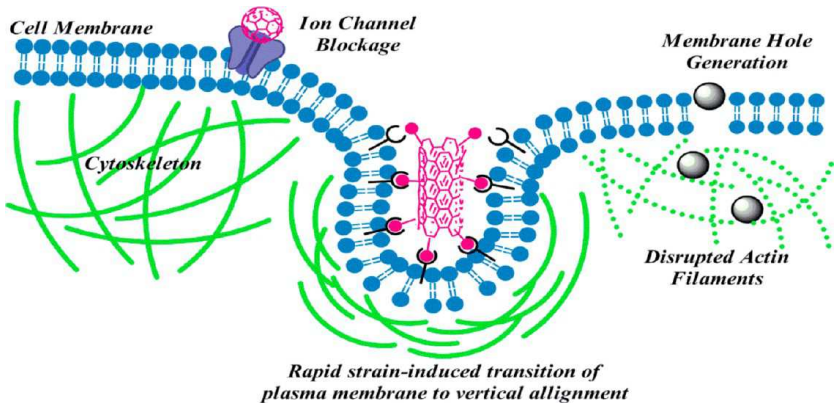

Fig.11 *Deformation of cellular membrane and reconstruction and disruption of cytoskeleton upon the interaction between nanomaterials and cells (Wu et al., 2013).*

As the primary defense barrier of the cell, the cell membrane forms the interface at which cells and ENMs first interact. When the they interact with the cellular membrane, may induce the disturbance of the phospholipids bilayer and blockage of membrane proteins (Fig. 11). It was found that the change in the cell membrane's local phase is closely related to the NPs' surface charge (*Dawson et al., 2009*; *Arvizo et al., 2007*). Negatively charged NPs bound to a fluid area of the membrane induced gelation, whereas positively charged NPs turned gelled areas into a fluid state for easier penetration. This may therefore explain why cationic particles are more toxic than net neutral analogues or anionic analogues of the same size (*Nel et al., 2009*). In addition, polymeric NPs were reported to induce “holes” in the living cell membrane, which corresponded to regions of reduced lipid or protein levels and are associated with cytotoxicity (*Leroueil et al., 2007*; *Verma et al., 2008*). This structural change of permeabilized cell membranes could lead to the leakage of cytosolic enzymes and result in toxicity. The formation of “holes” may be induced by the surface positive charges of NPs that could in turn cause the fluid phase change of lipid bilayer while the neutral or negative control does not show any cytosolic enzyme leakage. NPs of 1.2-22 nm could induce “holes” in lipid membranes, a process closely associated with nanotoxicity, while those nanoparticles with sizes less than 1.2 nm or more than 22 nm had no such effect.

Also the surface chemistry of NPs plays an important role in cell membrane disruption. Gold NPs (about 6 nm in diameter) with the same chemical composition but different surface ligand organization showed dramatic differences in cell membrane response (*Verma et al., 2008*).

Furthermore, besides the lipid bilayer of the cell membrane, NPs could also induce physical response in membrane proteins, which play an important role in the molecular transport and cell surface transmembrane signaling. As one of the most important membrane protein complexes, ion channels exhibit unique structures, especially the pore complex, that provide the physical pathway for ion movements across the plasma membrane and several charged domains that attract and/or repel ions. These characteristics make ion channels easy targets for nanomaterials that react with and block these channels as evidenced by the physical blocking of potassium ion channel by spherical fullerenes (diameter 0.72 nm) and carbon nanotubes (diameter 1-15 nm) (*Park et al., 2003*). Spherical fullerenes showed the highest blocking ability due to their similar diameter to the size of potassium channels, while the multiwalled carbon nanotube with bigger diameter did not show any blocking effects. Semiconductor NPs were reported to induce oxidative stress damage, leading to impairment of the ion channel structure and function (*Tang et al., 2008*; *Kirchner et al., 2005*). For example, oxidative stress induced by CdSe QDs could activate N-type calcium channels

and lead to the influx of extracellular calcium as well as rapid increase of intracellular calcium concentration, which is regarded as a possible mechanism of QD toxicity (*Peer et al., 2007*).

2.4.2 *Reconstruction and disruption of cytoskeleton*

After passing the cell membrane, NPs within the cell interact with the cytoskeleton, an interconnected network of filamentous proteins (microtubules, actin filaments, and intermediate filaments), and regulatory proteins which possess the ability to resist deformation. The cytoskeleton provides the mechanical stability and integrity of biological cells, transports intracellular cargo, and plays a key role during eukaryotic cell movement.

Cellular uptake of NPs is closely related to the deformation of cytoskeletal networks as well as changes in plasmamembrane tension and displacement of fluid in the cytoplasm. This process starts with the interaction between NPs coated with suitable ligands and cellular membrane receptor at the nano-bio interface (*Nel et al., 2009*). This specific binding of NPs to membrane receptors was driven by initial extension of cell membrane around the particle in a process that does not require actin polymerization. Active signaling from the receptor leads to the recruitment of numerous cytoskeletal proteins, including the Arp2/3 complex, which nucleates actin filaments beneath the particle. The formation of an actin network pushes the plasma membrane further around the target based on myosin-actin contractile activity, which leads to engulfment of the particle within the cell.

As a typical example, the cytotoxicity of single-wall carbon nanotubes that resulted from high amounts of cellular uptake is likely due to the changes induced in cytoskeleton and cell morphology (*Tian et al., 2006*). Human fibroblasts exposed to such nanotubes showed a random and irregular actin network compared with untreated cells with an organized radially distributed actin network.

2.4.3 *Induction of DNA damage and genotoxicity*

NPs, due to the minute size, charge, and high specific surface area, can cause a wide variety of DNA damage, ranging from chromosomal fragmentation, DNA strand breakages and the induction of gene mutations (*Singh et al., 2009*) (Fig. 12). Currently, there is an increasing focus on specific nanotoxic effects, and thus the advent of a subfield called “nanogenotoxicology” (*Donaldson et al., 2004*) which generally refers to the study of toxic effects of NMs on genomic stability and integrity.

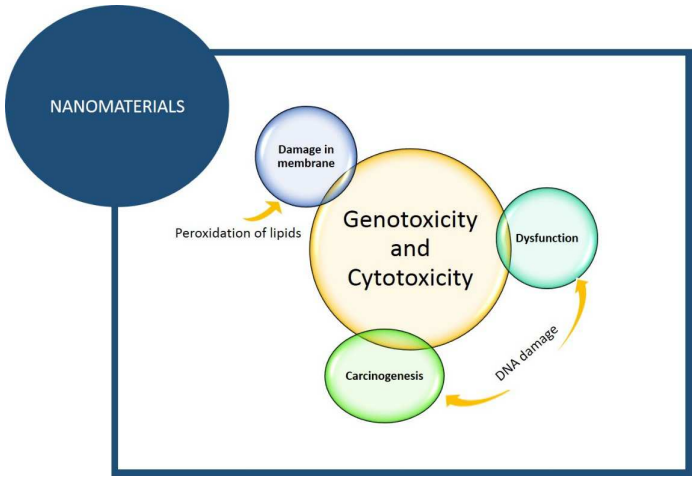

Fig. 12 *Genotoxic and Cytotoxic effects of NPs (Gonzalez-Munoz et al., 2015).*

For instance, gold NPs with smaller sizes (about 1.4 nm) have the ability to penetrate the nuclear compartment and could potentially bind to negatively charged DNA due to its electronegativity (*Rivera Gil et al., 2010*). Besides directly binding to DNA, NPs may cause DNA damage indirectly, by promoting oxidative stress and inflammatory responses (*Meng et al., 2009*). *In vitro* experiments have shown C60 to be generally noncytotoxic with no mutagenic response (*Shinohara et al., 2009*) in Chinese hamster ovary (CHO-K1) cells and mouse lung epithelial cells (*Jacobsen et al., 2008*) using the Ames test and CBMN tests, respectively. Another report has found that C60 treatment also increases formamidopyrimidine [fapy]-DNA glycosylase (FPG) sensitive sites, accounting for short-term DNA strand damage. Xu et al. *(2009*) observed that C60 induced an increase in mutation yield in primary mouse embryo fibroblast cells and dose-dependent formation of free radical $ONOO^-$ using dihydrorohodamine radical probes. However, *in vivo* setting, C60 treatment was found to be associated with increased DNA damage 8-hydroxydeoxyguanosine (8-OHdG) in mouse lung and liver (*Folkmann et al., 2009*). ZnO is quite well known to be cytotoxic to cells in culture (*Kim et al., 2010*), while the toxicity of TiO_2 NP is rapidly gaining attention due to the increased use and applications in many accessible medical and cosmetic products. TiO_2 NP comes in two common shapes, namely, the rutile and anatase forms. Although both are found to be genotoxic, one study showed that the anatase form induced greater DNA damage in human bronchial epithelium (*Pal et al., 2014*). TiO_2 NP could also increase cell sensitivity to phototoxicity (*Shi et al., 2010*), as well as induce more DNA adducts, strand breaks, base-pair mutations and chromosomal damage (*Wang et al., 2007*). Interestingly, Huang et al. *(2009)* reported that while long-term exposure to TiO_2 NP slowed down cell-division and induced aberrant multipolar spreads, chromatin alignment, and segregation, short-term exposure increased cell survival and growth and number of multinucleated cells. QDs, due to their small size, were able to enter the nucleus through the nuclear pore, inducing nuclear protein aggregation, as well as the inhibition of gene transcription and cell proliferation (*Nabiev et al., 2007*) and direct damage to chromosomes or nucleoproteins (*Singh et al., 2009*). One of the major effector molecules activated in response to DNA damage is p53. It plays a central role in DNA repair and cell cycle arrest, thereby preventing mutagenic events favouring the process of carcinogenesis (*Lane, 1992*). Cadmium-telluride QDs were found to significantly increase p53 levels and upregulate the p53-downstream effectors Bax, Puma and Noxa in human breast carcinoma cells (*Choi et al., 2008*). AgNPs were found to induce DNA damage in human glioblastoma cells as well as chromosomal aberrations in human fibroblast cells (*AshaRani et al., 2009*). Other genotoxic reactions include upregulation of p53 and DNA repair protein Rad51 observed in mouse embryonic stem cells and fibroblasts (*Ahamed et al., 2008*). In the same study, AgNP when functionalized with polysaccharide on its surface was more DNA damaging than uncoated AgNPs. A number of studies have also shown that AgNP treatment induced DNA damaging effects on aquatic and plant cells with impairment of cell-division (*Wise et al., 2010*).

2.4.4 *Induction of oxidative stress*

An important mechanism of nanotoxicity is the generation of reactive oxygen species (ROS), resulting in the subsequent oxidative stress (*Gonzalez et al., 2008*). ROS include free radicals such as the superoxide anion (O2•−), hydroxyl radicals (.OH) and the non-radical hydrogen peroxide (H_2O_2), which are constantly generated in cells under normal conditions as a consequence of aerobic metabolism. But cells are also endowed with an extensive antioxidant defense system to combat ROS, either directly by interception or indirectly through reversal of oxidative damage. The damage in cell function and development includes oxidative modification of proteins to generate

protein radicals (*Stadtman et al., 1997*), initiation of lipid peroxidation (*Butterfield et al., 2001*), DNA-strand breaks, modification to nucleic acids (*Evans M.D. et al., 2004*), modulation of gene expression through activation of redox-sensitive transcription factors (*Shi et al., 2004*), and modulation of inflammatory responses through signal transduction (*Bodamyali et al., 2002*), leading to cell death and genotoxic effects (*Fu et al., 2012*). NPs may promote the formation of pro-oxidants which, in turn, destabilizes he delicate balance between the biological antioxidant system and the reactive oxygen species (ROS) (*Curtis et al., 2006*; *Kabanov, 2006*) The generation of ROS and the subsequent production of oxidative stress is a predominant mechanism leading to nanotoxicity, including DNA damage, unregulated cell signaling, changes in cell motility, cytotoxicity, apoptosis, and cancer initiation and promotion (*Zhu et al., 2013*) (Fig. 13).

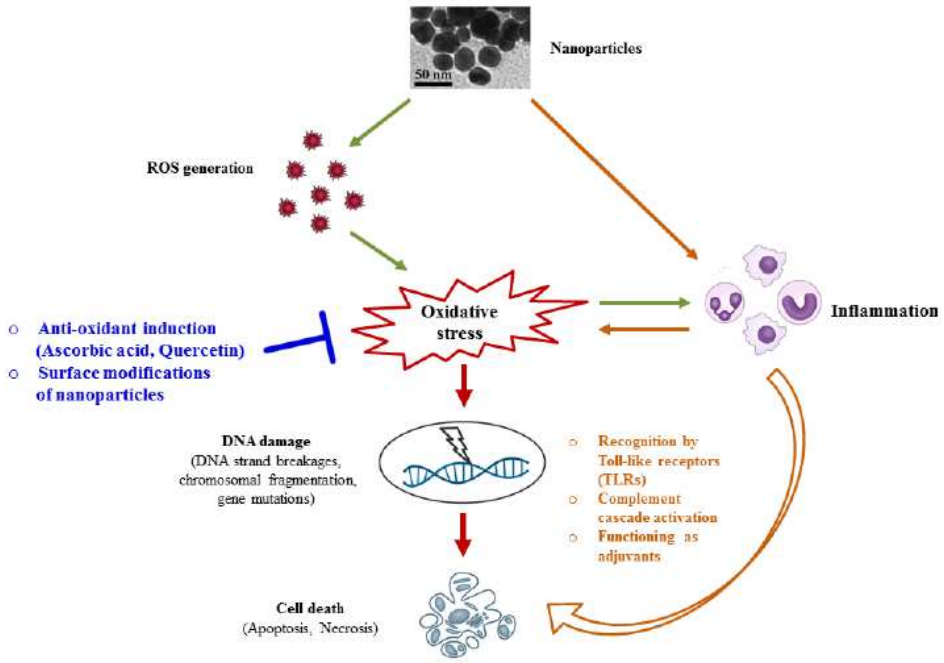

Fig. 13 *Overview of the signaling cascades mediating nanotoxicity and possible strategies to circumvent the toxicity (Khanna et al., 2015).*

Size, shape and aggregation are characteristics that can culminate in ROS generation (*Shvedova et al., 2005a, 2005b*). Compared to their bulk-size counterparts, ENMs possess a small size, high specific surface area, and high surface reactivity, leading to the production of higher levels of ROS and resulting in cytotoxicity and genotoxicity (*Oberdorster et al., 2005*) (fig. 14). A variety of ENMs has been found to induce toxicity mediated by ROS in many biological systems, such as human erythrocytes and skin fibroblasts (*Li et al., 2012*).

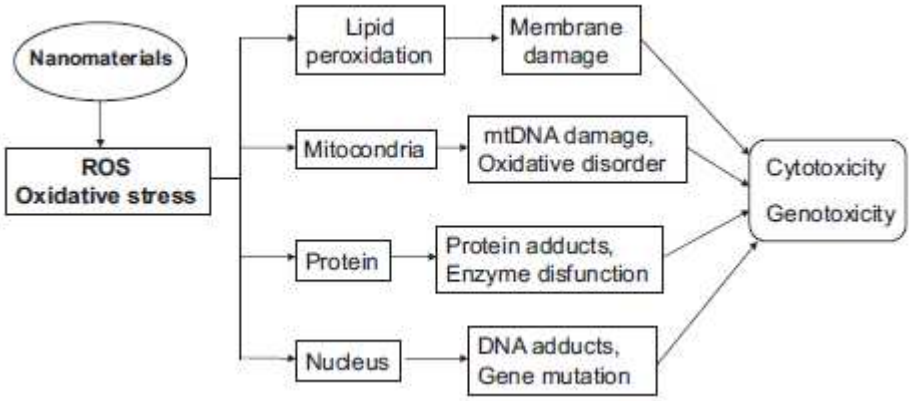

Fig. 14 *NP-induced toxicity mediated by ROS generation (Fu et al., 2014).*

Winnik et al. (*2013*) demonstrated that QDs produced oxidative stress and cell damage mediated by ROS. Akhtar et al. *(2010*) reported that silica NPs induced cytotoxicity and resultant oxidative stress in a dose dependent manner, mediated by the induction of ROS and lipid peroxidation in the cell membrane. Also *in vivo* studies with silica NPs indicated that single dose exposure to these NPs leads to ROS induction, consequently activating pro-inflammatory responses (*Park et al., 2009*).

2.4.5 Inflammation-mediated nanotoxicity

Inflammation is a defence mechanism of the body that involves several immune regulatory molecules, following the infiltration of phagocytic cells (Fig. 15). According to literature, NPs can activate and/or suppress immune response and the compatibility with this system is determined by its surface chemistry. Several studies with single and multi-walled carbon nanotubes and fullerene derivatives have shown the induction of inflammation in varied cell types, including alveolar and bronchial epithelial cells, epidermal keratinocytes and cultured monocyte-macrophage cells (*Qu et al., 2012*).

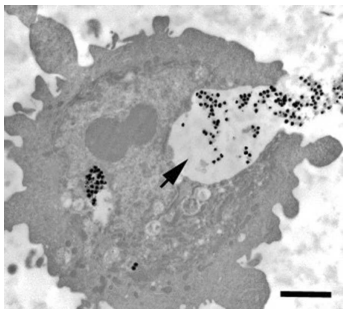

Fig. 15 *Transmission electron micrograph of an HEK engulfing 120 nm silica-coated silver nanoparticles. Arrow denotes silver nanoparticles within invagination (Monteiro-Riviere et al., 2012; by permission of Elsevier Ireland Ltd.). Bar, 2 μm.*

Many immunostimulatory reactions, driven by NPs, are mediated by the release of inflammatory cytokines. Cytokines are signaling molecules inducted by different types of nanomaterials: gold, dendrimers, or lipid NPs, among others. More recently, a study was carried out to provide a mechanistic explanation for immune and inflammatory responses observed upon exposure to carbon NPs. Importantly, inflammation has been shown to directly cause toxicity and promote cell death through the induction of toxic by-products of inflammation such as ROS and complement proteins, as well as via receptor-induced apoptosis/necrosis (*Wallach et al., 2015*). These cascades have not been well explored in the context of NP-induced cytotoxicity, and

investigations in this direction are required to fully identify and recognize the signaling networks mediating inflammation-driven cell death. Interestingly, oxidative stress also results in the release of pro-inflammatory mediators through the principal cascades such as the NF-κB (Nuclear Factor-κB), mitogen-activated protein kinase (MAPK) and phosphoinositide 3-kinase (PI3-K) pathways (*Poljak-Blaži et al., 2010*), suggesting that oxidative stress is linked to inflammation reciprocally (*Huang et al., 2010*). In the absence of a stimulus, NF-κB is sequestered in the cytoplasm by the Inhibitor of κB (IκB) family of inhibitors. However, in the event of oxidative stress, the IκB undergoes degradation, thus freeing NF-κB which then translocates into the nucleus to regulate the transcription of its target genes (*Allen et al., 2000*). Both *in vitro* and *in vivo* studies showed that nanoparticle-induced lung injury and pulmonary fibrosis lead to the ROS-mediated activation of NF-κB and production of pro-inflammatory mediators such as TNF-α, IL-8, IL-2 and IL-6 (*Byrne et al., 2008*). Several metal oxide NPs including zinc, cadmium, silica, and iron have also been shown to exert their toxicity via the production of inflammatory cytokines induced by NF-κB (*Hubbard et al., 2002*). NPs can also cause immunosuppression: one of the studies about immunosuppression has revealed that inhalation of carbon nanotube (CNT) results in a reduction of immune system in mice. This is produced through a mechanism that involves the release of TFG-β1 from lungs. Then, TFG-β1 goes into circulation and increases the expression of two molecules whose function is to inhibit T-cell proliferation (*Thompson et al., 2013*).

2.5 *Distribution and kinetics of nanoparticles in the body*

Humans can be exposed to nanomaterials via several routes such as inhalation, injection, oral ingestion and the dermal route (*Bystrzejewska-Piotrowska et al., 2009*) (fig. 16).

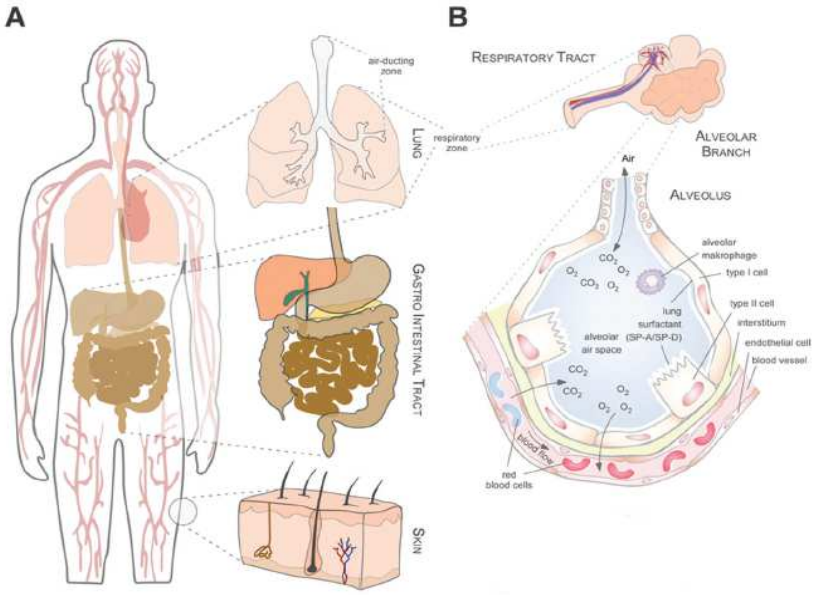

Fig. 16 *Biological complex environments: (A) possible application/entry routes for NPs. NPs can enter the human body via the bloodstream, via inhalation through the lung, via oral ingestion through the gastro-intestinal tract and, although less effective, through (damaged) skin. (B) Complex microenvironments of the lung. An alveolar duct and alveolus containing different cell populations and the pulmonary surfactant are depicted (Docter et al., 2015).*

Once nanoparticles cross these first biobarriers, they can easily reach vital organs such as lung, intestine and other organs by blood-stream transport. Specifically, the respiratory system, GI

tract, the circulatory system as well as the central nervous system are known to be adversely affected by NPs (*Medina et al., 2007*). For esample, TiO_2 NP used in sunscreen, cosmetics, paints and plastics, can cross bio-barriers such as spleen, liver, kidney and lung and, in *in vivo* exposure, cause effects such as spleen lesions, hepatocellular necrosis and apoptosis, hepatic fibrosis, renal glomerulus swelling and thrombosis in the pulmonary vascular system (*Chen et al., 2009*). Another study showed that silica NPs did not cause any toxicity in spleen, kidney and lung of mice, while chronic administration caused liver fibrosis, which can lead to hepatic cancer (*Nishimori et al., 2009*). Effects on the immune and inflammatory systems may include oxidative stress and/or activation of pro-inflammatory cytokines in the lungs, liver, heart and brain (*Mo et al., 2008*). Then, a greater understanding of the mechanisms whereby nanoparticles interact with target cells can impact significantly on assessing their potential toxicity (*Unfried et al 2007*). A complete analysis of the pharmacokinetics of NPs has to include absorption of biomolecules, distribution, metabolism, and excretion (*Sharifi et al., 2012*).

2.5.1 *Respiratory tract uptake, effects and clearance*

The respiratory system serves as a major portal for ambient particulate materials. Recently, the pathogenic effects and pathology of inhaled manufactured nanoparticles have received attention (*Donaldson et al., 2006; Lam et al., 2006; Nel et al., 2006; Oberdorster et al., 2005a*). After inhalation, NPs deposit throughout the entire respiratory tract, starting from nose and pharynx, down to the lungs (*Oberdorster 2001; Elder et al., 2006*). Being different than micron sized particles that are largely trapped and cleared by upper airway mucociliary escalator system, particles less than 2.5 μm can get down to the alveoli. In the upper airways, particle clearance is performed mainly by the mucociliary escalator (*Ferin, 2004*). The first contact of inhaled NPs in the respiratory tract is with the lining fluid, composed of phospholipids and proteins (*Wright et al., 1994*). This contact leads to particle wetting and displacement towards the epithelium by surface forces from the liquid-air interface (*Peters et al., 2006*). When in contact with esophageal epithelial cells, nanoparticles uptake by these cells is possible in the presence of preexistent inflammation (*Hopwood et al., 1995*). The adverse health effects of NPs depend on the residence time in the respiratory tract (*Peters A et al., 2006*). When the lung is subject to prolonged exposure, neutrophils are recruited to help. Experimental data show that, compared with larger particles, NPs smaller than 100-200 nm are more capable of evading alveolar macrophages phagocytosis (*Peters et al., 2006*), entering pulmonary interstitial sites, and interacting with epithelial cells to get access to the circulatory and lymphatic systems (*Oberdörster et al., 2005*; *Takenaka et al., 2001*). After absorption across the lung epithelium, NPs can enter the blood and lymph to reach cells in the bone marrow, lymph nodes, spleen and heart (*Hagens et al., 2007; Oberdorster et al., 2005a*). The latter could be of significance since the association between inhaled ambient ultrafine particles and cardiovascular events such as coagulation and cardiac rhythm disturbances has been proven (*Nurkiewicz et al., 2006; Yeates and Mauderly, 2001*). Other targets after translocation include the sensory nerve endings embedded in the airway epithelia, followed by ganglia and the central nervous system via axons (*Oberdorster et al., 2005b; Oldfors and Fardeau, 1983*). Smaller particles have a higher toxicity than larger particles of the same composition and crystalline structure, and they generate a consistently higher inflammatory reaction in the lungs (*Oberdörster et al., 1994*). Rat inhalation (*Oberdörster et al., 1994*) and instillation (*Oberdörster et al., 2005*) of titanium oxide NPs with two sizes, 20 nm and 250 nm diameter, having the same crystalline structure show that smaller particles led to a persistently high inflammatory reaction in the lungs

compared to larger size particles (*Oberdörster et al., 1994*). Takenaka et al. *(2001)* have demonstrated that in both inhalation and instillation experiments, ultrafine AgNPs were taken up by alveolar macrophages and aggregated silver particles persisted there for up to 7 days. Aggregated AgNPs have been shown to be cytotoxic to alveolar macrophage cells as well as epithelial lung cells (*Soto et al., 2007*).

The NPs that are cleared from the lung via the mucociliary escalator enter the gastro-intestinal tract (*Takenaka et al., 2001*; *Semmler et al., 2004*). In some interesting work, coating with pulmonary surfactant associated proteins enhanced the opsonin-dependent uptake of NPs (*Ruge et al., 2011*) Therefore, phagocytic uptake may be enhanced after the formation of a protein corona. The protein corona may, on the other hand, reduce interparticle agglomeration. Agglomeration is usually quite loose; thus, the protein corona could easily overcome the agglomeration tendency by reducing surface energy and increasing hydrophilicity and steric stability. Under such circumstances, well dispersed NPs with size below 100 nm could easily escape phagocytosis (*Geiser et al., 2010*). In addition, albumin adsorption significantly decreases the cellular association and uptake of NPs by Ams (*Ruge et al., 2011*). Given that a leak of serum albumin into alveoli is a common symptom of pulmonary exposure to NPs (*El-Ansary et al., 2009*) coating with albumin might sometimes prevent the AM-mediated clearance.

2.5.2 *Dermal uptake, effects and translocation*

Skin is the largest primary defense organ in our body and directly comes into contact with many toxic agents. The skin is structured organ comprising three layers: the epidermis, the dermis and the subcutaneous layer. The strongly keratinized stratum corneum acts as the primary protecting layer and may be the rate-limiting barrier to defend against the penetration of most micron sized particles and harmful exogenetic toxicants (*Hoet et al., 2004*). **S**kin exposure to NPs can also occur during the intentional application of topical creams and other drug treatments (*Curtis et al., 2006; Hagens et al., 2007; Oberdorster et al., 2005b*). A current area under discussion is whether or not TiO_2 NPs found in commercially available sunscreens penetrate the skin. For example, the application of a sunscreen containing 8% NPs (10-15nm) onto the skin of humans showed no penetration, while oilin-water emulsions showed penetration, higher penetration being present in hairy skin at the hair follicles site or pores (*Tsuji et al., 2006*). The quantity of NPs that penetrate is very small, with less than 1% of the total amount in the applied sunscreen being found in a given hair follicle (*Lademann et al., 1999*). Several studies show that NPs are able to penetrate the stratum corneum (*Borm et al., 2006*; *Oberdörster et al., 2005*; *Blundell et al 1989*; *Corachan et al., 1988*; *Toll et al., 2004; Tinkle et al., 2003*). NPs penetration through the skin typically occurs at hair follicles (*Toll et al., 2004*) and flexed (*Tinkle et al., 2003*) and broken skin (*Oberdörster et al., 2005*). In contradistinction to this finding, there are many reports that show deeper penetration of NPs (*Monteiro-Riviere et al., 2005*). Lademann et al. *(1999)* showed that TiO_2 NPs could get through the human stratum corneum and reach epidermis and even dermis. Flexing movement of normal skin was shown to facilitate the penetration of micrometer-size fluorescent beads into the dermis (*Tinkle et al., 2003*). Oberdorster et al. *(2005b)* demonstrated penetration of a variety of nanoparticles in the dermis and translocation to the systemic vasculature via lymphatic system and regional lymph. Translocation of nanoparticles through skin into the lymphatic system is demonstrated by soil particles found in lymph nodes of patients with podoconiosis (*Blundell et al 1989*; *Corachan et al., 1988*). Neuronal transport of small NPs along sensory skin nerves may be possible, in a similar way to the proven path for herpes virus (*Oberdörster et al., 2005*). Further,

Ryman-Rasmussen et al. *(2006)* demonstrated that QDs with diverse physicochemical properties could penetrate the intact stratum corneum barrier and get localized within the epidermal and dermal layers. Intradermally administered QDs could enter subcutaneous lymphatics (*Gopee et al., 2007*) and regional lymph nodes (*Kim et al., 2004*). Fullerene-based peptides were also shown to be capable of penetrating intact skin and mechanical stressors could facilitate their traversal into the dermis (*Rouse et al., 2007*). It is worth noting that some other types of NPs, i.e. single-/multi-wall CNTs, QDs with surface coating and nanoscale titania, have been shown to have toxic effects on epidermal keratinocytes and fibroblasts and are capable of altering their gene/protein expression (*Christie et al., 2006; Ding et al., 2005; Monteiro-Riviere et al., 2005; Ryman-Rasmussen et al., 2006; Sarkar et al., 2007; Tian et al., 2006; Witzmann and Monteiro-Riviere, 2006; Zhang et al., 2007*). MWCNTs are internalized by human epidermal keratinocytes (the major cell type of the epidermis) in cytoplasmic vacuoles and induce the release of pro-inflammatory mediators. Topically applied fine and ultrafine beryllium particles can be phagocytosed by macrophages and Langerhans cells possibly leading to perturbations of the immune system (*Tinkle et al., 2003*). Epidermal keratinocytes have also been shown to be capable of phagocytosing a variety of ENMs and setting off inflammatory responses (*Monteiro-Riviere et al., 2005*). Spherical particles with diameter between 750 nm and 6 microns selectively penetrate the skin at hair follicles with a maximum penetration depth of more than 2.4 mm (*Toll et al., 2004*). Broken skin facilitates the entry of a wide range of larger particles (500 nm - 7 μm) (*Oberdörster et al., 2005*).

2.5.3 *GI tract uptake*

NPs can reach the GI tract after mucociliary clearance from the respiratory tract through the nasal region (*Takenaka et al., 2001*), or can be ingested directly in food (such as colorants– titanium oxide), water, cosmetics (toothpaste, lipstick), drugs, and drug delivery devices (*Hagens et al., 2007; Oberdorster et al., 2005b*) and dental prosthesis debris (*Ballestri et al., 2001*). Gastro-intestinal tract is a complex barrier-exchange system, and is the most important route for macromolecules to enter the body. The epithelium of the small and large intestines is in close contact with ingested material, which is absorbed by the villi. The extent of particles absorption in the gastro-intestinal tract is affected by size, surface chemistry and charge, length of administration, and dose (*Hoet et al.,. 2004*). The absorption of NPs in the gastro-intestinal tract depends on their size, the uptake diminishing for larger particles (*Jani et al., 1990*). A study of polystyrene NPs with size between 50 nm and 3 μm indicated that the uptake decreases with increasing particle size from 6.6% for 50 nm, 5.8% for 100 nm nanoparticles, 0.8% for 1 μm, to 0% for 3 μm particles. The time required for NPs to cross the colonic mucus layer depends on the particle size, with smaller particles crossing faster than larger ones: 14 nm diameter latex NPs cross within 2 minutes, 415 nm within 30 minutes, and 1000 nm particles do not pass this barrier (*Hoet et al., 2004*). Moreover NPs in the GI tract have been linked to Crohn's disease and colon cancer (*Koeneman et al., 2009*). NPs that penetrate the mucus reach the enterocytes and are able to translocate further. Enterocyes are a type of epithelial cell of the superficial layer of the small and large intestine tissue, which aid in the absorption of nutrients. When in contact with the sub-mucosal tissue, NPs can enter the lymphatic system and capillaries, and then are able to reach various organs (*Hoet et al.,. 2004*). Furthermore, GI route of translocation of ingested ultrafine particles to the blood, is supported by studies in rats and humans that have shown that TiO_2 NPs (150–500 nm) taken in via food can translocate to the blood and are taken up by liver and spleen (*Bockmann J. et al., 2000*). Chung et al. *(2010)* recently reported occurrence of systemic argyria after ingestion of colloidal nanosilver proves its translocation from the intestinal tract.

2.5.4 *Nanoparticles uptake via injection and translocation*

When injected into the blood stream, foreign NPs encounter different blood constituents such as red blood cells, white blood cells, platelets, and a variety of proteins. NPs are known to interact with both proteins and blood cells. Protein binding and opsonization are processes that change the surface properties. There are three main types of cells in the blood: red cells in charge of oxygen transport; white cells responsible for fighting infections; and platelets that help prevent bleeding by forming blood clots. The uptake of NPs by each type of blood cells is essentially different. Uptake by red blood cells is entirely dictated by size (*Peters et al., 2006*), while the NP charge or material type have fewer importance (*Rothen-Rutishauser et al., 2006*) (Fig. 17).

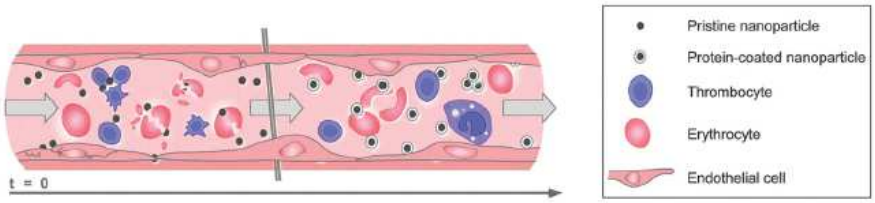

Fig. 17 *Illustration of how rapid corona formation kinetically impacts early nanopathology in the human blood system. Upon entry or parenteral application, pristine NPs only exist for a short period of time, but are still capable of immediately affecting the vitality of endothelial cells, triggering thrombocyte activation and aggregation, and may also induce hemolysis. Formation of the biomolecule corona rapidly modulates the NPs' decoration with bioactive proteins protecting the cells of the blood system against nanoparticle-induced (patho)biological processes, and can also promote cellularuptake (Docter et al., 2015).*

Hemolysis has been described for rigid materials such as silica NPs (*Yu et al., 2011*) or for soft NPs such as liposomes (*Quirion et al., 1991*). NP charge plays an essential role in their uptake by platelets and their influence on blood clot formation (*Nemmar et al., 2002*). Uncharged polystyrene particles do not have an effect on blood clots formation. Negatively charged NPs significantly inhibit thrombi formation, while positively charge NPs enhance platelet aggregation and thrombosis (*Nemmar et al., 2002*). The interaction between platelets and positively charged particles seems to be due to the net negative charge that platelets carry on their surface (*Nemmar et al., 2002*). The positively charged NPs interact with negatively charged platelets and reduce their surface charge, making them more prone to aggregation. NPs between 20 and 200nm can remain in the circulation for an extended period of time (*Petros et al., 2010*). In the blood stream, agglomerates may cause embolism with a potentially fatal outcome. Agglomerated NPs have a tendency to accumulate after injection within the lung since venous blood is directed from the right heart ventricle to this organ. Protein coating is a highly dynamic process, the resulting protein corona is complex and varies depending on the size (*Jansch et al., 2012*), hydrophobicity/surface charge (*Jansch et al., 2012*) and shape (*Gasser et al., 2010*) of the NPs. In the first instance, readily available proteins such as albumin are adsorbed onto the NPs surface, but may be replaced by other proteins (eg, lipoproteins or opsonins) over time, depending on the surface structure of the NPs. A prominent consequence of coating with proteins is the opsonization of NPs, which allows RES macrophages to easily recognize and their remove. Some researches have demonstrated that protein

corona assisted in the transcellular passage of NPs through the blood brain barrier (*Ragnaill et al., 2011; Koffie et al., 2011*).

Surface modification of NPs with chemical and biological agents, such as PEG can create a hydrophilic protective layer around the NPs, which sterically hinders absorption of opsonin proteins, thereby blocking the opsonization process. In addition, PEG may elicit an immunological response resulting in an accelerated blood clearance of NPs. As an alternative to PEGylation, NPs can be coated with amino acids such as lysine or cysteine. Such a mixed-charge monolayer-coating prevented protein adsorption in fetal bovine serum to 5 nm gold NPs (*Lipka et al., 2010*). Furthermore, it is established that NPs with neutral or negatively charged surfaces have a reduced plasma protein adsorption and low rate of nonspecific cellular uptake, while positively charged NPs are expected to have a high non specific internalization rate and short blood circulation half-life (*Alexis et al., 2008*).

The blood circulation of NPs and their exchange between tissue vasculature and interstitium is a multifaceted process, for istance, the translocation depends on the site of injection:

1. Intravenously injected nanoparticles quickly spread throughout the circulatory system, with subsequent translocation to organs
2. Intramuscular injection is followed by neuronal system uptake
3. Intradermal injection leads to lymph nodes uptake.

1. Intravenously injected nanoparticles (QDs, fullerenes, polystyrene) with size ranging from 10-240 nm show localization in different organs, such as liver, spleen, bone marrow, (*Oberdörster et al., 2005*), small intestine and lungs (*Rae et al., 2005*) (Fig. 18).

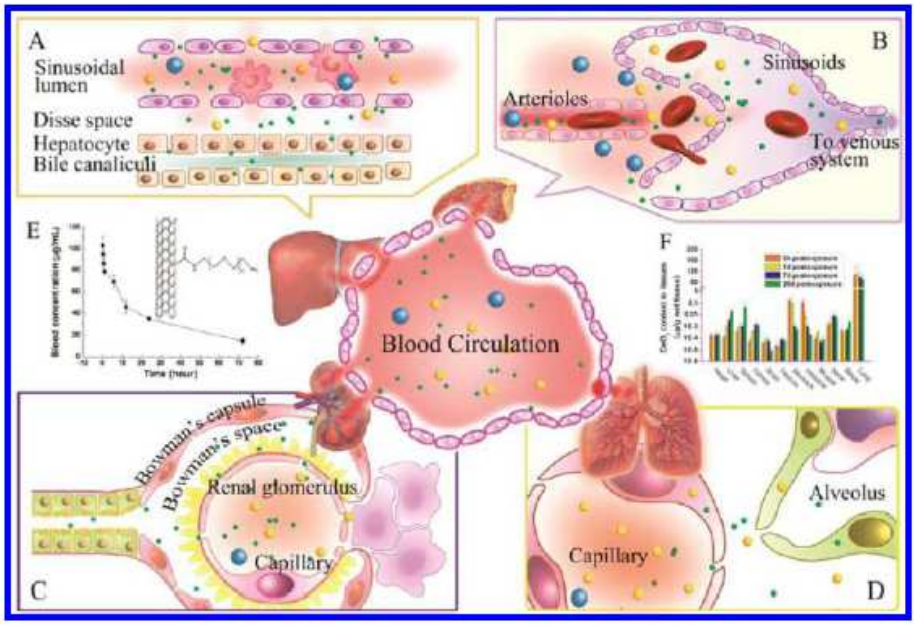

Fig. 18 *The tissue-specific extravasation of NMs. (A) The hepatic sinusoidal endothelial cells possess open fenestraes sized 100-200 nm that facilitate the NM diffusion. Smaller NMs (10-20 nm) are removed from blood via rapid liver uptake, whereas larger NMs (g200 nm) are effectively cleared by Kupffer cells. (B) In sinusoidal spleen (as in rat and human), blood flows through the discontinuous capillary into splenic venous system. Non deformable entities sized above 200 nm may be cleared from blood by splenic filtration. (C) The capillary fenestraes in the glomeruli have size between 10 and 100 nm, but the basal lamina can block the*

penetration of particles larger than 5 nm. (D) The endothelia of lung, muscle, and bone capillaries are generally characterized by a continuous morphology that allows only small particles sized below 3 nmto cross the interendothelial cell slits. (E) The blood concentration of PEG SWCNTs versus time following intravenous administration to mice. (F) The translocation to the secondary target organs and the intertissue redistribution of nanoceria via blood circulation (Wang et al., 2011).

Talc particles introduced by injection are found in the liver of intravenous drug users (*Gatti and Rivasi, 2002*). Liver is the main organ of metabolic clearance of most drugs and xenobiotics. Evidence has shown that NPs are preferentially deposited in liver under systemic exposure, resulting in prolonged retention within the organ and in some instances significant hepatotoxicity (*Abdelhalim et al., 2011*). The size of NPs plays an important role in modulating target cell type as well as the degradation pathway in liver. Generally, NPs larger than 200 nm are effectively cleared by KCs because slow blood flow in liver sinusoids allows enough time for phagocytosis and macropinocytosis. A work showed that polystyrene NPs (20 nm) were internalized by hepatocytes and were observed within bile canaliculi, indicating a possible elimination via bile (*Johnston et al., 2010*). Importantly, SWCNTs have been found to be biodegraded by enzymatic catalysis, including horseradish peroxidase, myeloperoxidase, and heme oxygenase-1 (*Kagan et al., 2010*). It is known that there are a large number of phase I and phase II enzymes in liver, for example, monooxygenase, transferases, esterases, and epoxide hydrolase, that are expressed. Thus, the hepatic clearance of NPs could be associated with enzyme-catalyzed biodegradation, although *in vivo* evidence is still lacking at this time. Chemical reactivity and composition of the shell and core materials play an important role in degradation. NPs known to "safely" degrade are porous silica NPs (*He et al., 2008*) and iron oxide particles (*Mahmoudi et al., 2011*). Degradation of silica NPs leads to the formation of silicic acid, which is excreted via feces and urine (*Park et al., 2009*). However, for another NPs is difficult to break down by intracellular processes, such as inert gold nanoparticles, NPs remain within the cells and deposit in the liver for a long time (*Sadauskas et al., 2009*). Increased liver accumulation was found for particles with a size of 5 nm as compared to particles with a size of 1.4 nm. Renal excretion represents a preferable clearance pathway for NPs from body. The understanding of renal clearance of NPs is fundamental for the toxicity assessment and the *in vivo* application of NPs. Work in mice orally exposed to copper and zinc oxide nanoparticles showed resultant morphological and pathological damage in the renal glomerulus and renal tubules (*Wang et al., 2008*). Renal clearance involves glomerular filtration, tubular secretion, and tubular reabsorption. Glomerular filtration is the first step in renal clearance of NPs and directly affects renal clearance capability: glomerular filtration eliminates NPs with a hydrodynamic diameter of ,5 nm to 10 nm. Size is an important parameter regarding circulation and distribution within the organism: small NPs might be removed from the blood by renal clearance (<5 nm) or rapid liver uptake (10-20 nm) (*Longmire et al., 2008*), whereas large NPs are filtered in the sinusoidal spleen (>200 nm) or are recognized and cleared by RES (Fig. 19).

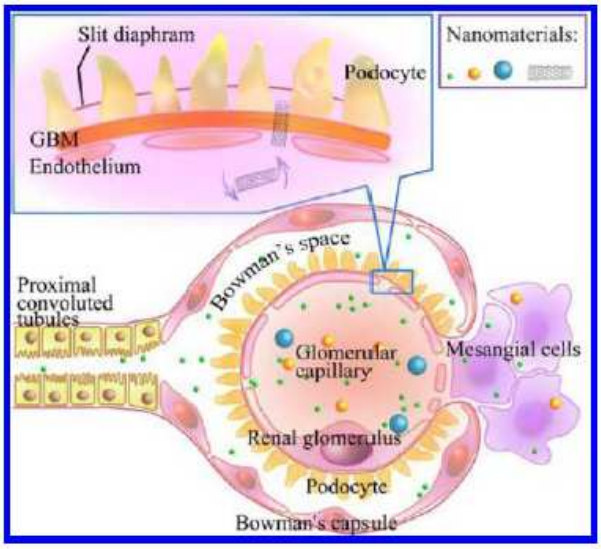

Fig. 19 *Glomerular filtration of NPs in vivo (Wang et al., 2011).*

Renal clearance studies in mice using QDs with zwitterionic cysteine demonstrated the size threshold for glomerular filtration of QDs was about 5.5 nm. The QDs less than 5.5 nm were effectively excreted in the urine, while renal excretion was prevented when the diameter was above this value (*Choi et al., 2007*). Protein adsorption has a profound effect on the hydrodynamic diameter and surface charge of NPs thus in turn influences the renal filterability and likely shifts the route of excretion from kidney to liver. Previous work indicated that because the anionic charged QDs absorbed serum albumin and γ-globulin and formed aggregations of several hundred nanometers, the aggregated QD particles could not be filtered via the glomerulus and were mainly metabolized in the liver (*Chen et al., 2008*). Under conditions when NPs deposit in kidney and are unable to be filtered by the glomerulus, they often induce severe kidney damage. The glomerular mesangial cells, glomerular capillary bed, and proximal tubular epithelial cells are considered important target sites for nephrotoxicity after exposure to NPs. It was reported that NPs with a 75-25 nm diameter could target the mesangium through the endothelial pore and accumulate in multiple clusters within the phagocytictype mesangial cells (*Choi et al., 2011*). Another work in mice showed that oral exposure to copper NPs induced grave morphological and pathological damages in the renal proximal convoluted tubule, such as reducing karyons, degeneration, and irreversibly massive necrobiosis in epithelial cells of the renal proximal convoluted tubules (*Chen e tal., 2006*).

2. Intramuscular injection is followed by neuronal system uptake. The nervous system is composed of the brain, spinal cord, and nerves that connect the brain and spinal cord to the rest of the body. Experiments performed on rats injected with ferritin macromolecules (with size around 10 nm) into the cerebrospinal fluid, demonstrated passage of ferritin into deep brain tissue. As esample, injection of magnetic NPs smaller than 100 nm into the tongues and facial muscles of mice resulted in synaptic uptake (*Oberdörster et al., 2005*). Blood brain barrier is a physical barrier with negative electrostatic charge between the blood vessels and brain (*Lockman et al., 2004*), selectively restricting the access of certain substances (Fig. 20). This anionic barrier is believed to stop most anionic molecules, while the cationic molecules increase the permeability of the blood-brain-barrier by charge neutralization (*Borm et al., 2006*). Regarding the passage of NPs, the blood-brain-barrier permeability is dependent upon the charge of NPs (*Lockman et al., 2004*) Penetration of NPs across blood brain barrier was observed in both *in vitro* and *in vivo* studies (*Ragnaill et al.,*

2011; Koffie et al., 2011). It allows a larger number of cationic NPs to pass compared to neutral or anionic particles, due to the disruption of its integrity (*Lockman et al., 2004*). In addition to uptake due to across blood brain barrier (BBB), nervous system uptake may occur via other pathways: uptake via olfactory nerves (*Borm et al., 2006*; *Oberdörster et al., 2005*). The nasal and tracheo-bronchial regions have many sensory nerve endings (*Oberdörster et al., 2005*).

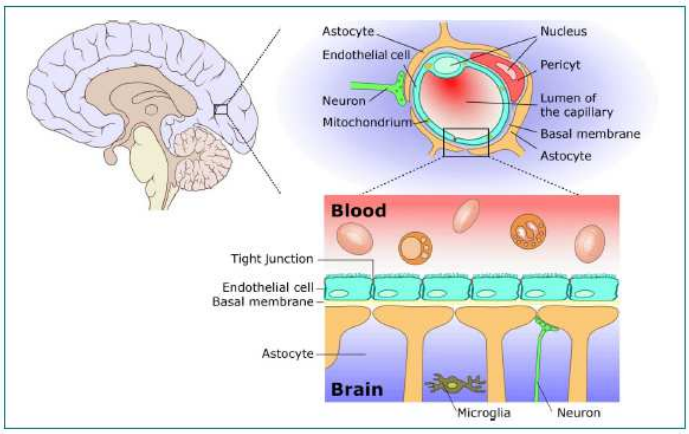

Fig. 20 *The blood-brain barrier (BBB); above, cross section through the brain; center, schematic representation of the BBB; below, cellular structure (Simkò et al., 2010).*

3. Translocation of NPs to lymph nodes is a topic of intense investigation today for drug delivery and tumor imaging. Progression of many cancers (lung, esophageal, mesothelioma, etc.) is seen in the spread of tumor cells to local lymph nodes. The detection and targeted drug delivery to these sites are the steps involved in the therapeutic treatment of cancer (*Cabral et al., 2015*) (Fig. 21). Several studies show that interstitially injected particles pass preferentially through the lymphatic system and not the circulatory system, probably due to permeability differences. After entering the lymphatic system, they locate in the lymph nodes (*Liu et al., 2006*). The free nanoparticles reaching the lymph nodes are ingested by resident macrophages (*Shwe et al., 2005*)**.** The adverse health effects of NP uptake by lymphatic system are not sufficiently explored.

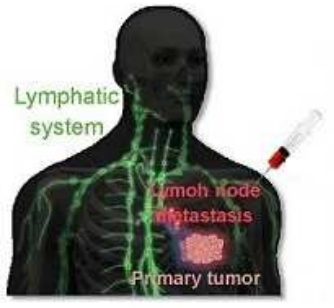

Fig. 21 *Translocation of NPs to lymph nodes is a topic of intense investigation today for drug delivery and tumor imaging (Cabral et al., 2015).*

3. PROTEIN CORONA

The rapid development of nanotechnology in the past decades offerswide prospects in using micro- and nano-scale materials in different areas of industry, technology, and medicine. NPs have unique properties that may be useful in a diverse range of applications and consequently they have attracted significant interest. Nevertheless, our knowledge about the bio-compatibility and risks of exposure to nanomaterials is limited. Exposure to nanomaterials for humans may be accidental, for example by occupational exposure, or intentional, for example in the case of the use of nano-enabled consumer products. Understanding the mechanisms of interactions between NPs and living matter is crucial for safe implementation of nanotechnologies in various fields. Therefore, we need to understand how NPs enter the body, tissues, and cells, where they go when they get there, and what are the consequences of them being there. Furthermore, if we want to fully understand the biological impact of NPs, we should address all the complicated molecular aspects of nano-bio interactions. Hence, there is an urgent need to understand the molecular mechanisms of nanoparticles-to-biological system interaction.

In physiological environments NPs are exposed not only to relatively high ion concentrations or drastic pH changes (*Li et al., 2010*), but also to a huge variety of complex biomolecules (*Monopoli et al., 2011*). Many body fluids (e.g. blood, lung lining fluid, saliva, intestinal juice, etc.) have one common characteristics, their composition is highly complex (*Anderson et al., 2011*). Thus, whereas the physico-chemical properties and behavior of NPs can be engineered and controlled in technically stable, protected environments, such as technical products, this is no longer the case in complex physiological or natural environments. Such 'complex environments' are not only represented by simple and higher organisms, including humans, but also by "complex (micro)environments", such as organs and cells, which also differ very dramatically in their physico-chemical composition. In this complex (micro)environments, once NPs interact with biological fluids and come into contact with tissues, they are exposed to active biomolecules that form a "crown" (*corona*) around them, thus transforming the bare NP into an NP that has a biological component: the so-called "protein corona". During the recent years, a large number of studies have been devoted to the characterization of protein corona (*Monopoli et al., 2012; Dos Santos et al., 2007*).

The surfaces of all NPs have higher free energy than the bulk material itself. This means that their surfaces will progressively and selectively adsorb biomolecules when they come into contact with complex biological fluids. This "corona" of biomolecules lowers the surface energy of the nanoparticle and promotes its dispersion and in many cases the biomolecular corona interacts with biological systems (*Aggarwal et al., 2009; Walczyk et al., 2010*). The protein corona is primarily composed of proteins. The presence of other biomolecules such as sugars, nucleic acids and lipids is expected but so far little studied (*Wan et al., 2015; Hellstrand et al., 2009*). The binding forces that are responsible for such interactions include van der Waals interactions, hydrogen bonds, hydrophobic interactions, electrostatic interactions, and π- π stacking (*Yang S.T. et al., 2013*).
The first studies on the interactions between NPs and plasma proteins were conducted between 1996 and 2000 (*Gessner et al., 2000; Diederichs et al., 1996*), but it was the group of Dawson that first introduced the NP– protein corona complex concept (*Cedervall et al., 2007*).

The physical and chemical interactions with proteins and/or other biomolecules (e.g. phospholipids, sugars, nucleic acids, etc.) will in most cases significantly affect the NPs' behavior and fate and understanding the corona formation process is crucial in predicting NP behavior in biological systems, including applications for nanotoxicology and development of drug delivery platforms at the nanolevel (*Shaw et al. 2012; Sisco et al. 2014*).

3.1 *Dynamics of protein corona formation*

The process of corona formation is determined by the competition of countless proteins to adsorb at the approaching NP surface. Miclăuş et al. *(2014)* suggested that protein adsorption is a dynamic process involving continuous adsorption/desorption equilibrium of proteins *on* and *off* on the NP surfaces. During such time dependent process, their kinetics might be also important, as described by the association (k_{on}) and dissociation (k_{off}) constants. The value of k_{on} depends on the contact frequency between the protein and NP, while the value of k_{off} depends on the binding energy of the protein–NP complex (Fig. 22). The balance between these two factors, k_{on} and k_{off}, determines the affinity of a protein to the NP and defines as the dissociation constant (K_d). For example, K_d for the adsorption of serum proteins to nanomaterials varies from approximately 10−4 to 10−9 M, which is similar to the range for antibody–antigen interactions. Then, these studies on the composition of the protein corona have demonstrated that the process of protein corona formation is in continuous evolution and that the adsorption of proteins on the surface is mainly governed by affinity interactions of proteins towards the NP surface and by affinity-based protein-to-protein interactions (*Monopoli et al., 2011*)

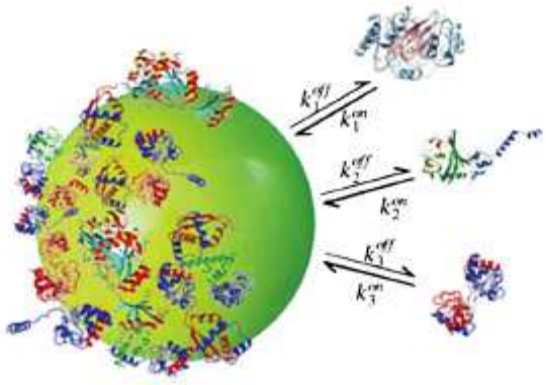

Fig. 22 *The protein corona in a biological environment. Biomolecules in the environment adsorb strongly to the bare liposome surface, forming a tightly bound shell – the protein corona – in immediate contact with the NP. Single type proteins attach to the NP surface at rate k_{on}, leaving the nanoparticle at rate k_{off} (Sahneh et al., 2013).*

Based on the exchange time of its composition, the protein corona is classified into hard and soft: proteins with higher affinity for the surface exchange slowly, forming the hard corona, the inner most layer composed of tightly bound proteins (over longer periods of hours). On top of this "hard" corona there is a "soft" corona formed by loosely-bound proteins, maybe via protein-protein interaction, with lower affinity for the nanoparticle surface and rapidly exchanging (over short time scales of seconds or minutes) (*Walczyk et al., 2010; Milani et al., 2012*) (Fig. 23).

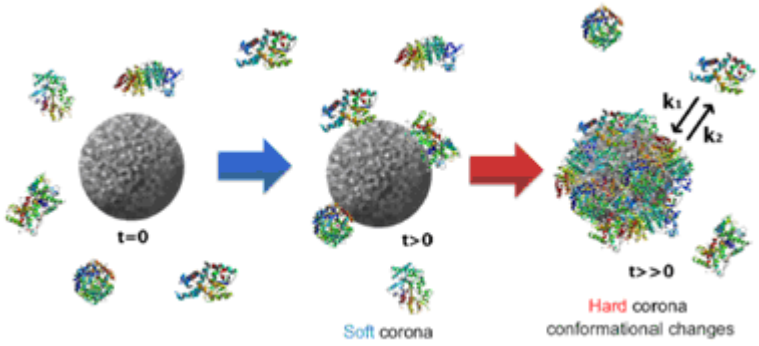

Fig. 23 *Schematic illustration and characteristics of a hard and a soft corona. The protein corona encompassing the nanoparticles. Hard coronas are characterized by slow exchange (i.e., several hours) and lower abundance, with a high affinity of proteins, whereas soft coronas are typified by rapid exchange (i.e., several minutes) and lower affinity of proteins with weakly bound outer layers on nanoparticles (Duran et al., 2015).*

Furthermore, Simberg et al. *(2009)* introduced a model for the protein corona which includes "primary binders" that interact with the NPs surface at first followed by "secondary binders" that binds to the primary binders by way of protein–protein interactions. This multilayered structure plays an important role in the physiological response as the interaction of the primary binders can be changed by the secondary binders or being "masked" by them, thereby hindering their interaction with the biological environment.

Crucially, it is observed that only a few of the biomolecules available in typical biological environments are found in the hard corona. For example, although blood plasma is constituted by thousands of proteins (≈4000) and some of which are more abundant than others (*Anderson et al., 2004*), their abundance in the plasma does not correspond to their abundance in the protein corona (*Zhang et al., 2011; Martel et al.,2011*). The formation and evolution of protein layers on flat surfaces was first analyzed by Vroman (*Vroman, 1962*), describing a time-dependent composition of the bio-coating, in which highly abundant proteins adsorbing only weakly dominate the early state. These adsorbed proteins are later replaced by less abundant proteins, which however bind with higher affinity, resulting in adsorption and displacement step (*Vogler, 2012*). This model has been widely discussed and implies the existence of a highly dynamic protein corona formed over time. More recently, Tenzer et al. *(2013)* described the early evolution and impact of the NP–protein corona complex, using their LC-MS based method to measure time-resolved corona compositions on silica and polystyrene NPs in human serum. By using NPs of various sizes (diameters of about 35, 120, 140 nm), and surface functionalities (amine, carboxylate, unmodified), they were able to provide insights into the consequences of these factors for corona composition and dynamics. They demonstrated in their study that interaction between NP surface and plasma proteins was formed very rapidly: quantitatively detected 166 different plasma proteins within the corona after 0.5 min. Interestingly, they also found that the amount of protein in the corona changes over time, while the types of bound protein remain relatively constant. These findings led to the introduction of a novel model of protein corona formation, which implies new binding kinetics independent from the Vroman effect (*Docter et al., 2015*). Indeed this effect was demonstrated only for a mixture of a few proteins and is unable to predict protein binding kinetics to NPs in complex mixtures (*Vogler, 2012*).

3.2 *Composition of the protein corona*

The protein corona can be considered unique for each given NP and greatly depends on their physicochemical properties. The relation between the pristine NP characteristics and the nature of the corona in complex environments is thus far from being trivial and currently still remains impossible to predict in complex physiological environments (*Tenzer et al., 2013, Gebauer et al., 2012; Walkey et al., 2014*). The different physico-chemical properties, such as material size and surface properties, but also the relative ratio of the physiological fluid to the nanoparticle dispersion and the exposure time play an important role for the composition and evolution of the protein corona (*Walkey et al., 2014; Dobrovolskaia et al., 2014; Caracciolo et al., 2011*). Moreover, when NPs move from one biological (micro)environment to another, e.g. from the blood system via different cellular uptake mechanisms into cells (e.g. monocytes or macrophages), a key issue is whether the original corona remains stable or is subjected to substantial changes (*Monopoli et al., 2012*), which adds an additional level of complexity.

Kelly et al. *(2015)* have recently presented an approach to map protein binding sites on the biomolecular corona which will help to understand the spatial location of the proteins and their binding sites after binding to NPs.

3.2.1 *Factors influencing NP-corona composition, fate and toxicity: physico-chemical properties of NPs*

Size (*Lundqvist et al., 2008*), shape (*Deng et al., 2009*) and surface charge (*Lundqvist et al., 2008; Qiu et al., 2010; Pozzi et al.,2015*), together with the surface modification (*Cedervall et al., 2007*) are key factors in determining the composition of the protein corona. For instance, hydrophobic NPs, e.g. carbon nanotubes, usually attract proteins with several hydrophobic residues (*Ge et al., 2011*). In addition, enhanced protein adsorption is observed with increased NP size (*Cedervall et al., 2007*). This size-dependent effect can be explained by taking into account the curvature of NPs. Larger NPs have reduced curvature, which enables proteins to more freely interact with a larger surface area. For istance, gold NPs of larger size were coated with a thicker layer of absorbed proteins as compared to gold NPs of smaller size (*Dobrovolskaia et al. 2009*). Tenzer and colleagues discovered that the size of the particles is a critical physico-chemical determinant of the human blood plasma corona (*Tenzer et al., 2011*). They could show that even differences in SiO_2 NP size of only 10 nm significantly affected the protein corona composition around three different SiO_2 NPs (with diameters of 20, 30, and 110 nm). At the physiological pH of blood plasma (pH=7.3), preferential binding of negatively charged proteins (pI < 7) onto the SiO_2 NP surfaces was reported. The protein size also played a significant role: while proteins with a high molecular mass were enriched on the NP surfaces as compared to their abundance in the plasma, proteins with low molecular mass were less abundant in the corona than in the surrounding plasma. The proteins that show such size-dependence in their adsorption behavior are involved in all kinds of biological processes, hence, they could not be attributed to a functional class. Interestingly, they were able to identify individual proteins (e.g., prothrombin or gelsolin) showing a higher affinity for larger SiO_2 NPs (110 nm) but also other proteins (e.g., clusterin) with higher affinities to smaller SiO_2 NPs (20 nm). Many other proteins such as immunoglobulin G or actin showed no dependence on the NP size. The surface curvature has an important role in protein absorption and corona composition (*Lundqvist et al. 2008*). Roach et al. *(2006)* studied the effects of curvature on two structurally different proteins — bovine serum albumin (BSA) and fibrinogen. Although albumin retained more native-like structure on smaller particles, fibrinogen was denatured to a greater extent

on smaller particles; the influence of surface curvature on the structure of an adsorbed protein therefore seems to depend on the nature of the protein. A similar 'protein-dependent' behavior was reported by Karajanagi et al. (*2004*) on single-walled carbon nanotubes (SWNTs). Spectroscopic measurements in conjunction with kinetic analysis revealed that soybean peroxidase (SBP) retained more of its native structure and activity when adsorbed onto SWNTs than chymotrypsin, which exhibited a nearly complete loss in activity and structure.

The shape of NPs also governs the type of protein corona that forms. Notable, titanium dioxide nanotubes and nanorods display different protein corona characteristics (*Deng et al., 2012*). The authors found that clusterin and apolipoprotein D were only observed on spherical NPs and were not detected on nanorods or nanotubes.

The surface chemistry of a NP also influences the structure and function of adsorbed proteins. Roach et al. *(2006)* reported a greater change in the secondary structure of both bovine serum albumin and fibrinogen on hydrophobic silica spheres than on hydrophilic ones. Moreover, Rotello and coworkers (*2014*) demonstrated the ability to control protein structure and function by tailoring the surface chemistry of NPs. By controlling the surface chemistry, they achieved three distinct levels of interaction of chymotrypsin with CdSe NPs: no interaction (i.e. no binding to the nanoparticles), enzyme inhibition with denaturation and enzyme inhibition with retention of structure (Hong et al*., 2004*). Collectively, these studies suggest that the structure, activity and stability of adsorbed proteins can be strongly influenced by both the surface chemistry of the NP and its curvature, but in a protein-dependent manner.

Functionalization appears here as a decisive parameter for the quantity and identity of proteins implicated in NP corona. For istance, in order to prevent absorption of proteins and to control the protein corona composition, the surface of NPs can be functionalized with different groups. Appropriate polymers, such as PEG can also be applied to coat the surface of NPs to decrease protein binding and to reduce opsonization (Fig. 24).

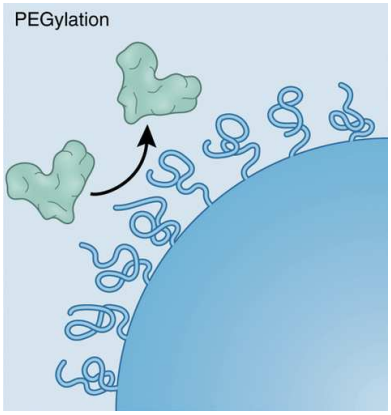

Fig. 24 *PEG applied to coat the surface of NPs to decrease protein binding (Blanco et al., 2015).*

Finally, polystyrene NPs with different functional groups (i.e., PEG, amidine, carboxyl, amine, lysine, methyl, and cysteine) were used in cultured endothelium cells (*Ehrenberg et al., 2009*). It was concluded that the protein binding capacity to these functionalized surface of NPs demonstrate their tendency to interact with the cells. Additionally, NP-cell association is not influenced by the identity of bound proteins. Surface charge of the NPs is a crucial factor in determining the protein corona composition and consequentially its eventual fate in the biological system. In a study conducted on gold NPs provided with negative, positive and neutral ligands, it has been demonstrated that charged ligands (both positive and negative) induce protein distortion,

whereas neutral ligands allow preservation of protein structure (*Lynch and Dawson, 2008*). Gessner and co-workers studied the impact of surface charge density of negatively charged polymeric NPs and found enhancement in plasma protein absorption with an increase in the surface charge density of NPs (*Gessner et al., 2002*). Studies on polystyrene NPs demonstrated that proteins with isoelectric points (pIs) of less than 5.5 (e.g., albumin) adsorbed on positively charged particles whereas proteins with pIs of higher than 5.5 (e.g., IgG) bound to negatively charged particles.

A recent study revealed that a positive surface charge is typically correlated with increased protein adsorption (*Alexis et al., 2008*). In addition, Deng et al. *(2009)* have studied the binding of human plasma proteins to commercially available metal oxide NPs such as titanium dioxide, silicon dioxide, and zinc oxide with the same surface charge. The authors revealed that similar proteins adsorb to titanium and silicon dioxide NPs, whereas significantly different proteins composed the hard corona of zinc oxide NPs. In particular, clusterin, apolipoprotein D, and alpha-2-acid glycoprotein were detected in the corona of TiO_2 and SiO_2 NPs while those were not observed in the corona of ZnO. Interestingly, some other proteins like transferrin, Ig heavy chain alpha, and haptoglobin (alpha) only were found in the corona of ZnO NPs alone.

Another important parameter for NP–corona interactions is the hydrophilicity/hydrophobicity that is correlated with the surface charge. In general, more proteins can adsorb onto the surface of hydrophobic NPs than their hydrophilic counterparts (*Cedervall et al., 2007a*). This results in more available protein-binding sites on the surfaces of hydrophobic copolymers (*Lindman et al., 2007; Saha et al., 2014*).

3.2.2 *Factors influencing NP-corona composition, fate and toxicity: biological environment factors*

The characteristics of the biological environment also play a determinant role in the formation of a protein corona: the type of plasma (e.g., human or murine) or biological fluid, incubation time, temperature, pH and the physiological state of the plasma (alterations due to disease/medical conditions) (*Tenzer et al., 2013*) may also affect the protein adsorption on the NP surface. Typically, corona protein abundance differs significantly from the protein composition in the biological fluid investigated (*Gebauer et al., 2012; Monopoli et al., 2012; Walkey et al., 2012*).
These factors may synergistically influence the recognition and uptake by cells (*Babic et al. 2009; Lunov et al. 2011; Mok et al. 2008; Shang et al. 2014; Yang et al. 2011*). The impact of media composition on the formation of protein corona was studied by Maiorano and co-workers (*Maiorano et al. 2010*). The study was performed by incubating various sized citrate-capped gold NPs, in commonly used cellular media including Roswell Park Memorial Institute medium (RPMI) and Dulbecco modified Eagle's medium (DMEM) that were supplemented with the fetal bovine serum (FBS). A number of techniques (dynamic light scattering, UV-visible, and plasmon resonance light scattering) were used to evaluate the corona formation on gold NPs mediated by DMEM and RPMI. It was concluded that formation of protein corona by utilizing DMEM is significantly time dependent, while using RPMI leads to distinct dynamics and reduction of protein corona.
Viability assays in both cultured media DMEM and RPMI were performed on two cell lines HeLa (human epithelial cervical cancer cell line) and U937 (human leukemic monocyte lymphoma cell line) for 15 nm gold NPs. This approach revealed substantial differences in cellular uptake, dynamics and NP–protein complexes biodistribution. More specifically, internalization of protein-NP complexes in cells that were formed in RPMI media was notably higher than those formed in DMEM, resulting in higher cytotoxic effects. Moreover, the protein corona formed in DMEM was

more abundant and stable compared to protein corona formed in RPMI. Thus these authors conclude that in dynamic extracellular environments, the original biological identity may become altered, and with it cellular uptake. Biological fluid also play a determinant role in the formation of a protein corona: since the majority of NPs are intended for intravenous administration (*Webster, 2013*), most of the studies in the current literature are devoted to the characterization of the protein corona adsorbed on NPs after incubation in plasma (*Landgraf et al., 2015*).

Despite this great variability, a similar subset of about 125 proteins has been shown to be adsorbed on various nanomaterials in different amounts when incubated in plasma (*Walkey et al., 2014*). These proteins are involved in the same cellular processes, namely, complement activation, pathogen recognition and blood coagulation. Among these, IgG, serum albumin, fibrinogen, clusterin and apolipoproteins are generally present in the protein corona of most analyzed NPs after exposure to plasma (*Aggarwal et al., 2009*). Studies of the corona of NPs recovered from many other biologic fluids, such as urine, synovial fluid, cerebrospinal fluid and pleural effusion, are also emerging (*Martel et al., 2011*) However, when other administrative routes are used, NPs are subjected to interactions with biomolecules of other biological fluids before reaching the plasma. For example, NPs could derive their initial biomolecular corona from different sources, for example, lung entry leads to contact with lung fluids and early studies have focused on protein surfactants, such as surfactant protein A (*Schleh et al., 2011*) and related biomolecules (*Choi et al., 2010*); that corona has a very different composition than blood plasma (*Kumar et al., 2015*) (Fig. 25). In a recent study, the selective adsorption of surfactant was demonstrated on SWCNs recovered from broncheo-alveolar lavage of mice and the presence of this surfactant lipid–protein corona was shown to influence the degree of macrophage uptake (*Kapralov et al., 2012*). Instead, NPs administrated via oral ingestion are subjected to contact with saliva and then with fluids of the gastrointestinal tract: an environment characterized by a low pH and the presence of enzymes that may hinder the bioavailability of NPs. Little information is available about the interactions of NPs with the biological milieu of the GI tract (*Lee et al., 2015*).

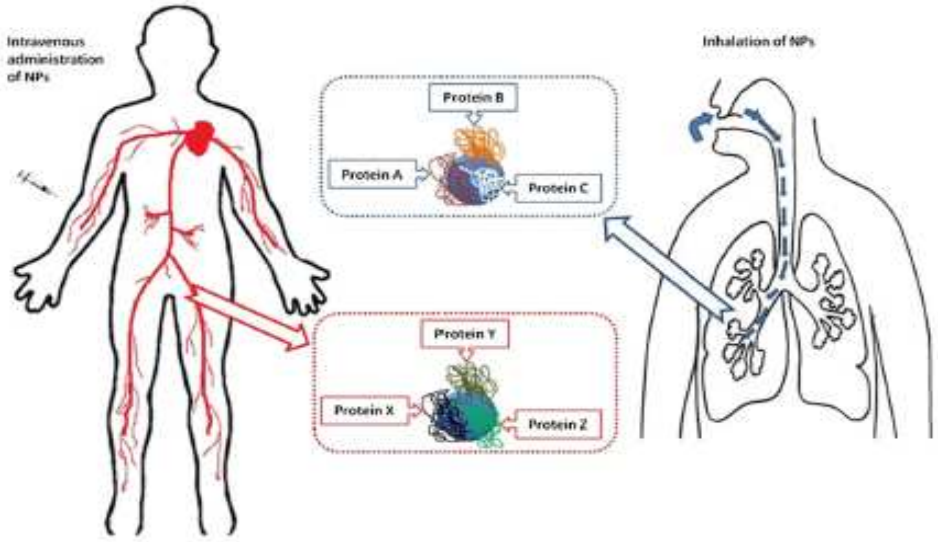

Fig. 25 *Schematic illustration of difference in the hard corona composition on NPs depending on the route of administration; intravenous and inhalation.The proteins that adsorbs on NP may vary depending on its exposure to the different types of biological fluids in the human body (Foroozandeh and Aziz, 2015).*

The effect of plasma concentration on the composition of protein corona *in vitro* was investigated by Monopoli and co-workers (*Monopoli et al., 2011*). They employed polystyrene NPs

($PSOSO_3$) and hydrophilic SiO_2 NPs to study the protein adsorption and protein corona. When plasma proteins were applied at concentrations between 3% and 80% of plasma, they observed that the proteins bound to NPs varied with plasma concentration, while relative amounts of some abundant proteins adsorbed on surfaces of silica or $PSOSO_3$ NPs increased with increasing plasma concentrations (*Monopoli et al., 2011*) (Fig. 26). In addition, it was observed that the structure of NP-protein complexes *in situ* is roughly the same with the structure of those *in vitro* after separation from excess plasma. More specifically, the concept that the hard corona may evolve remarkably as a function of protein concentrations will have significant impact when studies conducted on *in vitro* cell culture conditions were used to extrapolate over to *in vivo* conditions.

Temperature is another important parameter that influences protein corona composition. Body temperature varies in the range of 35 to 39°C. Mahmoudi and co-workers have studied the effect of temperature variation on the formation and composition of protein corona (*Mahmoudi et al., 2013*). Fluorescently labeled, negatively charged polymer-coated FePt NPs were applied to incubate with human serum albumin and fluorescence correlation spectroscopy was used to quantify protein absorption at different concentrations and temperatures.

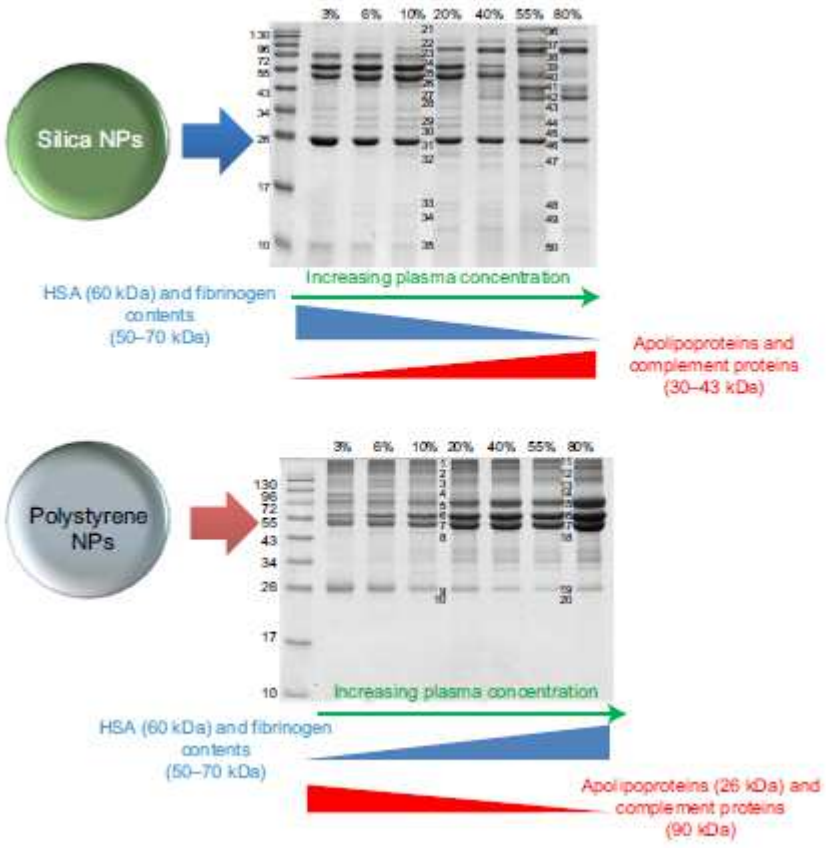

Fig.26 *NP-protein complexes based on sulfonated polystyrene and silica NPs (Monopoli et al. 2011).*

3.3 *Experimental approaches used to characterize the protein corona*

Many studies have revealed the identity (*Cedervall et al., 2015; Sund et al., 2011; Gossmann et al., 2007; Caracciolo et al., 2011*) and, more recently, also the quantity (*Tenzer et al., 2013; Sakulkhu et al., 2014; Capriotti et al., 2013*) of the proteins in the protein corona using proteomics-

based approaches coupled with MS. In a typical experimental plan, NPs are incubated in a biological fluid that ideally should replicate the features of the *in vivo* biological milieu. After incubation, the NPs are recovered by centrifugation, ultrafiltration (*Capriotti et al., 2010*) or, more recently, by a combination of size exclusion chromatography and ultrafiltration (*Hadjidemetriou et al., 2015*), and extensively washed to avoid contamination of nonbound proteins. Finally, the adsorbed proteins are eluted from the NP surface and analyzed by two different methods: gel-based or gel-free proteomics (*Salvatore et al., 2015*). While there are numerous reports which describe the protein corona at the surface of NPs *in vitro*, reports describing the *in vivo* protein corona are limited. Despite many good attempts to simulate the biological systems, *in vitro* experiments lack several dynamic parameters that exist *in vivo* and are hard to reproduce. The lack of similarities between these two models could explain why NPs that seem promising *in vitro* are less promising in preclinical trials. On the other hand, *in vivo* experiments are complicated by the fact that NPs cannot be readily recovered once they are injected in animals for protein adsorption analysis. Moreover, the biological identities adsorbed on the NPs in mice and humans could be different from one another (*Caracciolo et al., 2014*) (Fig. 27).

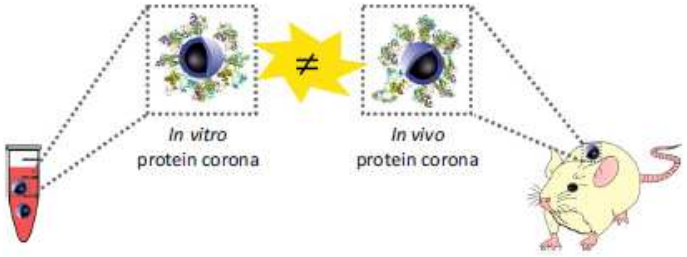

In vitro protein corona	*In vivo* protein corona
• Comprises the same amount of protein as *in vivo* corona	• Comprises a wider variety of biomolecular species
• Does not have a role in fasting, diet body tempeature, etc.	• Has a role as a fasting, diet, body temperature, etc.
• Does not have a role in personlized corona	• Has a role as a personalized corona
• Cannot mimic the dynamic and fluidic variations protein as *in vivo* corona	• Effects of dynamic and fluidic variations are considered

Trends in Biotechnology

Fig. 27 *Predicting the In vivo Behavior and Fate of NPs. Following exposure to biological fluids, NPs adsorb biomolecules toform a protein corona,which confers a new biological identity to the NPs. To investigate the structure, composition, and biological impact of the protein corona, NPs are typically exposed to static plasma or serum in vitro (on the left). NP–protein interactions under realistic in vivo conditions have been poorly explored so far.Recent findings have shown that the spontaneous coating of NPs in vivo differs from that formed following in vitro incubation. Along with other factors,this is principally due to dynamic flow, which introduces shear stress and provides a continual source of new biomolecules (Caracciolo et al., 2014).*

Recently, Hadjidemetriou et al. *(2015)* investigated *in vivo* protein corona formation on commercially available liposomes that are used in the clinical setting (i.e., the anticancer agent *Doxil*). In particular, they compared *in vivo* and *in vitro* protein coronas in terms of morphology, function and composition. The results revealed that the two protein coronas differ in morphology: electron microscopy imaging showed that liposomes incubated in plasma *in vitro* create fibrillar structures, whereas liposomes retrieved after *in vivo* systemic administration did not. Moreover, the composition of the *in vivo* protein corona was more complex, in terms of variety of molecular species adsorbed, than the *in vitro* protein corona. Finally, both *in vitro* and *in vivo* protein coronas affect the targeting capabilities of NPs, thereby decreasing cellular internalization. However, the impact of the *in vivo* protein corona was weaker. An another main obstacle limiting the progress in

this area is the lack of effective techniques allowing for separation of NPs from the *in vivo* environment after administration. However, Sakulkhu et al. *(2014)* were able to overcome this barrier by using polyvinyl-alcohol-coated SPIONs delivered to rats and deployed these NPs to investigate the in vivo protein corona formation. It is noteworthy that the unique magnetic properties of the particles made the particles separation possible using a strong external magnetic field. This study was able to demonstrate that there are substantial differences between the *in vitro* and *in vivo* protein corona profiles. For example, we found that positive and neutral NPs have 50% proteins in common between *in vivo* and *in vitro* conditions, and surprisingly, there wereonly 8% similarities for the negative particles.

3.4 *Effect of the corona presence and composition on cellular uptake*

The effect of protein corona formation on the cellular uptake of NPs was studied in numerous studies (*Lesniak et al., 2012; Treuel et al., 2013)* (Fig. 28)**.**

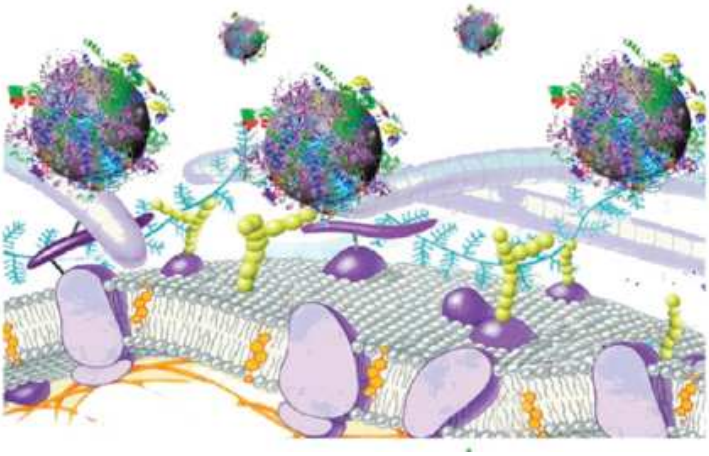

Fig. 28 *Schematic representation of the possible exchange/interaction scenarios at the bionanointerface at the cellular level (Mahmoudi et al., 2011).*

For example, it is reported that graphene oxide nanosheets can induce the irreversible cell damage after uptake of these NPs into the A549 cell. In contrast, when the NPs are incubated into fetal bovine serum (FBS) at near body temperature, the formation of protein corona reduces negative effects on the integrity of cell membranes after NP uptake (*Hu et al. 2011*). This study reveals that the protein corona can protect the cell from destruction by NPs. However, such protection also shows selectivity. When CNTs are coated with fibrinogen (FBG), the release of lactate dehydrogenase is the same as the control, which indicates that the FBG-CNTs have no effect on the destruction of the platelet membranes. In most cases, a protein coating has been shown to decrease adhesion of NPs to the cell membrane, thereby reducing cellular internalization (*Salvati A. et al., 2013*). The presence of PEG was shown to suppress protein absorption resulting in a decreased uptake by macrophages (*Kah et al., 2009*) and longer circulation times in the blood as well as altered bio-distribution upon injection in mice (*Owens et al., 2006*). Attempts were also made to coat NPs by specific proteins. For example, transferrin, well known to be internalized via its cognate receptor, was used to create a protein corona and study its effect on cellular uptake (*Jiang et al., 2012*). To elucidate how the presence of a protein adsorption layer around NPs affects their cellular uptake, Jiang et al. *(2012)* compared the uptake of small (diameter about 10 nm),

carboxyl-functionalized polymer-coated FePt NPs (fluorescently labeled by DY-636 dye molecules in the polymer shell), by live HeLa cells in the presence or absence of human transferrin (TF) and human serum albumin (HSA) in phosphate-buffered saline (PBS) medium. They studied the uptake of the NPs by quantitative confocal fluorescence microscopy. For comparison, they also studied the cellular uptake of fluorescently labeled (ca. 1:1 ratio) transferrin and HSA molecules. Whilst transferrin was endocytosed in significant amounts, HSA was barely internalized by HeLa cells under otherwise identical conditions. In contrast, the uncoated NPs were taken up in large amounts, whereas the presence of an HSA or transferrin corona both reduced the amount of endocytosed NPs with the exact causes for this behavior remaining uncertain. Also focusing on the transferrin corona, Salvati, Dawson and co-workers were able to demonstrate how transferrin-functionalized NPs can lose their targeting capabilities when a biomolecule corona adsorbs on their surface (*Salvati et al., 2013*). They studied the uptake of transferrin-decorated SiNPs with PEG8 spacers by A549 lung epithelial cells. After adding bovine serum to their experiments, proteins from the surrounding medium reportedly formed a corona around their pre-functionalized NPs shielding transferrin from binding to both its cognate receptors on cells and also to soluble transferrin receptors. While NPs were still taken up by the cells, the targeting specificity of transferrin was lost. These findings underline very well, the complexity of the situation where even protein mediated cell-targeting suffers from corona formation under physiological conditions. In a different approach, Treuel et al. *(2014)* studied the uptake of DHLA coated QDs by HeLa cells, comparing the uptake of the as-synthesized NPs to the cellular uptake of the same NPs carrying an HSA corona or a corona consisting of aminated (HSAam) or succinylated (HSAsuc) HSA, respectively. The cellular uptake was studied by confocal fluorescence microscopy and fluorescence intensities were quantified for the membrane associated and intracellular fractions of QDs. Their results revealed that the unfunctionalized NPs were taken up in the largest amounts while the presence of all corona reduced the cellular uptake. A possible contribution to this observation is that, in presence of free proteins, the cellular endocytosis machinery was also occupied with internalization of the freely dissolved protein. However, intriguing differences were found between the effects of the different coronas, essentially all consisting of HSA with just minor chemical modifications. Internalization of HSAam-coated NPs by the cells was completely suppressed within the sensitivity limits of their experiment. In addition the time-dependent NP uptake by HeLa cells was investigated, using spinning disk confocal microscopy. In these experiments, all QDs were found to accumulate at the cell membrane within minutes after exposure.

These findings will clearly help to design NPs for directed cellular uptake. The notion that rather the kinetics of membrane binding can be affected by the presence and nature of the protein corona, than the kinetics of the actual endocytosis process, allows novel strategies in this context. The role of this finding for the passive uptake of NPs by cells, remains unresolved, however, NP-membrane interactions will likely also play a central role.

3.4.1 *Cellular selectivity*

Distinction in the identity of the protein corona therefore takes very important role for cellular uptake, especially the ones mediated by the receptors. For example, the complement proteins often found in plasma are critical in activating the complement system, which serves as part of the innate immune system to assist phagocytes to clear up pathogens. When NPs adsorb such kind of proteins, the NP is easily internalized by phagocytes (*Gaucher et al. 2009; Mosqueira et al. 2001; Walkey et al. 2011*). Similarly, adsorption of immunoglobulins can also promote the uptake by macrophages because immunoglobulin also serves in the immune system with similar functions (*Gaucher et al.*

2009). When apolipoproteins are adsorbed on the NPs, they can easily cross the blood–brain barrier and be taken up by brain capillary endothelial cells (*Kreuter et al. 2007; Wagner et al. 2012*). Thus, there are multiple receptors for apolipoprotein complexes at cell surfaces that NPs with surface-adsorbed apolipoproteins can potentially exploit to enter cells (*Kim, et al., 2007*). Apolipoprotein E has been found to associate to some NPs (*Cedervall et al, 2007*), this has potentially significant consequences for neurotoxicity and the development of neurotherapies, as apolipoprotein E is known to be involved in trafficking to the brain (*Kim et al.,2007*). Furthermore, the uptake also shows cellular selectivity due to different identities of protein corona. Pre-coating with fetuin can promote the cellular uptake of polystyrene NPs by liver macrophages, such as Kupffer cell (*Nagayama et al. 2007a,b*). The uptake level of TiO_2 NPs by A549 cell (in lung) can increase after adsorbing vitronectins onto the surface, which is regulated by a clathrin-mediated pathway (*Tedja et al. 2012*). SWNTs and 10 nm amorphous SiO_2 NPs coated with albumin have been shown to induce anti-inflammatory responses in macrophages, measured as inhibited induction of cyclooxygenase-2 (Cox-2) by lipopolysaccharide under serum-free conditions (*Dutta et al., 2007*).

3.5 *Nanotoxicology of protein corona*

The formation of a protein corona impacts not only on the delivery properties of NPs (e.g. biodistribution and clearance), it can also influence their toxicity and pathophysiology (*Tenzer et al., 2013*). In fact, the nano-plasma interface can trigger toxicity due to modification of endogenous proteins (*Pelaz et al., 2013*). Such modifications can disrupt the normal function of proteins and potentially cause complications, since misfolded proteins have been associated with various diseases (*Chiti et al., 2006*). For instance, NP-induced conformational changes in fibrinogen were shown to activate inflammatory signaling pathways (*Chiti et al., 2006*). Shannahan et al. *(2014)* showed that AgNPs (with or without protein corona) were able to induce a concentration-dependent cytoxicity and that corona-coated AgNPs were found to activate cells by inducing IL-6 mRNA expression. For example, TiO_2 NPs were shown to induce conformational changes of tubulin, thus inhibiting its polymerization properties (*Gheshlaghi et al., 2008*), while gold NPs instead can induce changes in the conformation of serum albumin (*Wangoo et al., 2008a*). It was hypothesized that the cytotoxic mechanism underlying this phenomenon is the potential increased immunogenicity that the particles can exert by exposing protein epitopes on their surface in an aberrant conformation (*Nel et al., 2009*) (Fig. 29).

In addition, intracellular proteins, such as cytochrome c (*Shang et al., 2009*) and ribonuclease A (*Teichroeb et al., 2008*) have also been found to undergo structural changes when exposed to NPs.

Notably, a correlation between NP size and protein unfolding has been observed. Larger NPs with lower surface curvature cause more conformational changes in protein structure (*Teichroeb et al., 2008*) Since the structure-function relationship is strong for proteins, NP coronas may also alter the behavior of these macromolecules. Iron oxide NPs were found to change the conformation of transferrin, causing the protein to prematurely release iron (*Teichroeb et al., 2006*). Moreover, the conformational alteration is irreversible, indicating permanent damage to the function of this protein in iron transport.

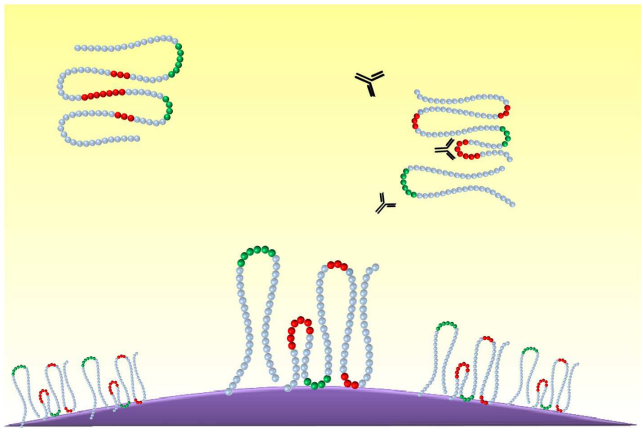

Fig. 29 *Schematic representation of NP surface induced unfolding of the interacting protein molecule and consequences. (A) Protein molecules adsorb on to the NP surface, to form a complex termed as the (B) NP-protein corona. NP surface may induce conformational change to the native structure of the adsorbed protein molecule, causing it to unfold. Such protein conformational changesmay either (C) alter the function of the native protein moleculeor even lead to (D) exposure of "cryptic" epitopes which may result in immunological recognition of the complex (Saptarshis et al., 2013).*

To study the structure of proteins in solution and adsorbed onto NP surfaces, a large range of experimental techniques has been employed (*Treuel et al., 2013*). This includes spectroscopic techniques such as fluorescence spectroscopy (*Mátyus et al., 2006*), Fourier transform infrared spectroscopy (*Wang et al., 2012*), Raman spectroscopy and surface-enhanced Raman spectroscopy (SERS) (*Shao et al., 2009*) as well as circular dichroism spectroscopy (*Shang et al., 2007*). Also, other established techniques were used to study protein adsorption such as isothermal titration calorimetry (ITC) (*Nienhau et al., 2005*), and surface plasmon resonance (SPR) (*Cheng et al., 2011*).

For example, it was demonstrated that the presence of poly(acrylic) acid on the surface of gold NPs induced unfolding of adsorbed fibrinogen that, in turn, interacted with the leukocyte receptor MAC-1, thereby triggering an inflammatory response (*Deng et al., 2011*). The surface interaction of proteins at the nanoscale also affects protein fibrillation, which is at the base of neurodegenerative diseases such as Parkinson's and Alzheimer's (*Saptarshi et al., 2013*). Recently, Mirsadeghi et al. *(2015)* found that the protein corona of gold NPs impacts the fibrillation process in a way that strongly depends on the protein source and concentration. Studies in animals have shown that C60 hydrated fullerene may have anti-amyloidogenic capacity resulting from inhibition of the fibrillation of amyloid-beta 25–35 peptide (*Podolski et al., 2007*). A single intracerebroventricular injection of a C60 hydrated fullerene at a dose of 7.2 nmol/ventricle significantly improves the performance of a cognitive task in control rats. TEM studies have confirmed that C60 hydrated fullerene inhibits the fibrillation of amyloid-beta 25–35 peptide.

On the contrary, the formation of a protein corona can also mitigate the cytotoxicity of NPs. Especially in the case of NP–cell membrane interactions, the presence of a protein coat can decrease cell damage (*Ge et al., 2011*). Indeed, NPs that are not precoated with a protein layer may instead interact with cell membrane proteins, causing damage to these structures. For instance, it has been shown that the toxicity of CNTs (*Ge et al., 2011*)and gold nanorods (*Wang L. et al., 2013*) decreases upon coating with plasma proteins. While albumin protein coronas decreased the platelets aggregation, histone H1 and gamma globulins protein coronas caused platelet aggregation and fragmentation, respectively (*De Paoli et al., 2014*).

Furthermore, the protein coating that occurs in biological fluids can increase the stability of particles, which is important from the standpoint of cellular toxicity if the secondary degradation products of the carriers pose a potential threat. This phenomenon was shown in ZnO (*Yin et al., 2015*) and AgNPs *(Kittler et al., 2010)* in which the formation of a protein corona inhibited NPs dissolution and consequent release of Zn and Ag ions that eventually became toxic for cells. Lastly, the formation of a protein corona can increase the safety of NPs by inhibiting the generation of ROS, by which several compounds exert their cytotoxic activity (*Sies et al., 1992*). In this context, ZnO NPs are again an example of this phenomenon because their pristine surface is a natural trigger of ROS, but the formation of a protein corona on their surface inhibits this phenomenon (*Yin et al., 2015*).

4. ENMs USED IN THE PRESENT STUDY: QUANTUM DOTS

In the past years, a new class of fluorescent particles emerged as a good candidate for single molecule and single particle tracking (SPT) in living cells and organisms, the semiconductor QDs (*Pierobon et al., 2012*). QDs are inorganic fluorescent nanoscale crystals with considerable enhanced optical properties in terms of brightness, photostability, blinking and bleaching compared to conventional organic and protein fluorophores (Fig. 30). QD core sizes are in the range 2 - 10 nm and the individual nanocrystals contain from a few hundred to several thousands of atoms each. The most commonly used QDs fall within this size range, but larger NPs have also been fabricated and used for other specific applications. QDs are nanometer-scale semiconductor crystals composed of groups II to VI or III to V elements and are defined as particles with physical dimensions smaller than the exciton Bohr radius (*Chan et al., 2002*). The core of the QD nanocrystals is typically composed of binary mixtures of semiconductor materials (ZnS, CdS, CdSe, InP, CdTe, PbS, PbTe).

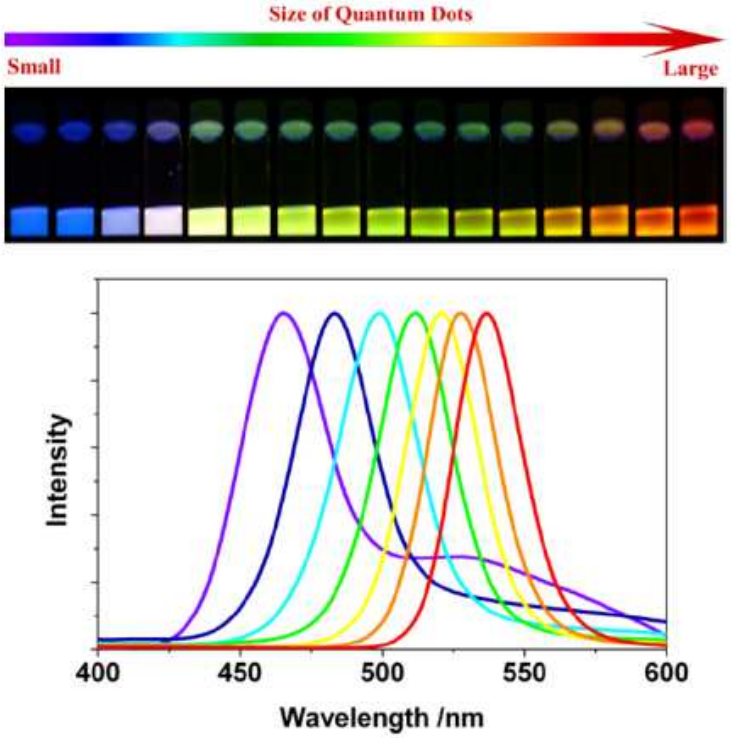

Figure 30 *Top: Sixteen emission colors from small (blue) to large (red) CdSe QDs excited by a near-ultraviolet lamp; size of QDs can be from ~1 nm to ~10 nm (depends on several parameters, see text for details). Bottom: Photoluminescence spectra of some of the CdSe QDs (Bera et al., 2009).*

The optical properties of QDs stem from their composition: a semiconductor material core, such as cadmium selenide, lead selenide, or indium arsenide (CdSe, PbSe, or InAs), passivated by a coating, or shell, also of semiconductor material (*Bruchez et al. 1998*; *Dabbousi et al., 1997*). The core semiconductor material has a narrow bandgap, defined as the minimum amount of energy required to excite an electron from its ground state to the next highest energy level. This excitation of the QDs core occurs through absorption of energy, which causes an electronic transition from the ground state to the first excited state. Absorption is followed by the release of energy in the form of a photon when the electron relaxes back to the ground state. The core-shell architecture not only confines excitation and emission to the core, but also enhances the photoluminescence quantum yield of the core emission and protects the core from photobleaching (*Bruchez et al 1998*; *Hines et al., 1996*; *Dabbousi et al., 1997*; *Kuno et al., 1997*; *Talapin et al., 2001*). The increase in

photoluminescence quantum yield results from a surface passivation effect of the core, where the number of nonradiative recombination sites, such as holes and gap states, are reduced, enhancing the charge transfer (*Hines et al., 1996*; *Dabbousi et al., 1997*; *Weller, 1993*; *Peng et al., 1997*). QDs have been estimated to be up to 20 times brighter and 100 times more stable than traditional fluorescent reporters (*Chan et al 1998*). Most commercial available QDs have emission spectra situated in the visual part of the electromagnetic spectrum and include QDs such as (CdS, CdSe, CdTe). QDs emitting in the Ultra Violet range have mainly been made of ZnS and ZnSe while emission in the near infrared range has been accomplished with materials such as CdS/HgS/CdS, InP, InAs (*Deng et al., 2012*).

4.1 *Applications of QDs*

QDs have featured in a range of optoelectronic devices, including LCD TVs, light emitting devices (LEDs), solar cells, photodiodes, thermoelectrics, photoconductors and field-effect transistors, while QD solutions have been used in a number of *in vivo* and *in vitro* imaging, sensing and labelling techniques (Fig. 31, 32). QDs display many improved optical qualities desirable for biological applications, and are advantageous for both singleand multi-color experiments as compared to organic dyes (*Bruchez et al 1998*; *Chan et al 1998*). The enhanced optical properties of QDs, in particular the significant brightness and photostability, make these materials more practical in ultrasensitive detection, longterm imaging, and rapid-detection applications, such as flow cytometry (*Chan et al 1998*; *Gao et al., 2004*; *Chen et al., 2004*). QDs properties are controllable and their signal strength is robust, and as such, are desirable for a wide range of *in vivo* studies and labeling applications, immunoassays, optical encoding for multiplexed analyses, cell tracking, and fluorescence resonance energy transfer (FRET) (*Bruchez et al 1998*; *Chan et al 1998*; *Mattheakis et al., 2004*; *Chen et al., 2004*; *Dubertret et al., 2002*; *Larson et al., 2003*; *Medintz et al., 2004*; *Cui et al., 2007*; *Akerman et al., 2002*; *Gao et al., 2002*; *Parak et al., 2002*; *Voura et al., 2004*). In animal bioimaging, Goldman et al. used biotinylated CTxB in conjunction with QD-avidin conjugates (*Goldman et al., 2002*) for labeling of the live HeLa cells. Punctuate labeling of the cell surface by QD bioconjugate is typical for molecules such as GM1 that is present in membrane rafts (*Jaiswal et al., 2004*). In another study, they labeled live HeLa cells which were biotinylated using sulfo-NHS-SS biotinylating reagent and then incubated with the avidin-conjugated yellow-emitting QDs (*Jaiswal et al., 2003*). The interaction of QDs with cells was successfully controlled by the amino group content of the CHPNH2 nanogel (*Hasegawa et al., 2005*). For in vivo bioimaging, Maysinger et al. (*2007*) visualized CdSe and CdTe quantum dots detectable at one hour-, one day-, three days-, and seven days post intracortical injection using in vivo imaging techniques. Mice were injected subcutaneously and scanned for fluorescence, in particular in the brain, where peak fluorescence was observable at three days post injection and persisted for seven days. Sub-cellular resolution was achieved and allowed the identification of the location of the conjugates.

In prokaryote bioimaging, sensitive and selective staining of bacterial mutants using QD labels was demonstrated by Smith's group. This principle of detection is based on selective targeting affinity of Zn(II)- dipicolylamine coordination complex to phospholipids on the bacterial cell surface of specific strain (*Leevy et al., 2008*; *Tallury et al., 2010*). In another study, authors demonstrated the use of magnetic beads coated with anti-*E.coli* O157 antibodies and streptavidin-coated QDs for measuring the bacterial cell concentration (*Su et al., 2004*). Yang and Li, using QDs with different emission wavelengths (525 nm and 705 nm), reported the simultaneous detection of *E. coli* O157:H7 and *Salmonella typhimurium* (*Yang et al., 2006*). Indeed, the development of

multifunctional NPs combining diagnostic and therapeutic purpose has recently attracted intensive interests (*Gautrot et al., 2009*; *Wu, 2010*). The clinical applications of QDs include biomarker detection in various cancers and imaging and sensing of infectious diseases. As biomarker detection in various cancers, the detection of cancer biomarkers is important for diagnosis, disease stage forecasting, and clinical management. Multicolor and multiplexing potentialities of QDs are used for the detection of four protein biomarkers CD15, CD30, CD45, and Pax5 of Hodgkin's lymphoma from lymphoma tissues. Simultaneous visualization using multiplexed QD staining was advantageous for the selective identification of rare Hodgkin (Reed-Sternberg) cells, a primary diagnostic target for Hodgkin's disease, which was not achievable using traditional immunohistochemistry assays (*Liu, 2010*; *Ray, 2011*).

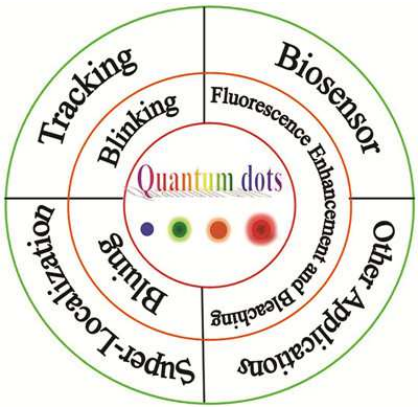

Fig. 31 *Applications of QDs (Xingba S. et al., 2014).*

Although QDs exhibit these numerous advantageous optical properties, inorganic semiconductor materials are toxic to living systems, effectively limiting their use in biological systems. While nanoparticle toxicity continues to be an area of much research and debate, numerous experiments have documented modified QDs as having limited cytotoxicity, and surface coatings have been developed in an effort to minimize toxicity (*Mattheakis et al., 2004*; *Chen et al., 2004*; *Ryman-Rasmussen et al., 2006*; *Duan et al., 2007*).

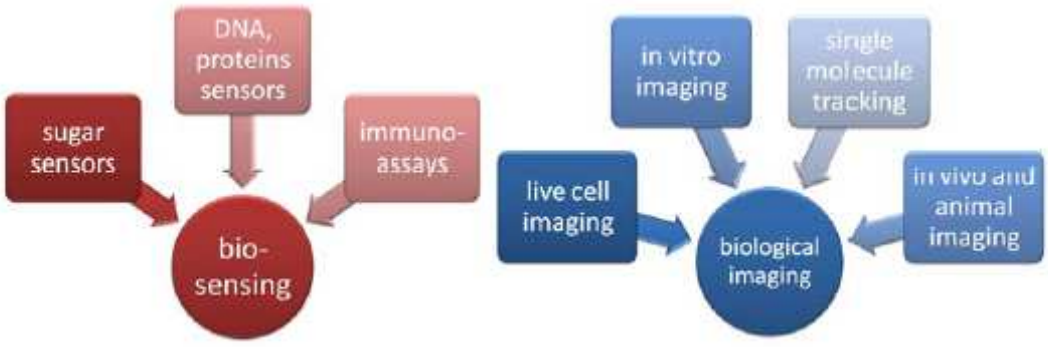

Fig. 32 *Examples of QDs' bioanalytical and biomedical applications (Drbohlavova et al., 2009).*

4.2 *Toxicity of QDs*

The quality and specific degree of QD toxicity has been extensively explored. The nature of the surface coatings obviously plays an important role in cytotoxicity. Because QD cores are made with elements that are inherently toxic to cells and living systems, concerns exist over their potential toxicity for in vivo applications.

Cadmium ions have been shown to bind to thiol groups on critical molecules in the mitochondria and cause enough stress and damage to cause significant cell death (*Derfus et al., 2004*; *Rikans et al., 2000*). Cadmium is the most widely used material for QD cores, so its release into the cell would be a logical mechanism of toxicity. In amoeba it has been determined that QD labeling had no detectable effect on cell growth and had no deleterious effects on cellular signaling and motility during development of the Dictyostelium discoideum cells (*Jaiswal et al., 2003*). In plant, the ratio of reduced glutathione levels (GSH) relative to the oxidized glutathione (GSSG) suggests that QDs caused oxidative stress (*Navarro et al., 2012; Marmiroli et al., 2015*).

Yan et al. (*2011*) investigated the potential vascular endothelial toxicity of mercaptosuccinic acid (2-sulfanylbutanedioic acid)-capped QDs *in vitro*. Their results suggested that QDs could not only impair mitochondria but also exert endothelial toxicity through activation of mitochondrial death pathway and induction of endothelial apoptosis. Chen et al. (*2012*) have studied the cytotoxicity of CdTe/CdS (core-shell) and CdTe/CdS/ZnS (core-shell-shell); their results suggest that the cytotoxicity of CdTe QDs not only comes from the release of cadmium ions but also from the intracellular distribution of QDs in cells and the associated nanoscale effects.

Derfus et al. (*2004*) used hepatic cells to monitor toxic effects of QDs, as the liver is the primary site for acute damage from cadmium and a major accumulation site for NPs. Results indicated that oxidation of the NP surface, either induced by exposure to air before solubilization or catalyzed by UV light, caused oxidation of selenium and/or sulfur, exposing free cadmium (*Murray et al., 1993*; *Dabbousi et al., 1997*; *Katari et al., 1994*; *Alivisatos, 1996*). Exposure to air before solubilization or moderate to prolonged exposure to UV light after incubation increased the amount of cadmium in the cells enough to cause observable cell death. Further efforts demonstrated that cells labeled with quantum dots synthesized under stable, inert conditions showed no toxic effects. In addition to air and UV exposure, QD surface oxidation can occur in oxidative solutions, such as hydrogen peroxide, which is relevant because such environments are possible *in vivo*. In a separate report using CdSe/ZnS core/shell NPs solubilized with mercaptoacetic acid, Kirchner et al. (*2005*) showed that Cd^{2+} was released into cells at toxic levels over time (48 hours), under standard synthesis and imaging conditions.

Cell death caused by cadmium ion release is not the only type of toxicity exhibited by NPs. QDs can also damage DNA and disrupt normal cell activity caused by factors such as the surface coatings themselves. Zhang et al. (*2006*) made phenotype and whole genome measurements of human fibroblast cells exposed to PEG-silica-coated quantum dots, as they were proven to be the least toxic and most stable. The fibroblast cells were monitored for other activity interruptions based on exposure to nanomolar QD concentrations. DNA damage was observed based on interactions with QDs coated with carboxylic acids (*Hoshino et al., 2004*).

By examining the effects of the free core materials in solution, cadmium was determined as the primary cause of cytotoxicity, but its levels could be reduced or eliminated by adding additional surface coatings (*Derfus et al., 2004*), (*Kirchner et al., 2005*). Prevention of core material oxidation is essential to reducing toxicity and increasing biocompatibility of QDs. Coatings used to increase the quantum yield of the core, or for solubility and conjugation, have been shown to reduce

cytotoxicity of QDs. The fundamental notion is that additional layers act as a physical barrier to the core, preventing access, with different surface coatings having varying levels of passivation. A common surface shell coating for CdSe core-QDs is ZnS, and as mentioned, the additional semiconductor layer increases the material's photoluminescence (*Hines et al., 1996*; *Dabbousi et al., 1997*). Additionally, the semiconductor shell aids in reducing the cytotoxicity of the core material, as the concentration where cell death was first observed was approximately nine times higher for CdSe/ZnS (core/shell) QDs than with CdSe core QDs alone. The ZnS shell protects the core from oxidation and other environmental factors that contribute to cadmium release (*Kirchner et al., 2005*).

5. ENMs USED IN THE PRESENT STUDY: NANOSILICA

SiO_2 NPs, also know as silica nanoparticles or nanosilica, are the basic for a great deal of biomedical research due to their stability, low toxicity and ability to be functionalized with a range of molecules and polymers. Moreover, the precise control of silica particle size, porosity, crystallinity, and shape strengthen their possibilities in nanobiotechnology (*Liberman et al., 2014*) (fig. 33).

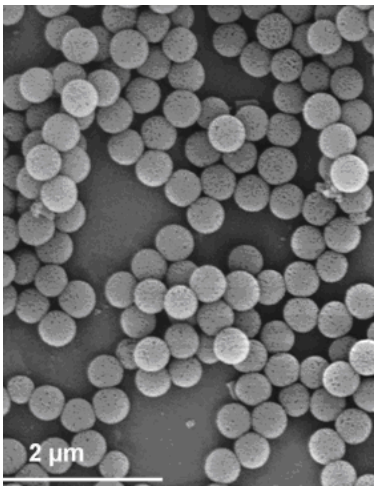

Fig. 33 *SEM imaging of silica nanospheres (provided by Polshettiwar's NanoCat Group*).

Nanosilica can be synthetized through two main methods, the high-temperature thermal route, to yield *pyrogenic silica,* or low-temperature wet routes to form *precipitated*, *colloidal*, *mesoporous* silica or *silica gel* (*Napierska et al., 2010*). Colloidal silicas (silica sols) are stable dispersions in a liquid, usually water. Furthermore, which are generally hydrophilic, may be rendered hydrophobic by surface treatment. Nanosilica exist as highly pure, white, fluffy powders or milky-white dispersions of these powders in fluids.

Furthermore, nanosilica, which are generally hydrophilic, may be rendered hydrophobic by surface treatment on an industrial scale, either by physical or chemical treatment. Methods for chemical modification of the silica particle surface, i.e. silylation, are many and various. The most common treating agents are organosilicon compounds like dimethyldichlorosilane, hexamethyldisilazane and polydimethylsiloxane fluids. With respect to particle size, the German standard DIN 53206 distinguishes between primary particles, aggregates and agglomerates (*DIN, 1972*). Primary particles are recognisable by electron (transmission, scanning) microscopy as sub-units of pyrogenic and precipitated nanosilica or individual particles in sols. For nanosilica gels,

primary particles are not visible: nucleation and condensation give rise to further particle growth. Primary particles in the case of pyrogenic or precipitated do not exist in isolation (*Degussa, 1984b*). Aggregates are assemblies of primary particles which are grown together face-to-face in the form of chains or clusters. The aggregates are formed by the collision of primary particles during particle growth and/or by the further deposition of silica onto these aggregates. Nanosilica aggregates represent the smallest, stable, non-dispersible particle units of three-dimensional structure, with a size ranging from 100 to 1,000 nm for pyrogenic and precipitated. These aggregates can be found at infinite dilution or after blending in a polymer matrix, e.g. composites. For gels, aggregates form macroscopic structures. Nanosilica sols consist of primary particles and aggregates only in a fluid like water, organic solvent or a polymeric matrix but typically agglomerate irreversibly under drying. Agglomerates are assemblies of aggregates, held together by strong physical adhesion forces.

5.1 *Applications of amorphous silica NPs*

Nanosilica has been commercialised since the 1950 and is currently used in a wide variety of industrial applications. The main use of nanosilica is as reinforcement and thickening agent in various systems. It exhibits a high absorption capacity due to their high porosity, therefore it is used as adsorbing agents. In coating for ink-jet paper, absorbs large volumes of water from ink drops which lead to fast drying times.

Nanosilica is integrated in a wide variety of commercial products for human use, such as pharmaceutical products, paints, cosmetics, food (eg. food additive E551) and is also used in beer and wine clarification. In addition, the unique physicochemical properties of nanosilica make it attractive for a variety of biomedical and biotechnological applications such as cancer therapy, drugs and gene delivery and biosensors (*Vivero-Escoto et al., 2012; Malvindi et al., 2012*).

5.2 *Cytotoxicity of amorphous silica NPs*

The emerging commercialization of the nanosilica products has increased the environment and human exposure.

Human exposure to nanosilica may occur during production, storage, transportation, and consumer use (*Napierska et al., 2010*). Due to their very small density, nanosilica can be readily evaporated into air and can be inhaled. Following inhalation, NPs have been reported to rapidly cross the alveolar capillary barrier and penetrate into to the systemic circulation and reach various organs (*Nemmar et al., 2002; Oberdorster et al., 2002*). In contrast to cristaline silica like quartz or cristobalite which are known to be carcinogenic and which cause the lung disease silicosis after chronic inhalation, amorphous silica NPs were classified as harmless in 1997, as there is inadequate evidence for carcinogenicity (*Napierska et al., 2010; IARC, 1997*).

The potential toxicity of nanosilica has been extensively investigated in several studies and experimental evidence of a dose dependent oxidative stress, cytotoxicity and inflammatory effects has been reported (*Athinarayanan et al., 2014; Lin et al., 2006; Morishige et al., 2010; Park et al., 2009*). Cytotoxicity of silica NPs was observed to be dependent on nanoparticle size (*Waters et al., 2009; Nabeshi et al., 2010; Nabeshi et al., 2011*), particle concentration, number or surface area (*Napierska et al., 2009; Li et al., 2011a; Sun et al., 2011; Yang et al., 2010*), surface properties and porosity (*Napierska et al., 2009; Morishige et al., 2010*), incubation time (*Sun et al., 2011b*), proteins in the cell medium (*Drescher et al., 2011; Al-Rawi et al., 2011*) and the cell type (*Palomaki et al., 2010; Chang et al., 2007*) as well as the metabolic activity of the cells (*Chang et al., 2007*). The experiments were carried out on a variety of cells including endothelial cells

(*Napierska et al., 2009*), human and mouse macrophages (*Morishige et al., 2010; Palomaki et al., 2010*), liver cells (*Li et al., 2011a; Sun et al., 2011b*), keratinocytes (*Nabeshi et al., 2011; Yang et al., 2010*), epithelial cells (*Chang et al., 2007*), dendritic cells (*Palomaki et al., 2010*), several types of fibroblasts (*Drescher et al., 2011; Chang et al., 2007*), cancer cells (*Al-Rawi et al., 2011*) and Langerhans cells (*Nabeshi et al., 2010*).

It has been reported that intravenous administration of nanosilica induces consumptive coagulopathy in mice (*Nabeshi et al., 2012*). More recently, we have demonstrated that intraperitoneal administration of amorphous nanosilica cause prothrombotic events, endothelial dysfunction and systemic inflammation in mice (*Nemmar et al., 2002*). However, little is known about the direct *in vitro* effect of amorphous SiNP on platelets.

In the study, Di Cristo and colleagues (*Di Cristo et al., 2015*), studied effects of two representative preparations of nanosilica, NM-203 (pyrogenic) and NM-200 (precipitated), of comparable size, specific surface area, surface charge and hydrodynamic radius in complete growth medium, in two murine macrophage cell lines (MH-S and RAW264.7 cells). The results presented in this study indicate that pyrogenic NM-203 nanosilica are more biologically reactive and pro-inflammatory than precipitated NM-200 nanosilica. In particular, NM-203 resulted more cytotoxic and exhibit larger effects on macrophage activation than NM-200, suggesting that the thermally produced synthetic amorphous silica is correlated to the presence of crucial determinants of biological responses.

They shown that, when incubated in protein-rich fluids, NM-203 adsorbed on their surface more proteins than NM-200 and, once incubated with macrophages, elicited a greater oxidative stress, assessed from *Hmox1* induction and ROS production. Flow cytometry and helium ion microscopy indicated that pyrogenic NM-203 interacted with macrophages more strongly than the precipitated NM-200 and triggered a more evident inflammatory response, evaluated with *Nos2* induction, NO production, and the secretion of TNF-α, IL-6 and IL-1β. The greater biological reactivity of pyrogenic nanosilica does not seem to depend on a different agglomeration behaviour when dispersed in biological media but may, instead, derive from their higher surface reactivity associated with a higher capability to: i) adsorb proteins and, possibly, other bioactive organic molecules, ii) interact with cell membranes and iii) induce oxidative stress in exposed cells.

Mesoporous nanosilica (i.e. nanosilica with pores in their matrix) were mainly tested with regard to their hemolytic properties. They showed mainly to be non-hemolytic, regardless of their size, surface groups, and dosage (*Yu et al., 2011; Slowing et al., 2009*). Furthermore, certain cell lines are less susceptible of getting damaged in the presence of nanosilica than others (*Schrurs and Lison, 2012*). In another study, Nemmar and colleagues, discovered that the *in vitro* incubation of nanosilica in whole blood caused oxidative stress, increased intracellular calcium and platelet aggregation in a dose-dependent fashion (*Nemmar et al., 2002*). Nanosilica as carriers of drug delivery systems are generally injected into the body intravenously and translated to organs via the systemic circulation (*Brook et al., 2010*). It was reported that the liver is the target organ in which the nanosilica could be accumulated and retained for over 30 days (*Nishimori et al., 2009; Xie et al., 2010*). Therefore, it is essential to understand the biological effects and potential hepatotoxicity of nanosilica either *in vivo* or *in vitro*. Currently, several studies have reported that the nanosilica can penetrate the cell membrane, deposit in mitochondria or even the nucleus, and eventually lead to cell death (*García-Saucedo et al., 2011*; *Fruijtier-Pölloth et al., 2012*). Yua and colleagues demonstrated that autophagy and autophagic cell death was induced as a result of ROS generation in HepG2 cells after exposed to the nanosilica (*Yua et al., 2014*)

Zhang et al. (*Zhang et al., 2012*) found that the lung toxicity of pyrogenic nanosilica was comparable to or even exceeding that of crystalline silica NPs (*Fubini and Hubbard 2003*).

Moreover, relatively high doses of pyrogenic nanosilica resulted in rat liver fibrosis after 84 days of exposure (*van der Zande et al., 2014*). However, also nanosilica produced with wet methods have been found to be endowed with some toxicity (*Kaewamatawong et al., 2005; Morishige et al., 2010; Nishimori et al., 2009*). As far as precipitated nanosilica are concerned, they have been found to produce only transient and reversible neutrophilic lung inflammatory responses at 24 h (*Sayes et al., 2007*). In addition, precipitated nanosilica seem nearly inert when assayed for hemolytic activity (*Pavan et al., 2013*) and failed to induce significant increases in the frequency of micronucleated binucleate cells (MNBCs) in human lymphocyte populations (*Tavares et al., 2014*). An inhalation toxicity study in Wistar rats (*Arts et al., 2007*) demonstrated that pyrogenic silica induced a more pronounced increase in the expression of lung inflammation markers and, although equally cleared from the tissue, produced more severe histopathological changes than the precipitated form.

6. CELLULAR MODELS USED IN THE PRESENT STUDY: YEAST

The yeast *Saccharomyces cerevisiae,* one of the most important model fungal organisms, plays an important role as a model of eukaryotic cells for biochemical and physicochemical experiments (*Gromozova et al., 2007*) (Fig. 34).

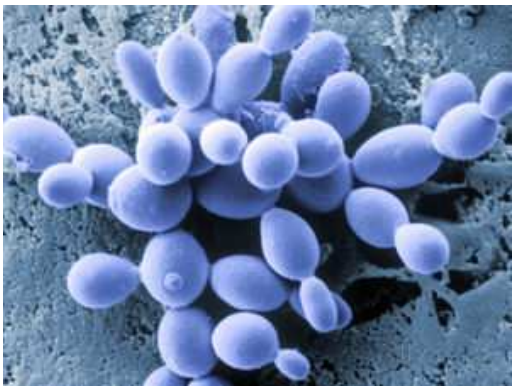

Fig. 34 *Saccharomyces cerevisiae*

In the ensuing 8000 years, this fungus played a central role in food production and conservation thanks to its ability to ferment glucose to ethanol and carbon-dioxide. But not only being useful in daily brewers and bakers practice, yeast, as a simple, unicellular eukaryote developed to a unique powerful model system for biological research: it is still the most facile organism for studying the relationship of genotype to phenotype in eukaryotic cells. Since its cellular structure and functional organization have a high degree of similarity to cells belonging to higher-level organisms.

Indeed, *Saccharomyces* has already begun to play a central role in both the pharmaceutical and the industrial arenas. *S. cerevisiae* is a popular and widely used eukaryotic model organism for the study of the oxidative stress and aging (*Unlu and Koc, 2007*) as 30% of known genes involved in human disease have yeast orthologues, that is, functional homologues (*Ploger et al., 2000; Mager and Winderickx, 2005*), and the high conservation of metabolic and regulatory mechanisms has contributed to the wide-spread use of yeast to as a model eukaryotic system for diversed biological studies. *S. cerevisiae* is also growingly used in the toxicological evaluation of chemicals such as heavy metals (*Kungolos et al., 1999; De Freitas et al., 2003; Schmitt et al., 2004*), anticancer drugs (*Buschini et al., 2003*), herbicides (*Cabral et al., 2003*) or food preservatives such as monocarboxylic acids (*Kasemets et al., 2006*).

Yeast has also a number of advantages for processes that require production on a large scale: the low cost of culture media and a history of efficient fermentation technology. Moreover, the yeast itself, a by-product of the production process, is a valuable commodity for animal feed and thus does not incur additional costs required for disposal.

6.1 *Yeast cells exposed to NPs*

S. cerevisiae is a promising unicellular eukaryotic organism for the toxicological evaluation of NPs. So far, few studies have investigated the potential impact of NPs on yeast. Marmiroli and colleagues (*Marmiroli et al., 2015*) studied CdS QD cytotoxicity. Results obteined shown that several haploid mutants sensitive to CdS QD treatment; these mutants are deleted in genes associated with the abiotic stress response, various metabolic processes, mitochondrial organization,

transport and DNA repair and NP sensitivity could not have been due to the release of Cd^{2+} from these QDs. A gene ontology analysis highlighted the role of oxidative stress in determining the cellular response.

In another work, Han and colleagues (*Han et al., 2012*) studied the toxicity and subcellular localization of CdTe QDs and the mechanism of QD induced cell death. Their results reveal that QDs are toxic to yeast cells in a concentration-dependent manner. TEM images suggested that QD-induced cytotoxicity is due to endocytosis and is partially dependent on the QD size.

Instead, Sun and colleagues (*Sun et al., 2014*) investigated the potential effect of synthesized CdSe NPs. The results revealed that these nanoparticles (20–30 nm) showed a strong inhibitory effect on the growth of yeast cells. Most importantly, contrary to the findings in mammalian cells, the toxicity seems to be not attributed to mitochondrial dysfunction and autophagy, because mitochondrial membrane potential (MMP) was not affected by the NPs, and deletion of the autophagy-required gene, ATG1, had no impact on the toxicity. The mitochondria showed intact membrane and normal function in the CdSe NP-treated yeast cells, implying that ROS is mainly produced by other sources rather than the mitochondria. One possible mechanism of ROS production in the CdSe treated yeast cells is the direct contact of the NP surfaces and electron donor groups of biomolecules, which observed by Li and colleagues (*Li et al., 2014*). Then this toxicity is associated with a novel mechanism, the enhancement of vacuolar membrane permeabilization (VMP), finding a dose-dependent effect of CdSe NPs on VMP in yeast cells. This is associated with ROS accumulation and depends on End3-mediated endocytosis: deletion of the endocytosis required gene, END3, led to a significant decrease of the inhibitory effect of the CdSe NPs. These results reveal a key role of the vacuole during the interaction between CdSe NPs and yeast cells.

Kasemets and colleagues (*Kasemets et al., 2009*) evaluated the toxic effect of ZnO, CuO and TiO_2 NPs on the growth of *S. cerevisiae*. Results indicate that TiO_2 NPs were not toxic for yeast cells, instead ZnO NPs, as well as bulk ZnO, showed concentration-dependent effects on yeast growth and about 80% inhibition of the growth was observed at 250 mg/L. In this study, also CuO NPs were 32-fold more toxic to a wild-type *S. cerevisiae* strain than bulk-CuO: complete inhibition of growth occurred at 40 mg/L. These authors suggested that CuO NPs adsorbed onto the outer surface of these yeasts and that this process increased NP solubility in the close vicinity of yeast cells, resulting in the increased uptake of Cu^{2+}.

In another study, same authour and colleagues (*Kasemets et al., 2013*) used eight oxidative stress response-deficient haploid mutants (*sod1*Δ, *sod2*Δ, *yap1*Δ, *cta1*Δ, *ctt1*Δ, *gsh1*Δ, *glr1*Δ, and *ccs1*Δ) and one copper-vulnerable mutant (*cup2*Δ). Results indicate that the toxicity of CuO NPs is not mediated by oxidative stress. The most vulnerable strain was the copper stress response-deficient strain *cup2*Δ, indicating that the toxic effect of CuO NPs proceeds via dissolved cupper ions.

Lee and colleagues (*Lee et al. 2009*) reported that *S. cerevisiae* showed a higher survival rate than *Escherichia coli* and *Bacillus subtilis* after exposure to nanosized silver powder. Schwegmann and colleagues (*Schwegmann et al. 2010*) showed that *S. cerevisiae* was less affected by the presence of iron oxide NPs compared with *E. coli*. Hadduck and colleagues (*Hadduck et al. 2010*) mentioned that no reduction in the cell yield of *S. cerevisiae* was observed in the presence of fullerene. Garciá–Saucedo and colleagues (*García-Saucedo et al., 2011*) demonstrated that nanoscale HfO, HfO_2, SiO_2, Al_2O_3, and CeO_2 displayed low or no toxicity toward *S. cerevisiae*. Interestingly, in another study (*García-Saucedo et al.,2013*), García-Saucedo and colleagues reported that dispersant supplementation (Dispex A40) enhanced the toxicity of CeO_2 (at 1000 mg/L) toward *S. cerevisiae*. Same author in another study (*Otero-González et al., 2013*) evaluated the toxicity in yeast of a variety of commonly used inorganic NPs (TiO_2, ZrO_2, Mn_2O_3, Fe0, and

Fe_2O_3). Cytotoxicity was evaluated based on measurements of O_2 consumption rate and membrane integrity. In addition, the effect on toxicity of NP dispersion was assessed by using a dispersant to reduce NPs agglomeration in the assay medium, as for CeO_2. Indeed, aggregation and settling of NPs during toxicity testing, leading to a decrease in the concentration effectively dispersed, is a concern because of the uncertainty in the actual NP concentration in contact with the microorganisms. Moreover, the formation of large aggregates exceeding the typical dimensions of NPs (1–100 nm) may hinder the evaluation of nanotoxicity. They reported that Mn_2O_3 NPs were toxic to the yeast based on O_2 consumption (IC50 = 170 mg/L) and cell membrane damage (30% cells with compromised membrane at 1000 mg/L and 5.4% of the cells completely dead). FeO NPs showed low toxicity (44% inhibition at 1000 mg/L) in the O_2 uptake test, but slightly negative on the cell membrane integrity. The other NPs (TiO_2, ZrO_2, and Fe_2O_3) did not affect the O_2 consumption of the cells and did not display any significant effect on membrane integrity. The effect of aggregation of NPs in their toxicity was evaluated using a dispersant. The dispersant increased the stability and decreased the aggregation of TiO_2, ZrO_2, and Mn_2O_3 in YEPD medium; the presence of dispersant did not alter the non-toxic behavior of TiO_2 and ZrO_2 NPs. For the toxic NPs, such as Mn_2O_3, there was a small decrease in the toxicity when the dispersion stability was increased with a dispersant, potentially due to particle surface modifications that altered the interaction between the NPs and the cells.

Zhang and colleagues *(2016)* investigated the cytotoxicity of ZnO NPs to the wild-type cells and three yeast mutants (*yap1*Δ; quadruple mutant, 4Δ; quintuple mutant; 5Δ). In particular, *yap1*Δ has a single deletion in the *yap1* gene, which regulates the enzymatic response to oxidative and metal stress; this mutant is sensitive to NP-related oxidative stress. The quadruple gene deletion mutant (4Δ: *cwp1*Δ *cwp2*Δ *snq2*Δ *pdr5*Δ) has several mutation in genes that control cell membrane permeability and is sensitive to metal ions or mechanical damage-induced toxicity. The quintuple gene deletion mutant (5Δ: *cwp1*Δ *cwp2*Δ *snq2*Δ *pdr5*Δ *yap1*Δ) has several mutation in genes that govern both the effect of oxidative defense and cell membrane permeability and is sensitive to oxidative and/or mechanical damage toxicity. Results show high toxicity of ZnO NPs in these yeast mutants.

In another study, Sun and colleagues (*Sun et al., 2014*) demonstrated that PbS NPs (80 nm, diameter) exhibited high toxicity in yeast through induction of mitochondria-associated apoptosis. Furthermore observed that *S. cerevisiae,* in response to NP exposure, increased the synthesis of chitin and activated cell wall integrity signalling pathway. They observed activation of the CWI (conserved cell wall integrity) pathway supported by the increased *PRM5* and *FKS2* gene expression in cells treated with PbS NPs. Therefore, the CWI pathway is spontaneously activated in *S. cerevisiae* to maintain cell wall integrity in response to cell wall stress: as a protective strategy, yeast cells deposit an increased amount of chitin in the cell walls and activate CWI signaling to maintain cell wall integrity.

7. CELLULAR MODELS USED IN THE PRESENT STUDY: HUMAN INTESTINAL CELL LINE

The intestinal epithelium is the main barrier preventing molecules from the lumen (e.g. food and toxins) reaching the systemic circulation. Metabolism and transport of drugs across intestinal membrane are therefore multifaceted and dynamic process involving both passive and active transport mechanisms. The epithelium is composed of several cell types: enterocytes, goblet cells, Paneth cells, enteroendocrine cells and stem cells. However, absorptive and goblet cells constitute the two major cell types of the intestine. The Caco-2 cell line was derived from intestinal absorptive cell types.

7.1 *Caco-2 cell line*

The Caco-2 cell line derived from human colon adenocarcinoma is considered the most common *in vitro* model used for investigation and prediction of intestinal drug and food absorption (*Sambuy et al. 2005*). It is derived from heterogenous human epithelial colorectal adenocarcinoma cells, developed through research by Jorgen Fogh in 1975 at Sloan-Kettering Institute for Cancer Research (*Fogh et al.,1975*). Caco-2 cells differentiate spontaneously on reaching confluence in the presence of normal culture conditions and exhibit structural and functional differentiation patterns characteristic of mature enterocytes (Fig. 35)

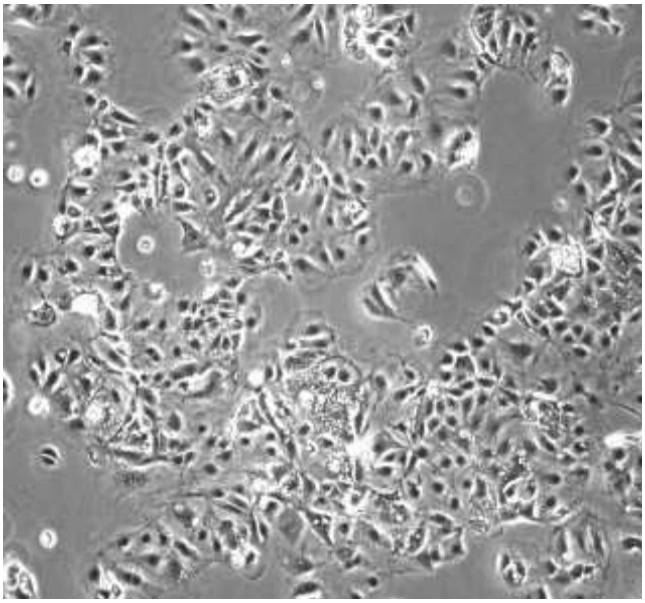

Fig. 35 *Caco-2 cell line.*

At confluence, there is progressive development of brush border. The surface occupied by each cell gradually reduces from 5 to 20 days post-confluence and intimate intercellular junctions are developed (*Pinto et al., 1983*). During the same period, the length and density of microvilli increase. The Caco-2 cells form well - developed tight junctions after 21 days of culturing. At day - 30 post-confluence, the cell surface reaches minimum with typical enterocytes-like morphology. Most cells develop complete brush borders with tall and regular microvilli when the full structural polarization is achieved after 30 days (*Vachon et al., 1992*) .

The complete polarized Caco-2 cells resemble human small intestinal mucosa cells expressing brush borders, tight junctions and, efflux and uptake transporters at both apical and basolateral

compartments (P-gp, MRP 1-3). The polarized cells depict several functions of normal enterocytes including expression of brush border enzymes, some cytochrome (CYP) isoenzymes and phase II enzymes (*Bohets et al., 2001*). The differentiated cells exhibit high levels of alkaline phosphatase, sucrase isomaltase and aminopeptidase activity characteristic to enterocyte brush border microvilli. Although Caco-2 cells express many enzymes and transporters present in the small intestine, the high TEER (200-600 Ωcm^2, grown on polycarbonate filters) and poor paracellular permeability properties resemble colonic cells (mannitol (m.w. 182 g/mol), Lucifer yellow (453 g/mol), polyethylene glycol (4000 g/mol), inulin (5000 g/mol), and dextran (70000 g/mol) (*Grasset et al., 1984; Hidalgo et al., 1989; Artursson et al., 1993*).

Caco-2 cell monolayers have been used for studying mechanisms of passive paracellular (*Artursson et al., 1993*) and passive transcellular permeability (*Artursson 1990*), carrier mediated absorptive transport of amino acids (*Thwaites et al. 1995b*), amino acid analogues (*Hu and Borchardt, 1990*; *Thwaites et al., 1995a*), oligopeptides (*Thwaites et al. 1993*), ß-lactam antibiotics and ACE-inhibitors (*Inui et al. 1992*) and peptidomimetic thrombin inhibitors (*Walter et al. 1995*). Carrier mediated efflux (combined with metabolism inside the enterocytes) of several drugs has been intensively studied over the last years (*Benet et al. 1999; Walgren et al. 1999; Polli et al. 2001; Eneroth et al. 2001; Tran et al. 2002; Troutmann and Thakker 2003; Collett et al. 2004*), as well as cocktail dosing of several different drugs (*Bu et al. 2000; Markowska et al. 2001; Tannergren et al. 2001; Larger et al. 2002; Augustijns and Mols 2004; Palmgren et al. 2004*). TC-7, a subclone of Caco-2 cells, is also used for permeability screening of tests compounds. The TC-7 clone displays morphological features of brushborder membrane, microvilli and tight junctions similar to Caco-2 monolayer (*Balimane et al., 2005*). There is a good correlation of passive transcellular absorption of compounds through TC7 and the parental Caco-2 cell monolayer comparable to the extent of permeability in humans. The TC-7 model therefore offers an alternative to Caco-2 for intestinal permeability assessment of test compounds. In addition, TC-7 has an advantage over Caco-2 by expressing high levels of CYP3A4 enzymes well represented in the intestine.

However, TC-7 unlike Caco-2 cell lacks transport proteins and therefore its application is skewed towards metabolism of drug employing CYP3A4. The intestinal epithelial cell line 2/4/A1 originates from fetal rat intestine and is considered to mimic intestinal passive paracellular permeability in humans better than Caco-2 monolayer (*Tavelin et al., 2003a, Tavelin et al, 2003b*). This immortalized cell is reported to differentiate monolayers with tight junctions, brush-border membrane enzymes and transporter proteins. Unlike, Caco-2, tight junctions expressed in 2/4/A1 are loose and better for studies of compounds absorbed in the human intestine via the paracellular route. The model has been proven tobe excellent for prediction of poorly absorbed compounds such as mannitol and creatinine better than Caco-2 but comparable to that of human jejunum (*Tavelin et al., 2003a, Tavelin et al, 2003b*).

8. BIOLOGICAL SAMPLES USED IN THE PRESENT STUDY: HUMAN BLOOD

Human blood is a non-homogeneous system composed of deformable cells suspended in plasma. It contains 55% of plasma and 45% of cells. These cells (erythrocytes, leukocytes and thrombocytes) are suspended in plasma. Leukocytes and thrombocytes form a small fraction. The erythrocytes are about 5 millions/cu.mm, White cells vary from 5000 to 8000 /cu.mm and platelets from 250000 to 300000/cu.mm. The ratio of cells in normal blood is 600 erythrocytes for each leucocyte and 40 thrombocytes. The plasma is about 90% water by weight containing 7% plasma proteins, 1% inorganic and 1% other organic substances (Fig. 36).

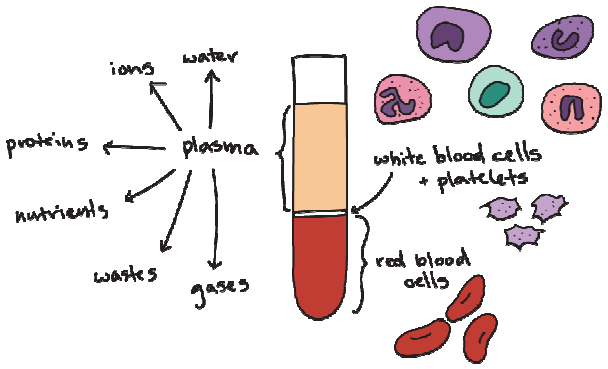

Fig. 36 *Components of human blood. Sal Khan Khanacademy*

The plasma viscosity is determined by its dissolved macro molecular components and its primary component is water. The contribution of individual protein fraction is related to the mass and shape of the molecules. The normal range of plasma viscosity is between 1.10 and 1.35 m Pas at 37 degrees centigrade. Flow behavior of blood plasma or serum is affected by protein components. The contribution of proteins is related to their molecular weight and shape. Small globular molecules such as albumin are of less significance. On the other hand fibrinogen, a high molecular weight protein, has strong effect on plasma viscosity. Fibrinogen affects also the aggregability of erythrocytes, then adhesion which is the cause of disturbances in microcirculation.
Blood was first emphasized diagnostically by Hippocrates, who proposed that disease was due to an imbalance of four humors: blood, phlegm, yellow bile, and black bile. The importance of this idea was to propose a physical cause, and not a divine one, for human disease, and it remained basic to medical practice for over a thousand years. With Wohler's synthesis of urea in 1828, the distinction between living matter and chemicals began to disappear, and with the enunciation of the cell theory by Schleiden and Schwann, the question of the location of disease could be productively revisited: Virchow described the cellular (as opposed to humoral) basis of disease and finally put an end to phlebotomy as general therapy. Despite not being a humor or "vital principle," plasma remained a subject of interest throughout this period: in the 1830 Liebig and Mulder analyzed a substance called "albumin," in 1862 Schmidt coined the term "globulin" for the proteins that were insoluble in pure water, and in 1894 Gurber crystallized horse serum albumin (*Putnam, 1975–1987*).

Elaborating on Putnam's classification from a functional viewpoint, the protein content of plasma is classified into the following design/function groups:

- *Proteins Secreted by Solid Tissues and That Act in Plasma*
  The classical plasma proteins are largely secreted by the liver and intestines. A key aspect of plasma proteins is a native molecular mass larger than the kidney filtration cutoff (~45 kDa) and thus an extended residence time in plasma (albumin, which is just larger than the cut off, has a life time of about 21 days).

- *Immunoglobulins*
  Although the antibodies typically function in plasma, they represent a unique class of proteins because of their complexity: there are thought to be on the order of 10 million different sequences of antibodies in circulation in a normal adult.

- *"Long Distance" Receptor Ligands*
  This group included the classical peptide and protein hormones. These proteins come in a range of sizes, which may indicate a range of time scales for their control actions (*i.e.* rapid adjustment with small hormones such as insulin and slower adjustments with larger hormones such as erythropoietin).

- *"Local" Receptor Ligands*
  These include cytokines and other short distance mediators of cellular responses. In general these proteins have native molecular weights under the kidney filtration cutoff (and hence relatively short residence times in plasma) and appear to be designed to mediate local interactions between cells followed by dilution into plasma at ineffective levels. High plasma levels may cause deleterious effects remote from the site of synthesis, *e.g.* sepsis.

- *Temporary Passengers*
  These include non-hormone proteins that traverse the plasma compartment temporarily on their way to their site of primary function, *e.g.* lysosomal proteins that are secreted and then taken up via a receptor for sequestration in the lysosomes.

- *Tissue Leakage Products*
  These are proteins that normally function within cells but can be released into plasma as a result of cell death or damage. These proteins include many of the most important diagnostic markers, *e.g.* cardiac troponins, creatine kinase, or myoglobin used in the diagnosis of myocardial infarction.

- *Aberrant Secretions*
  These proteins are released from tumors and other diseased tissues, presumably not as a result of a functional requirement of the organism. These include cancer markers, which may be normal, non-plasma-accessible proteins expressed, secreted, or released into plasma by tumor cells.

- *Foreign Proteins*
  These are proteins of infectious organisms or parasites that are released into, or exposed to, the circulation.

MATERIALS AND METHODS

9. MATERIALS AND METHODS

9.1 ENM used in the present study

9.1.1 CdS QDs

CdS QDs were manufactured by IMEM-CNR (Parma), following the method described by *Villani M. et al.* (2012). Briefly, dimethylformamide (DMF) is used as solvent: 10 ml of thiourea solution (1E5 M) were mixed with 100 ml DMF and the solution was heated at 70°C; 10 ml of cadmium acetate (1E5 M) were then added to the solution and the temperature raised to 90°C. The reaction was stopped after 5 minutes, the solid phase was washed with water and collected by centrifugation.

X-ray diffraction, TEM and physical property analysis (photoluminescence, photocatalytic activity, electrical properties, alternating gradient force and vibrating sample magnetometry) are used to characterize these ENMs (*Villani et al., 2012*). The bulk density of CdS QDs was 4.82 g cm^{-3} and their mean diameter was 5 nm. The estimated mass of a single NP was 2,5E-18 g/mol. Cd represented 78% of the dry weight of each NP (*Marmiroli et al., 2014*). Zeta potential of CdS QDs (240 µg) in 20 mM Tris-HCl pH=7.4 was measured using ZetaPlus Zeta Potential Analyzer (Brookhaven Instrument). CdS QDs were sonicated for 16 min with a sonicator bath (Transsonic 460, Elma) prior to incubation in cellular media.

9.1.2 SiO_2 NPs

SiO_2 NPs were provided by prof. Bussolati (Department of S.Bi.Bi.T, University of Parma) and has a diameter of 200 nm (NM200). According to the NANOGENOTOX dispersion protocol (http://www.nanogenotox.eu/), these NPs were pre-wetted using EtOH (0.5%), dispersed at a concentration of 2.56 g/L in sterile milliQ water containing 0.05% BSA and sonicated for 16 min with a sonicator bath (Transsonic 460, Elma) prior to incubation in cellular media.

9.2 Cellular models and biological samples used in the present study

9.2.1 Yeast strains and growth conditions

S. cerevisiae BY4742 (*MATα his3Δ1 leu2Δ0 lys2Δ0 ura3Δ0*) wild-type strain and a subset of haploid deletion strains (background BY4742) from the Yeast Knockout Collection (Thermo Scientific) were used in this study.
S. cerevisiae TAP-tag strains (*MATa his3Δ1 leu2Δ0 met15Δ0 ura3Δ0*) from the yeast TAP-tagged ORF library (Dharmacon, GE Healthcare) were also utilized for proteomic experiments. In this library, Open Reading Frames (ORFs) were tagged with a high-affinity epitope and expressed from their natural chromosomal locations. The tandem affinity purification (TAP) tag consists of a calmodulin binding peptide, a TEV cleavage site and two IgG binding domains of *Staphylococcus aureus* protein A.
Cells are grown at 30°C on yeast extract-peptone (YP) or synthetic medium (S) supplemented with glucose (2% w/v) as carbon source.

9.2.2 Human cell line: growth conditions and cell viability assay

Caco-2 human colorectal adenocarcinoma cell line was provided by Prof. Bussolati (S.Bi.Bi.T, Parma). Human cells were grown in RPMI medium, supplemented with 20% fetal bovine serum (FBS), 1% L-glutamine and 1% penicillin/streptomycin (100 U/100 µg/mL), and cultured on 24-well plates in a 5% CO_2 humidified atmosphere at 37°C.

Human cell viability was determined by the AlamarBlue® viability assay. In this assay, a non-fluorescent, membrane permeant molecule (resazurin) is converted by mitochondrial enzymes in the fluorescent compound resorufin (λ_{em} = 572 nm). After 24h of incubation, cell viability was tested replacing medium with a solution of resazurin (44 μM) in serum-free medium. After 1 hour, fluorescence was measured (excitation 530-560 nm; emission 590 nm) with a multimode plate reader Enspire (Perkin Elmer Waltham, MA, USA).

9.2.3 Human Plasma

Human plasma was provided from Medical Center of Parma, was aliquoted and stored at −80°C. For NP-binding experiments, plasma was thawed and centrifuged for 2 min at 14000 rpm at 4 °C to remove protein precipitates.

9.3 Proteomic analysis

9.3.1 Protein extraction procedure

Yeast cell pellets (1E8 cells) were washed in ice cold PBS and resuspended in cold extraction buffer (200 mM Tris-HCl pH=8.0, 150 mM ammonium sulfate, 10% glycerol), containing protease inhibitor cocktail (Sigma Aldrich). Acid-washed glass beads were added to the samples and yeast cells were mechanically lysed by FastPrep® Cell Disrupter (Savant), vortexing six times (four time for 45 s with other two steps for 10 s, interspersed with 5 min rests of the tube on ice to minimize sample heating). Cells lysates were transferred to a fresh tube and particulates were removed by centrifugation (30 min, 14000 rpm at 4 °C).

Human monolayer cells to approximately 80% confluence (3E6 cells) were gently wash with ice cold PBS and resuspended in cold extraction buffer (200 mM Tris-HCl pH=8.0, 150 mM ammonium sulfate, 10% glycerol), with the addition of protease inhibitors. Using a cell scraper, human cells were detached from the 24-well plates and the lysate was transfer to a 1.5 ml microtube and incubated on ice for 15 minutes. The lysate was sonicates (Sonicator Ultrasonic Processor XL, Misonix) three times for five seconds each with at least one minute rest on ice between each five-second pulse and incubated in ice an additional 15 minutes. The cell lysate was centrifugated (30 min, 14000 rpm at 4°C) and the supernatant containing soluble proteins was collected.

Protein concentration was determined using Bradford assay (BioRad).

9.3.2 Proteomic analysis of ENM-protein interactions

For the binding assay (Fig. 37), cell lysates (from yeast or human cell lines) or human plasma proteins were incubated with ENMs (CdS QDs or silica NPs) in the reaction buffer (200 mM Tris-HCl pH=8.0, 150 mM ammonium sulfate, 10% glycerol). The proteins (7 g/L, final concentration) and the ENMs (0.5 g/L, final concentration) were incubated at 4°C for 24 h in gentle agitation (*Sund J. et al., 2011*), in a reaction volume of 142 μL. After incubation, ENMs and the adsorbed (corona) proteins were recovered by centrifugation (14000 rpm, 5 min, 4 °C) and unbound proteins were removed by washing the pellets five times with no-salt wash buffer A (20 mM Tris-HCl, pH=7.4) and three times with low-salt wash buffer B (0.1 M NaCl, 20 mM Tris-HCl, pH=7.4). After each wash, pellets were gently vortexed and centrifuged (14000 rpm, 5 min, 4 °C). Corona proteins were removed from ENMs by incubation for 60 min at 30°C in hot solubilization buffer (60 mM Tris-HCl pH=6.8, 2% SDS, 10% glycerol), heated at 100°C for five minutes.

Aliquots of each wash and corona proteins were dissolved in SDS-sample buffer (62.5 mM Tris-HCl pH=6.8, 2.5 % SDS, 0.02 % Bromophenol Blue, 2% β-mercaptoethanol, 10% glycerol), denatured at 95°C for 5 min and analyzed in 12% SDS-polyacrylamide gel electrophoresis (SDS-PAGE).

9.3.3 Identification of corona proteins: in-solution protein digestion and LC-MS/MS analysis

Corona proteins were denatured by adding 6 M urea in 25 mM ammonium bicarbonate solution. Disulfide bonds were reduced by adding DTT (35 mM, final concentration) for 1 hour at room temperature and reduced cysteine residues were alkylated by adding iodoacetamide (32 mM, final concentration) for 1 hour at room temperature, in the dark. After the urea concentration was lowered to 0.6 M by adding 25 mM ammonium bicarbonate, trypsin (Sigma Aldrich) was added in a 1:30 ratio (trypsin: proteins, w/w) and the digestion took place for 18 hours at 37°C. The samples were then acidified with formic acid (0.5%, final concentration) to stop the digestion, incubated with gentle agitation at 37°C for 15 min and lyophilizated (Speedvac, Savant).

The dried samples were resuspended in 0.1% formic acid and analyzed with a Liquid chromatography (LC)–mass spectrometry system. Tryptic peptide analysis was performed with a Dionex Ultimate 3000 micro HPLC coupled with an LTQ-Orbitrap XL (Thermo Fisher) mass spectrometer equipped with a conventional electrospray ionization (ESI) source. LC-MS/MS analyses were performed by Dr. Faccini (CIM, University of Parma; *Bencivenni M. et al., 2014*). The UniProt database (www.uniprot.org) was employed to retrieve information on all the known protein sequences from *S. cerevisiae* and *H. sapiens*.

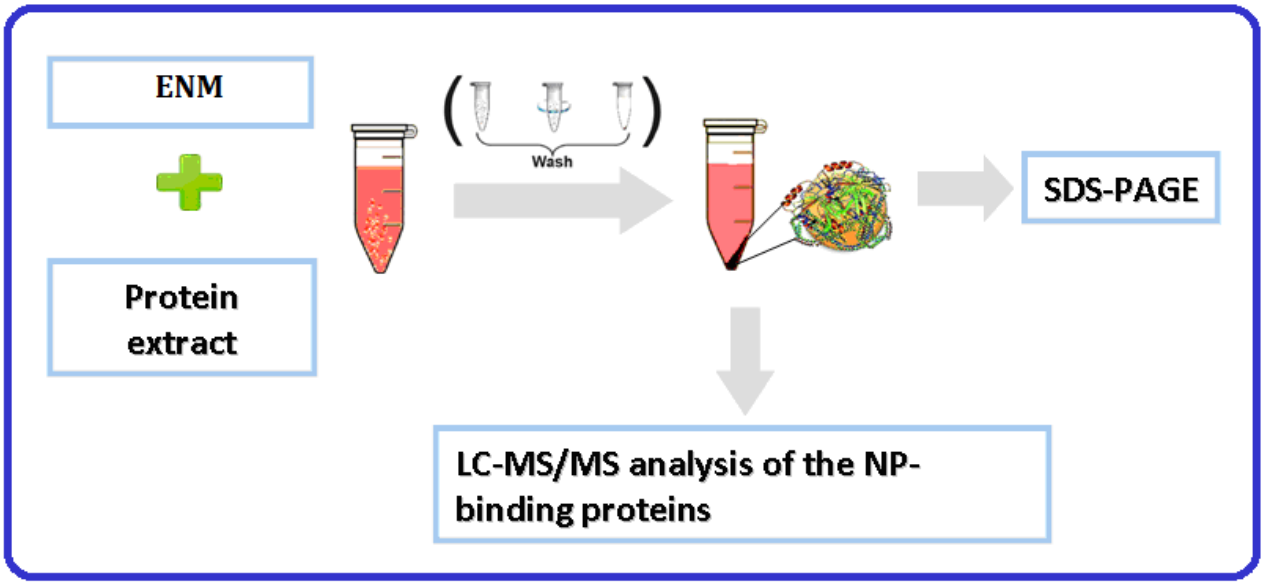

Fig. 37 *Schematic representation of the strategy to identify ENM-adsorbed proteins. Incubation of ENM with protein solutions results in adsorption of corona proteins onto the ENM surface. Wash-centrifugation steps are important for the isolation of "hard protein corona"and removal of unbound proteins. The adsorbed proteins can thus be visualized using one dimensional gel electrophoresis (SDS-PAGE). Corona proteins can further be subjected to in-solution tryptic digestion and subsequently identified using LC-mass spectrometry.*

9.4 Real-time PCR analysis

S. cerevisiae cells were treated with and without CdS QDs (250 mg/L) in YPD media at 30°C for 2 hours. Cells (2E6 cells) were collected by centrifugation and total RNA (2 µg) was extracted using the RNeasy® kit (Qiagen) following the manufacturer's instructions. cDNAs were synthesized using the QuantiTect Reverse Transcription kit (Qiagen) as described by the manufacturer. The primers used in Real-time PCR were designed using Primer Express® software (Applied Biosystems) and were reported in Table 2. Real-time PCR was performed with a ABI

PRISM 7000 Sequence Detection System (Applied Biosystems) according to the manufacturer's instructions. Briefly, reaction mixtures (25 µl final volume) were assembled with the following components: 2.5 µl of 10-fold serial dilutions of cDNAs, optimized amounts of each primer set (Table 2), 2X Power SYBR® Green RT-PCR Mix (Applied Biosystems). The housekeeping *ACT1* mRNA served as an independent internal standard. All primer pairs produced only one amplification band (ranging from 67 to 114 bp) when tested by conventional reverse transcription-PCR. The specificity of individual real-time PCR products was assessed by melting curve analysis carried out immediately after Real-time PCR completion. Melting curves for individual PCR products displayed a single peak. Melting temperatures (Tm) were determined with the Dissociation Curve software (Applied Biosystems). All sets of reactions were conducted in triplicate, and each included a nontemplate control (NTC). The threshold cycle (C_T) was used to calculate relative gene expression levels using the "Comparative C_T ($2^{-\Delta\Delta CT}$) Method".

Table 2. *Primers used in Real-time PCR analysis.*

Gene name	Amplicon length	Primer sequence (5'-3')	Primer concentration (final)
CDC19	104 bp	FW: ATCTTCACCACCGATGACAAGT RE: TAGATGATTCTACCAGCGGAGA	50 nM
PDC1	114 bp	FW: ATGCTGAATCCGAAAAGGAAGTC RE: TCAGCCTTGACGTCGTGTCTG	250 nM
TDH3	107 bp	FW: TCATGAGAATTGCTTTGTCTAGAC RE: TAAGTAGCAATCTTCTTACCATCG	250 nM
EFT2	111 bp	FW: ATGCTAAGAAATTCGGTGTCGAC RE: CTTCAGCATCAGTGTCCTTGTTG	75 nM
YEF3	99 bp	FW: ATGCCAGAATTGATTCCAGTC RE: AGTTTCGGTAGCCTTGGTCATG	40 nM
TEF1	106 bp	FW: ATGGTCAAACCAGAGAACACGC RE: AATCTGGATTCGTCCCATTTGAC	200 nM
SSB2	114 bp	FW: ATGTTTCCTTGTTGCACATTGCTG RE: CAGCCTTGAAGTGTTCCAACAAG	100 nM
ACT1	67 bp	FW: GAGGTTGCTGCTTTGGTTATTGA RE: CGTCGTCACCGGCAAAA	50 nM

9.5 Western Blot analysis

Yeast TAP-tag strains (Yef3-TAP-tag, Eft2-TAP-tag, SSb2-TAP-tag, Tdh2-TAP-tag, Tdh3-TAP-tag, Pdc1-TAP-tag) were treated with and without CdS QD (250 mg/L) in YPD media at 30°C for 6 hours. After incubation time, the cells were collected and cell lysis was conducted using the extraction method described previously (*see before*). Protein concentration was determined using Bradford assay (BioRad).

Total protein extracts (10 µg/sample) were then separated on a 12% SDS-PAGE gel and transferred to a nitrocellulose membrane (Thermo Fisher Scientific). Membranes were blocked for 2 hours at room temperature in Tris-Buffered Saline (TBS) containing 0.1% Tween20 and 5% skim milk (TTS buffer) with gentle agitation. Rabbit anti-TAP-tag polyclonal antibody (CAB1001, Open Biosystems) was used for detection of TAP-tagged proteins. Mouse anti-phosphoglycerate kinase 1 (Pgk1; Abcam) monoclonal antibody served as loading control. Membranes were incubated with the primary antibodies in TTS buffer over-night a 4°C with gentle agitation. Goat anti-rabbit and anti-mouse (680 RD; LI-COR) antibodies were used as secondary antibodies and visualization was carried out with the Odyssey® Imaging System (LI-COR).

9.6 Spot assay

S. cerevisiae wild type (BY4742) and a subset of haploid mutant strains were grown at 30°C in YPD medium. After 24 hours, the OD_{600} of individual cultures was determined with a UV-Visible spectrophotometer (Cary 50, Varian), adjusted with sterile water to an OD_{600} value of 1.0 and serially diluted in tenfold increments. Aliquots (4 µl) of each dilution were spotted onto SD-agar plates in the presence or absence of CdS QDs (0-250 mg/L) or SiO_2 NPs (0-5 g/L). Yeast growth was examined after incubation at 30°C for 2 days.

9.7 GAPDH enzymatic activity assay

Glyceraldehyde 3 phosphate dehydrogenase (GAPDH) Activity Assay Kit (Abcam) was used following the manufacturer's instructions. Briefly, GAPDH catalyzes the conversion of Glyceraldehyde-3-Phosphate (GAP) into 1,3-Bisphosphate Glycerate (BPG) and an intermediate, which reacts with a developer to form a colored product that absorbs maximally at 450 nm.
Yeast protein extract (1 µg) and CdS QDs (0-20 µg/mL) were added to kit reagents and the assay was run for 60 min at 37°C. Finally, the absorbance at 450 nm was measured with a Microplate Reader (BioRad) (Fig. 38).

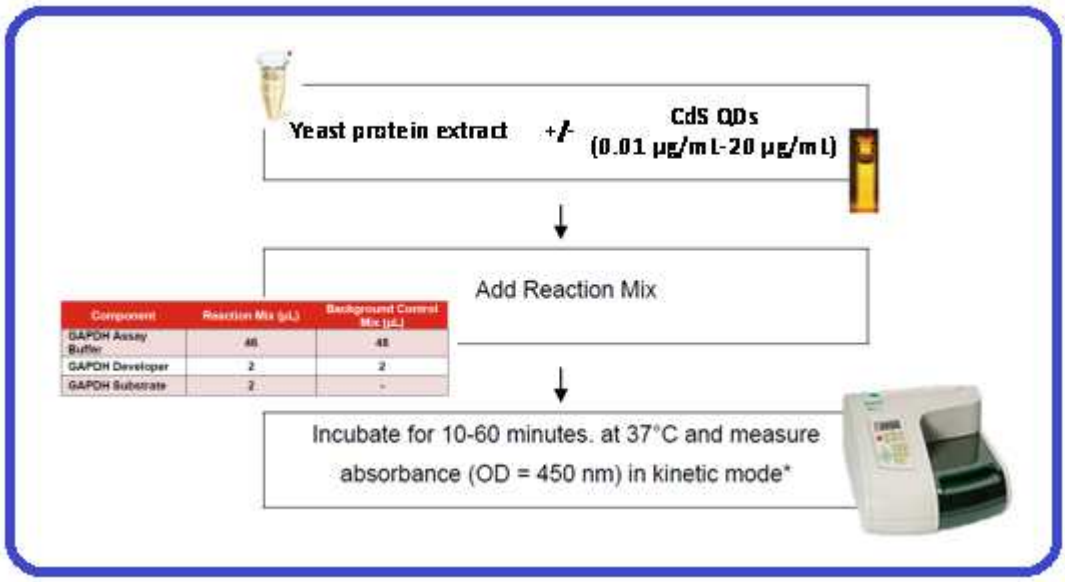

Fig. 38 *Schematic procedure of the GAPDH Activity Assay Kit (Colorimetric).*

9.8 Computational analysis of corona protein sequences

We have downloaded 5,783 *S. cerevisiae* protein sequences from the Saccharomyces Genome Database (http://www.yeastgenome.org/) and calculated amino acid residue frequencies. The proteome-average amino acid frequency for all proteins was determined. Protein-specific amino acid frequencies for each *S. cerevisiae* protein was analyzed to compute a protein-specific amino acid Z-score [(protein-specific amino acid frequency - average amino acid frequency)/standard deviation for 5,783 proteins]. Z-score measures whether an amino acid is over- or under-represented in a protein sequence relative to the average proteome value. Corresponding *P*-values were determined for all over-represented or under-represented amino acids using a one-tailed test and normal approximation.

9.9 Statistical analysis

Statistical analysis was performed using GraphPad Prism software (version 6). Each experiment was performed 3 to 5 times and results are expressed as mean ± SD. Statistical significance of differences between average values was determined by ANOVA, the order of significance was determined using the Bonferroni's multiple comparisons test and P-value ≤ 0.05 was considered significant.

RESULTS AND DISCUSSION

10. RESULTS AND DISCUSSION: CdS QDs

10.1 Proteomic analysis of CdS QD-protein interactions in *S. cerevisiae*.

Nanotoxicity of CdS QDs has been studied in *S. cerevisiae* (*Marmiroli et al., 2016*), but the mechanisms that affect the toxicity of these NPs are not yet completely understood. The aim of this work is to investigate the formation of protein corona on the CdS QD surface to study the implications of yeast protein adsorption on the bioactivity of these NPs.

CdS QDs are inorganic fluorescent nanoscale crystals (Fig. 42a) with enhanced optical properties in terms of brightness, photostability, blinking and bleaching compared to conventional organic and protein fluorophores. Synthesis and characterization of water-soluble CdS QDs are performed by Dr. Zappettini and colleagues (IMEM-CNR, Parma; *Villani et al., 2012; Marmiroli et al., 2014*). Briefly, TEM and X-ray diffractometry analysis showed that CdS QDs exhibited hexagonal or cubic shape and an average size of 5 nm.

10.1.1 CdS QD-protein interaction assay

To identify yeast proteins which were adsorbed on the NP surface, CdS QDs and protein extracts were incubated with gentle agitation in a medium that replicate the features of the *in vivo* biological milieu. After incubation, the NPs and corona proteins were recovered by centrifugation and washed to remove nonbound proteins. After three centrifugation steps followed by resuspension in wash buffer, the adsorbed proteins were eluted from the NP surface and analyzed with SDS-polyacrylamide gel electrophoresis to estimate molecular masses and relative abundance of polypeptides (Fig. 42; *see "Materials and Methods" for additional details*).

There are many factors influencing the composition of the protein corona: related to the NPs (chemical composition, size, shape, surface charge), the biological samples (e.g., amount of proteins) and the experimental conditions (temperature, incubation time).

To determine the optimal conditions for the binding assay, adsorption of yeast proteins to the surface of CdS QDs was analyzed in the presence of different amount of yeast protein extracts (0.1-1 mg), different times of exposure (1-24 hours) and temperature (4°C-37°C) incubation. For each condition tested, CdS QD-corona proteins were analyzed with SDS-polyacrylamide gel electrophoresis.

Based on a visual evaluation of the SDS-PAGE gels, the total amounts of adsorbed proteins were strongly increased with the increase of the protein extract concentration (Fig. 39b) and the time of exposure (Fig. 39c). Importantly, not statistically significant, qualitative differences were detected in the protein profiles analyzed in these conditions (Fig. 39b and c).

NP-protein binding assays performed for 1 hour at 4°C or 37°C do not show qualitative and quantitative differences in the observed electrophoretic profiles (Fig. 39d).

Thus, to maximize the amount of adsorbed proteins, we proceeded to carry out the following experiments in these conditions: yeast extracts (1 mg, total protein extract) were incubated for 24 hours in the presence of NPs and, to minimize protein degradation, binding assays were run at 4°C.

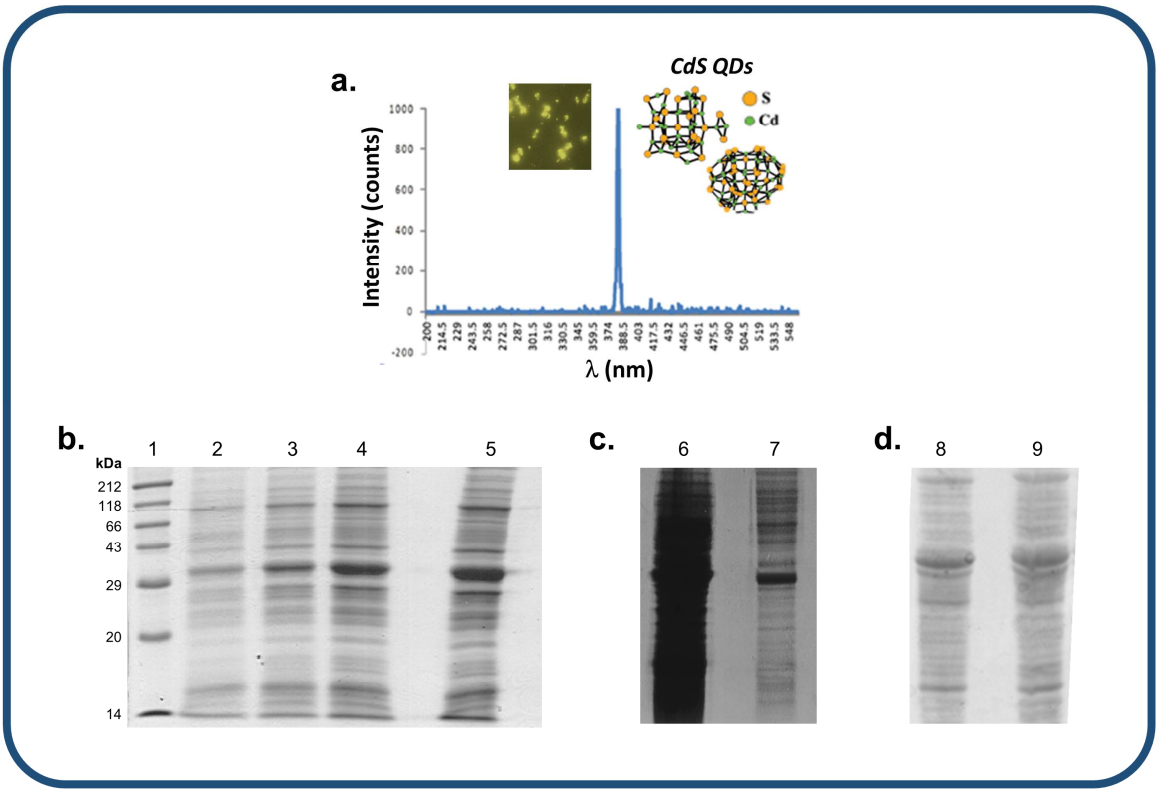

Fig. 39 *Yeast proteins adsorbed onto CdS QD surface. a) CdS QDs used in the present study. These NPs are synthetized by Dr. Zappettini (IMEM-CNR, Parma). CdS QDs exhibited hexagonal or cubic shape and showed strong fluorescence at emission wavelengths of 370-390 nm.*
b-d) Different amounts of yeast proteins were adsorbed to CdS QDs; increasing yeast protein extract concentration [0.1 mg (2), 0.3 mg (3), 0.6 mg (4), 1 mg (5)] corresponded to a greater adsorption on the NPs. Increased amounts of corona proteins were observed at higher time of exposure [24h (6) or 1h (7)] to CdS QDs. NP-protein binding assays performed at 4°C (8) and 37°C (9) do not show qualitative and quantitative differences (d). In all these experiments (b-d), only three washes with wash buffer A (see "Materials and Methods", section 9.3.2, for additional details) of the NP-protein pellet were conducted.
1) Protein molecular marker; the molecular weights (in kDa) of the standard marker on the left lane were reported for reference.

10.1.2 Identification of yeast proteins with high affinity for CdS QDs

The process of corona formation is determined by the competition of countless proteins to adsorb at the approaching NP surface. Protein coronas are categorized as either "soft" or "hard" (*Walczyk et al., 2010; Milani et al., 2012*). The soft corona represents loosely bound proteins on a NP surface over short time scales (i.e., seconds to minutes) or weak interactions compared with the hard corona. In contrast, the hard corona represents tightly bound proteins with high affinity on the NP surface and for longer periods (i.e., hours).

To identify yeast proteins that form the NP corona, we have used a proteomics-based approach coupled with MS analysis. CdS QDs and protein extracts were incubated with gentle agitation for 24 hours at 4°C and proteins bound to the NPs were recovered by multiple centrifugation steps and extensively washed to remove almost all nonbound and soft corona proteins. We used different ionic strengths to separate the proteins from the NPs (*see "Materials and Methods" for additional details*): no-salt solution to separate the loosely bound proteins and low-salt solution to investigate the hard corona.

Finally, hard corona proteins were eluted from the NP surface, visualized by gel electrophoresis and quantitatively analyzed (after tryptic digestion) using liquid chromatography–high-resolution mass spectrometry. Sample preparation for MS analysis involves protein denaturation, reduction and alkylation of cysteines, digestion of the sample into peptides, sample concentration and analysis by ESI-based MS strategies (LC-MS/MS) using LTQ-ORBITRAP XL mass spectrometer. The experiments were carried out in five independent replicates.

In yeast, the hard corona of the CdS QDs was composed of many different proteins with molecular weights between 30 and 100 kDa (Fig. 40 and Table 3). The proteins that contribute predominantly to the formation of this protein corona were involved in translation processes, in energy metabolism and belong to the superfamily of molecular chaperones (Table 4).

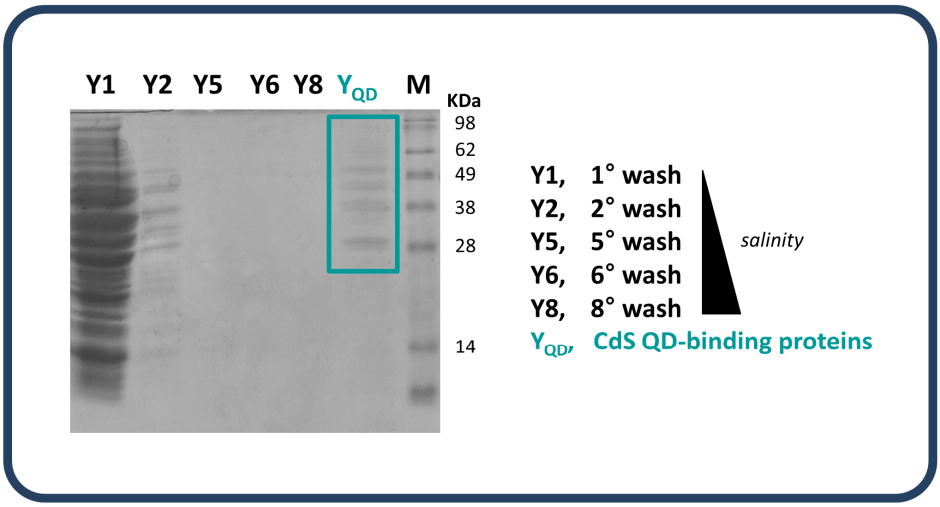

Fig. 40 *Proteomic analysis of the yeast proteins adsorbed on the surface of CdS QDs with high affinity. Aliquots of the wash solutions (Y1-Y8; 30% of the total sample) and yeast-derived hard corona proteins (Y_{QD}; 15% of the total sample) were visualized by 12% SDS-PAGE. Hard protein corona was composed of many different proteins with molecular weights between 30 and 100 kDa.*
Y1-Y5) Washes (first, second and fifth) of the CdS QD-protein pellet with no-salt wash buffer; Y6-Y8) Washes (sixth and eighth) of the CdS QD-protein pellet with low-salt wash buffer (see "Materials and Methods" for additional details).

Table 3. *Yeast-derived hard corona proteins identified by LC-MS/MS analysis (LTQ-ORBITRAP XL).*

Identified proteins	Coverage (%)[1]	Score[2]	Isoelectric point (pI)
Tdh2	74.7	186.8	6.46
Tdh3	83.7	181.6	6.46
Pdc1	71.2	308.7	5.8
Cdc19	46.8	85.9	7.56
Ssb2	48.6	73.9	5.37
Tef1	75.8	285.9	9.14
Eft2	36.27	72.15	5.92
Yef3	56.9	313.7	5.73

[1]The coverage (%) was calculated by dividing the number of amino acids in all found peptides by the total number of amino acids in the entire protein sequence.
[2]The score was based on the probability (*P*) that the observed match between the experimental data and the database sequence was not a random event.

Table 4. *Characteristics of hard corona proteins adsorbed to CdS QDs.*

Identified proteins	Description (UniProt Accession N.)	Mol. weight (kDa)	Biological process
Tdh2	Glyceraldehyde-3-phosphate dehydrogenase (P00358)	36	Energy metabolism
Tdh3	Glyceraldehyde-3-phosphate dehydrogenase (P00359)	36	
Cdc19	Pyruvate kinase (P00549)	54	
Pdc1	Pyruvate decarboxylase isozyme 1 (P06169)	61	
Ssb2	Ribosome-associated molecular chaperone (P40150)	66	Molecular chaperone
Tef1	Translation Elongation Factor I (P02994)	50	Translation process
Eft2	Elongation Factor II (P32324)	93	
Yef3	Translation Elongation Factor III (P16521)	116	

Several proteins isolated in CdS QD-protein corona were involved in **energy metabolism** (Table 4): glyceraldehyde-3-phosphate dehydrogenase (two isoforms, Tdh2 and Tdh3), pyruvate decarboxylase (Pdc1) and pyruvate kinase (Cdc19).

GAPDH is a cytosolic glycolytic enzyme that catalyzes the conversion of glyceraldehyde-3-phosphate to 1,3 bis-phosphoglycerate, but also displays activities that are unrelated to glycolysis in different subcellular locations (*Sirover, 2005*; *Shen et al., 2014*). *S. cerevisiae* contain three related, but not identical, GAPDH isoforms (Tdh1, Tdh2, Tdh3) with different specific activities (*McAlister et al., 1985a*). None of the *TDH* genes are individually essential for cell viability, but a functional copy of either *TDH2* or *TDH3* is required since *tdh2Δtdh3Δ* cells are not viable (*McAlister et al., 1985b*). GAPDH isoforms were detected in cytoplasm, nucleus (Tdh2 and Tdh3) and cell wall (*Delgado et al., 2001*).

Pdc1 is the major of three pyruvate decarboxylase isozymes and is involved in the nonoxidative conversion of pyruvate to acetaldehyde and carbon dioxide during alcoholic fermentation. Furthermore, it is involved in amino acid catabolism and activated by phosphorylation in response to glucose levels (*Kellermann et al., 1986; Foyn et al., 2013*).

Cdc19 is a homotetramer involved in glycolysis to convert phosphoenolpyruvate to pyruvate and is regulated via allosteric activation by fructose bisphosphate.

Hard corona proteins were also involved in **translation process** (Table 4): translation elongation factor I (Tef1), elongation factor II (Eft2) and translation elongation factor III (Yef3).

Tef1 is a elongation factor that binds to and delivers aminoacylated tRNA to the A-site of ribosomes during protein biosynthesis; Tef1 may also have a role in export of aminoacyl-tRNAs from the nucleus and in translational quality control by targeting cotranslationally damaged proteins to the proteasome. Also, Tef1 exhibits actin filament-binding and filament-bundling activities and is involved in cytoskeleton organization (Bodman et al., 2015).

Eft2 is an essential protein that catalyzes the translocation of the ribosome along messenger RNA during protein synthesis and is highly conserved in all eukaryotes. Eft2 has been highly conserved throughout evolution: the *S. cerevisiae* protein sharing 66% identity and 85% homology to human ortholog.

Yef3 is a elongation factor required for the ATP-dependent release of deacylated tRNA from the ribosomal E-site during protein biosynthesis.

Ssb2 is a ribosome-associated **molecular chaperone**, member of the HSP70 family. Ssb2 is involved in the folding of newly-synthesized polypeptide chains and prevents from interfering with translation by clogging the ribosome channel.

Interestingly, Tef1, Tdh2/3, Eft2, Cdc19 and Ssb2 are highly conserved proteins and have human orthologs (Ensembl database; http://www.ensembl.org/index.html).

10.1.3 Physico-chemical characterization of the hard corona proteins isolated on the surface of the CdS QDs

We have demonstrated that the CdS QDs are able to adsorb several proteins from yeast cell lysates with high affinity. Recently, Zhang et al. (*2011*) showed that the protein-binding patterns onto the NPs were closely related to the NP surface properties, size as well as physical properties of corona proteins. To further characterize the nature of protein binding to CdS QDs and identify potential regions that influence the interaction between NPs and proteins, amino acid composition, isoelectric point (pI) values and structural features of the NP-bound proteins were compared. Analysis of the amino acid composition (Table 5) showed an enrichment of non-polar amino acids with small lateral residues (Ala, Gly, Val) and a lower frequency of aromatic amino acids (especially, Tyr and Phe) in the CdS QD-corona protein sequences respect to the average amino acid frequencies of the yeast proteome (Table 5 and "Material and Methods"). Proteins with this amino acid composition are generally characterized by a high structural flexibility that may mediate the protein interaction with CdS QDs. Notably, Gly residues was often found at the surface of these corona proteins within loop- or coil (without secondary structure) regions, providing high flexibility to the polypeptide chain at these locations.

In addition, electrostatic interactions are also responsible for mediating molecular recognition among NPs and corona proteins (*Mu et al., 2014*). The measured zeta potential of CdS QDs in aquaeus solution was –14 ± 1.03 mV, indicating that these NPs are anionic, but have a tendency toward agglomeration and sedimentation, as previously identified (*Marmiroli et al., 2016*). Curiously, except for Cdc19 and Tef1, the majority of the isolated corona proteins presents a pI below 6.5 (Table 3), suggesting that these CdS QD-binding proteins would have a net negative charge at physiological pH. It is possible that anionic CdS QDs may interact with positively charged regions in cavity on the surface of these corona proteins (Fig. 41), previously described as the cationic "hot spots" (*Xiao et al., 2008*). For istance, the binding between functionalized QDs and human serum albumin occurs near a protein pocket centered at Lys199 residue (*Xiao et al., 2008*). Shen et al. (*2007*) showed that hemoglobin have a relatively high affinity for CdS QDs through the electrostatic interactions as well as the chemical bonds with sulfur atoms of cysteine residues. Ishii et al. (*2003*) showed that CdS QDs were trapped in the cylindrical cavity of chaperonin proteins (GroEL, *Escherichia coli* and *Thermus thermophiles*) and become thermally stable and tolerant to electrolytes (Fig. 41a).

Identified corona proteins are homodimers or homotetramers with ring-shaped architecture (Fig. 41b and c) and, similarly to GroEL-QD binding, these protein rings could capture CdS QDs; notably, ring cavities are rich in basic amino acids (lysine, arginine and histine; Fig. 41c).

Table 5. *Amino acid frequencies in the corona protein sequences.*

	Yeast proteome (mean)[1]	Corona proteins[2]							
		Cdc19	**Eft2**	**Pdc1**	**Tdh2**	**Tdh3**	**Yef3**	**Tef1**	**Ssb2**
Hydrophobic amino acids									
Ala	5.7	8.6 (*)	8.1 (*)	9.6 (*)	9.9 (*)	9.6 (*)	8.7 (*)	8.1 (*)	10.0 (*)
Gly	5.2	6.8 (*)	7.0 (*)	7.5 (*)	7.5 (*)	7.8 (*)	6.0 (*)	9.2 (*)	6.9 (*)
Val	5.8	9.6 (*)	9.6 (*)	7.1 (*)	10.8 (*)	11.1 (*)	6.8 (*)	10.0 (*)	8.5 (*)
Pro	4.3	5.0 (*)	4.8	4.6	3.3 (#)	3.6 (#)	4.1	5.0 (*)	3.3 (#)
Ile	6.5	7.4	5.9	6.6	6.0	5.7	7.5	6.6	5.9
Leu	9.6	7.0 (#)	8.2 (#)	9.6	6.3 (#)	6.3 (#)	8.3 (#)	5.2 (#)	8.3 (#)
Phe	4.7	3.0 (#)	4.2	4.1	3.3 (#)	3.0 (#)	3.4 (#)	3.7 (#)	4.2
Trp	1.1	0.2	1.0	1.2	0.9 (#)	0.9 (#)	1.1	1.3	0.2 (#)
Tyr	3.4	3.0	2.4 (#)	3.0	3.0	3.3	1.9 (#)	1.7 (#)	1.5 (#)
Acidic amino acids (negatively charged)									
Asp	5.5	6.4 (*)	6.9 (*)	5.2	7.2 (*)	7.2 (*)	5.6	5.2	6.2
Glu	6.3	5.6 (#)	6.5	5.3	4.5	4.5	8.8 (*)	6.8	8.0 (*)
Basic aminoacids (positively charged)									
Arg	4.7	4.8	4.9	2.7 (#)	3.3 (#)	3.3 (#)	4.3	3.9 (#)	4.7
His	2.2	1.4 (#)	1.9	2.1	2.4	2.4	2.3	2.4	0.8 (#)
Lys	7.4	7.4	7.2	6.2	7.8	7.8	8.0	10.7 (*)	7.7
Polar amino acids with uncharged groups									
Cys	1.5	1.4	1.0 (#)	0.7 (#)	0.6 (#)	0.6 (#)	1.4	1.5	0.3 (#)
Ser	8.7	5.4 (#)	5.2 (#)	5.3 (#)	7.5 (#)	7.8	5.7 (#)	4.6 (#)	7.2 (#)
Thr	5.8	7.6 (*)	5.7	7.8 (*)	6.9 (*)	7.2 (*)	6.0	6.1	7.3 (*)
Asn	5.7	5.2	3.1 (#)	5.2	4.2	3.9 (#)	4.7 (#)	3.5 (#)	3.6 (#)
Gln	3.9	2.0 (#)	3.8	3.9	1.8 (#)	1.5 (#)	2.8 (#)	2.6 (#)	4.1
Met	2.2	2.2	2.7 (*)	2.3	2.4	2.1	2.4	1.7 (#)	1.5 (#)

[1]*The average frequency of each amino acid residue in the yeast proteome (http://www.yeastgenome.org/).*
[2]*The amino acid residue frequencies in the corona protein sequences. Increased (*) or decreased (#) abundance of a given amino acid in the corona protein sequence relative to proteomic frequency (average) was indicated (see "Material and Methods" for details).*

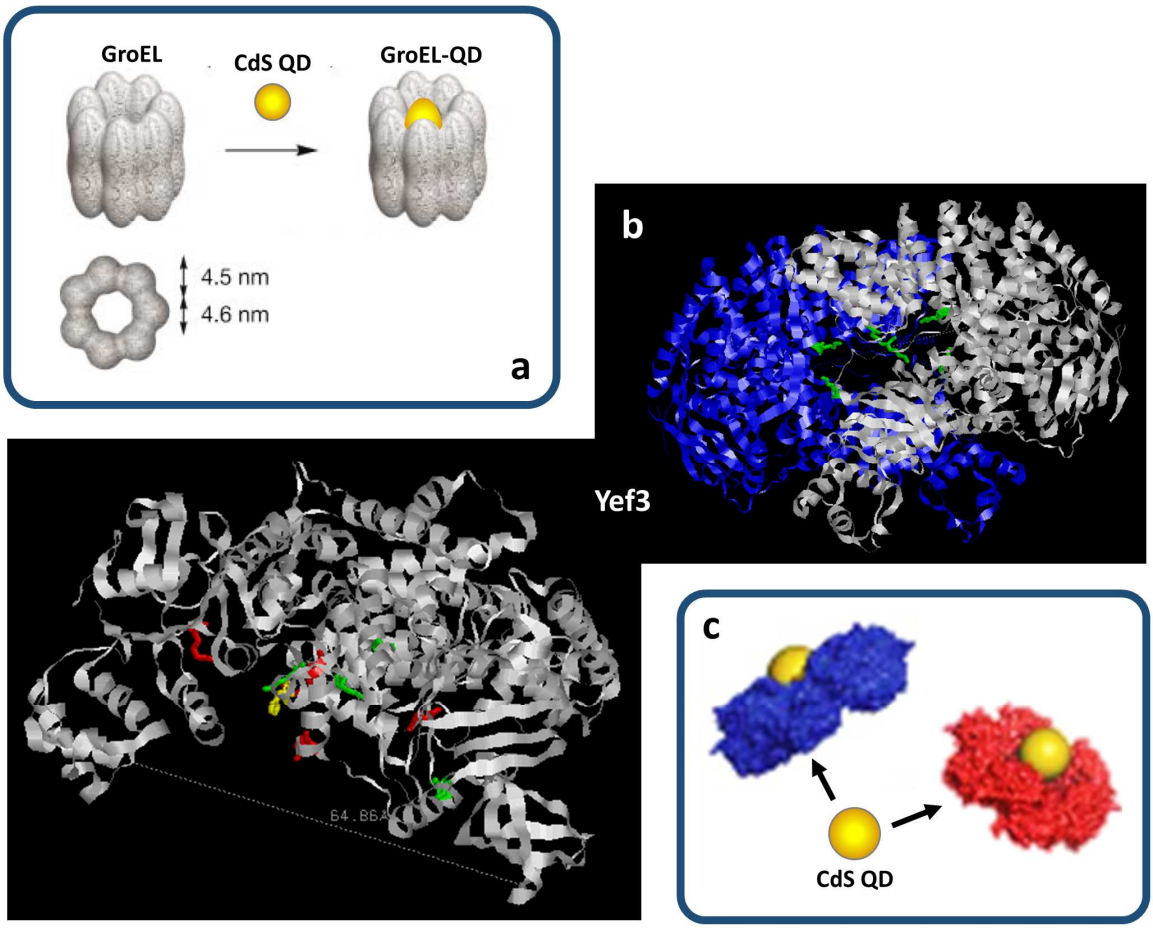

Fig. 41 *3-D structure of the CdS QD-binding proteins. a) Schematic representation of the formation of GroEL–CdS QD complexes by inclusion of NPs into the cylindrical cavity of GroEL (image adapted by Ishii et al., 2003). b) 3-D structure of Yef3 in homodimeric (up) e monomeric (down) forms. The lysine, arginine and histidine residues are shown in green, red and yellow, respectively (image was generated with RasMol software). c) Schematic representation of the CdS QD-yeast protein complexes.*

The adsorption of proteins on the surface of NPs was governed by protein–NP binding affinities as well as protein–protein interactions. Indeed, the CdS QD-corona can be composed by only a single layer of adsorbed proteins or multiple layers generated by protein–protein interactions. We observed the existence of well known and documented physical interactions between the proteins identified in the corona on the surface of CdS QDs (Biogrid database, https://thebiogrid.org/; Fig. 42a) and the presence of a highly connected node or "hub" (Ssb2), in this small protein–protein interaction network (*Rual et al., 2005; Stelzl et al., 2005*). This could be expected because Ssb2 belongs to the superfamily of the molecular chaperones, a group of highly interactive proteins that modulate the folding and unfolding of other proteins, or the assembly and disassembly of protein–protein complexes.

AFM analysis of the yeast protein corona (Fig. 42b) showed a lot of small round structures with a central core of ca. 5 nm in height and width, and the absence of aggregates or large clusters of QDs. Protein binding seems to reduce the CdS QD agglomeration (Fig. 42b) and these circular structures could be CdS QDs encapsulated in yeast protein rings (Fig. 41c). Notably, interaction with BSA significantly enhanced stability of functionalized CdTe QDs in aqueous solution and prevented NPs from aggregating (*Poderys et al., 2011*). As the yeast proteins identified in the hard corona of CdS QDs presented a hydrodynamic diameter of about 3–7 nm, it is possible to hypothesize a competitive adsorption of these proteins rather than the formation of multiple layers of proteins on the surface of CdS QDs.

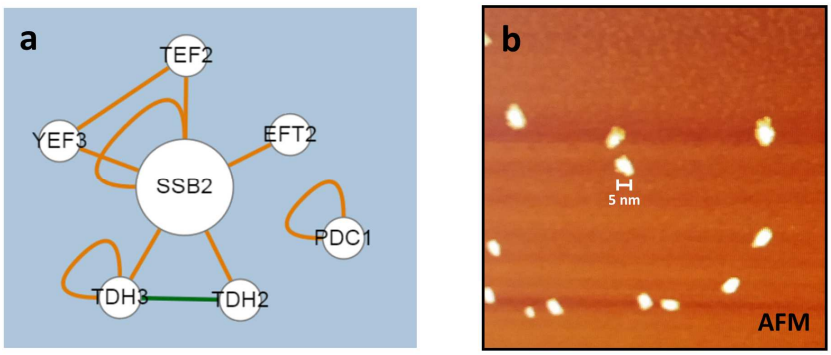

Fig. 42 *Structural analysis of the yeast protein corona.* a) *Genetic (green) and physical (orange) interactions between hard corona proteins. Biological network was built with the online tool esyN (http://www.esyn.org).*
b) AFM analysis of CdS QD-protein corona dispersed on mica in Phosphate-buffered saline (PBS). Images were collected on the dried sample with a Nanoscope IIIa AFM (Digital Instruments) operating in tapping mode. Commercial silicon cantilevers for noncontact AFM (MikroMasch, Tallin, Estonia) were used. Round structures observed in AFM image could be CdS QDs coated with yeast proteins.

10.1.4 Western blot analysis to confirm the presence of corona proteins on the surface of CdS QDs

To confirm the presence of the hard corona proteins on the surface of CdS QDs, we used a targeted approach based on the use of *S. cerevisiae* TAP-tagged ORF library (Dharmacon, GE Healthcare). As proof of concept, we used two strains (Tdh2-TAP-tag and Pdc1-TAP-tag) in which two proteins isolated in the corona are TAP-tagged (*see "Materials and Methods" for details*).

Using the standardized protocol developed for NP-binding assay (*see Section 10.1.3*), CdS QDs were incubated with protein extracts obtained from Pdc1-TAP-tag and Tdh2-TAP-tag strains. After incubation, the NPs and corona proteins were recovered by centrifugation and washed to remove nonbound proteins. The adsorbed proteins (which should contain the corona TAP-tagged proteins) were eluted from the NP surface and analyzed with Western blot analysis (Fig. 43; *see "Materials and Methods" for additional details*). Anti-Pgk1 monoclonal antibody served as negative control.

The results clearly showed the presence of these proteins in the adsorbed fractions from both NP-coronas (Fig. 43). No immunodetection was observed in total protein extracts obtained from wild-type strain (BY4742) using anti-TAP-tag antibody.

Protein levels of Pgk1, an abundant protein, not present in CdS QD corona, was detected only in yeast extracts obtained from BY4742, using an anti-Pgk1 antibody.

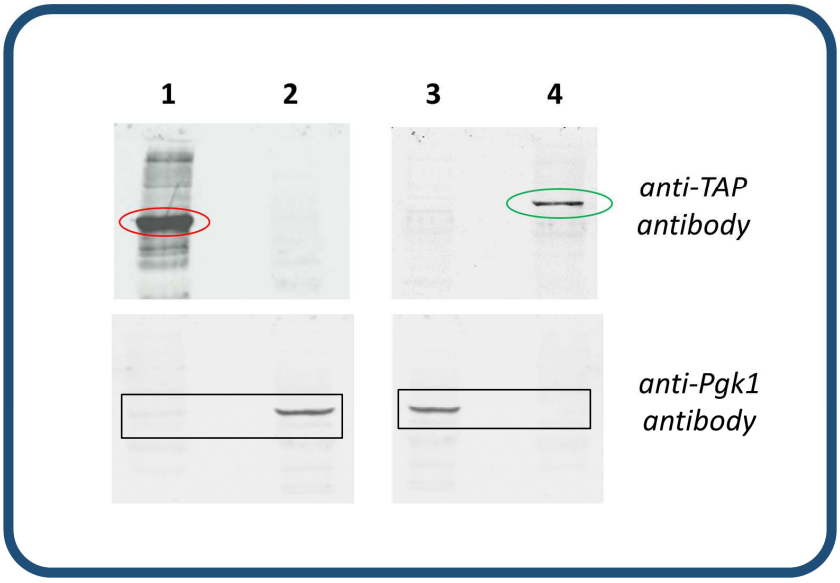

Fig. 43 *Western Blot analysis. Tdh2 and Pdc1 levels were detected in the protein corona isolated by TAP-tagged strains (lane 1, Tdh2-TAP-tag; lane 4, Pdc1-TAP-tag) using an anti-TAP antibody; no immunodetection was observed in total protein extracts obtained from the wild-type (BY4742; lanes 2 and 3) strain. Pgk1 levels were only detected in total protein extracts from the wild-type strain using an anti-Pgk1 antibody.*

10.1.5 CdS QDs affect the expression of genes coding for corona proteins

We evaluated the effect of CdS QD treatment on expression of the genes coding for corona proteins. *S. cerevisiae* wild-type (BY4742) cells were traited for 2 hours with or without CdS QDs (250 mg/L), total RNA was extracted from these samples and cDNAs were synthesized (*see "Materials and Methods" for details*). Real-time PCR analysis was performed on cDNA prepared from treated and untreated samples, using *ACT1* as housekeeping gene.
Gene expression analysis showed that all genes analyzed were up-regulated by CdS QD treatment (Fig. 44). Transcriptional up-regulation of these genes could represent a cellular mechanism in response to "physical sequestration" of the corona proteins adsorbed onto CdS QD surface. In fact, the cellular levels of these proteins can be reduced by the absorption to the NPs and an increase of the transcriptional levels of the genes coding for these proteins could be important for cell survival. Notably, *CDC19*, the most up-regulated gene (Fig. 44), codes for an essential protein (pyruvate kinase) involved in glycolytic process.

A strong up-regolation of *SSB2*, a molecular chaperone of the Hsp70 family, could be necessary to maintain a correct folding of newly-translated proteins and prevent aggregation/misfolding (*Gupta et al., 2010*). Notably, Hsps have been shown to be induced by several stress conditions, including exposure to heavy metals (*Guven and de Pomerai, 1995; Mutwakil et al., 1997*).

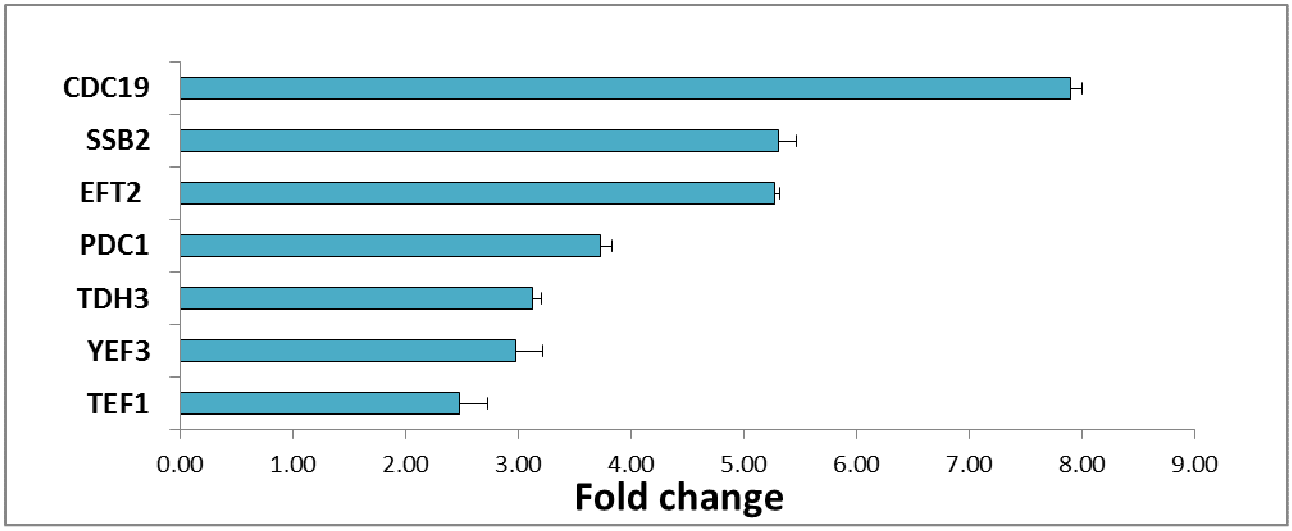

Fig. 44 *Up-regulation of the genes coding for corona proteins in response to CdS QD treatment. Gene expression levels were normalized to ACT1 gene expression. Histograms in the graph represent mean and SD values of two independent reactions performed in triplicate.*

10.1.6 CdS QDs reduce the cellular levels of the corona proteins in S. cerevisiae

We also analyzed the effect of CdS QD treatment on the modulation of the abundance of the proteins identified in NP corona. Yeast TAP-tag strains (Yef3-, Eft2-, Ssb2-, Tdh2-, Tdh3- and Pdc1-TAP-tag) and wild-type (BY4742) cells were grown for 6 h with or without CdS QD treatment. Total protein extracts were prepared and then subjected to Western blot analysis (*see "Materials and Methods" for details*). The protein levels of Cdc19 and Tef1 were not analyzed in this work because their TAP-tagged strains are not present in our yeast collection.
Our results demonstrated that CdS QDs strongly reduced the abundance of the corona proteins, with the exception of Pdc1, whose protein levels are low and not affected by the NP treatment in the tested conditions (Fig. 45).

It's possible that the "physical sequestration" caused by CdS QD-protein corona formation could lead to a reduction in cellular levels of the proteins involved. In addition, different proteins associated with the NP corona are translation elongation factors (Eft2, Tef1 and Yef3) and it is possible that the adsorption of these proteins on the surface of the QDs may lead to their functional inactivation which might cause a reduction of the translational levels of other proteins, including Ssb2, Tdh2 and Tdh3. Notably, silica NPs can inhibit protein synthesis *in vitro* (*Klein et al., 2016).*

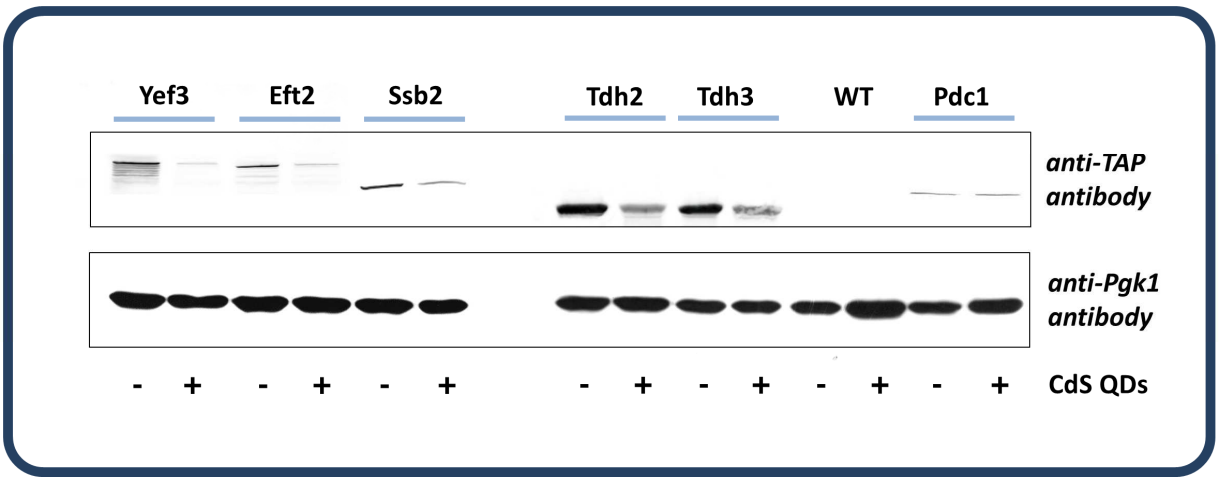

Fig. 45 *Western Blot analysis shows a reduction of the corona protein levels under NP treatment. TAP-tagged proteins (Yef3, Eft2, Ssb2, Tdh2, Tdh3 and Pdc1) were detected using an anti-TAP antibody. Pgk1 protein levels were detected using an anti-Pgk1 antibody and served as loading control. Total protein extract from the wild-type cells (no TAP) was used as negative control for anti-TAP immunoreactivity.*

10.1.7 Mutations in genes coding for corona proteins affect cell viability

We then evaluated the fitness of yeast strains deleted in genes coding for corona proteins (*TDH2*, *TDH3*, *PDC1* and *EFT2*) exposed to CdS QDs (Fig. 46). Strain deleted in *CDC19*, *YEF3*, *SSB2* and *TEF1* genes were not present in our yeast haploid deletion mutant collection and were not tested.

Serial dilution assay of wild-type (BY4742) cells and haploid mutant strains (*tdh2Δ*, *tdh3Δ*, *pdc1Δ*, *eft2Δ*) were performed on standard synthetic media supplemented with glucose (2%) as carbon source (SD) in the absence or in the presence of CdS QDs (20-250 mg/L; *see "Materials and Methods" for details*).

Mutant strains deleted in genes coding for corona proteins showed a tolerant phenotype also in presence of high concentrations of CdS QDs (250 mg/L) that suppress the viability of the wild-type strain. Tolerant phenotype of these mutant strains suggest that the formation of protein corona may mediate the cytotoxicity of CdS QDs in yeast.

It is known that the adsorption of proteins on the NP surface can induce protein inactivation and denaturation by decreasing their thermal stability and favoring conformational changes of the adsorbed proteins (*Corbo et al., 2016*). CdS QDs could induce the exposure of protein epitopes on their surface in an aberrant conformation or the formation of the protein corona could promote the binding of NPs with other cellular components, causing an increased toxicity.

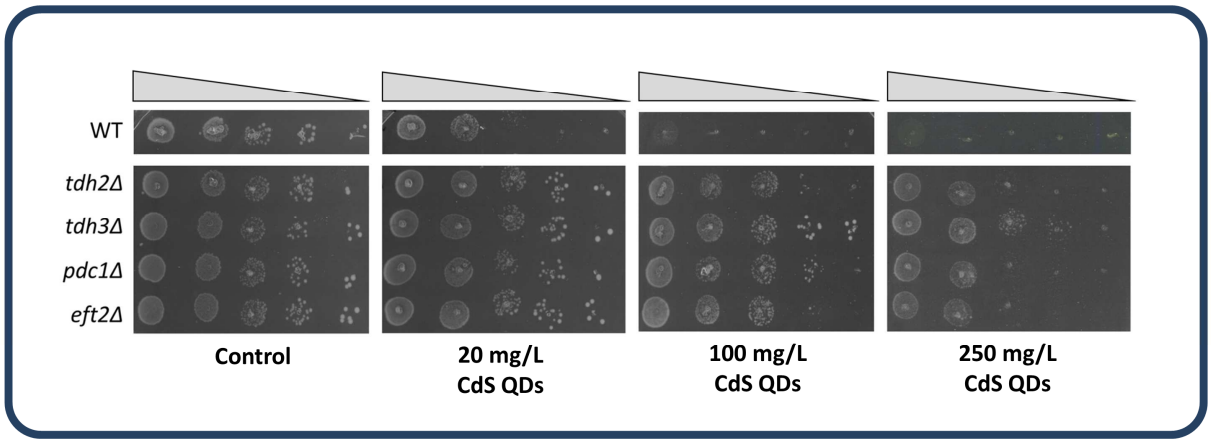

Fig. 46 *Phenotypic analysis of haploid mutants deleted in genes coding for corona proteins. Serial dilution assay (spot assays) of wild-type (WT) cells and haploid mutant strains (tdh2Δ, tdh3Δ, pdc1Δ, eft2Δ) grown in the absence (left) or in the presence of CdS QDs (20-250 mg/L), on standard synthetic media supplemented with glucose (2%) as carbon source (SD).*

10.1.8 Inhibition of GAPDH activity by CdS QDs

Several studies showed that proteins adsorbed onto NP surface may result in unfolding, with consequent loss of functionality (*Gheshlaghi et al., 2008*; *Wangoo et al., 2008a*; *Nel et al., 2009*; *Deng et al., 2011*; *Yoo et al., 2011*). For instance, NPs can induce conformational changes in fibrinogen (*Deng et al., 2011*), tubulin (*Gheshlaghi et al., 2008*), serum albumin (*Wangoo et al., 2008a*), RNase A (*Lee and Belfort, 1989*), hemoglobin (*Shen et al. 2007*) and inhibit the fibrillation process of the amyloid peptide (*Yoo et al., 2011*). In addition, certain NPs induced conformational changes in proteins, but this effect is isozyme-dependent (*Lundqvist et al., 2005*). The cytotoxic mechanism underlying this phenomenon was the potential increased immunogenicity that the NPs can exert by exposing protein epitopes on their surface in an aberrant conformation (*Nel et al., 2009*).

The adsorption of proteins to QD surface leads to the changes in the protein conformation and/or changes in the surface of these NPs (*Shen X. et al., 2007*; *Manokaran et al., 2010*). For instance, the interaction of CdS QDs with human hemoglobin (Hb) results in a significant alteration of its secondary and tertiary structures that leads to quenching of the intrinsic fluorescence of this protein. Raman spectra indicated that the sulfur atoms of the Cys residues form chemical bonds on the surface of the CdS QDs (*Shen X. et al., 2007*).

We performed an *in vitro* enzymatic activity assay (*see "Materials and Methods" for details*) to evaluate if the protein adsorption on CdS QD surface could reduce the activity of the GAPDH, a yeast corona protein. We observed a dose-dependent inhibition of the activity of yeast GAPDH by CdS QDs (Fig. 47). In particular, a strong reduction of the enzyme activity was observed at concentrations of NPs (20 mg/L; Fig. 50) that reduced the viability of wild-type cells (Fig. 46).

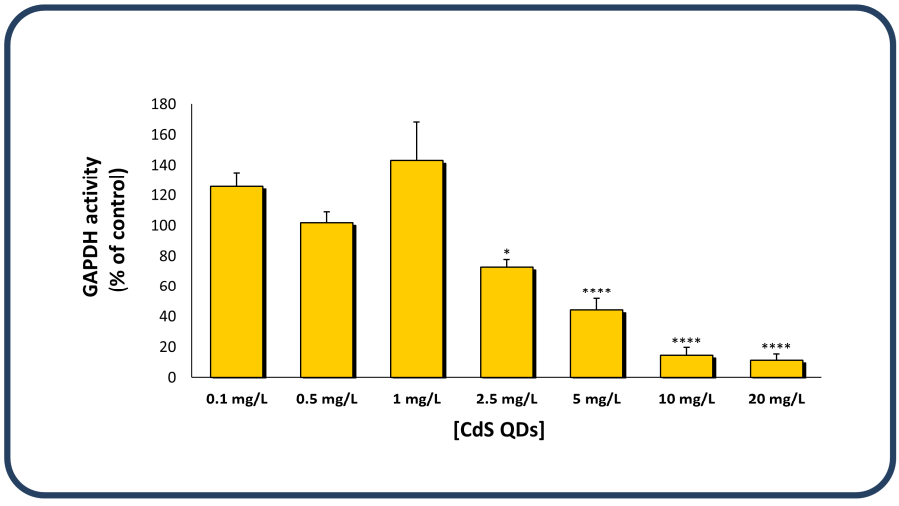

Fig. 47 *Inhibition of GAPDH activity by CdS QDs. Data are reported as means ± SD (*, P-value ≤ 0.05; ****, P ≤ 0.0001).*

GAPDH is a multifunctional protein with defined functions in different subcellular processes, namely a primary role in glycolysis, apoptosis and in a variety of critical nuclear pathways (*Sirover, 2005*). *GAPDH* is overexpressed in various cancer cells, such as lung cancer, prostatic adenocarcinoma, renal cell carcinoma, breast carcinoma cells or hepatocellular carcinoma (*Sirover, 1997*; *Révillion et al., 2000*), and is considered as a novel target for anticancer therapy (*Ray et al.,* 1997; *Pathania et al., 2009*; *Zhang et al., 2015*).

Ghosh and collaborators (*2014*) showed that functionalized metal chalcogenide QDs have a marked affinity towards mouse GAPDH isoforms. These QDs inhibit reversibly GAPDH enzyme activity from normal mouse tissues, whereas isoforms of this enzyme from tumour-associated tissues are irreversibly inhibited at a significantly low concentration of QDs. When cancer cells are exposed to QDs, loss of cellular GAPDH activity causes metabolic perturbation during glycolysis. This suggests a possible mechanism of impaired energy homeostasis during QDs-mediated cellular injury that can cause cell death (*Ghosh et al., 2014*). Spectroscopic evidence reveals that the binding of QDs to rabbit and mouse GAPDHs retains the protein structure (*Ghosh et al, 2014*). Since the active site of GAPDH is surrounded by positively charged amino acid residues, the negatively surface-functionalized QDs can alter the structure of active site and reduce the accessibility of negatively charged substrates (such as GAP).

A critical cysteine residue (Cys-149) in the active site (*Smith et al., 1979*) was supposed to be the target for QD-binding (*Ghosh et al, 2014*). This residue is highly conservated in yeast, mouse and human enzymes and thus these observations suggest that CdS QDs can inhibit yeast GAPDH activity via electrostatic interaction with Cys residue in the active site.

10.2 CdS QDs: human protein corona

10.2.1 Formation of human blood plasma corona on CdS QD surface

The interactions between ENMs and macromolecules in the blood plasma dictate the biocompatibility, delivery and the effects (positive or negative) of these materials. Human blood plasma is constituted by thousands of proteins (ca. 4000), some of which are more abundant (e.g., serum albumin; *Anderson et al., 2004*).

To identify human plasma proteins that form the NP corona, CdS QDs and human plasma proteins were incubated with gentle agitation for 24 hours at 4°C and proteins bound to the NPs were recovered by multiple centrifugation steps and extensively washed to remove almost all nonbound and soft corona proteins. Proteins absorbed on CdS QDs were identified by LC-MS/MS analysis (Fig. 48; Table 6 and 7); among these, apolipoproteins, proteins involved in complement system and in clotting process. These proteins were also detected on other NP-coronas (*Cedervall et al., 2007; Lundqvist et al., 2008; Dobrovolskaia et al., 2008; Deng et al., 2011; Sund et al., 2011; Tenzer et al., 2013*; *Walkey et al., 2014; Chen et al., 2016*).

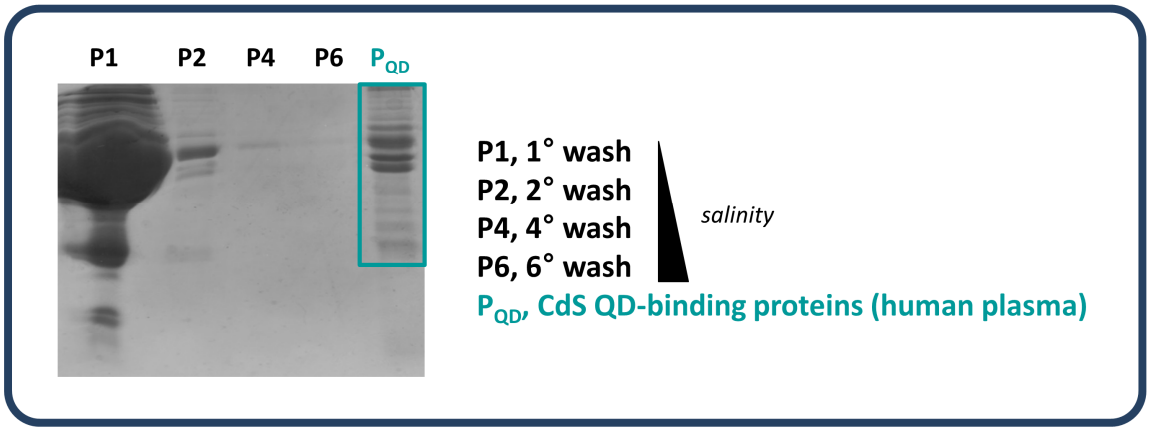

Fig. 48 *Proteomic analysis of the human plasma proteins adsorbed on the surface of CdS QDs with high affinity. Aliquots of the wash solutions (P1-P6; 50% of the total sample) and plasma-derived hard protein corona (P_{QD}; 15% of the total sample) were visualized by 12% SDS-PAGE. Hard protein corona was composed of many different proteins with molecular weights between 30 and 500 kDa.*
P1-P4) Washes (first, second and fourth) of the CdS QD-protein pellet with wash buffer A; P6) Wash (sixth) of the CdS QD-protein pellet with wash buffer B (see "Materials and Methods" for additional details).

Table 6. *Plasma-derived hard corona proteins identified by LC-MS/MS analysis.*

Identified proteins	Score	Coverage	pI
Apolipoprotein B100	629.31	52.58	6.58
Apolipoprotein A1	121.18	76.4	5.56
Apolipoprotein L1	30.50	26.84	5.6
Complement component III (C3)	39.44	25.86	6.02
Fibrinogen, alpha chain	197.89	57.61	5.7
Fibrinogen, beta chain	104.02	47.25	8.54
Fibrinogen, gamma chain	111.12	42.79	5.37
Kininogen I	25.39	25.37	6.34

At the physiological pH of blood plasma (pH=7.3), preferential binding of negatively charged proteins (pI < 7) onto the CdS QD surfaces was observed (Table 6). As reported for yeast protein corona (*see Section 10.1*), these observations leads to suppose that electrostatic interactions may be established between hard corona proteins and CdS QDs.

Interestingly, the most abundant proteins in the plasma (serum albumin and immunoglobulins) were not identified in the hard corona of the CdS QDs. Among other proteins identified in this study, only Apolipoprotein B100 and Apolipoprotein A1 were relatively abundant plasma proteins.

The protein size also played a significant role: few proteins with high molecular mass (> 90 kDa) were find on the NP surfaces (Table 7).

Table 7. *Characteristics of hard corona-plasmatic proteins adsorbed to CdS QDs.*

Identified proteins	UniProt Acc. N.	Mol. weight (kDa)	Biological Process
Apolipoprotein B100	P04114	515	Lipid metabolism
Apolipoprotein A1	P02647	31	Lipid metabolism
Apolipoprotein L1	O14791-3	42	Lipid metabolism
Complement component III (C3)	P01024	187	Complement system
Fibrinogen alpha chain	P02671	69	Clotting process
Fibrinogen beta chain	P02675	56	Clotting process
Fibrinogen gamma chain	P02679	49	Clotting process
Kininogen I	P01042	72	Clotting process

Apolipoproteins, plasma proteins highly enriched in the CdS QD-corona, were involved in lipid transport and metabolism. Apolipoprotein B100 (ApoB100) have been studied extensively because they play central roles in lipoprotein assembly, plasma lipid metabolism and atherogenesis. This lipoprotein is the major protein constituent of cholesterol-rich low density lipoproteins (LDL) and very low density lipoproteins (VLDL). ApoB100 functions as a recognition signal for the cellular binding and internalization of LDL particles by the apoB/E receptor.

Apolipoprotein A1 (ApoA1) is the major protein constituent of high-density lipoprotein (HDL) that transports lipids and cholesterol in the bloodstream, is involved in reverse cholesterol transport and is thought to play an important role in lowering the risk of coronary artery disease. ApoA1 participates in the reverse transport of cholesterol from tissues to the liver for excretion by promoting cholesterol efflux from tissues and by acting as a cofactor for the lecithin cholesterol acyltransferase (LCAT). The most common receptor is scavenger receptor class B type 1 (SR-BI), which mediates the bidirectional lipid transfer between VLDL, LDL and HDL and cells (*Zannis et al., 2006*). SR-BI is expressed mainly in the liver and steroidogenic glands, but also in brain, intestine, and placenta, and in cells such as macrophages and endothelial cells (*Zannis et al., 2006*). Apolipoprotein L1 is a secreted high density lipoprotein which binds to ApoA1. This apolipoprotein L family member may play a role in lipid exchange and transport throughout the body, as well as in reverse cholesterol transport from peripheral cells to the liver.

Several members of the apolipoprotein family, as well as lipid molecules, have also been detected on other ENMs, e.g. polystyrene, solid lipid NPs and carbon nanotubes (*Lundqvist et al., 2008; Cedervall et al., 2007*). Protein binding is one of the key elements that affects biodistribution of the ENMs throughout the body and the interaction between lipoprotein and these materials could affect their biodistribution. In another study, functionalization of the surface of QDs with 5,6-secosterol atheronal-B induced the binding to and misfolding of apolipoprotein B-100 (Apo-B100) in low-density lipoprotein (LDL) in the protein corona. The conformational change induced by the

misfolding of Apo-B100 causes the exposure of epitopes that bind cell-surface receptors on macrophage cells, which ultimately favors the selective uptake of atheronal-modified LDL particles by cells and foam cell formation (*Prapainop et al., 2012*). Furthermore, the discovery that NPs can bind intact lipoprotein complexes offers a new window on nanomedicine, as NPs may also "hitch a lift" on existing cellular lipidic transport pathways

The complement system is a critical component of the innate immunity in the blood and comprising over thirty proteins. The complement system is a proteolytic cascade that converge to generate the same set of effector molecules at the **third component of complement** (C3). C3 plays a central role in the activation of the complement system and also promotes phagocytosis, supports local inflammatory responses against pathogens and instructs the adaptive immune response to select the appropriate antigens for a humoral response. In addition, its interactions with the proteins of foreign pathogens may provide a mechanism by which these microorganisms evade complement attack. In chronic inflammation, C3 acts as a chemoattractant for neutrophils. It induces the contraction of smooth muscle, increases vascular permeability and causes histamine release from mast cells and basophilic leukocytes. C3 is an ancient molecule; its identification in echinoderms and tunicates suggests that it emerged at least 700 million years ago, long before the appearance of immunoglobulins.

Complement proteins were consistently identified in high-throughput proteomic screens of NP coronas (*Lundqvist et al., 2008*; *Tenzer et al., 2013*; *Walkey et al., 2014; Chen et al., 2016*). Complement proteins deposit on the surface of NPs in a process called "opsonization". C3 activation by pathway-specific C3 convertases generates C3b and iC3b; these species prime the surface of a NP for engulfment by leukocytes and macrophages through complement receptors (*Moghimi et al., 2003*). The ways complement proteins assemble on NPs have remained unclear. Activation of the complement cascade on exposure to several NPs leads to hypersensitivity reactions and anaphylaxis (*Dobrovolskaia et al., 2008*). Moreover, binding of complement proteins to NPs can activate complement processes that eventually cause inflammation (*Qu et al., 2012*). Inflammation has been shown to directly cause toxicity and promote cell death through the induction of toxic by-products of inflammation such as ROS and complement proteins, as well as via receptor-induced apoptosis/necrosis (*Wallach et al., 2015*). NPs may be designed to avoid such immune toxicity and so improve their safety.

Human plasma proteins isolated in CdS QD-corona were also involved in clotting process: fibrinogen (alpha, beta and gamma chain) and kininogen 1. **Fibrinogen** is synthesized in the liver and constitutes 7% of blood proteins. The intact protein has a molecular weight of 340 kDa and is composed of 3 pairs of disulphide-bound polypeptide chains named Aα, Bβ and γ. Fibrinogen is a triglobular protein consisting of a central E domain and terminal D domains. Proteolysis by thrombin results in release of Fibrinopeptide A (FPA, Aα1-16) followed by Fibrinopeptide B (FPB, Bβ1-14) and the fibrin monomers that result polymerize in a half-overlap fashion to form insoluble fibrin fibrils. The chains of fibrin are referred to as α, β and γ, due to the removal of FPA and FPB. Fibrin has a major function in hemostasis as one of the primary components of blood clots. Fibrinogen is essential for platelet aggregation and acts during the early stages of wound repair to stabilize the lesion and guide cell migration during re-epithelialization. It's known that fibrinogen was denatured to a greater extent on the surface of small NPs (*Roach et al., 2006; Deng et al., 2011*). Complement factors and fibrinogen can promote phagocytosis and removal of the NPs from systemic circulation via cells of the reticuloendothelial system. These NPs were sequested in the reticuloendothelial system organs very rapidly and concentrated in the liver and spleen (*Dobrovolskaia et al., 2007*).

Kininogen 1 (Kng1), also known as alpha-2-thiol proteinase inhibitor, is the precursor protein of low-molecular-weight kininogen (LMWK) and high molecular-weight kininogen (HMWK), essential for blood coagulation. Kng1 was adsorbed on hydrophilic inorganic NPs, polymer NPs and NPs with hydrophobic surface component (*Karmali and Simberg, 2011*).

We observed that CdS QDs bind several proteins involved in blood coagulation and some reports suggest that ENMs can induce platelet aggregation, but the underlying mechanisms are largely unknown (*Dobrovolskaia et al., 2009a*).

Adsorbtion onto NP surface may caused conformational changes, exposure of protein epitopes that can mediate cytotoxic mechanisms (*Nel et al., 2009*). For example, it was demonstrated that functionalized gold NPs induced unfolding of adsorbed fibrinogen that, in turn, interacted with the leukocyte receptor MAC-1, thereby triggering an inflammatory response (*Deng et al., 2011*).

It is possible hypothesize that conformational changes in the identified plasma proteins may also occur during the adsorption on CdS QDs and facilitate this interaction. About this hypothesis, we observed that the identified proteins have a high frequency of disordered regions (DRs; Fig. 49). DRs are defined as regions of proteins that lack a fixed tertiary structure; DRs are involved in a variety of functions (*Dunker et al., 2001*), including DNA/RNA/protein recognition, modulation of specificity/affinity of protein binding, molecular threading and activation by cleavage. For example, 16 DRs, of which a very long DR (129 amino acids; Fig. 49), were predicted in the fibrinogen alpha chain (FibA) sequence using PONDR® (Predictors of Natural Disordered Regions; www.pondr.com) software.

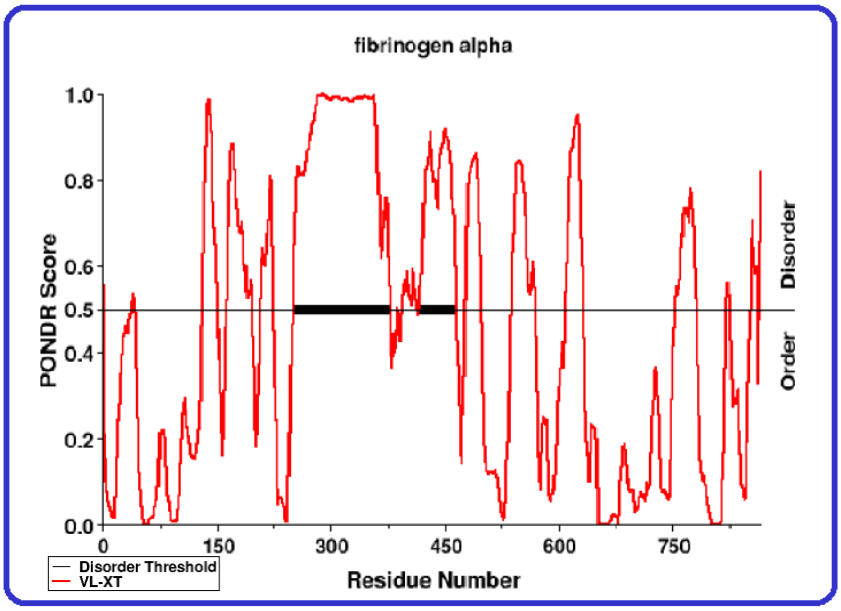

Fig. 49 *Prediction of DRs in the human FibA protein. Graphical representation of the PONDR® output that showed long DRs (indicated with black segments) in FibA sequence. PONDR software use the VL-XT algorithm (www.pondr.com).*

10.2.2 Identification of human proteins (Caco-2 cell line) with high affinity for CdS QDs

The respiratory system and the GI tract are considered to be the main routes by which ENMs may access the body. After inhalation, the majority of ENMs are transported out of the lung by the mucociliary clearance mechanism, swallowed and enter in the GI tract (*Docter et al., 2014*). The GI tract is a major biobarrier target organ for ENMs due to its huge surface area. Also, GI is specialized in the uptake and excretion of various molecules and thus, connects the environment to the bloodstream. A well accepted *in vitro* model to study ENM exposure via the oral route is the epithelial colonic carcinoma cell line Caco-2, which has features consistent with differentiated small intestinal enterocytes (*Docter et al., 2014*).

Here, we employed CdS QDs and Caco-2 cell line as a model to study the protein corona formation in the GI tract cells. Firstly, we evaluated the effect of CdS QDs (dose range 10–160 µg/ml) on the viability of Caco-2 cells after 24 hour of exposure using AlamarBlue® viability assay (Fig. 50). CdS QDs slightly lowered cell viability inducing a maximal decrease of 16%.

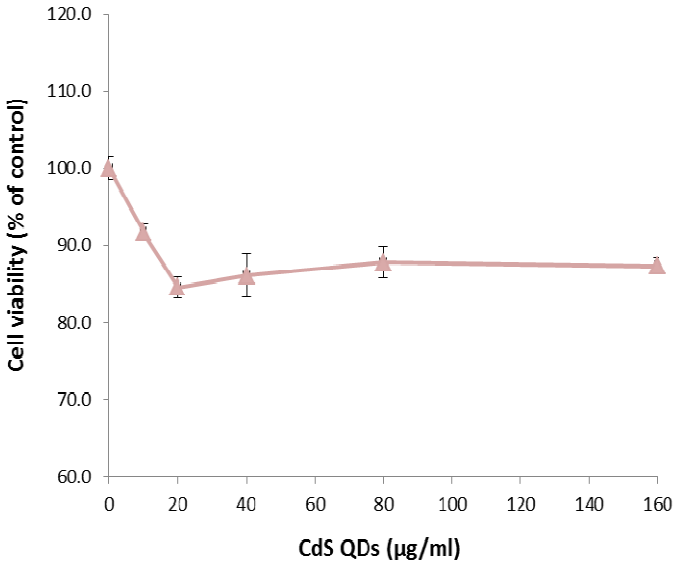

Fig. 50 *Effect of CdS QDs on cell viability of Caco-2 cell line. Untreated Caco-2 cells were used as control sample (100%).*

To identify Caco-2 proteins that form the NP corona, CdS QDs and human protein extracts were incubated with gentle agitation for 24 hours at 4°C and proteins bound to these NPs were recovered by multiple centrifugation steps and extensively washed to remove almost all nonbound and soft corona proteins. Proteins absorbed on CdS QDs were identified by LC-MS/MS analysis (Fig. 51; Table 8); among these, proteins involved in acid nucleic binding, in transporter activity and cytoskeleton components were adsorbed to CdS QDs (Table 9).

As observed for yeast and plasma corona, most of the identified proteins have a pI <6.5 (70%; Table 8) and a molecular weight of less than 90 kDa (100%; Table 9) supporting the hypothesis that negatively charged proteins with sizes comparable to thse NPs were adsorbed to the surface of CdS QDs.

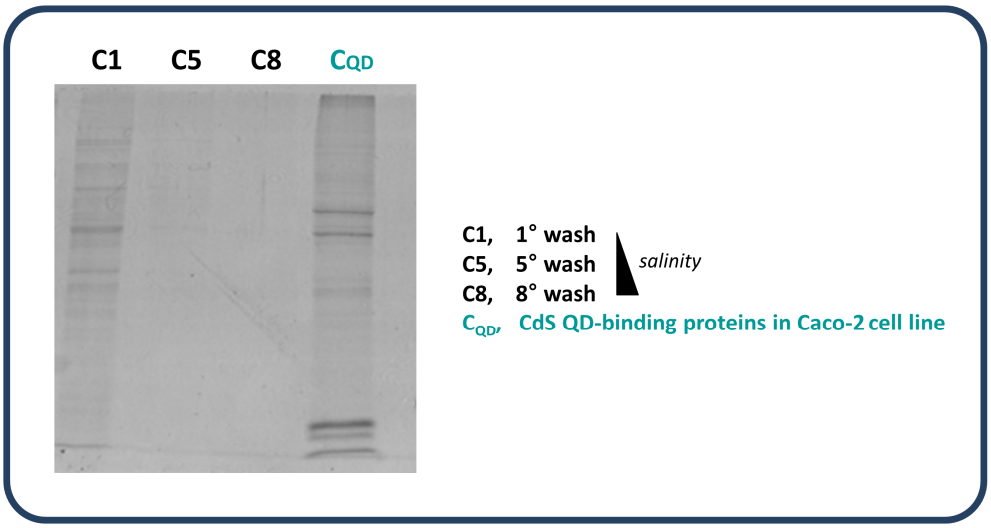

Fig. 51 *Proteomic analysis of the human proteins (Caco-2 cell lines) adsorbed on the surface of CdS QDs with high affinity. Aliquots of the wash solutions (C1-C8; 50% of the total sample) and human-derived hard protein corona (C_{QD}; 15% of the total sample) were visualized by 12% SDS-PAGE. Hard protein corona was composed of many different proteins with molecular weights between 10 and 100 kDa.*
C1-C5) Washes (first and fifth) of the CdS QD-protein pellet with wash buffer A; C8) Wash (eighth) of the CdS QD-protein pellet with wash buffer B (see "Materials and Methods" for additional details).

Table 8. *Human-derived hard corona proteins identified by LC-MS/MS analysis.*

Identified proteins	Score	Coverage	pI
Tubulin beta chain	86.83	54.95	4.89
Tubulin alpha-1B chain (Isoform 2)	58.91	42.09	4.94
Keratin (type II), cytoskeletal 8	102.74	43.69	5.59
Keratin (type I), cytoskeletal 18	142.49	35.58	5.45
Heterogeneous nuclear ribonucleoprotein U	20.60	11.99	6.43
Histone H2B	123.35	60.24	10.32
Histone H3	40.13	57.58	11.30
Facilitated glucose transporter, member 3 variant	22.13	16.96	5.92
Glutamate dehydrogenase 1, mitochondria	18.71	12.28	7.58

Table 9. *Characteristics of hard corona proteins adsorbed to CdS QDs.*

Identified proteins	UniProt Accession N.	Mol. weight (kDa)	Biological Process
Tubulin beta chain (Tbb5)	P07437	49.6	Cytoskeleton
Tubulin alpha-1B chain (Tba1b)	P68363	37.2	Cytoskeleton
Keratin (type II), cytoskeletal 8 (K2c8)	P05787	53.7	Cytoskeleton
Keratin (type I), cytoskeletal 18 (K1c18)	P05783	48	Cytoskeleton
Heterogeneous nuclear ribonucleoprotein U (HnRNPu)	Q00839	86.8	DNA and RNA binding
Histone H2B	B4DR52	18	DNA binding
Histone H3 (H33)	P84243	14.9	DNA binding
Facilitated glucose transporter, member 3 variant	Q59F54	31.9	Transporter activity
Glutamate dehydrogenase 1, mitochondria (Glud1)	P00367	42.9	Biosynthetic process

Interestingly, we observed that several proteins involved in acid nucleic binding are adsorbed to CdS QDs, in particular, two histones (H2B and H3), a ribonucleoprotein (heterogeneous nuclear ribonucleoprotein U) and HMG-I/Y protein. Histones are a family of basic proteins that associate with DNA in the nucleus and form the chromatin. The complex array of histone modifications/variants alter the overall charge and conformation of chromatin which helps in recruitment of factors at damage site to facilitate repair, and thus in maintaining genomic integrity in response to DNA damaging agents. Furthermore, histones are involved in transcription regulation and DNA replication. Notably, it is known that QDs, due to their small size, were able to enter the nucleus through the nuclear pore, inducing nuclear protein aggregation, as well as the inhibition of gene transcription and cell proliferation (*Nabiev et al., 2007*) and direct damage to chromosomes or nucleoproteins (*Singh et al., 2009*). Insteed, QDs exhibit strong affinity to core histones and histone-rich cell organelles (*Conroy et al., 2008*). Histone binding is driven by electrostatic interactions between negatively charged QDs and positively charged core histone proteins.

Heterogeneous **nuclear ribonucleoproteins** (hnRNPs) are a family of proteins which share common structural domains; they have central roles in DNA repair, telomere biogenesis, cell signaling and in regulating gene expression at both transcriptional and translational levels. Through these key cellular functions, individual hnRNPs have a variety of potential roles in tumour development and progression including the inhibition of apoptosis, angiogenesis and cell invasion. Furthermore, hnRNPs bind double- and single-stranded DNA and RNA molecules.

HMG-I/Y proteins binds preferentially to the minor groove of A/T rich regions in double-stranded DNA molecules. It is suggested that these proteins could function in nucleosome phasing and in the 3'-end processing of mRNA transcripts. They are also involved in the transcription regulation of genes containing or in close proximity to A/T-rich regions.

The interaction between these nuclear proteins and CdS QDs could result in alteration in their cellular role, from DNA damage susceptibility to aberrant transcriptional and replication processes.

CdS QDs bind with high affinity several cytoskeletal elements (Tables 8 and 9): keratins 8 and 18; tubulin beta chain (Tbb5) and tubulin alpha-1B chain (Tba1b). **Keratins** are fibrous

structural proteins that regulate protein synthesis and epithelial cell growth. Keratins 8 and 18 are major components of the intermediate filaments (IFs) of single-layered epithelia, as found in the GI tract, liver, and exocrine pancreas. Keratins have also involved in secretion and protection against chemical injury.

Tubulin is the major building block of microtubules, that are essential in many cell functions, as cell division, intracellular transport or flagellar movement. Notably, significant structural changes in actin and tubulin networks were observed in 3T3 fibroblasts after incubation with CdSe/ZnSe QDs (*Mahto et al. 2010*). In addition, exposure to metal-based NPs also leads to alterations in the cellular cytoskeletal network (*Pernodet et al., 2006*; *Mironava et al., 2010; Wu et al., 2010*; *Soenen et al., 2010*), inducing conformational changes in tubulin structure (*Gheshlaghi et al., 2008*).

NPs with different shapes could lead to different effects on the cytoskeleton of the same cell lines (*Huang et al., 2010*). For istance, gold nanomaterials have also been reported to induce cytoskeletal defects as well as profound effects on the morphology of several cell types, such as A549 human lung carcinoma cells (*Patra et al., 2007*). Gold NPs have also been described to have a concentration-dependent effect on the actin fibrils of human dermal fibroblasts (*Pernodet et al., 2006*). Furthermore, disruption of cytoskeletal filaments is a function of gold NPs exposure time, concentration and size, although actin or β-tubulin protein expression levels are not affected (*Pernodet et al., 2006*; *Mironava et al., 2010*). Furthermore, exposure to metal-oxide NPs, such as ZnO or Fe_2O_3, leads to alterations in the cellular cytoskeletal network. Fe_2O_3 NPs greatly disrupted actin fibers and tubulin network of human umbilical vein endothelial cells (HUVECs) and also impeded the maturation of focal adhesion complexes, which linked the cytoskeletal network to the extracellular matrix (*Wu et al., 2010*). A variety of Fe_2O_3 NPs, including lipid-dextran-and citrate-coated, induced actin and tubulin network deformations when high intracellular levels were reached in neural progenitor cells and primary human blood outgrowth endothelial cells (*Soenen et al., 2010*). Thus, the cytoskeleton plays an important role in the NP uptake process as well as cytotoxicity research.

Other proteins that have been found in the CdS QD-corona are a glucose transporter and a mitochondrial glutamate deydrogenase. Facilitated **glucose transporter** is responsible for constitutive or basal glucose uptake. This transporter has a very broad substrate specificity and can transport a wide range of aldoses, including both pentoses and hexoses.

Glutamate deydrogenase 1 (Glud1) is a mitochondrial enzyme that converts L-glutamate into alpha-ketoglutarate. Glud1 plays a key role in glutamine anaplerosis by producing alpha-ketoglutarate, an important intermediate in the tricarboxylic acid cycle.

As observed for plasma proteins, several DRs are predicted in most of the corona protein sequences identified in Caco-2 cells; in particular, Histone H3 and hnRNPu contain long DRs (Fig. 52 and 53).

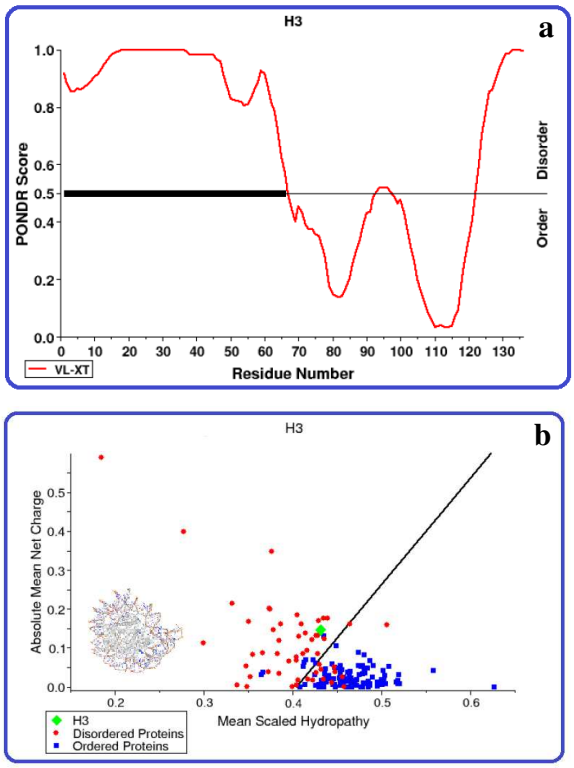

Fig. 52 *Prediction of DRs in histone H3 protein sequence. a) Graphical representation of the PONDR® output that showed long DRs (indicated with black segments) in histone H3 sequence. b) Charge-hydropathy (C-H) plot using PONDR®. The plot compares the absolute mean net charge and the mean scaled hydropathy of completely disordered proteins (red) and completely ordered proteins (blue). Ordered and disordered proteins can be separated to a significant degree by a linear boundary (black line), with proteins located above this boundary line being natively unfolded and with proteins below the boundary line being ordered. Histone H3 (green dot) is located in the protein disordered group.*

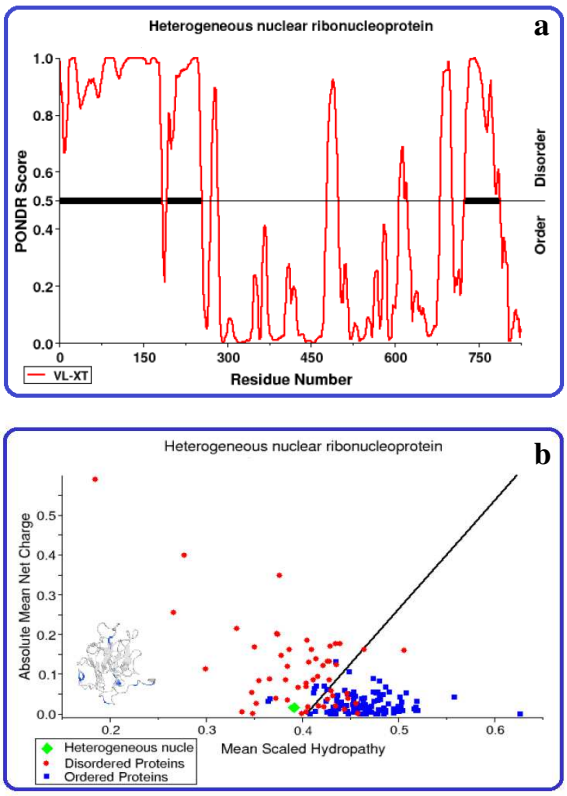

Fig. 53 *Prediction of DRs in hnRNPu protein sequence. a) Graphical representation of the PONDR® output that showed long DRs (indicated with black segments) in hnRNPu sequence. b) Charge-hydropathy plot using PONDR®. HnRNPu (green dot) is located in the protein disordered group.*

11. RESULTS AND DISCUSSION: SILICA NPs.

SiO_2 NPs is one of the most used ENMs (*Piccinno et al., 2012*). Silica NPs are applied as food additive (E551), but have also attracted much attention because offer great potential for various applications (e.g., as drug carriers) due to their unique properties such as the variety of surface modifications and their convenient synthesis.

The assessment of amorphous silica being non-toxic is mostly based on the testing of micrometer-sized bulk materials. Whether nano-sized amorphous silica should be considered as a completely novel entity of materials is still an ongoing debate in the growing field of nanotechnology. Consequently, the present PhD thesis investigated the potential toxic effects of SiO_2 NPs, focusing on the characterization of silica NPs-protein corona.

11.1 Characterization of SiO_2 NPs

A detailed physico-chemical characterization of the SiO_2 NPs was provided in the report on the synthetic amorphous SiO_2 NPs of the JRC Repository (*Rasmussen et al., 2013*). NPs used in this study are provided by Prof. Bussolati (Dep. S.Bi.Bi.T., University of Parma) and are produced via the thermal route, that is burning $SiCl_4$ in an oxygen-rich hydrocarbon flame to produce a fume of SiO_2 (*Rasmussen et al., 2013*).

Physico-chemical properties of SiO_2 NPs are indicated in Table 10. NPs were dispersed into 0.05% BSA in water, at the concentration of 2.56 g/L, as indicated by JRC Repository. Primary particle size is 13 ± 6 nm, but SiO_2 NPs form agglomerates with an average size of 138.3 ± 16 nm in our reaction conditions.

Notably, the surface of silica is composed of silanol groups (Si-OH), with hydrophilic properties and siloxane bridges (Si-O-Si) (*Napierska et al., 2010*). At neutral pH, the silanol groups tend to be deprotonated leading to a negatively charged surface (*Klein et al., 2016*), as indicated by a negative value of zeta potential (Table 10).

Table 10. *Physico-chemical properties of SiO_2 NPs.*

Indicative content of SiO_2 (% wt)	**Crystallinity**	**Primary particle size (nm)[1]**	**Specific surface area (m^2/g)[2]**	**Zeta potential (surface change)**
99% Si content: 46.3%	amorphous	13± 6	203.92	-46.1 mV (in milliQ water at pH=6.6)

[1]TEM analysis. The TEM specimens of suspended ASNP were prepared on 300-mesh Cu lacey carbon grids by drop-casting and were visualized under a Jeol 2100 TEM (Jeol Ltd) operating at 200 kV with a Lanthanum Hexaborise emission source.

[2]Brunauer-Emmett-Teller (BET) Surface Area Analysis provides precise specific surface area evaluation of materials by nitrogen multilayer adsorption measured as a function of relative pressure using a fully automated analyser. The technique encompasses external area and pore area evaluations to determine the total specific surface area in m^2/g yielding important information in studying the effects of surface porosity and particle size in many applications.

11.2 Exposure of S. cerevisiae to SiO_2 NPs

We evaluated the cytotoxic effects of SiO_2 NPs in *S. cerevisiae*. Serial dilution assay of wild-type (BY4742) cells were performed on standard synthetic media supplemented with glucose (2%) as carbon source (SD) in the absence or in the presence of SiO_2 NPs (0.25-2 g/L; *see "Materials and Methods" for details*). In contrast to CdS QDs (Fig. 54), the results showed a low toxicity of SiO_2 NPs in wild type strain, also exposed to high concentrations of NPs (2 g/L). It is possible that differences in cytotoxicity between the two types of NPs could be correlated with different uptake rates. In fact, SiO_2 NPs form aggregates in SD medium and the effective size of NPs (140 nm, average size) can greatly exceed their primary particle size (Table 10). Experiments to evaluate the internalization levels of SiO_2 NPs are still ongoing.

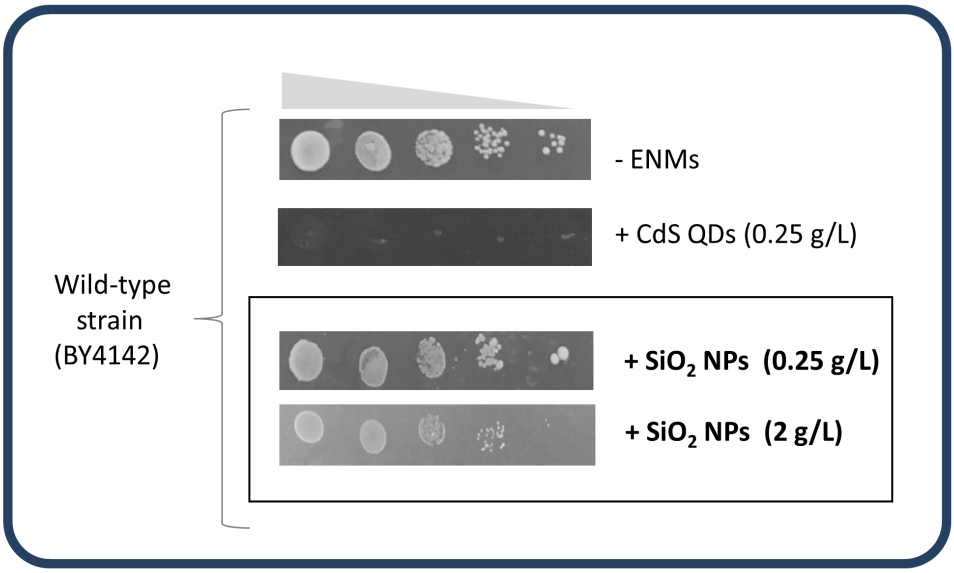

Fig. 54 *Silica NPs showed low toxicity in yeats cells. Serial dilution assay (spot assays) of wild-type strain grown in the absence (- ENMs) or in the presence of CdS QDs (0.25 g/L) or SiO_2 NPs (0.25-2 g/L), on standard synthetic media supplemented with glucose (2%) as carbon source (SD).*

11.2.1 SiO_2 NP-protein corona assay conditions

To identify yeast proteins which were adsorbed on the SiO_2 NP surface, NPs and protein extracts were incubated with gentle agitation. After incubation, the NPs and corona proteins were recovered by centrifugation and washed to remove nonbound proteins. After three centrifugation steps followed by resuspension in wash buffer, the adsorbed proteins were eluted from the NP surface and analyzed with SDS-polyacrylamide gel electrophoresis to estimate molecular masses and relative abundance of polypeptides (Fig. 55; *see "Materials and Methods" for additional details*).

As for CdS QDs, to determine the optimal conditions for the binding assay, adsorption of yeast proteins to the surface of SiO_2 NPs was analyzed in the presence of different amount of yeast protein extracts (0.1-1 mg), different times of exposure (1-24 hours) and temperature (4°C-37°C) incubation. For each condition tested, SiO_2 NP-corona proteins were analyzed with SDS-PAGE. Based on a visual evaluation of the SDS-PAGE gels, the total amounts of adsorbed proteins were strongly increased with the increase of the protein extract concentration (Fig. 55) and the time of

exposure (data not shown). Importantly, quantitative, but not qualitative, differences were detected in the protein profiles visualized in SDS-PAGE (Fig. 55).

Thus, to maximize the amount of adsorbed proteins, we proceeded to carry out the experiments in the same conditions used for CdS QDs: yeast extracts (1 mg, total protein extract), incubation time for 24 hours at 4°C.

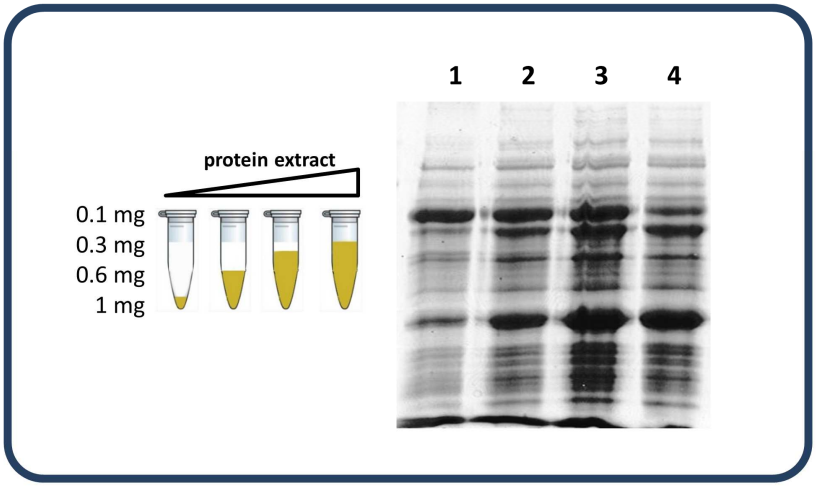

Fig. 55 *Yeast proteins adsorbed onto silica NP surface. Different amounts of yeast proteins were adsorbed to SiO_2 NPs; increasing yeast protein extract concentration [0.1 mg (1), 0.3 mg (2), 0.6 mg (3), 1 mg (4)] corresponded to a greater adsorption on the NPs. We loaded in 12% SDS-PAGE the 50% of the proteins eluted from samples 1,2 and 3, while we loaded the 25% of the proteins eluted from sample 4.*

11.2.2 Identification of yeast proteins with high affinity for SiO_2 NPs

To identify yeast proteins that form the hard corona in SiO_2 NPs, after incubation for 24 hours, proteins bound to the NPs were recovered by multiple centrifugation steps and extensively washed to remove almost all nonbound and soft corona proteins (*see "Materials and Methods" for additional details*). Hard corona proteins were eluted from the NP surface, visualized by gel electrophoresis and quantitatively analyzed (after tryptic digestion) using LC–high-resolution MS using LTQ-ORBITRAP XL mass spectrometer, as performed for CdS QDs. The experiments were carried out in three independent replicates. In yeast, the hard corona of the SiO_2 NPs was composed of many different proteins with molecular weights between 10 and 120 kDa (Fig. 56; Tables 11 and 12). The proteins that contribute to the formation of this protein corona were involved in translation processes, in energy and cell metabolism (Table 12).

SiO_2 NPs were prepared according to the protocol of the JRC Repository (*Rasmussen et al., 2013*) that includes the addition of BSA during the dissolution of the NPs. We wondered if the presence of the BSA could alter the binding of yeast proteins to silica NPs and we executed the binding assay under the same conditions described above, but using a silica NPs preparation obtained without BSA. Hard corona proteins adsorbed on SiO_2 NPs obtained by the two silica NP preparations were eluted and analysed with SDS-PAGE (Fig. 57). Quantitative differences were detected in the observed protein profiles: the band intensities of corona proteins from BSA-added NPs was higher than the silica preparation without BSA. Thus, the presence of BSA did not alter the protein pattern, but the relative protein abundance (Fig. 57). From a qualitative point of view, BSA is the only different protein band in the sample obtained by NPs dispersed in BSA (Fig. 57).

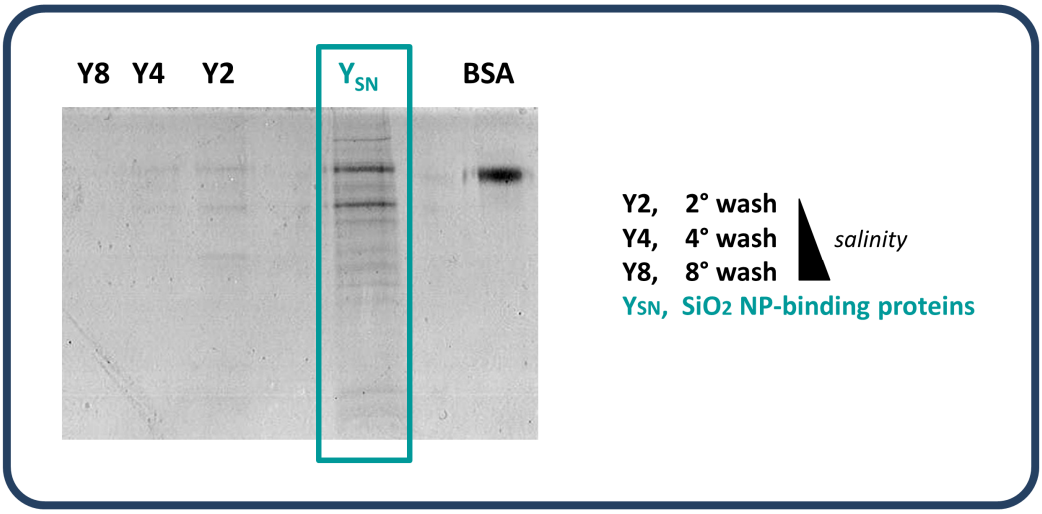

Fig. 56 *Proteomic analysis of the yeast proteins adsorbed on the surface of SiO_2 NPs with high affinity. Aliquots of the wash solutions (Y1-Y8; 50% of the total sample) and yeast-derived hard protein corona (Y_{SN}; 15% of the total sample) were visualized by 12% SDS-PAGE. Hard protein corona was composed of many different proteins with molecular weights between 10 and 120 kDa.*
Y2-Y4) Washes (second and fourth) of the SiO_2 NP-protein pellet with wash buffer A; Y8) Wash (eighth) of the SiO_2 NP-protein pellet with wash buffer B (see "Materials and Methods" for additional details).

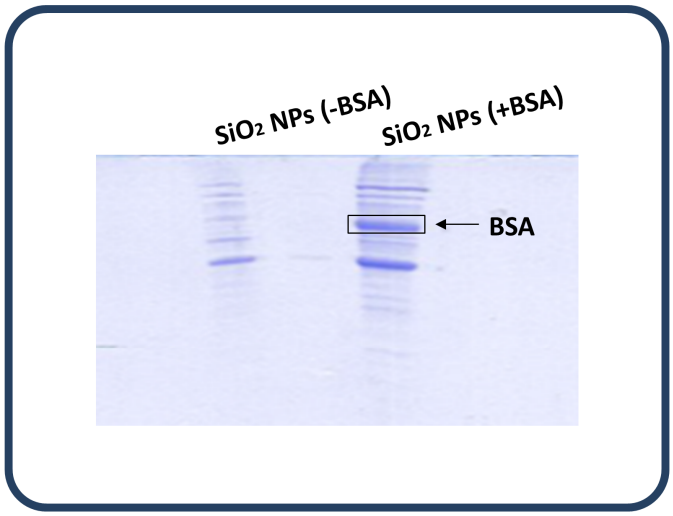

Fig. 57 *Hard protein corona obtained from SiO_2 NPs dispersed (+BSA) or not (-BSA) in 0.05% BSA-water milliQ. Yeast protein extract was exposed for 24h at 4°C to SiO_2 NPs (+/-BSA).*

Table 11. *Yeast-derived hard corona proteins identified by LC-MS/MS analysis.*

Identified proteins	***Score***	***Coverage***	***pI***
Tef1	234.62	71.83	9.14
Yef3	194.22	58.91	5.73
Stm1	63.41	55.68	9.66
Cdc19	63.14	43.80	7.56
Eft2	36.70	17.81	9.10
Tma10	32.56	67.44	9.75
Tif3	27.71	22.02	5.17
Rpl12a	25.62	55.76	10.10
Gus1	23.94	12.57	7.21
Shm2	20.95	17.06	6.98
Mbf1	20.33	27.15	10.61

Table 12. *Characteristics of hard corona proteins adsorbed to silica NPs.*

Identified proteins	**Sistematic name and description (SGD)**	**Mol. weight (kDa)**	**Biological Process**
Rpl12a	YOL039W, Ribosomal 60S subunit protein L12A	18	Translation process
Stm1	YLR150W, Protein required for optimal translation under nutrient stress	30	Translation process
Tma10	YLR327C, Translation Machinery Associated, protein of unknow function that associates with ribosomes	10	Translation process
Tif3	YPR163C, Translation Initiation Factor 3	49	Translation process
Tef1	YPR080W, Translation Elongation Factor	50	Translation process
Eft2	YDR385W, Elongation Factor 2	92	Translation process
Yef3	YLR249W, Translation Elongation Factor 3	116	Translation process
Cdc19	YAL038W, Pyruvate kinase	54	Energy metabolism
Mbf1	YOR298C, Transcriptional coactivator	16	Transcription
Gus1	YGL245W, Glutamyl-tRNA synthetase	81	Cell metabolism
Shm2	YLR058C, Serine hydroxymethyltransferase	52	Cell metabolism

Notably, several yeast proteins (Eft2, Tef1, Cdc19, Yef3) have also been identified in hard corona of CdS QDs (see Section 10.1).
Several corona proteins specifically adsorbed to silica NPs were involved in translation process. Among these, **Rpl12a** is a component of the large ribosomal subunit and is involved in the interaction between translational elongation factors and the ribosome. Notably, Taniguchi et al. (*2007*) showed that the *Escherichia coli* ribosomal protein L2 strongly adsorb to silica NPs.
Stm1 is a 30-kDa basic protein required for optimal translation under stress condition. Stm1 was originally identified as a protein with a high affinity for nucleic acid structures, as G4 quadruplex and antiparallel purine motif triplex. These structures may be present at DNA telomeres or in rRNAs. Recent studies have proposed a role for Stm1 in a variety of biological processes, ranging from telomere maintainance to apoptosis.
Tif3 is a translation initiation factor; this protein consists of three domains: the N-terminal domain (1–182 amino acids) with an RNA recognition motif (RRM); the middle region, composed by a seven-fold repeat of 26 amino acids rich in basic and acidic residues (183–350 amino acids); a C-terminal domain without homology to any known sequence (351–436 amino acids). Tif3 has RNA annealing activity, interacts with Rps20p at the head of the 40S ribosomal subunit and alters the structure of the mRNA entry channel.
Tma10 is a protein of unknown function that associates with ribosomes; its abundance increases in response to DNA replication stress.
Adsorption to silica NPs of translation initiation (Tif3) and elongator (Eft2, Tef1, Yef3) factors may lead one to suppose that these NPs (as well as the CdS QDs) can cause problems to protein synthesis in yeast. In fact, Klein et al. (*2016*) showed that NPs of smaller size (10-20 nm) than SiO_2 NPs are able to inhibit protein synthesis *in vitro*.

Other proteins specifically isolated in SiO_2 NP-corona were involved in several metabolic processes. **Gus1** is nucleic acid-transacting protein localized to the mitochondria and cytosol. Gus1 catalyzes the attachment of glutamate to $tRNA_{Glu}$ in a two-step reaction: glutamate is first activated by ATP to form Glu-AMP and then transferred to $tRNA_{Glu}$. In mitochondria, constitutes the nondiscriminating glutamyl-tRNA synthase that generates the mitochondrial mischarged glutamyl-$tRNA_{Glu}$ substrate for the tRNA-dependent amidotransferase, which generates mitochondrial glutaminyl-$tRNA_{Glu}$ by transamidation of glutamyl-$tRNA_{Glu}$.
Shm2 is a serine hydroxymethyltransferase, the major isoform involved in generating precursors for purine, pyrimidine, amino acid, and lipid biosynthesis; Shm2 is involved in the pathway of tetrahydrofolate interconversion that converts serine to glycine and methylenetetrahydrofolate.
Mbf1 is a transcriptional coactivator that connects a regulatory factor and TATA element-binding protein.

Interestingly, Tef1, Rpp2a, Tif3, Eft2, Tma10, Shm2 and Mbf1 are highly conserved proteins and have human orthologs (Ensembl database; http://www.ensembl.org/index.html).

In contrast to CdS QDs, 60% of the isolated corona proteins has a pI >7.5, indicating that these proteins exhibit a net positive charge at physiological pH. Notably, most of these proteins (Table 13) has a significantly high frequency of Lys and/or Arg residues (Fig. 58). These results are in agreement with the observation that silica NPs have a negatively charged surface (Table 10). Protein adsorption to silica NPs is known to depend on electrostatic interactions and flexibility properties (*Ikeda and Kuroda, 2011*; *Klein et al., 2016*). As observed for SiO_2 NPs of smaller size (10-20 nm) than those used in this work (*Klein et al., 2016*), we also highlighted a high frequency of non-polar amino acids with small lateral residues, especially in the coil/loop regions of these proteins, and the presence of long DRs in the N- and/or C-terminal regions of the identified corona protein sequences (Table 10 and Fig. 59). The high flexibility provided by long DRs could allow to establish large contact areas by conformational adaptation of the proteins to the NP surface (*Tosaka et al. 2010; Ikeda and Kuroda, 2011; Klein et al., 2016*). Indeed, Tosaka et al. (*2010*) showed that the *E. coli* ribosomal protein L2 strongly adsorb to silica NPs mainly through two DRs of 60 and 70 amino acids. Thus, it is possible that proteins that contain DRs can be adsorbed with a high affinity to SiO_2 NPs and that DRs act as binding sites, especially if parts of these regions are positively charged and can establish electrostatic interactions with the electronegative silica surface.

Karlsson et al. (*2005*) have demonstrated that the adsorption of human carbonic anhydrase II onto negatively charged silica nanoparticles appears to be specific to limited regions at the N-terminal domain of the protein. In this work, the orientation of the bound proteins is also pH-dependent. At pH 6.3, a histidine-rich area is the dominant binding region. At higher pH values (e.g., pH 9.3), the protein is adsorbed near a region, which contains several lysine and arginine residues. This absorption behavior indicates that specific binding may be a result of electrostatic interactions between the positively charged areas on the protein surface and the negatively charged NPs.

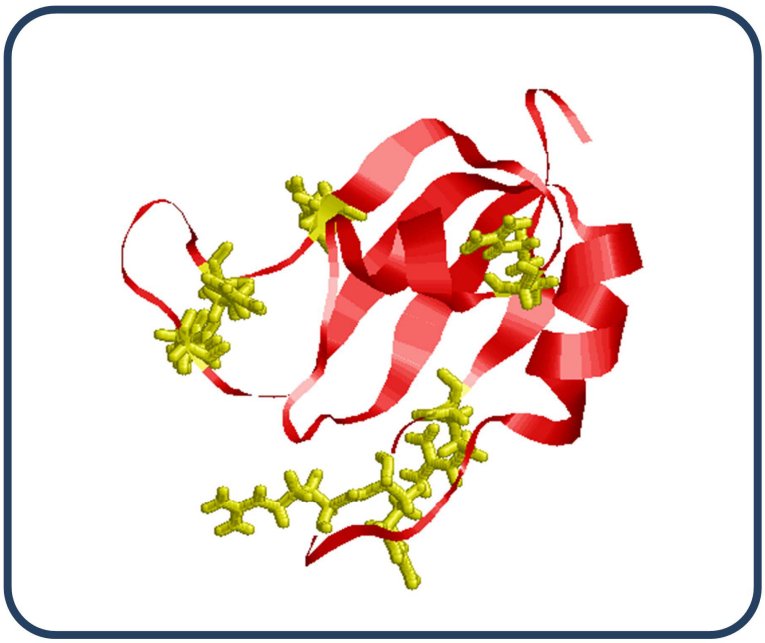

Fig. 58 *3-D structure of the Tif3 protein. Arg residues are shown in yellow (image was generated with RasMol software).*

Table 13. *Amino acid frequencies in the corona protein sequences.*

	Yeast proteome (mean)[1]	Corona proteins[2]										
		Cdc19	**Eft2**	**Yef3**	**Tef1**	**Gus1**	**Mbf1**	**Rpl12a**	**Shm2**	**Stm1**	**Tif3**	**Tma10**
Acidic amino acids (negatively charged)												
Ala	5.7	8.6 (*)	8.1 (*)	8.7 (*)	8.1 (*)	7.3	9.3 (*)	9.7 (*)	8.3	11.7 (*)	8.7 (*)	1.2 (#)
Gly	5.2	6.8 (*)	7.0 (*)	6.0 (*)	9.2 (*)	5.1	9.3 (*)	7.9 (*)	7.5	4.8	8.0 (*)	11.6 (*)
Val	5.8	9.6 (*)	9.6 (*)	6.8 (*)	10.0 (*)	7.1	7.3	7.9	6.6	5.9	6	3.5 (#)
Pro	4.3	5.0 (*)	4.8	4.1	5.0 (*)	4.2	4.6	6.7 (*)	5.1	4.8	6.9 (*)	3.5
Ile	6.5	7.4	5.9	7.5	6.6	6.8	5.3	9.1 (*)	6.6	1.8 (#)	2.8 (#)	4.7
Leu	9.6	7	8.2	8.3	5.2	8.5	6.0 (#)	6.7 (#)	7.9	4.4 (#)	4.8 (#)	3.5 (#)
Phe	4.7	3	4.2	3.4	3.7	4	0.0 (#)	2.4	3.2	2.2 (#)	3	3.5
Trp	1.1	0.2	1	1.1	1.3	1.7	0.7	0.0 (#)	0.6	0.4	2.5 (*)	2.3 (*)
Tyr	3.4	3	2.4	1.9	1.7	3.2	1.3 (#)	1.2 (#)	4.9	1.1 (#)	1.1 (#)	3.5
Acidic amino acids (negatively charged)												
Asp	5.5	6.4 (*)	6.9 (*)	5.6	5.2	9.0 (*)	6.6	4.8	5.5	7.7	8.9 (*)	4.7
Glu	6.3	5.6	6.5	8.8 (*)	6.8	6.2	3.3 (#)	7.3	6.2	7	9.2 (*)	5.8
Basic aminoacids (positively charged)												
Arg	4.7	4.8	4.9	4.3	3.9	5.1	9.9 (*)	4.8	4.9	7.3 (*)	9.6 (*)	7
His	2.2	1.4	1.9	2.3	2.4	2	0.0 (#)	1.2	3.4	0.4 (#)	0.2 (#)	4.7 (*)
Lys	7.4	7.4	7.2	8	10.7 (*)	10.2	10.6 (*)	10.9 (*)	6.6	11.7 (*)	6.2	9.3
Polar amino acids with uncharged groups												
Cys	1.5	1.4	1	1.4	1.5	1	0.0 (#)	0.6	1.1	0.0 (#)	0.0 (#)	0.0 (#)
Ser	8.7	5.4	5.2	5.7	4.6	4.0 (#)	6.6	6.1	6.2	7	7.8	8.1
Thr	5.8	7.6 (*)	5.7	6	6.1	5.1	6	3.6	5.5	7	4.8	7
Asn	5.7	5.2	3.1	4.7	3.5	5.1	7.3	4.2	4.3	11.4 (*)	5.7	11.6 (*)
Gln	3.9	2	3.8	2.8	2.6	2.3	4.6	3.6	3.2	3.3	3.2	3.5
Met	2.2	2.2	2.7	2.4	1.7	2.3	1.3	1.2	2.3	0.4 (#)	0.5 (#)	1.2

[1]*The average frequency of each amino acid residue in the yeast proteome (http://www.yeastgenome.org/).*
[2]*The amino acid residue frequencies in the corona protein sequences. Increased (*) or decreased (#) abundance of a given amino acid in the protein corona sequence relative to proteomic frequency (average) was indicated (see "Material and Methods).*

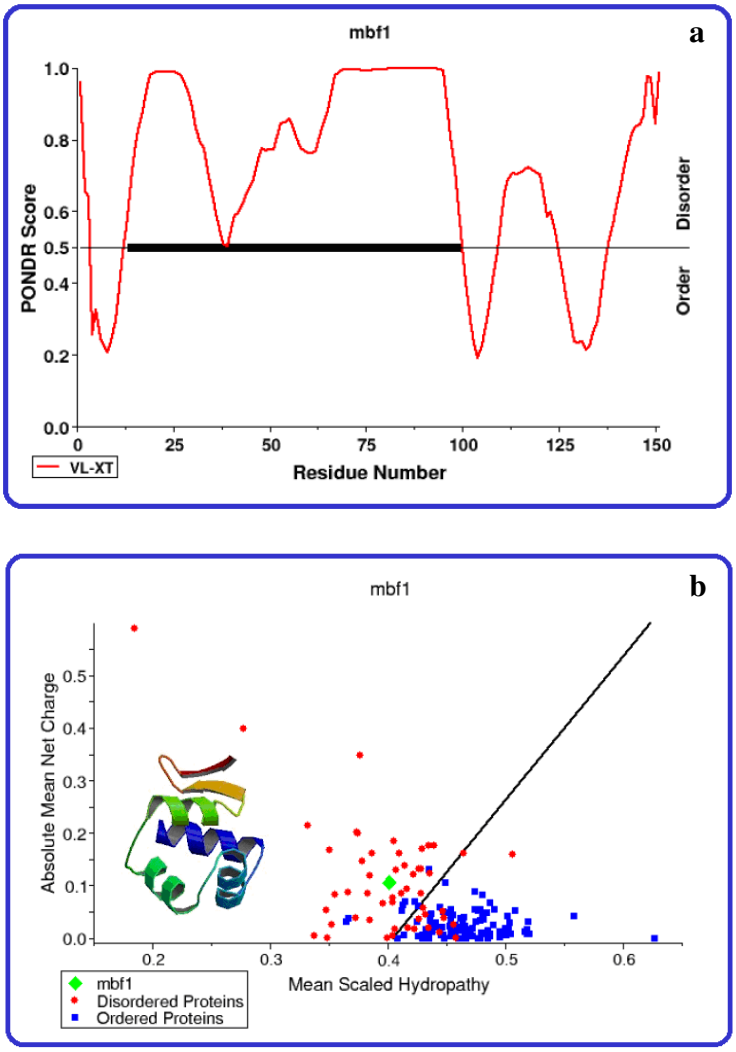

Fig. 59 *Prediction of DRs in yeast Mbf1 protein sequence. a) Graphical representation of the PONDR® output that showed long DRs (indicated with black segments) in Mbf1 sequence. b) Charge-hydropathy (C-H) plot using PONDR®. Mbf1 (green dot) is located in the protein disordered group.*

11.3 Identification of human proteins with high affinity for SiO_2 NPs

It is expected that in the future occupational and public exposure to silica and other NPs will further increase because of their huge potential and rising applications in technology and nanobiomedicine (*Docter et al., 2014*). To date, there are several reports about the potential toxicity of SiO_2 NPs in the GI tract, based on studies employing in vitro as well as *in vivo* murine models (*Napierska et al., 2010; Fu et al., 2013*). In addition, biochemical studies have characterized sets of proteins with strong binding properties to SiO_2 NPs using human plasma or serum (*Roach et al., 2006; Tenzer et al. 2011*; *Walkey and Chan, 2012*). However, the mechanistic impact of the physico-chemical parameters of silica NPs as well as of the protein corona is not yet resolved in detail.

We have evaluated the effect of silica NPs (dose range 10–80 μg/cm^2) on the viability of Caco-2 cells after 24 hour of exposure using AlamarBlue® viability assay (Fig. 60). As observed with CdS QDs, we showed that SiO_2 NPs slightly lowered cell viability inducing a maximal decrease of ca. 20%.

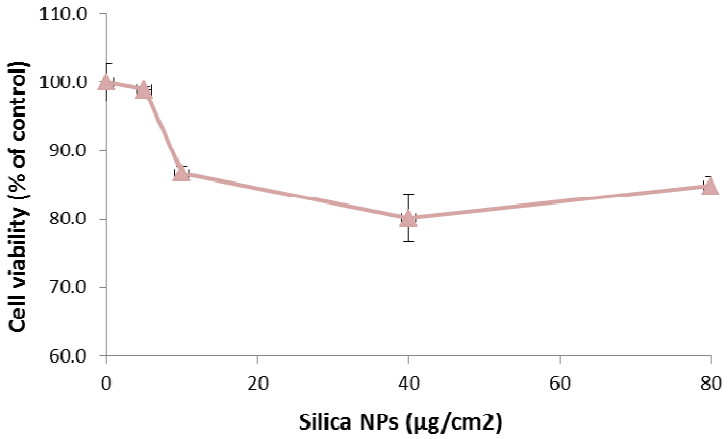

Fig. 60 *Effect of silica NPs on cell viability of Caco-2 cell line. Untreated Caco-2 cells were used as control sample (100%).*

To identify human proteins that form the NP corona, SiO_2 NPs and Caco-2 protein extracts were incubated with gentle agitation for 24 hours at 4°C and proteins bound to these NPs were recovered by multiple centrifugation steps and extensively washed to remove almost all nonbound and soft corona proteins. Proteins absorbed on silica NPs were identified by LC-MS/MS analysis (Fig. 61; Table 14); among these, proteins involved in cell division, two histones, translation process and a molecular chaperone were strongly associated to SiO_2 NPs. Notably, proteins involved in these processes were also identified in yeast corona of silica NPs (see Section 11.2), supporting the hypothesis that specialized proteins involved in metabolic processes in which is crucial a high flexibility in the protein structure are adsorbed to these NPs. Some of these proteins (Tubulin alpha-1B, Tubulin beta, Histone H2B) have also been isolated in the human protein corona of CdS QDs (see Section 10.2.2).

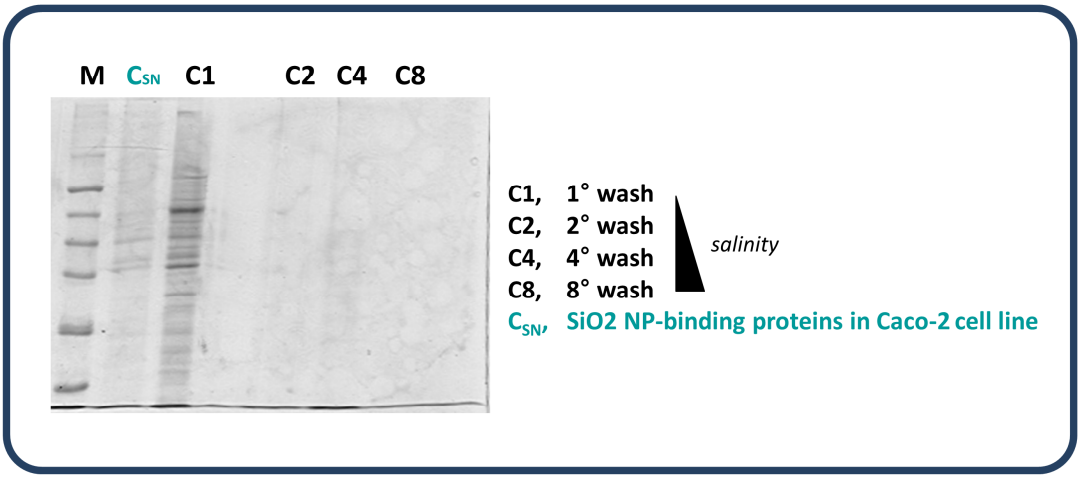

Fig. 61 *Proteomic analysis of the Caco-2 proteins adsorbed on the surface of SiO_2 NPs with high affinity. Aliquots of the wash solutions (C1-C8; 50% of the total sample) and human-derived hard protein corona (C_{SN}; 15% of the total sample) were visualized by 12% SDS-PAGE. Hard protein corona was composed of many different proteins with molecular weights between 10 and 50 kDa.*
C1-C4) Washes (first, second and fourth) of the SiO_2 NP-protein pellet with wash buffer A; C8) Wash (eighth) of the SiO_2 NP-protein pellet with wash buffer B (see "Materials and Methods" for additional details).

Two histones are identified in SiO_2 NP-protein corona: histone H4 and histone H2B. Histones are core component of chromatin that play a central role in transcription regulation, DNA repair, DNA replication and chromosomal stability. DNA accessibility is regulated via a complex set of post-translational modifications of histones and nucleosome remodeling. Thus, the interaction between these proteins and SiO_2 could result in alteration in their cellular role, from DNA damage susceptibility to aberrant transcriptional and replication processes. Indeed, Chen and Mikecz (*2005*) showed that silica NPs can penetrate into the cell nucleus, induce abnormal redistribution of nuclear proteins into protein aggregates and inhibit replication, transcription and cell proliferation. The authors suggest that these inhibitions result from protein adsorption and aggregation.

As observed in yeast, a protein involved in elongation translation process is identified in Silica NP-corona. **Elongation factor** 1-alpha 1 (Ef1-alpha) promotes the GTP-dependent binding of aminoacyl-tRNA to the A-site of ribosomes during protein biosynthesis. In addiction, Ef1-alpha forms a complex with Parp1 and Txk that acts as a T helper 1 (Th1) cell-specific transcription factor and binds the promoter of IFN-gamma to directly regulate its transcription, and is thus involved importantly in Th1 cytokine production.

60 kDa heat shock protein (Hspd1) is implicated in mitochondrial protein import and macromolecular assembly. Hspd1 may facilitate the correct folding of imported proteins and also prevent misfolding (or promote the refolding and proper assembly) of unfolded polypeptides generated under stress conditions in the mitochondrial matrix.

All corona proteins isolated have a molecular weight < 60 kDa (Table 15) and 50% of these proteins presents a pI>7.5 (Table 14). As observed in yeast, corona proteins have a high number of long DRs, which confers them a high disorder and structure flessibility (Fig. 62).

Table 14. *Human-derived hard corona proteins identified by LC-MS/MS analysis.*

Identified Proteins	***Score***	***Coverage***	***pI***
Tubulin alpha-1B chain (Isoform 2)	38.7	35.8	5.0
60 kDa heat shock protein, mitochondrial	37.8	14.7	5.6
Histone H4	35.3	14.5	10.4
Histone H2B	23.1	51.6	10.3
Elongation factor 1-alpha 1	22.2	22.3	9.0
Tubulin beta chain	20.3	30.9	4.9

Table 15. *Characteristics of hard corona proteins adsorbed to silica NPs.*

Identified proteins	***UniProt Acc. N.***	***Mol. weight (kDa)***	***Biological Process***
Tubulin alpha-1B chain (Isoform 2)	P68363-2	50	cell division
Tubulin beta-1 chain	Q9H4B7	50	cell division
Histone H4	P62805	11	DNA binding
Histone H2	P62807	13	DNA binding
Elongation factor 1-alpha 1	P68104	50	translation process
60 kDa heat shock protein, mitochondrial	B7Z5E7	55	molecular chaperone

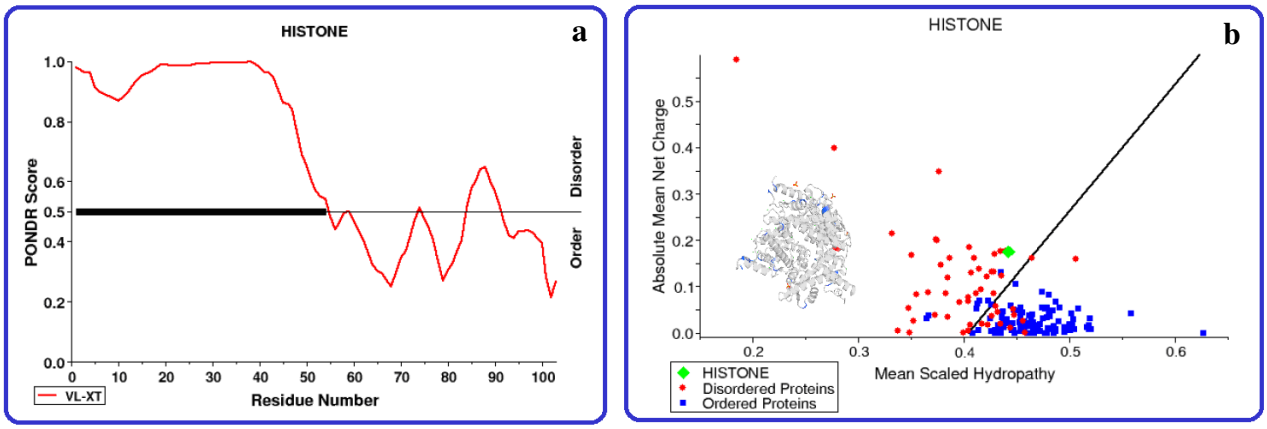

Fig. 62 *Prediction of DRs in human histone H4 protein sequence. a) Graphical representation of the PONDR® output that showed long DRs (indicated with black segments) in histone H4 sequence. b) Charge-hydropathy (C-H) plot using PONDR®. Histone H4 (green dot) is located in the protein disordered group.*

CONCLUSIONS

Identification of the composition of the NP-protein complex is crucial for understanding of the uptake mechanisms, biodistribution and clearance of NPs and for safety evaluation and biomedical applications of these materials (*Sund et al., 2011*).
Using a proteomics-based approach coupled with MS analysis, we showed in this PhD thesis that specific proteins from different biological models (yeast and Caco-2 cells or human plasma) were adsorbed with high affinity to CdS QDs and SiO_2 NPs. Considering the relationship between NP adsorption and the enzyme activity inhibition (*Gheshlaghi et al., 2008*; *Wangoo et al., 2008a*; *Nel et al., 2009*; *Deng et al., 2011*; *Yoo et al., 2011*; *Shannahan et al. 2014*), the identification of essential cellular proteins prone to adsorption may contribute to a better understanding of the potential toxicological effects of NPs.

Surface charge of the NPs is a crucial factor in determining the protein corona composition and consequentially its eventual fate in a biological system (*Gessner et al., 2002; Lynch and Dawson, 2008*). In fact, yeast and human proteins identified in CdS QD-coronas have a net negative charge at physiological pH; in contrast, proteins adborbed to negatively charged silica NPs exhibit a net positive charge and a significantly high frequency of Lys and/or Arg residues in NP surface. Indeed, electrostatic interactions can mediate the NP interaction with different cellular proteins in both cases.

A high frequency of long DRs were observed in protein sequences of human-derived coronas of both NPs and yeast corona of silica NPs, suggesting that these regions may favor interactions and adsorption with these materials. These regions are characteristic of Intrinsically Unstructured Proteins (IUPs), entire proteins or large segments of proteins that lack a well-structured three-dimensional fold (*Wright and Dyson, 1999*). IUPs are highly abundant in nature and are involved in processes such as transcription, translation, folding, signal transduction and cell-cycle control; the presence of DRs is crucial for their function (*Bychkova et al., 1996; Daughdrill et al., 1997; Riek et al., 1996, Uversky et al., 1996*). Notably, proteins involved in these processes are identified in the hard coronas of both NPs. It is possible that proteins that contain long DRs, having a more flexible structure, can be adsorbed with a high affinity to these NPs; DRs may act as binding sites and allow a better formation of electrostatic interactions with charged NP surface.

Several proteins showing a high affinity for both CdS QDs and silica NPs are nuclear (as histones) or cytosolic (e.g., cytoskeletal) components and it is possible that an alteration in cellular pathways in which they are involved can cause the toxicity of these NPs. Access to the cytosol and nucleus is somewhat limited as the process of NPs translocation into the cells that generally involves the formation of vesicles (*Saptarshi et al., 2013*). Some NPs can be found in the cytosol or nucleus (*Chen and Mikecz, 2005*; *Nabiev et al., 2007*; *Singh et al., 2009*) and it would be enough for these NPs to bind, with very high affinity, low abundant essential proteins to induce important cellular effects.

Incubation of CdS QDs with human plasma resulted in the formation of NP-biomolecular corona enriched with complement factors and proteins involved in clotting process. A similar subset of plasma proteins has been shown to be adsorbed on various ENMs (as silica NPs) in different amounts when incubated in human plasma, but it was observed a different physiological impact (negative or positive) depending on ENMs (*Monopoli et al 2012; Tenzer et al., 2011; Tenzer et al., 2013*). For example, binding of complement proteins to NPs can activate complement processes that eventually cause inflammation (*Qu et al., 2012*). Inflammation has been shown to directly cause toxicity and promote cell death and NPs may be designed to avoid such immune toxicity to improve their safety.

Our results demonstrated by using independent experimental methods that the protein adsorption can mediate CdS QD-induced toxicity in yeast cells. We observed a general transcriptional up-regulation of genes coding for yeast corona proteins; this effect could represent a cellular mechanism in response to "physical sequestration" of the corona proteins adsorbed on CdS QD surface. Whereas the cellular levels of the corona proteins can be reduced by the absorption to

the NPs, an increase of the transcriptional levels of the genes coding for these proteins could be important for cell survival. Notably, *CDC19*, the most up-regulated gene, codes for an essential protein (pyruvate kinase) involved in glycolysis process.

CdS QDs strongly reduced the abundance of several yeast corona proteins. It is possible that the hard corona formation could lead to a reduction of the cellular levels of the involved proteins; as observed also in the corona of silica NPs, most of the identified proteins are translation elongation factors and it is possible that the adsorption of these proteins on the NP surface may lead to their functional inactivation which might cause a reduction of the translational levels of other proteins. Notably, silica NPs can inhibit protein synthesis *in vitro* (*Klein et al., 2016).*

Yeast mutant strains deleted in genes coding for corona proteins showed a tolerant phenotype also in presence of concentrations of CdS QDs that suppress the viability of the wild-type strain. Tolerant phenotype of these mutants suggest that the formation of protein corona may mediate the cytotoxicity of CdS QDs in yeast. In these conditions, NPs could induce the exposure of protein epitopes on their surface in an aberrant conformation or the formation of the protein corona could promote the binding of NPs with other cellular components, causing an increased toxicity. The adsorption of proteins on the NP surface can induce protein denaturation and we observed a dose-dependent inhibition of the activity of the yeast GAPDH by CdS QDs. A critical cysteine residue in the active site (*Smith et al., 1979*) was supposed to be the target for QD-binding (*Ghosh et al, 2014*).

Notably, we observed here a time- and dose-dependent toxicity for the CdS QDs in yeast cells, but a lower toxicity in Caco-2 cell line and this suggests a lower uptake of QDs in these cells. In contrast, exposure even to high doses (2 g/mL) of larger silica NPs (> 100 nm) under identical experimental conditions have less impact on the yeast cell vitality and a similar effect is observed in Caco-2 cell line. Previous studies reported a toxicity-dependent on the particle size of NPs in different cell models (*Napierska et al., 2009; Park et al. 2011; Ma et al. 2014*) and it was postulated that the smaller particles always affected the exposed cells faster and at a lower dose.

Our preliminary results obtained with other human cell lines (data not shown) displayed that CdS QDs and silica NPs strongly reduce the viability of human monocytic cell line (THP-1) and we are just now characterizing the proteins that form the respective hard coronas. It will be interesting to see if the identified proteins belong to the same functional classes and whether the corona formation can mediate the NP toxicity in these cells, as observed in *S. cerevisiae*.

In conclusion, it is conceivable to speculate that, depending on the type of ENMs, the formation of a biologically active protein corona may change the physico-chemical properties of the NPs and these effects will ultimately be relevant for nano–bio responses. In prospect, the protein corona formation can be used to deliver drugs in the body, including the treatment of cancer. Clearly, the analysis of the NP corona alone is not a generally applicable predictive parameter for nanotoxicity. *In vivo* context, NPs do not reach alveolar or intestinal cells as naked NPs but covered with mucus proteins and surfactants that have been encountered on their route to the interior of the cells. Adsorption of cellular proteins on such "pre-coated NPs" can be different from the *in vitro* assay using naked NPs described in this work. Further developments, using pre-coated NPs with surfactants and mucus proteins, are required to test this approach for toxicological studies and resolve the mechanisms and (patho)biological effects of ENMs *in vivo*.

REFERENCES

Abdelhalim M. and Jarrar B. 2011. *Gold nanoparticles administration induced prominent inflammatory, central vein intima disruption, fatty change and Kupffer cells hyperplasia.* Lipids Health Dis. 10:133-138.

Abdelhamid M.A.A., Motomura K., Ikeda T., Ishida T., Hirota R., Kuroda A. 2014. *Affinity purification of recombinant proteins using a novel silica-binding peptide as a fusion tag.* Applied Microbiology and Biotechnology. 98(12):5677-5684.

Agasti S.S., Chompoosor A., You C.C., Ghosh P., Kim C.K., Rotello V.M.J. 2009. *Photoregulated release of caged anticancer drugs from gold nanoparticles*. J. Am. Chem. Soc. 131(16):5728-9.

Aggarwal P., Hall J.B., McLeland C.B., Dobrovolskaia M.A., McNeil S.E. 2009. *Nanoparticle interaction with plasma proteins as it relates to particle biodistribution, biocompatibility and therapeutic efficacy.* Adv. Drug. Deliv. Rev. 61(6):428-437.

Ahamed M., Karns M., Goodson M., Rowe J., Hussain S.M., Schlager J.J., Hong Y. 2008. *DNA damage response to different surface chemistry of silver nanoparticles in mammalian cells.* Toxicology and Applied Pharmacology. 233(3):404-410.

Akerman M.E., Chan W.C.W., Laakkonen P., Bhatia S.N., Ruoslahti E. 2002. *Nanocrystal targeting in vivo*. Proc. Natl. Acad. Sci. USA 99(20):12617-12621.

Akhtar M.J., Ahamed M., Kumar S., Siddiqui H., Patil G., Ashquin M., Ahmad I. 2010. *Nanotoxicity of pure silica mediated through oxidant generation rather than glutathione depletion in human lung epithelial cells*. Toxicology. 276(2):95-102.

Alberts A.J.B., Lewis J., Raff M., Roberts K., Walter P. 2002. *Molecular biology of the cell.* Garland Science, Taylor and Francis Group, New York.

Alexis F., Pridgen E., Molnar L., Farokhzad O. 2008. *Factors affecting the clearance and biodistribution of polymeric nanoparticles*. Mol. Pharmaceutics. 5(4):505-515.

Alfaro-Moreno E., Nawrot T.S., Nemmar A., Nemery B. 2007. *Particulate matter in the environment: pulmonary and cardiovascular effects*. Curr. Opin. Pulm. Med. 13:98-106.

Alivisatos A.P. 1996. *Semiconductor clusters, nanocrystals, and quantum dots.* Science. 271(5251):933-937.

Alivisatos A.P. and Chen F.F. 2006. *Cellular effect of high doses of Silica-coated quantum dot profiled with high throughput gene expression analysis and high content cellomics measurements*. Nano. Lett. 6(4):800-808.

Allen R. and Tresini M. 2000. *Oxidative stress and gene regulation.* Free Radic. Biol. Med. 28(3):463-499.

Al-Rawi M., Diabate S., Weiss C. 2011. *Uptake and intracellular localization of submicron and nano-sized SiO2 particles in Hela cells*. Archives of toxicology. 85(7):813-26.

American Heritage Dictionary. 2010.

Anderson N.L. 2011. *The clinical plasma proteome: a survey of clinical assays for proteins in plasma and serum.* Clin. Chem. 56:177-85.

Anderson N.L., Polanski M., Pieper R., Gatlin T., Tirumalai R.S., Conrads T.P., Veenstra T.D., Adkins J.N., Pounds J.G., Fagan R., Lobley A. 2004. *The human plasma proteome.* Mol. Cell. Proteomics. 3(4):311-326.

Arts J.H., Muijser H., Duistermaat E., Junker K., Kuper C.F. 2007. *Five-day inhalation toxicity study of three types of synthetic amorphous silicas in Wistar rats and post-exposure evaluations for up to 3 months.* Food. Chem. Toxicol. 45:1856-1867.

Artursson P. 1990. *Epithelial transport of drugs in cell culture. I: A model for studying the passive diffusion of drugs over intestinal absorptive (Caco-2) cells*. J. Pharm. Sci. 79:476-482.

Artursson P., Ungell A.L., Löfroth J.E. 1993. *Selective paracellular permeability in two models for intestinal absorption: cultured monolayers of human intestinal epithelial cells and rat intestinal segments*. Pharm. Res. 10:1123-1129.

Arvizo R.R., Miranda O.R., Thompson M.A., Pabelick C.M., Bhattacharya R., Robertson J.D., Rotello V.M., Prakash Y.S., Mukherjee P. 2010. *Effect of nanoparticle surface charge at the plasma membrane and beyond.* Nano. Lett. 10:2543-2548.

Asare N., Instanes C., Sandberg W.J., Refsnes M., Schwarze P., Kruszewski M., Brunborg G. 2012. *Cytotoxic and genotoxic effects of silver nanoparticles in testicular cells*. Toxicology. 291(1-2):65-72.

AshaRani P.V., Low Kah Mun G., Hande M.P., Valiyaveettil S. 2009. *Cytotoxicity and genotoxicity of silver nanoparticles in human cells.* ACS Nano. 3(2):279-290.

Astruc D., Lu F., Aranzaes J.R. 2005. *Nanoparticles as recyclable catalysts: the frontier between homogeneous and heterogeneous catalysis.* Angew. Chem. Int. Ed. Engl. 44(48):7852-72.

Athinarayanan J., Periasamy V.S., Alsaif M.A., Al-Warthan A.A., Alshatwi A.A. 2014. *Presence of nanosilica (E551) in commercial food products: TNF-mediated oxidative stress and altered cell cycle progression in human lung fibroblast cells.* Cell. Biol. Toxicol. 30:89-100.

Augustijns P. and Mols R. 2004. *HPLC with programmed wavelength fluorescence detection for the simultaneous determination of marker compounds of integrity and P-gp functionality in the Caco-2 intestinal absorption model.* J. Pharm. Biomed. Anal. 34:971-978.

Babic M., Horák D., Jendelová P., Glogarová K., Herynek V., Trchova M., Likavanová K., Lesný P., Pollert E., Hájek M., Syková E. 2009. *Poly(N,N-dimethylacrylamide)-coated maghemite nanoparticles for stem cell labeling.* Bioconjug Chem. 20(2):283-94.

Bai Y., Zhang Y., Zhang J., Mu Q., Zhang W., Butch E.R., Snyder S.E., Yan B. 2010. *Repeated administrations of carbon nanotubes in male mice cause reversible testis damage without affecting fertility.* Nat. Nanotechnol. 5(9):683-9.

Bal R., Turk G., Tuzcu M., Yilmaz O., Ozercan I., Kuloglu T., Gur S., Nedzvetsky V.S., Tykhomyrov A.A., Andrievsky G.V., Baydas G., Naziroglu M. 2011. *Protective effects of nanostructures of hydrated C(60) fullerene on reproductive function in streptozotocin-diabetic male rats*. Toxicology. 282(3):69-81.

Balimane P.V. and Chong S. 2005. *Cell culture-based models for intestinal permeability: a critique.* Drug. Discovery Today. 10:335-343.

Ballestri M., Baraldi A., Gatti A.M., Furci L., Bagni A., Loria P., Rapaa M., Carulli N., Albertazzi A. 2001. *Liver and kidney foreign bodies granulomatosis in a patient with malocclusion, bruxism, and worn dental prostheses.* Gastroenterology.121:1234-1238.

Barabasi A.L. and Oltvai Z.N. 2004. *Network biology: Understanding the cell's functional organization.* Nature Reviews Genetics. 5, 101-U115.

Baughman R.H., Zakhidov A.A., De Heer W.A. 2002. *Carbon nanotubes-the route toward applications*. Science. 297:787-92.

Bencivenni M., Faccini A., Zecchi R., Boscaro F., Moneti G., Dossena A., Sforza S. *Electrospray MS and MALDI imaging show that non-specific lipid-transfer proteins (LTPs) in tomato are present as several isoforms and are concentrated in seeds.* J Mass Spectrom. 2014 Dec,49(12):1264-71.

Benet L.Z., Izumi T., Zhang Y., Silverman J.A., Wacher V.J. 1999. *Intestinal MDR transport proteins and P-450 enzymes as barriers to oral drug delivery*. J. Control Release. 62:25-31.

Blundell G., Henderson W., Price E.W.1989. *Soil particles in the tissues of the foot in endemic elephantiasis of the lower legs.* Ann. Trop. Med. Parasitol. 83:381-385.

Bockmann J., Lahl H., Eckert T., Unterhalt B. 2000. *Titanium blood levels of dialysis patients compared to healthy volunteers*. Pharmazie. 5(5):468.

Bodamyali T., Stevens C.R., Blake D.R., et al. 2000. *Reactive oxygen/nitrogen species and acute inflammation: a physiological process*. In: Winyard PG, Blake DR, Evans CH, editors. Free radicals and inflammation. Basel: Springer. 11-9.

Bodman J.A., Yang Y., Logan M.R., Eitzen G. 2015. *Yeast translation elongation factor-1A binds vacuole-localized Rho1p to facilitate membrane integrity through F-actin remodeling.* J Biol Chem. 290(8):4705-16.

Bohets H., Annaert P., Mannens G., van Beijsterveldt L., Anciaux K., Verboven P., Meuldermans W., Lavrijsen K. 2001. *Strategies for absorption screening in drug discovery and development*. Curr. Top. Med. Chem. 1:367-383.

Borkovich K.A., Farrelly F.W., Finkelstein D.B., Taulien J., Lindquist S. 1989. *Hsp82 is an essential protein that is required in higher concentrations for growth of cells at higher temperatures.* Mol Cell Biol. 9(9):3919-30.

Borm P.J.A., Robbins D., Haubold S., Kuhlbusch T., Fissan H., Donaldson K., Schins R.P.F., Stone V., Kreyling W., Lademann J., Krutmann J., Warheit D. 2006. *The potential risks of nanomaterials: a review carried out for ECETOC.* Part. Fibre Toxicol. 14(3):11.

Bosi S., da Ros T., Spalluto G., Prato M. 2003. *Fullerene derivatives: an attractive tool for biological applications*. Eur. J. Med. Chem. 38(11):913-923.

Boverhof D.R. and David R.M. 2010. *Nanomaterial characterization: Considerations and needs for hazard assessment and safety evaluation.* Anal. Bioanal. Chem. 396:953-961.

Boyoglu C., He Q., Willing G., et al. 2013. *Microscopic studies of various sizes of gold nanoparticles and their cellular localizations*. ISRN Nanotechnol.

Bradley G.W., McKenna G.B., Dunn H.K., Daniels A.U., Statton W.O. 1979. *Effects of flexural rigidity of plates on bone healing*. J. Bone Joint. Surg. 61(6):866-72.

Brook R.D., Rajagopalan S., Pope C.A., Brook J.R., Bhatnagar A., Diez-Roux A.V., Holguin F., Hong Y., R.V., Luepker M.A., Mittleman. 2010. *Particulate matter air pollution and cardiovascular disease an update to the scientific statement from the American heart association.* Circulation. 121:2331-2378.

Bruchez M. Jr., Moronne M., Gin P., Weiss S., Alivisatos A.P. 1998. *Semiconductor nanocrystals as fluorescent biological labels*. Science. 281(5385):2013-2016.

BSI PD. 6699-1:2007. *Nanotechnologies-part 1: good practice guide for specifying manufactured nanomaterials*. British Standards Institute, UK.

Bu H.Z., Poglod M., Micetich R.G., Khan J.K. 2000. *High-throughput Caco2 cell permeability screening by cassette dosing and sample pooling approaches using direct injection/on-line gurard cartridge extraction/tandem mass spectrometry*. Rapid. Commun. Mass. Spectrom. 14:523-528.

Buschini A., Poli P., Rossi C. 2003. *Saccharomyces cerevisiae as an eukaryotic cell model to assess cytotoxicity and genotoxicity of three anticancer anthraquinones*. Mutagenesis. 18:25-36.

Butterfield D.A. and Kanski J. 2001. *Brain protein oxidation in agerelated neurodegenerative disorders that are associated with aggregated proteins*. Mech. Ageing. Dev. 122(9):945-62.
Bychkova V.E, Dujsekina A.E., Klenin S.I., Tiktopulo E.I, Uversky V.N., Ptitsyn O.B. 1996. *Molten globule-like state of cytochrome c under conditions simulating those near the membrane surface*. Biochemistry. 35, 6058-6063.

Byrne J.D. and Baugh J.A. 2008. *The significance of nanoparticles in particle-induced pulmonary fibrosis*. McGill J. Med. 11(1):43-50.

Bystrzejewska-Piotrowska G., Golimowski J., Urban P.L. 2009. *Nanoparticles: their potential toxicity, waste and environmental management.* Waste Manage. 29(9):2587-95.

Cabral H., Makino J., Matsumoto Y., Mi P., Wu H., Nomoto T., Toh K., Yamada N., Higuchi Y., Konishi S., Kano M.R., Nishihara H., Miura Y., Nishiyama N., Kataoka K. 2015. *Systemic Targeting of Lymph Node Metastasis through the Blood Vascular System by Using Size-Controlled Nanocarriers.* ACS Nano. 9(5):4957-67.

Cabral M.G., Viegas C.A., Teixeira M.C., Sá-Correia I. 2003. *Toxicity of chlorinated phenoxyacetic acid herbicides in the experimental eukaryotic model Saccharomyces cerevisiae: role of pH and of growth phase and size of the yeast cell population.* Chemosphere. 51:47-54.

Campen A., Williams R.M., Brown C.J., Uversky V.N., Dunker A.K. 2008. *TOPIDP-Scale: A new amino acid scale measuring propensity for intrinsic disorder.* Protein and Peptide Letters. 15(9):956-963.

Capriotti A.L., Caruso G., Cavaliere C., Pozzi D., Samperi R., Laganà A. 2013. *Label-free quantitative analysis for studying the interactions between nanoparticles and plasma proteins*. Anal. Bioanal. Chem. 405(2-3):635-645.

Capriotti A.L., Caruso G., Cavaliere C., Pozzi D., Samperi R., Laganà A. 2010. *Analysis of plasma protein adsorption onto DC-Chol-DOPE cationic liposomes by HPLC-CHIP coupled to a Q-TOF mass spectrometer.* Anal. Bioanal. Chem. 398(7-8):2895-2903.

Caracciolo G., Pozzi D., Capriotti A.L., Cavaliere C., Piovesana S., La Barbera G., Amici A., Laganà A. 2014. *The liposome-protein corona in mice and humans and its implications for in vivo delivery*. J. Mater. Chem. B 2(42):7419-7428.

Caracciolo G., Pozzi D., Capriotti A.L., Cavaliere C., Foglia P., Amenitsch H., Laganà A. 2011. *Evolution of the protein corona of lipid gene vectors as a function of plasma concentration.* Langmuir: ACS J. Surfaces Colloids. 27:15048-53.

Cedervall T., Lynch I., Foy M. Berggård T., Donnelly S.C., Cagney G., Linse S., Dawson K.A. 2007a. *Detailed identification of plasma proteins adsorbed on copolymer nanoparticles*. Angew. Chem. Int. Ed. Engl. 46(30):5754-5756.

Cedervall T., Lynch I., Lindman S., Berggard T., Thulin E., Nilsson H., Dawson K.A., Linse S. 2007b. *Understanding the nanoparticle protein corona using methods to quantify exchange rates and affinities of proteins for nanoparticles*. Proc. Natl. Acad. Sci. USA 104(7):2050-2055.

Champion J.A., Katare Y.K., Mitragotri S. 2007. *Particle shape: a new design parameter for micro and nanoscale drug delivery carriers.* J. Control Release. 121(1-2):3-9.

Chan W.C., Maxwell D.J., Gao X., Bailey R.E. 2002. Han M: *Luminescent quantum dots for multiplexed biological detection and imaging*. Curr. Opin. Biotechnol. 13(1):40-46.

Chang E., Yu W.W., Colvin V.L., Drezek R. 2005. *Protease-activated quantum dot probes*. Biochem. Biophys. Res. Commun. 334(4):1317-21.

Chang J.S., Chang K.L., Hwang D.F., Kong Z.L. 2007. *In vitro cytotoxicitiy of silica nanoparticles at high concentrations strongly depends on the metabolic activity type of the cell line.* Environ. Sci. Technol. 41(6):2064-8.

Chavalarias D., Wallach J.D., Li A.H., Ioannidis J.P. 2016. *Evolution of Reporting P Values in the Biomedical Literature*. 1990-2015. JAMA. 315(11):1141-8.

Chen F., Gerion D. 2004. *Fluorescent CdSe/ZnS nanocrystal-peptide conjugates for long-term, nontoxic imaging and nuclear targeting in living cells*. Nano. Lett. 4(10):1827-1832.

Chen J., Dong X., Zhao J., Tang G. 2009. *In vivo acute toxicity of titanium dioxide nanoparticles to mice after intraperitioneal injection*. J. Appl. Toxicol. 29(4):330-7.

Chen K., Zhang J., Gu H. 2012. *Dissolution from inside: a unique degradation behaviour of core-shell magnetic mesoporous silica nanoparticles and the effect of polyethyleneimine coating*. J. Mater. Chem. 22(41):22005-22012.

Chen M. and Mikecz von, A., 2005. *Formation of nucleoplasmic protein aggregates impairs nuclear function in response to SiO_2 nanoparticles*. Experimental cell research. 305 (1), 51–62.

Chen N. 2012. *The cytotoxicity of cadmium-based quantum dots*. Biomaterials. 33(5):1238-1244.

Chen Z., Chen H., Meng H., Xing G., Gao X., Sun B., Shi X., Yuan H., Zhang C., Liu R., Zhao F., Zhao Y., Fang X. 2008. *Bio-distribution and metabolic paths of silica coated CdSeS quantum dots*. Toxicol. Appl. Pharmacol. 230(3):364-371.

Chen Z., Meng H., Xing G., Chen C., Zhao Y., Jia G., Wang T., Yuan H., Ye C., Zhao F., Chai Z., Zhu C., Fang X., Ma B., Wan L. 2006. *Acute toxicological effects of copper nanoparticles in vivo*. Toxicol. Lett. 163(2):109-120.

Chen F., Wang G., Griffin J.I., Brenneman B., Banda N.K., Holers V.M., Backos D.S., Wu L., Moghimi S.M., Simberg D. 2016. *Complement proteins bind to nanoparticle protein corona and undergo dynamic exchange in vivo*. Nat. Nanotechnol. Dec 19.

Cheng Y., Wang M., Borghs G., Chen H. 2011. *Gold nanoparticle dimers for plasmon sensing*. Langmuir. 27(12):7884-91.

Chiti F. and Dobson C.M. 2006. *Protein misfolding, functional amyloid, and human disease.* Annual Review of Biochemistry. 75:333-366.

Cho E.C., Xie J.W., Wurm P.A., Xia Y.N. 2009. *Understanding the role of surface charges in cellular adsorption versus internalization by selectively removing gold nanoparticles on the cell surface with a I2/KI etchant*. Nano. Lett. 9(3):1080-4.

Choi A.O., Brown S.E., Szyf M., Maysinger D. 2008. *Quantum dot induced epigenetic and genotoxic changes in human breast cancer cells*. J. Mol. Med. 86(3):291-302.

Choi C., Zuckerman J., Webster P., Davis M. 2011. *Targeting kidney mesangium by nanoparticles of defined size*. Proc. Natl. Acad. Sci. U.S.A. 108(16):6656-6661.

Choi H.S., Ashitate Y., Lee J.H., Kim S.H., Matsui A., Insin N., Bawendi M.G., Semmler-Behnke M., Frangioni J.V., Tsuda A. 2010. *Rapid translocation of nanoparticles from the lung airspaces to the body*. Nat. Biotechnol. 28(12):1300-1303.

Choi H.S., Liu W., Misra P., Tanaka E., Zimmer J., Itty Ipe B., Bawendi M., Frangioni J. 2007. *Renal clearance of quantum dots*. Nat. Biotechnol. 25:1165-1170.

Christie M.S., Wahi R., Preetha A.K., Liu Y., Jennifer L.W., Kevin D.A., David B.W., Vicki L.C. 2006. *Correlating nanoscale titania structure with toxicity: a cytotoxicity and inflammatory response study with human dermal fibroblasts and human lung epithelial cells*. Toxicol. Sci. 92:174-185.

Chung I.S., Lee M.Y., Shin D.H., Jung H.R. 2010. *Three systemic argyria cases after ingestion of colloidal silver solution*. Int. J. Dermatol. 49:1175-1177.

Cliften P., Sudarsanam P., Desikan A., Fulton L., Fulton B., Majors J., Waterston R., Cohen B.A., Johnston M. 2003. *Finding functional features in Saccharomyces genomes by phylogenetic footprinting*. Science. 301(5629):71-6.

Collett A., Tanianis-Hughes J., Warhurst G. 2004. *Rapid induction of P-glycoprotein expression by high permeability compounds in colonic cells in vitro: a possible source of transporter mediated drug interactions?* Biochem. Pharmacol. 68:783-790.

Connor E.E., Mwamuka J., Gole A., Murphy C.J., Wyatt M.D. 2005. *Gold nanoparticles are taken up by human cells but do not cause acute cytotoxicity.* Small. 1:325-327.

Conroy J., Byrne S.J., Gun'ko Y.K., Rakovich Y.P., Donegan J.F., Davies A., Kelleher D., Volkov Y. 2008. *CdTe nanoparticles display tropism to core histones and histone-rich cell organelles*. Small. 4(11):2006-15.

Corachan M. 1988. *Endemic non-filarial elephantiasis of lower limbs–podonconiosis*. Medicina Clinica. 91:97-100.

Corbo C., Molinaro R., Parodi A., Toledano Furman N.E., Salvatore F., Tasciotti E. 2016. *The impact of nanoparticle protein corona on cytotoxicity, immunotoxicity and target drug delivery*. Nanomedicine (Lond.) 11(1): 81–100.

Coyle P., Philcox J.C., Carey L.C., Rofe A.M. 2002. *Metallothionein: the multipurpose protein.* Cell. Mol. Life Sci. 59(4):627-47.

Crisp T.M., Clegg E.D., Cooper R.L., Wood W.P., Anderson D.G., Baetcke K.P., Hoffmann J.L., Morrow M.S., Rodier D.J., Schaeffer J.E., Touart L.W., Zeeman M.G., Patel Y.M. 1998. *Environmental endocrine disruotion: an effects assessment and analysis.* Health Persp. 106(1):11-56.

Cui B., Wu C., Chen L., Ramirez A., Bearer E.L., Li W.P., Mobley W.C., Chu S. 2007. *One at a time, live tracking of NGF axonal transport using quantum dots*. Proc. Natl. Acad. Sci. USA. 104(34):13666-13671.

Curtis J., Greenberg M., Kester J., Phillips S., Krieger G. 2006. *Nanotechnology and nanotoxicology: a primer for clinicians*. Toxicol. Sci. 25:245-260.

Dabbousi B.O., Rodriguez-Viejo J., Mikulec F.V., Heine J.R., Mattoussi H., Ober R., Jensen K.F., Bawendi M.G. 1997. *(CdSe)ZnS core-shell quantum dots: synthesis and characterization of a size series of highly luminescent nanocrystallites*. J. Phys. Chem. B. 101(46):9463-9475.

Daughdrill G.W., Chadsey M.S., Karlinsey J.E., Hughes K.T., Dahlquist F.W. 1997. *The C-terminal half of the anti-sigma factor, FlgM, becomes structured when bound to its target, sigma.* Nature Structural. Biology. 4, (28):285-291.

Dawson K.A., Salvati A., Lynch I. 2009. *Nanoparticles reconstruct lipids.* Nat. Nanotechnol. 4:84-85.

De Freitas J.M., Wintz H., Kim J.H., Poynton H., Fox T., Vulpe C. 2003. *Yeast, a model organism for iron and copper metabolism studies.* Bio. Metals. 16:185-197.

De Paoli S.H., Diduch L.L., Tegegn T.Z., Orecna M., Strader M.B., Karnaukhova E., Bonevich J.E., Holada K., Simak J. 2014. *The effect of protein corona composition on the interaction of carbon nanotubes with human blood platelets.* Biomaterials. 35(24):6182-6194.

Degussa. 1984. *Zur Bedeutung und Existenz von Primärteilchen bei hochdispersen Stoffen.* Ferch H, Seibold K. Schriftenreihe Pigmente Nummer 60. Degussa, Frankfurt am Main, Germany.

Delgado M.L., O'Connor J.E., Azorín I., Renau-Piqueras J., Gil M.L., Gozalbo D. 2001. *The glyceraldehyde-3-phosphate dehydrogenase polypeptides encoded by the Saccharomyces cerevisiae TDH1, TDH2 and TDH3 genes are also cell wall proteins.* Microbiology. 147(Pt 2):411-7.

Deng Z., Samanta A., Nangreave J., Yan H., Liu Y. 2012. *Robust DNA-functionalized core/shell quantum dots with fluorescent emission spanning from UV-vis to near-IR and compatible with DNA-directed self-assembly.* Journal of the American Chemical Society. 134:17424-17427.

Deng Z.J., Liang M., Monteiro M., Toth I., Minchin R.F. 2011. *Nanoparticle-induced unfolding of fibrinogen promotes Mac-1 receptor activation and inflammation.* Nat. Nanotechnol. 6(1):396-44.

Deng Z.J., Mortimer G., Schiller T., Musumeci A., Martin D., Minchin R. F. 2009. *Differential plasma protein binding to metal oxide nanoparticles.* Nanotechnology. 20(45):455101.

Derfus A.M., Chan W.C.W., Bhatia S.N. 2004a. *Intracellular delivery of quantum dots for live cell labeling and organelle tracking.* Adv. Mater. 16:961-966.

Derfus A.M., Chan W.C.W., Bhatia S.N. 2004b. *Probing the cytotoxicity of semiconductor quantum dots.* Nano. Lett. 4(1):11-18.

Di Comite G., Grazia Sabbadini M., Corti A., Rovere-Querini P., Manfredi A.A. 2007. *Conversation galante: how the immune and the neuroendocrine systems talk to each other.* Autoimmun Rev. 7(1):23-9.

Di Cristo L., Movia D., Bianchi M.G., Allegri M., Mohamed B.M., Bell A.P., Moore C., Pinelli S., Rasmussen K., Riego-Sintes J., Prina-Mello A., Bussolati O., Bergamaschi E. 2016. *Pro-inflammatory effects of pyrogenic and precipitated amorphous silica nanoparticles in innate immunity cells.* Toxicological Sciences. 150(1):40-53.

Diederichs J.E. 1996. *Plasma protein adsorption patterns on liposomes: establishment of analytical procedure.* Electrophoresis. 17(3):607-611.

DIN. 1972. Prüfung von Pigmenten; Teilchengrößenanalyse, Grundbegriffe (Testing of pigments; particle size analysis, basic terms). DIN 53206. Deutsches Institut für Normung, Berlin, Germany.

Ding L., Stilwell J., Zhang T., Elboudwarej O., Jiang H., Selegue J.P., Cooke P.A., Gray J.W., Chen F.F. 2005. *Molecular characterization of the cytotoxic mechanism of multiwall carbon nanotubes and nano-onions on human skin fibroblast*. Nano. Lett. 5:2448-2464.

Dobrovolskaia M.A. and McNeil S.E. 2007. *Immunological properties of engineered nanomaterials*. Nat. Nanotechnol. 2(8):469-78.

Dobrovolskaia M.A., Aggarwal P., Hall J.B., McNeil S.E. 2008. *Preclinical studies to understand nanoparticle interaction with the immune system and its potential effects on nanoparticle biodistribution.* Mol. Pharm. 5(4):487-495.

Dobrovolskaia M.A., Neun B.W., Man S., Ye X., Hansen M., Patri A.K., Crist R.M., McNeil S.E. 2014. *Protein corona composition does not accurately predict hematocompatibility of colloidal gold nanoparticles*. Nanomed: Nanotechnol. Biol. Med. 10:1453-63.

Dobrovolskaia M.A., Patri A.K., Zheng J., Clogston J.D., Ayub N., Aggarwal P., Neun B.W., Hall J.B., McNeil S.E. 2009. *Interaction of colloidal gold nanoparticles with human blood: effects on particle size and analysis of plasma protein binding profiles.* Nanomed. Nano. Biol. Med. 5(2):106-117.

Docter D., Bantz C., Westmeier D., Galla H.J., Wang Q., Kirkpatrick J.C., Nielsen P., Maskos M., Stauber R.H. 2014. *The protein corona protects against size- and dose-dependent toxicity of amorphous silica nanoparticles*. Beilstein J. Nanotechnol. 5:1380-1392.

Docter D., Westmeier D., Markiewicz M., Stolte S., Knauer S., Stauber R. 2015. *The nanoparticle biomolecule corona: lessons learned-challenge accepted?* Chem. Soc. Rev. 44(17): 6094-6121.

Dominguez-Medina S., Blankenburg J., Olson J., Landes C.F., Link S. 2013. *Adsorption of a protein monolayer via hydrophobic interactions prevents nanoparticle aggregation under harsh environmental conditions*. ACS Sustainable Chemistry & Engineering. 1:833-842.

Donaldson K., Aitken R., Tran L., Stone V., Duffin R., Forrest G., Alexander A. 2006. *Carbon nanotubes: a review of their properties in relation to pulmonary toxicology and workplace safety.* Toxicol. Sci. 92:5-22.

Donaldson K., Stone V., Borm P.J.A., Jimenez L.A., Gilmour P.S., Schins R.P.F., Knaapen A.M., Rahman I., Faux S.P., Brown D.M., MacNee W. 2003. *Oxidative stress and calcium signaling in the adverse effects of environmental particles PM10.* Free Radical Biol. & Med. 34:1369-1382.

Donaldson K., Stone V., Tran C., Kreyling W., Borm P.J.A. 2004. Nanotoxicology occup Environ. Med. 61(9):727-728.

Dos Santos N., Allen C., Doppen A.M., Anantha M., Cox K.A., Gallagher R.C., Karlsson G., Edwards K., Kenner G., Samuels L., Webb M.S., Bally M.B. 2007. *Influence of poly(ethylene glycol) grafting density and polymer length on liposomes: relating plasma circulation lifetimes to protein binding*. Biochim. Biophys. Acta. 1768(6):1367-1377.

Dos Santos T., Varela J., Lynch I., Salvati A., Dawson K.A. 2011. *Quantitative assessment of the comparative nanoparticle-uptake efficiency of a range of cell lines*. Small. 7:3341-3349.

Drescher D., Orts-Gil G., Laube G., Natte K., Veh R.W., Osterle W., Kneipp J. 2011. *Toxicity of amorphous silica nanoparticles on eukaryotic cell model is determined by particle agglomeration and serum protein adsorption effects.* Analytical and Bioanalytical Chemistry. 400(5):1367-73.

Duan H., Nie S. 2007. *Cell-penetrating quantum dots based on multivalent and endosomi-disrupting surface coatings*. J. Am. Chem. Soc. 129(11):3333-3338.

Dubertret B., Skourides P., Norris D.J., Noireaux V., Brivanlou A.H., Libchaber A. 2002. *In vivo imaging of quantum dots encapsulated in phospholipid micelles.* Science. 298(5599):1759-1762.

Dunker A.K. and Obradovic Z. 2001. *The protein trinity - linking function and disorder.* Nature Biotechnology. 19, 805-806.

Dunker A.K., Lawson J.D., Brown C.J., Williams R.M., Romero P., Oh J.S., Oldfield C.J., Campen A.M., Ratliff C.M., Hipps K.W, et al. 2001. *Intrinsically disordered protein.* J. Mol. Graph. Model. 19(1):26-59.

Dunker A.K., Obradovic Z., Romero P., Garner E.C., Brown C.J. 2000. *Intrinsic protein disorder in complete genomes.* Genome Inform. Ser. Workshop Genome Inform. 11, 161-171.

Dutta D., Sundaram S.K., Teeguarden J.G., Riley B.J., Fifield L.S., Jacobs J.M., et al. 2007. *Adsorbed proteins influence the biological activity and molecular targeting of nanomaterials.* Toxicol. Sci. 100(1):303-15.

Ehrenberg M.S., Friedman A.E., Finkelstein J.N., Oberdorster G., McGrath J.L. 2009. *The influence of protein adsorption on nanoparticle association with cultured endothelial cells.* Biomaterials. 30(4):603-610.

Ekimov A.I. and Onushchenko A.A. 1981. *Quantum size effect in three-dimensional microscopic semiconductor crystals*. JETP Lett. 34(6):345-349.

El-Ansary A. and Al-Daihan S. 2009. *On the toxicity of therapeutically used nanoparticles: An overview.* J. Toxicol. 1-9.

Elder A., Gelein R., Silva V., Feikert T., Opanashuk L., Carter J., Potter R., Maynard A., Ito Y., Finkelstein J., Oberdorster G. 2006. *Translocation of inhaled ultrafine manganese oxide particles to the central nervous system* Environ. Health Perspect. 114:1172-1178

Ellis-Behnke R.G., Liang Y.X., You S.W., Tay D.K., Zhang S., So K.F., Schneider G.E. 2006. *Nano neuro knitting: peptide nanofiber scaffold for brain repair and axon regeneration with functional return of vision.* Proc. Natl. Acad. Sci. USA. 103(13):5054-5059.

Elsabahy M. and Wooley K.L. 2012. *Design of polymeric nanoparticles for biomedical delivery applications.* Chem. Soc. Rev. 41(7):2545-2561.

Eneroth A., Åström E., Hoogstraate J., Schrenk D., Conrad S., Kauffmann K-M., Gjellan K. 2001. *Evaluation of a vincristine resistant Caco-2 cell line for use in a calcein AM extrusion screening assay for P-glycoprotein interaction.* Eur. J. 0Pharm. Sci. 12:205-214.

Evans M.D., Dizdaroglu M., Cooke M.S. 2004. *Oxidative DNA damage and disease: induction, repair and significance.* Mutat. Res. 567:1-61.

Ferin J. 2004. *Pulmonary retention and clearance of particles* Toxicol. Lett. 72:121-125

Fernández-García M., Martínez-Arias A., Hanson J.C., Rodríguez J.A. 2004. *Nanostructure oxides in chemistry: characterization and properties.* Chem. Rev. 104(9):4063-104.

Ferrari M. 2008. *Nanogeometry: beyond drug delivery.* Nat. Nanotechnol. 3(3):131-132.

Feynman R.P. 1959. *There's plenty of room at the bottom, an invitation to enter a new field of physics.* Annual meeting of the american physical society. California Institute of Technology.

Fogh J. and Trempe G. 1975. *Human Tumor Cells In Vitro* (J. Fogh, ed.). Plenum.115-141.

Folkmann J.K., Risom L., Jacobsen N.R., Wallin H., Loft S., Møller P. 2009. *Oxidatively damaged DNA in rats exposed by oral gavage to C60 fullerenes and single-walled carbon nanotubes*. Environmental Health Perspectives. 117(5):703-708.

Fowell R.R. 1952. *Sodium acetate agar as a sporulation medium for yeast.* Nature. London. 170(4327):578.

Foyn H., Van Damme P., Støve S.I., Glomnes N., Evjenth R., Gevaert K., Arnesen T. 2013. *Protein N-terminal acetyltransferases act as N-terminal propionyltransferases in vitro and in vivo.* Mol. Cell. Proteomics. 12(1):42-54.

Freidfelder D. 1960. *Bud position in Saccharomyces cerevisiae*. J. Bacteriol. 80:567-8.

Fruijtier-Pölloth C. 2012. *The toxicological mode of action and the safety of syntheticamorphous silica-a nanostructured material.* Toxicology. 294:61-79.

Fu P.P., Xia Q., Sun X., Yu H. 2012. *Phototoxicity and environmental transformation of polycyclic aromatic hydrocarbons (PAHs)-light-induced reactive oxygen species, lipid peroxidation, and DNA damage.* J. Environ. Sci. Health C. Environ. Carcinog. Ecotoxicol. Rev. 30(1):1-41.

Fu C., Liu T., Li L., Liu H., Chen D., Tang F. 2013. *The absorption, distribution, excretion and toxicity of mesoporous silica nanoparticles in mice following different exposure routes*. Biomaterials. 34(10):2565-2575.

Fubini B. and Hubbard A. 2003. *Serial review: role of reactive oxygen and nitrogen species (ROS/RNS) in lung injury and diseases*. Free Radmn. Biol. Med. 34:1507-1516.

Gao X. and Nie S. 2004. *Quantum dot-encoded mesoporous beads with high brightness and uniformity: rapid readout using flow cytometry*. Anal. Chem. 76(8):2406-2410.

Gao X., Chan W.C.W., Nie S. 2002. *Quantum-dot nanocrystals for ultrasensitive biological labeling and multicolor optical encoding*. J. Biomed. Opt. 7(4):532-537.

Garcia-Garcia E., Andrieux K., Gil S., Kima H.R., Le Doana T., Desmaele D., d'Angelo J., Taran F., Georgin D., Couvreur P. 2005. *A methodology to study intracellular distribution of nanoparticles in brain endothelial cells.* Int. J. Pharm. 298:310-314

García-Saucedo C., Field J.A., Otero-Gonzalez L., Sierra-Álvarez R. 2011. *Low toxicity of HfO_2, SiO_2, Al_2O_3 and CeO_2 nanoparticles to the yeast, Saccharomyces cerevisiae.* J. Hazard. Mater. 192(3):1572-1579.

Gasser M., Rothen-Rutishauser B., Krug H.F., Gehr P., Nelle M., Yan B., Wick P. 2010. *The adsorption of biomolecules to multi-walled carbon nanotubes is influenced by both pulmonary surfactant lipids and surface chemistry.* J. Nanobiotechnology. 8:31.

Gatti A.M. and Rivasi F. 2002 *Biocompatibility of micro- and nanoparticles. Part I: in liver and kidney* Biomater. 23 2381-2387

Gaucher G., Asahina K., Wang J.H., Leroux J.C. 2009. *Effect of poly(Nvinyl-pyrrolidone)-block poly (D, L-lactide) as coating agent on the opsonization, phagocytosis, and pharmacokinetics of biodegradable nanoparticles.* Biomacromolecules. 10(2):408-416.

Gaumet M., Vargas A., Gurny R., Delie F. 2008. *Nanoparticles for drug delivery: The need for precision in reporting particle size parameters.* Eur. J. Pharm. Biopharm. 69(1):1-9.

Gautrot J.E. and Zhu X.X. 2009. *Macrocyclic bile acids: from molecular recognition to degradable biomaterial building blocks*. J. Mater. Chem. 19(32):5705-5716.

Ge C., Du J., Zhao L., Wang L., Liu Y., Li D., Yang Y., Zhou R., Zhao Y., Chai Z., Chen C. 2011. *Binding of blood proteins to carbon nanotubes reduces cytotoxicity.* Proceedings of the National Academy of Sciences of the United States of America. 108:16968-16973.

Gebauer J.S., Malissek M., Simon S., Knauer S.K., Maskos M., Stauber R.H., Peukert W., Treuel L. 2012. *Impact of the nanoparticle-protein corona on colloidal stability and protein structure.* Langmuir: ACS J. Surface Colloids. 28:9673-9.

Geiser M. 2010. *Update onmacrophage clearance of inhaledmicro-and nanoparticles.* J. Aerosol. Med. Pulm. Drug. Delivery. 23(4):207-217.

Gessner A., Lieske A., Paulke B.R., Müller R.H. 2002. *Influence of surface charge density on protein adsorption on polymeric nanoparticles: analysis by two-dimensional electrophoresis.* Eur. J. Pharm. Biopharm. 54(2):165-170.

Gheshlaghi Z.N., Riazi G.H., Ahmadian S., Ghafari M., Mahinpour R. 2008. *Toxicity and interaction of titanium dioxide nanoparticles with microtubule protein.* Acta. Biochim. Biophys. Sin. 40(9):777-782.

Ghosh S., Ray M., Rani Das M., Chakrabarti A., Khan A.H., Sarma D.D., Acharya S. 2014. *Modulation of glyceraldehyde-3-phosphate dehydrogenase activity by surface functionalized quantum dots.* Phys.Chem.Chem.Phys., 16, 5276

Gleiter H. 1995. *Nanostructured materials: state of the art and perspectives.* Nanostructured Materials. 6:3-14.

Goffeau A., Barrell B.G., Bussey H., Davis R.W. Dujon B., Feldmann H., Galibert F., Hoheisel J. D., Jacq C., Johnston M., Louis E.J., Mewes H.W., Murakami Y., Philippsen P., Tettelin H., Oliver S.G. 1996. *Life with 600 genes*. Science. 25:546-567.

Gokarna A. 2008. *Quantum dot-based protein micro- and nanoarrays for detection of prostate cancer biomarkers*. Proteomics. 8(9):1809-1818.

Goldman E.R., Balighian E.D., Mattoussi H., Kuno M.K., Mauro J.M., Tran P.T., Anderson G.P. 2002. *Avidin: a natural bridge for quantum dot-antibody conjugates.* J. Am. Chem. Soc. 124(22):6378-6382.

Gonzalez L., Lison D., Kirsch-Volders M. 2008. *Genotoxicity of engineered nanomaterials: a critical review.* Nanotoxicology. 2:252-73.

Gopee N.V., Roberts D.W., Webb P., Cozart C.R., Siitonen P.H., Warbritton A.R., Yu W.W., Colvin V.L., Walker N.J., Howard P.C. 2007. *Migration of intradermally injected quantum dots to sentinel organs in mice.* Toxicol. Sci. 98(1):249-57.

Gordon S. and Taylor P.R. 2005. *Monocyte and macrophage heterogeneity.* Nat. Rev. Immunol. 5(12):953-64.

Gossmann R., Fahrländer E., Hummel M., Mulac D., Brockmeyer J., Langer K. 2015. *Comparative examination of adsorption of serum proteins on HSA-and PLGA-based nanoparticles using SDS–PAGE and LC–MS.* Eur. J. Pharm. Biopharm. 93:80-87.

Gosso S., Gavello D., Giachello C.N., Franchino C., Carbone E., Carabelli V. 2011. *The effect of CdSe-ZnS quantum dots on calcium currents and catecholamine secretion in mouse chromaffin cells.* Biomaterials. 32(34):9040-50.

Grasset E., Pinto M., Dussaulx E., Zweibaum A. 1984. *Epithelial properties of human colonic carcinoma cell line Caco-2; electrical parameters*. J. Am. Physiol. 247:C260-267.

Gromozova E.N. and Voychuk S.J. 2007. *In Biophotonics and Coherent Systems in Biology* (Eds.: L.V. Beloussov, V.L. Voeikov,V.S. Martynyuk), Springer New York. pp. 167-175.

Gupta A.K. and Gupta M. 2005. *Cytotoxicity suppression and cellular uptake enhancement of surface modified magnetic nanoparticles.* Biomater. 26:1565-1573.

Gupta S.C., Sharma A., Mishra M., Mishra R.K., Chowdhuri D.K. 2010. *Heat shock proteins in toxicology: How close and how far?* Life Sci. 86:377-384

Gurr J.R, Wang A.S.S., Chen C.H., Jan K.Y. 2005. *Ultrafine titanium dioxide particles in the absence of photoactivation can induce oxidative damage to human bronchial epithelial cells.* Toxicol. 213:66-73.

Guven K., De Pomerai D.I. 1995 *Differential expression of HSP70 proteins in response to heat and cadmium in Caenorhabditis elegans.* J. Therm. Biol. 20:355-363.

Hadduck A.N., Hindagolla V., Contreras A.E., Li Q., Bakalinsky A.T. 2010. *Does aqueous fullerene inhibit the growth of Saccharomyces cerevisiae or Escherichia coli?* Appl. Environ. Microbiol. 76:8239-8242.

Hadjidemetriou M., Al-Ahmady Z., Mazza M., Collins R.F., Dawson K., Kostarelos K. 2015. *In vivo biomolecule corona around blood-circulating, clinically used and antibody-targeted lipid bilayer nanoscale vesicles.* ACS Nano. 9(8):8142-8156.

Hafner J.H., Cheung C.L., Woolley A.T., Lieber C.M. 2001. *Structural and functional imaging with carbon nanotube AFM probes*. Prog. Biophys. Mol. Biol. 77(1):73-110.

Hagens W.I., Oomen A.G., de Jong W.H., Cassee F.R., Sips A.J. 2007. *What do we (need to) know about the kinetic properties of nanoparticles in the body?* Regul. Toxicol. Pharmacol. 49:217-219.

Han X., Lai L., Tian F., Jiang F.L., Xiao Q., Li Y., Yu Q., Li D., Wang J., Zhang Q., Zhu B., Li R., Liu Y. 2012. *Toxicity of CdTe Quantum Dots on Yeast Saccharomyces cerevisiae.* Small. 8(17):2680-2689

Handy R.D, von der Kammer F., Lead J.R., Hassellov M., Ower R., Crane M. 2008. *The ecotoxicology and chemistry of manufactured nanoparticles.* Ecotoxicology. 17(4):287-314

Harisinghani M.G., Barentsz J., Hahn P.F., Deserno W.M., Tabatabaei S., van de Kaa C.H., de la Rosette J., Weissleder R. 2003. *Noninvasive detection of clinically occult lymph-node metastases in prostate cancer.* N Engl J Med. 348(25):2491-9.

Harush-Frenkel O., Debotton N., Benita S., Altschuler Y. 2007. *Targeting of nanoparticles to the clathrin-mediated endocytic pathway.* Biochem. Biophys. Res. Commun. 353(1):26-32.

Hasegawa U., Nomura S.M., Kaul S.C. 2005. *Nanogel-quantum dot hybrid nanoparticles for live cell imaging.* Biochem. Biophys. Res. Commun. 331(4):917-921.

Hauck T.S., Anderson R.E., Fischer H.C., Newbigging S., Chan W.C. 2010. *In vivo quantum dot toxicity assessment.* Small. 6:138-44.

He X., Nie H., Wang K., Tan W., Wu X., Zhang P. 2008. *In vivo study of biodistribution and urinary excretion of surface-modified silica nanoparticles.* Anal. Chem. 80(24):9597-9603.

Hellstrand E., Lynch I., Andersson A., Drakenberg T., Dahlbäck B., Dawson K.A., Linse S., Cedervall T. 2009. *Complete highdensity lipoproteins in nanoparticle corona.* FEBS J. 276(12):33723381.

Henrich V.E. and Cox P.A. 1994. *The surface chemistry of metal oxides.* Cambridge University Press: Cambridge, UK.

Hidalgo I.J., Raub T.J., Borchardt R.T. 1989. *Characterization of the human colon carcinoma cell line (Caco-2) as a model system for intestinal epithelial permeability.* Gastroenterology. 96:736-749.

Hilgendorf C., Spahn-Langguth H., Regårdh C., Lipka E., Amidon G.L., Langguth P. 2000. *Caco-2 versus Caco-2/HT29-MTX co-cultured cell lines: Permeabilities via diffusion, inside-and outside-directed carrier-mediated transport.* J. Pharm. Sci. 89:63-75.

Hines M.A. and Guyot-Sionnest P. 1996. *Synthesis and characterization of strongly luminescing ZnS-Capped CdSe nanocrystals.* J. Phys. Chem. 100(2):468-471.

Hoet P.H.M., Bruske-Hohlfeld I., Salata O.V. 2004. *Nanoparticles - known and unkown health risks.* J. Nanobiotechnol. 2:12-27.

Hogan J. 2004. *Smog-busting paint soaks up noxious gases.* New Scientist 4 February.

Hong R., Fischer N. O., Verma A., Goodman C. M., Emrick T., Rotello V. M. 2004. *Control of protein structure and function through surface recognition by tailored nanoparticle scaffolds.* J. Am. Chem. Soc. 126:739-743.

Hoshino A., Fujioka K., Oku T., Suga M., Sasaki Y.F., Ohta T., Yasuhara M., Suzuki K., Yamamoto K. 2004. *Physicochemical poperties and cellular toxicity of nanocrystal quantum dots depend on their surface modification.* Nano. Lett. 4(11):2163-2169.

Houghton J. 2005. *Global warming*. Rep. Prog. Phys. 68:1343-1403.

Hu M. and Borchardt R.T. 1990. *Mechanism of L-α-methyldopa transport through a monolayer of polarized human intestinal epithelial cells (Caco-2).* Pharm. Res. 7:1313-1319.

Hu W., Peng C., Lv M., et al. 2011. *Protein corona-mediated mitigation of cytotoxicity of graphene oxide.* ACS Nano. 5(5):3693-3700.

Huang J., Bu L., Xie J., Chen K., Cheng Z., Li X., Chen X. 2010. *Effects of nanoparticle size on cellular uptake and liver MRI with polyvinylpyrrolidone-coated iron oxide nanoparticles.* ACS Nano. 4:7151-7160.

Huang S., Chueh P.J., Lin Y.W., Shih T.S., Chuang S.M. 2009. *Disturbed mitotic progression and genome segregation are involved in cell transformation mediated by nano-TiO2 longterm exposure.*Toxicology and Applied Pharmacology. 241(2):182-194.

Huang X.L., Zhang B., Ren L., Ye S.F., Sun L.P., Zhang Q.Q., Tan M.C., Chow G.M. 2008. *In vivo toxic studies and biodistribution of near infrared sensitive Au-Au(2)S nanoparticles as potential drug delivery carriers.* J. Mater. Sci. Mater. Med. 19(7):2581-8.

Huang Y.W., Wu C.H., Aronstam R.S. 2010. *Toxicity of transition metal oxide nanoparticles: Recent insights from in vitro studies.* Materials. 3(10):4842-4859.

Hubbard A.K., Timblin C.R., Shukla A., Rincón M., Mossman B.T. 2002. *Activation of NF-κB-dependent gene expression by silica in lungs of luciferase reporter mice.* J. Am. Physiol. Lung. Cell. Mol. Physiol. 282(5):L968-L975.

Huet C., Sahuquillo-Merino C., Coudrier E., Louvard D. 1987. *Absorptive and mucus-secreting subclones isolated from a multipotent intestinal cell line (HT-29) provide new models for cell polarity and terminal differentiation.* J. Cell. Biol. 105:345-357.

IARC. 1997. *Iarc monographs on the evaluation of carcinogenic risks to humans.* vol. 86, silica.

Ikeda T. and Kuroda A. 2011. *Colloids and Surfaces B.* Biointerfaces. 86 (2):359-363.

International Standards Organization. 2008. ISO/TS 27687:2008 and 2010. ISO/CD TS 80004-1:2010.

Inui K., Miyamoto M., Saito H. 1992. *Transepithelial transport of oral cephalosporins by monolayers of intestinal epithelial cell line Caco-2; Specific transport systems in apical and basolateral membranes.* J. Pharmacol. Exp. Ther. 261:195-201.

Ishii D., Kinbara K., Ishida Y., Ishii N., Okochi M., Yohda M., Aida T. 2003. *Chaperonin-mediated stabilization and ATP-triggered release of semiconductor nanoparticles*. Nature. 423(6940):628-32.

Iversen T.G., Skotland T., Sandvig K. 2011. *Endocytosis and intracellular transport of nanoparticles: present knowledge and need for future studies.* Nano. Today. 6:176-185.

Jacobsen N.R., Pojana G., White P., Møller P., Cohn C.A., Korsholm K.S., Vogel U., Marcomini A., Loft S., Wallin H. 2008. *Genotoxicity, cytotoxicity, and reactive oxygen species induced by singlewalled carbon nanotubes and C60 fullerenes in the FE1- MutaTMmouse lung epithelial cells.* Environmental and.Molecular Mutagenesis. 49(6):476-487.

Jain M.P., Vaisheva F., Maysinger D. 2012. *Metalloestrogenic effects of quantum dots*. Nanomedicine. 7(1):23-37.

Jaiswal J.K., Goldman E.R., Mattoussi H., Simon S.M. 2003. *Long-term multiple color imaging of live cells using quantum dot bioconjugates.* Nat. Biotech. 21(1):47-51.

Jaiswal J.K., Mattoussi H., Mauro J.M., Simon S.M. 2004. *Use of quantum dots for live cell imaging*. Nat. Meth. 1(1):6.

Jani P., Halbert G.W., Langridge J., Florence A.T. 1990. *Nanoparticle uptake by the rat gastrointestinal mucosa: quantitation and particle size dependency.* J. Pharm. Pharmacol. 42:821-826.

Jansch M., Stumpf P., Graf C., Rühl E., Müller R.H. 2012. *Adsorption kinetics of plasma proteins on ultrasmall superparamagnetic iron oxide (USPIO) nanoparticles.* Int. J. Pharm. 428(1-2):125-133.

Jiang W., Kim B.Y.S, Rutka J.T, Chan W.C.W. 2008. *Nanoparticle-mediated cellular response is size-dependent.* Nat. Nanotechnol. 3:145-150.

Jiang X., Röcker C., Hafner M., Brandholt S., Dörlich R.M., Nienhaus G. U. 2010. *Endoand exocytosis of zwitterionic quantum dot nanoparticles by live HeLa cells*. ACS Nano. 4: 6787-6797.

Jiang X., Weise S., Hafner M., Röcker C., Zhang F., Parak W.J., Nienhaus G.U. 2010. *Quantitative analysis of the protein corona on FePt nanoparticles formed by transferrin binding*. J. R So. Interface 7:S5-S13.

Jirage K.B., Hulteen J.C., Martin C.R. 1997. *Nanotubule based molecular-filtration membranes.* Science. 278(5338):655-658.

Johnstone S.A., Masin D., Mayer L., Bally M.B. 2001. *Surface associated serum proteins inhibit the uptake of phosphatidylserine and poly (ethylene glycol) liposomes by mouse macrophages.* Biochim. Biophys. Acta. 1513(1):25-37.

Jøssang T., Feder J., Rosenqvist E. 1988. *Photon correlation spectroscopy of human IgG.* J. Protein Chem. 7(2):165-171.

Kabanov A.V. 2006. *Polymer genomics: an insight into pharmacology and toxicology of nanomedicines.* Adv. Drug. Deliv. Rev. 58:1597-1621.

Kaewamatawong T., Kawamura N., Okajima M., Sawada M., Morita T., Shimada A. 2005. *Acute pulmonary toxicity caused by exposure to colloidal silica: particle size dependent pathological changes in mice.* Toxicol. Pathol. 33:743-749.

Kagan V., Konduru N., Feng W., Allen B., Conroy J., Volkov Y., Vlasova I., Belikova N., Yanamala N., Kapralov A., Tyurina Y., Shi J., Kisin E., Murray A., Franks J., Stolz D., Gou P., Klein-Seetharaman J., Fadeel B., Star A., Shvedova A. 2010. *Carbon nanotubes degraded by neutrophil myeloperoxidase induce less pulmonary inflammation.* Nat. Nanotechnol. 5:354-359.

Kah J.C.Y., Wong K.Y., Neoh K.G., Song J.H., Fu J.W.P., Mhaisalkar S., Olivo M., Sheppard C.J.R. 2009. *Critical parameters in the pegylation of gold nanoshells for biomedical applications: an in vitro macrophage study.* J. Drug. Targeting. 17:181-193.

Kairdolf B.A., Mancini M.C.M., Smith A., Nie S.M. 2008. *Minimizing nonspecific cellular binding of quantum dots with hydroxyl-derivatized surface coatings.* Anal. Chem. 80(8):3029-34.

Kangwansupamonkon W., Lauruengtana V., Surassmo S., et al. 2009. *Antibacterial effect of apatite-coated titanium dioxide for textiles applications.* Nanomedicine. 5(2):240-9.

Kapralov A.A., Feng W.H., Amoscato A.A., Yanamala N., Balasubramanian K., Winnica D.E., Kisin E.R., Kotchey G.P., Gou P., Sparvero L.J., Ray P., Mallampalli R.K., Klein-Seetharaman J., Fadeel B., Star A., Shvedova A.A., Kagan V.E. 2012. *Adsorption of surfactant lipids by single-walled carbon nanotubes in mouse lung upon pharyngeal aspiration.* ACS Nano. 6:4147-4156.

Karajanagi S.S., Vertegel A.A., Kane R.S., Dordick J.S. 2004. *Structure and function of enzymes adsorbed onto single-walled carbon nanotubes.* Langmuir. 20:11594-11599.

Karlsson J., Wikman A., Artursson P. 1993. *The mucus layer as a barrier to drug absorption in monolayers of human intestinal HT29-H goblet cells.* Int. J. Pharm. 99:209-218.

Karmali P.P. and Simberg D. 2011. *Interactions of nanoparticles with plasma proteins: implication on clearance and toxicity of drug delivery systems*. Expert. Opin. Drug. Deliv. 8(3):343-357.

Kasemets K., Ivask A., Dubourguier H.C., Kahru A. 2009. *Toxicity of nanoparticles of ZnO, CuO and TiO_2 to yeast Saccharomyces cerevisiae*. Toxicology in Vitro. 23:1116-1122.

Kasemets K., Kahru A., Laht T.M., Paalme T. 2006. *Study of the toxic effect of the short- and medium-chain monocarboxylic acids on the growth of Saccharomyces cerevisiae using CO_2-auxo-accelerostat fermentation system.* International Journal of Food Microbiology. 111:206-215.

Kasemets K., Suppi S., Kunnis-Beres K., Kahru A. 2013. *Toxicity of CuO Nanoparticles to Yeast Saccharomyces cerevisiae BY4741 Wild-Type and Its Nine Isogenic Single-Gene Deletion Mutants*. Chem. Res. Toxicol. 26:356-367.

Katari J.E.B., Colvin V.L., Alivisatos A.P. 1994. *X-ray photoelectron spectroscopy of CdSe nanocrystals with applications to studies of the nanocrystal surface.* J Phys Chem. 98(15):4109-4117.

Kellermann E., Seeboth P.G., Hollenberg C.P. 1986. *Analysis of the primary structure and promoter function of a pyruvate decarboxylase gene (PDC1) from Saccharomyces cerevisiae*. Nucleic Acids Res. 14(22):8963-77.

Kellis M., Patterson N., Endrizzi M., Birren B., Lander E.S. 2003. *Sequencing and comparison of yeast species to identify genes and regulatory elements.* Nature. 423(6937):241-54.

Kelly P.M., Åberg C., Polo E., O'Connell A., Cookman J., Fallon J., Krpetić Ž., Dawson K.A. 2015. *Mapping protein binding sites on the biomolecular corona of nanoparticles*. Nat. Nanotechnol. 10:472-9.

Khan J.A., Pillai B., Das T.K., Singh Y., Maiti S. 2007. *Molecular effects of uptake of gold nanoparticles in HeLa cells.* Chem. Biochem. 8(11):1237-40.

Kim B.S., Kim C.S., Lee K.M. 2008. *The intracellular uptake ability of chitosan-coated Poly (D,L-lactide-co-glycolide) nanoparticles.* Arch. Pharmacal. Res. 31(8):1050-4.

Kim C.S., Nguyen H.D., Ignacio R.M., Kim J.H., Cho H.C., Maeng E.H., Kim Y.R., Kim M.K., Park B.K., Kim S.K. 2005. *Immunotoxicity of zinc oxide nanoparticles with different size and electrostatic charge.* Int. J. Nanomedicine. 9(2):195-205.

Kim H.R., Gil S., Andrieux K., Nicolas V., Appel M., Chacun H., Desmaële D., Taran F., Georgin D., Couvreur P. 2007 *Low-density lipoprotein receptor-mediated endocytosis of PEGylated nanoparticles in rat brain endothelial cells.* Cell. Mol. Life Sci. 64(3):356-64.

Kim I.S., Baek M., Choi S.J. 2010. *Comparative Cytotoxicity of Al2O3 , CeO2 , TiO2 and ZnO nanoparticles to human lung cells*. Journal of Nanoscience and Nanotechnology. 10(5):3453-3458.

Kim K.Y., Truman A.W., Levin D.E. 2008. *Yeast Mpk1 mitogen-activated proteinkinase activates transcription through Swi4/Swi6 by a noncatalytic mechanismthat requires upstream signal.* Mol. Cell. Biol. 28:2579-2589.

Kim S., Lim Y.T., Soltesz E.G., De Grand A.M., Lee J., Nakayama A., Parker J.A., Mihaljevic T., Laurence R.G., Dor D.M., Cohn L.H., Bawendi M.G., Frangioni J.V. 2004. *Near-infrared fluorescent type II quantum dots for sentinel lymph node mapping.* Nat. Biotechnol. 22:93-97.

Kirchner C., Liedl T., Kudera S., Pellegrino T., Javier A.M., Gaub H.E., Stolzle S., Fertig N., Parak W.J. 2005. *Cytotoxicity of colloidal CdSe and CdSe/ZnS nanoparticles*. Nano. Lett. 5:331-338.

Kittelson D.B. 2001. *Recent measurements of nanoparticle emission from engines. Current research on Diesel Exhaust Particles Japan Association of Aerosol Science and Technology.* Tokyo, Japan and references therein.

Kittler S., Greulich C., Diendorf J., Koller M., Epple M. 2010. *Toxicity of silver nanoparticles increases during storage because of slow dissolution under release of silver ions.* Chem. Mater. 22(16):4548-4554.

Klaine S.J., Alvareez J.J., Batley G.E., et al. 2008. *Nanomaterials in the environment: behaviour, fate, bioavailability and effects.* Environ. Toxicol. Chem. 27(9):1825-51.

Klein G., Mathé C., Biola-Clier M., Devineau S., Drouineau E., Hatem E., Marichal L., Alonso B., Gaillard J.C., Lagniel G., Armengaud J., Carrière M., Chédin S., Boulard Y., Pin S., Renault J.P., Aude J.C., Labarre J. 2016. *RNA-binding proteins are a major target of silica nanoparticles in cell extracts.*Nanotoxicology. 10(10):1555-1564.

Koeneman B.A., Zhang Y., Hristovski K., et al. 2009. *Experimental approach for an in vitro toicity assay with non-aggregated quantum dots.* Toxicol. in vitro. 23(5):955-62.

Koffie R., Farrarc C., Saidia L., Williama C., Hymana B., Spires-Jones T. 2011. *Nanoparticles enhance brain delivery of blood brain barrier-impermeable probes for in vivo optical and magnetic resonance imaging*. Proc. Natl. Acad. Sci. USA.108:18837-18842.

Koper O.B., Klabunde J.S., Marchin G.L., Klabunde K.J., Stoimenov P., Bohra L. 2002. *Nanoscale powders and formulations with biocidal activity toward spores and vegetative cells of bacillus species, viruses, and toxins*. Curr. Microbiol. 44:49-55.

Krege J.H., Hodgin J.B., Couse J.F., Enmark E., Warner M., Mahler J.F., Sar M., Korach K.S., Gustafsson J.A., Smithies O. 1998. *Generation and reproductive phenotypes of mice lacking estrogen receptor beta.* Proc. Natl. Acad. Sci. USA. 95(26):15677-82.

Kreuter J., Hekmatara T., Dreis S., Vogel T., Gelperina S., Langer K. 2007. *Covalent attachment of apolipoprotein A-I and apolipoproteine B-100 to albumin nanoparticles enables drug transport into the brain.* J. Control. Release. 118(1):54-58.

Kubiak M. 2014. *Dendrimers-fascinating nanoparticles in the application in medicine.* Chem. 68(2):141-150.

Kumar A., Forbes B., Mudway I., Bicer E.M., Dailey L.A. 2015. *What are the biological and therapeutic implications of biomolecule corona formation on the surface of inhaled nanomedicines?* Nanomedicine. London. 10(3):343-345.

Kung H.H. 1989. *Transition metal oxides: surface chemistry and catalysis.* Elsevier Amsterdam.

Kungolos A., Aoyama I., Muramoto S. 1999. *Toxicity of organic and inorganic mercury to Saccharomyces cerevisiae.* Ecotoxicology and Environmental Safety. 43:149-155.

Kuno M. and Lee J.K. 1997. *The Band edge luminescence of surface modified CdSe nanocrystallites: probing the luminescing state.* J. Chem. Phys. 106(23):9869-9882.

Lademann J., Weigmann H., Rickmeyer C., Barthelmes H., Schaefer H., Mueller G., Sterry W. 1999. *Penetration of titanium dioxide microparticles in a sunscreen formulation into the horny layer and the follicular orifice.* Skin Pharmacol. Appl. Skin. Physiol. 12:247-256.
Lancaster D.L., Dobson C.M., Rachubinski R.A. 2013. *Chaperone proteins select and maintain [PIN+] prion conformations in Saccharomyces cerevisiae.* J Biol Chem. 288(2):1266-76

Landgraf L., Christner C., Storck W., Schick I., Krumbein I., Dähring H., Haedicke K., Heinz-Herrmann K., Teichgräber U., Reichenbach J.R., Tremel W., Tenzer S., Hilger I. 2015. *A plasma protein corona enhances the biocompatibility of Au@ Fe3O4 Janus particles.* Biomaterials. 68:77-88.

Lane D.P. 1992. *Cancer P53, guardian of the genome.* Nature. 358(6381):15-16.

Larger P., Altamura M., Catalioto R.M., Giuliani S., Maggi C.A., Valenti C., Triolo A. 2002. *Simultaneous LC-MS/MS determination of reference pharmaceuticals as a method for the characterization of Caco-2 cell monolayer absorption properties.* Anal. Chem. 74: 5273-5281.

Larson D.R., Zipfel W.R., Williams R.M., Clark S.W., Bruchez M.P., Wise F.W., Webb W.W. 2003. *Water-soluble quantum dots for multiphoton fluorescence imaging in vivo.* Science. 300(5624):1434-1436.

Lee C.C., Mackay J.A., Frechet J.M.J., Szoka F.C. 2005. *Designing dendrimers for biological applications.* Nat. Biotech. 23(12):1517-1526.

Lee J.A., Kim M.K., Kim H.M., Oh J.M., Choi S.J. 2015. *The fate of calcium carbonate nanoparticles administered by oral route: absorption and their interaction with biological matrices.* Int. J. Nanomedicine. 10:2273-93.

Lee K.H. 2012. *Quantitative molecular profiling of biomarkers for pancreatic cancer with functionalized quantum dots.* Nanomedicine. 8(7):1043-51.

Lee S., Lee J., Kim K., Sim S.J., Gu M.B., Yi J., Lee J. 2009. *Ecotoxicity of commercial silver nanopowders to bacterial and yeast strains.* Biotechnol. Bioprocess. Eng. 14:490-495.

Lee C.S. and Belfort G., 1989. *Changing activity of ribonuclease A during adsorption: a molecular explanation.* Proc Natl Acad Sci USA. 86(21): 8392–8396.

Leevy W.M., Lambert T.N., Johnson J.R., Morris J., Smith B.D. 2008. *Quantum dot probes for bacteria distinguish Escherichia coli mutants and permit in vivo imaging*. Chem. Commun. (Camb). 20:2331-2333.

Leroueil P.R., Hong S., Mecke A., Baker J.R. Jr, Orr B.G., Banaszak Holl M.M. 2007. *Nanoparticle interaction with biological membranes: does nanotechnology present a Janus face?* Acc. Chem. Res. 40(5):335-42.

Lesniak A., Fenaroli F., Monopoli M.P., Aberg C., Dawson K.A., Salvati A. 2012. *Effects of the presence or absence of a protein corona on silica nanoparticle uptake and impact on cells.* ACS Nano. 6(7):5845-5857.

Lesuffleur T., Barbat A., Dussaulx E., Zweibaum A. 1990. *Growth adaptation to methotrexate of HT-29 human colon carcinoma cells is associated with their ability to differentiate into columnar absorptive and mucus-secreting cells*. Cancer. Res. 50:6334-6343.

Lesuffleur T., Barbat A., Luccioni C., Beaumatin J., Clair M., Kornowski A., Dussaulx E., Dutrillaux B., Zweibaum A. 1991 b. *Dihydrofolate reductase gene ampli®cation-associated shift of differentiation in methotrexate-adapted HT-29 cells.* J. Cell. Biol. 115:1409-1418.

Lesuffleur T., Kornowski A., Luccioni C., Muleris M., Barbat A., Beaumatin J., Dussaulx E., Dutrillaux B., Zweibaum A. 1991 a. *Adaptation to 5-fuorouracil of the heterogeneous colon tumor cell line HT-29 results in the selection of cells commited to differentiation.* Int. J. Cancer. 49:721-730.

Lewinski N., Colvin V., Drezek R. 2008. *Cytotoxicity of nanoparticles*. Small. 4:26-49.

Li J., Chang X., Chen X., Gu Z., Zhao F., Chai Z., Zhao Y. 2014. *Toxicity of inorganic nanomaterials in biomedical imaging*. Biotechnol. Adv. 32:727-743.

Li S-D., Huang L. 2008. *Pharmacokinetics and biodistribution of nanoparticles*. Mol. Pharm. 5:496-504.

Li T., Shi T., Li X., Zeng S., Yin L., Pu Y. 2014. *Effects of nano-MnO2 on dopaminergic neurons and the spatial learning capability of rats.* Int. J. Environ. Res. Public Health. 11(8):7918-7930.

Li W., Chen C.Y., Ye C., Wei T.T., Zhao Y.L., Lao F., Chen Z., Meng H., Gao Y.X., Yuan H., Xing G.M., Zhao F., Chai Z.F., Zhang X.J., Yang F.Y., Han D., Tang X.H., Zhang Y.G. 2008. Nanotechnology. 19-12.

Li X., Liu W., Sun L., Aifantis K.E., Yu B., Fan Y., Feng Q., Cui F., Watari F. 2014. *Effects of phy-icochemical properties of nanomaterials on their toxicity.* J. Biomed. Mater. Res. A. 103(7):2499-507.

Li Y., Leung P., Yao L., Song Q.W., Newton E. 2006. *Antimicrobial effect of surgical masks coated with nanoparticles*. J. Hosp. Infect. 62(1):58-63.

Li Y., Sun L., Jin M., Du Z., Liu X., Guo C., Huang P., Sun Z. 2011. *Size-dependent cytotoxicity of amorphous silica nanoparticles in human hepatoma HepG2 cells.* Toxicology in vitro: an international journal published in association with BIBRA.

Li Y., Yu S., Wu Q., Tang M., Pu Y., Wang D. 2012. *Chronic Al2O3-nanoparticle exposure causes neurotoxic effects on locomotion behaviors by inducing severe ROS production and disruption of ROS defense mechanisms in nematode Caenorhabditis elegans.* J. Hazard Mater. 219-220:221-30.

Liberman A., Mendez N., Trogler W.C., Kummel A.C. 2014. *Synthesis and surface functionalization of silica nanoparticles for nanomedicine.* Surf. Sc.i Rep. 69:132-158.

Lien Z.Y., Hsu T.C., Liu K.K., Liao W.S., Hwang K.C., Chao J.I. 2012. *Cancer cell labeling and tracking using fluorescent and magnetic nanodiamond*. Biom. 33(26):6172-6185.

Lim D., Roh J.Y., Eom H.J., Choi J.Y., Hyun J., Choi J. 2012. *Oxidative stress-related PMK 1 P38 MAPK activation as a mechanism for toxicity of silver nanoparticles to reproduction in the nematode Caenorhabditis elegans.* Environ Toxicol. Chem. 31(31):585-92.

Lin W., Huang Y.W. Zhou X.D., Ma Y. 2006. *In vitro toxicity of silica nanoparticles in human lung cancer cells*. Toxicol. Appl. Pharmacol. 217(3):252-259.

Lindman S., Lynch I., Thulin E., Nilsson H., Dawson K.A., Linse S. 2007. *Systematic investigation of the thermodynamics of HAS adsorption to N-iso-propylacrylamide/N-tert butylacrylamide copolymer nanoparticles. Effects of particle size and hydrophobicity.* Nano. Lett. 7(4):914-920.

Lipka J., Semmler-Behnke M., Sperling R.A., Wenk A., Takenaka S., Schleh C., Kissel T., Parak W. J., Kreyling W.G. 2010. *Biodistribution of PEG-modified gold nanoparticles following intratracheal instillation and intravenous injection.* Biomaterials. 31(25):6574-6581.

Liu J. 2010. *Multiplexed detection and characterization of rare tumor cells in Hodgkin's lymphoma with multicolor quantum dots.* Anal. Chem. 82(14):6237-6243.

Liu J., Wong H.L., Moselhy J., Bowen B., Wu X.Y., Johnston M.R. 2006. *Targeting colloidal particulates to thoracic lymph nodes.* Lung Cancer. 51:377-386.

Liu Y., Li X., Bao S., et al. 2013a. *Plastic protein microarray to investigate the molecular pathways of magnetic nanoparticle-induced nanotoxicity.* Nanotechnology. 24:175501.

Liu Y., Xu Z., Li X. 2013b. *Cytotoxicity of titanium dioxide nanoparticles in rat neuroglia cells.* Brain Inj. 27(7-8):934-939.

Lockman P.R., Koziara J.M., Mumper R.J., Allen D.D. 2004. *Nanoparticle syrface charges alter bloodbrain barrier integrity and permeability.* J. Drug Targeting. 12:635-641.

Longmire M., Choyke P., Kobayashi H. 2008. *Clearance properties of nano-sized particles and molecules as imaging agents: considerations and caveats*. Nanomedicine. 3(5):703-717.

Lovrić J., Bazzi H.S., Cuie Y., Fortin G.R.A., Winnik F.M., Maysinger D. 2005. *Differences in subcellular distribution and toxicity of green and red emitting CdTe quantum dots*. J. Mol. Med. 83(5): 377-385.

Lu F., Wu S.H., Hung Y., Mou C.Y. 2009. *Size effect on cell uptake in wellsuspended, uniform mesoporous silica nanoparticles.* Small. 5:1408-1413.

Lühmann T., Rimann M., Bittermann A.G., Hall H. 2008. *Cellular uptake and intracellular pathways of PLL-g-PEG-DNA nanoparticles*. Bioconjug. Chem. 19(9):1907-1916.

Lundqvist M., Sethson I., Jonsson B. 2005. *High-resolution 2D 1H-15N NMR characterization of persistent structural alterations of proteins induced by interactions with silica nanoparticles*. Langmuir. 21:5974–5979.

Lundqvist M., Stigler J., Elia G., Lynch I., Cedervall T., Dawson K.A. 2008. *Nanoparticle size and surface properties determine the protein corona with possible implications for biological impacts.* Proc. Natl. Acad. Sci. USA. 105(38):14265-14270.

Lunov O., Syrovets T., Loos C., et al. 2011. Differential *uptake of functionalized polystyrene nanoparticles by human macrophages and a monocytic cell line.* ACS Nano. 5(3):1657-1669.

Lynch I. and Dawson K.A. 2008. *Protein-nanoparticle interactions.* Nano. Today. 3(1-2):40-47.

Ma Z., Bai J., Wang Y., Jiang X. 2014. *Impact of shape and pore size of mesoporous silica nanoparticles on serum protein adsorption and RBCs hemolysis*. ACS Appl. Mater. Interfaces. 6(4):2431-8.

Maffre P., Nienhaus K., Amin F., Parak W.J., Nienhaus G.U. 2011. *Characterization of protein adsorption onto FePt nanoparticles using dual-focus fluorescence correlation spectroscopy.* Beilstein J. Nanotechnol. 2:374-383.

Mager W.H. and Winderickx J. 2005. *Yeast as a model for medical and medicinal research.* Trends in Pharmacological Sciences. 26:265-273.

Mahmoudi M., Abdelmonem A. M., Behzadi S., Clement J. H., Dutz S., Ejtehadi M. R., et al. 2013. *Temperature: the "ignored" factor at the nanobio interface*. ACS Nano. 7(8):6555-62.

Mahmoudi M., Hofmann H., Rothen-Rutishauser B., Petri-Fink A. 2012. *Assessing the in vitro and in vivo toxicity of superparamagnetic iron oxide nanoparticles.* Chem. Rev. 112(4):2323-2338.

Mahmoudi M., Lynch I., Ejtehadi M.R., Monopoli M.P., Bombelli F.B., Laurent S. 2011. *Protein-nanoparticle interactions: opportunities and challenges.* Chem. Rev. 111:5610-5637.

Mahto S.K., Park C., Yoon T.H., Rhee S.W. 2010. *Assessment of cytocompatibility of surfacemod fied CdSe/ZnSe quantumdots for BALB/3T3 fibroblast cells.* Toxicol. in vitro. 24:1070-1077.

Mailänder V. and Landfester K. 2009. *Interaction of nanoparticles with cells.* Biomacromolecules. 10(9):2379-2400.

Maiorano G., Sabella S., Sorce B., Brunetti V., Malvindi M.A., Cingolani R., et al. 2010. *Effects of cell culture media on the dynamic formation of protein-nanoparticle complexes and influence on the cellular response.* ACS Nano. 4(12):7481-7491.

Maïté L., Carlesso N., Tung C.H., Tang X.W., Cory D., Scadden D.T., Weissleder R. 2000. *Tat peptide-derivatized magnetic nanoparticles allow in vivo tracking and recovery of progenitor cells.* Nat. Biotechnol. 18(4):410-414.

Malugin A. and Ghandehari H. 2010. *Cellular uptake and toxicity of gold nanoparticles in prostate cancer cells: a comparative study of rods and spheres*. J. Appl. Toxicol. 30:212-217.

Malvindi M.A., Brunetti V., Vecchio G., Galeone A., Cingolani R., Pompa P.P. 2012. *SiO2nanoparticles biocompatibility and their potential for gene delivery andsilencing,* Nanoscale. 4:486-495.

Manokaran S., Zhang X., Chen W., Srivastava D.K. 2010. *Differential modulation of the active site environment of human carbonic anhydrase XII by cationic quantum dots and polylysine*. Biochim. Biophys. Acta. 1804(6):1376-84.

Mao C. 2004. *Introduction: nanomaterials characterization using microscopy.* Microscopy Research and Technique. 64:345-346.

Markowska M., Oberle R., Juzwin S., Hsu C.P., Gryszkiewicz M., Streeter A.J. 2001. *Optimizing Caco-2 cell monolayers to increase throughput in drug intestinal absorption analysis*. J Pharmacol. Toxicol. Methods. 46:51-55.

Marmiroli M., Pagano L., Pasquali F., Zappettini A., Tosato V., Bruschi C.V., Marmiroli N. 2016. *A genome-wide nanotoxicology screen of Saccharomyces cerevisiae mutants reveals the basis for cadmium sulphide quantum dot tolerance and sensitivity*. Nanotoxicology. 1-10.

Martel J., Young D., Young A., Wu C.Y., Chen C.D., Yu J.S., Young J.D. 2011. *Comprehensive proteomic analysis of mineral nanoparticles derived from human body fluids and analyzed by liquid chromatography–tandem mass spectrometry.* Anal. Biochem. 418(1):111-125.

Matsusaki M., Larsson K., Akagi T., Lindstedt M., Akashi M., Borrebaeck C.K. 2005. *Nanosphere induced gene expression in human dendritic cells.* Nano. Lett. 5(11):2168-73.

Mattheakis L.C., Dias J.M., Choi Y.J., Gong J., Bruchez M.P., Liu J., Wang E. 2004. *Optical coding of mammalian cells using semiconductor quantum dots.* Anal. Biochem. 327(2):200-208.

Mátyus L., Szöllősi J., Jenei A.J. 2006. *Steady-state fluorescence quenching applications for studying protein structure and dynamics.* Photochem. Photobiol. B. Biol. 83:223-236.

Maysinger D., Behrendt M., Lalancette-Hebert M., Kriz J. 2007. *Real-time imaging of astrocyte response to quantum dots: in vivo screening model system for biocompatibility of nanoparticles.* Nano. Lett. 7(8):2513-2520.

McAlister L., Holland M.J. 1985a. *Isolation and characterization of yeast strains carrying mutations in the glyceraldehyde-3-phosphate dehydrogenase genes*. J. Biol. Chem. 260:15013-15018.

McAlister L., Holland M.J. 1985b. *Differential expression of the three yeast glyceraldehyde-3-phosphate dehydrogenase genes*. J. Biol. Chem. 260:15019-15027.

McLaren A., Valdes-Solis T., Li G., Tsang S.C. 2009. *Shape and size effects of ZnO nanocrystals on photocatalytic activity.* J. Am. Chem. Soc. 131(5):12540-1.

Medina C., Santos-Martinez M.J., Radomski A., Corrigan O.I., Radomski M.W. 2007. *Nanoparticles: pharmacological and toxicological significance*. Br. J. Pharmacol. 150(5):552-558.

Medintz I.L., Konnert J.H., Clapp A.R., Stanish I., Twigg M.E., Mattoussi H., Mauro J.M., Deschamps J.R. 2004. *A fluorescence resonance energy transfer-derived structure of a quantum dot-protein bioconjugate nanoassembly.* Proc. Nat. Acad. Sci. USA. 101:9612-9617.

Meng H., Xia T., George S., Nel A.E. 2009. *A predictive toxicological paradigm for the safety assessment of nanomaterials.* ACS Nano. 3:1620-1627.

Miclăuş T., Bochenkov V.E., Ogaki R., Howard K.A., Sutherland D.S. 2014. *Spatial mapping and quantification of soft and hard protein coronas at silver nanocubes.* Nano. Lett 14(4):2086-2093.

Milani S., Baldelli Bombelli F., Pitek A.S., Dawson K.A., Rädler J. 2012 *Reversible versus irreversible binding of transferrin to polystyrene nanoparticles: soft and hard corona.* ACS Nano. 6:2532-2541.

Milic M., Leitinger G., Pavicic I., Zebic Avdicevic M., Dobrovic S., Goessler W., Vinkovic Vrcek I. 2014. *Cellular uptake and toxicity effects of silver nanoparticles in mammalian kidney cells*. J. Appl. Toxicol. 35(6):581-92.

Mironava T., Hadjiargyrou M., Simon M., Jurukovski V., Rafailovich M.H. 2010. *Gold nanoparticles cellular toxicity and recovery: Effect of size, concentration and exposure time.* Nanotoxicology. 4:120-137.

Mirsadeghi S., Dinarvand R., Ghahremani M.H., Hormozi-Nezhad M.R., Mahmoudi Z., Hajipour M.J., Atyabi F., Ghavami M., Mahmoudi M. 2015. *Protein corona composition of gold nanoparticles/nanorods affects amyloid beta fibrillation process.* Nanoscale. 7(11):5004-5013.

Mo Y.Q., Zhu X.Q., Hu X., Tollerud D.J., Zhang Q.W. 2008. *Cytokine and NO release from peripheral blood neutrophils after exposure to metal nanoparticles: In vitro and ex vivo studies.* Nanotoxicology. 2(2):79-87.

Mochalin V.N., Shenderova O., Ho D., Gogotsi Y. 2012. *The properties and applications of nanodiamonds.* Nat. Nanotechnol. 7(1):11-23.

Moghimi S.M. and Szebeni J. 2003. *Stealth liposomes and long circulating nanoparticles: critical issues in pharmacokinetics, opsonization and protein-binding properties*. Prog. Lipid Res. 42, 463–478.

Mok H., Bae K.H., Ahn C.H., Park T.G. 2008. *PEGylated and MMP-2 specifically DePEGylated quantum dots: comparative evaluation of cellular uptake.* Langmuir. 25(3):1645-1650.

Monopoli M.P., Aberg C., Salvati A., Dawson K.A. 2012 *Biomolecular coronas provide the biological identity of nanosized materials*. Nat. Nanotechnol. 7(12):779-786.

Monopoli M.P., Walczyk D., Campbell A., Elia G., Lynch I., Baldelli Bombelli F., Dawson K.A. 2011. *Physical−chemical aspects of protein corona: relevance to in vitro and in vivo biological impacts of nanoparticles.* J. Am. Chem. Soc. 133:2525-2534.

Monteiro-Riviere N.A., Nemanich R.J., Inman A.O., Wang Y.Y., Riviere J.E. 2005. *Multi-walled carbon nanotube interactions with human epidermal keratinocytes*. Toxicol. Lett. 155:377-384.

Morishige T., Yoshioka Y., Inakura H., Tanabe A., Yao X., Narimatsu S., Monobe Y., Imazawa T., Tsunoda S., Tsutsumi Y., Mukai Y., Okada N., Nakagawa S. 2010a. *The effect of surface modification of amorphous silica particles on NLRP3 inflammasome mediated IL- 1beta production, ROS production and endosomal rupture.* Biomaterials. 31:6833-6842.

Morishige T., Yoshioka Y., Inakura H., Tanabe A., Yao X., Tsunoda S., Tsutsumi Y., Mukai Y., Okada N., Nakagawa S. 2010b. *Cytotoxicity of amorphous silica particles against macrophage-like thp-1 cells depends on particle-size and surface properties.* Die Pharmazie. 65(8):596-9.

Morishige K., Kacher D.F., Libby .P, Josephson L., Ganz P., Weissleder R., Aikawa M. 2010. *High-resolution magnetic resonance imaging enhanced with superparamagnetic nanoparticles measures macrophage burden in atherosclerosis.* Circulation. 122(17):1707-15.

Mortensen L.J., Oberdorster G., Pentland A.P., DeLouise L.A. 2008. *In vivo skin penetration of quantum dot nanoparticles in the murine model: the effect of UVR.* Nano. Lett. 8(9):2779-87.

Mortimer R.K. 1958. *Radiobiological and genetic studies on a polyploid series (haploid to hexaploid) of Saccharomyces cerevisiae.* Radiation Res. 9(3):312-26.

Mosqueira V.C.F., Legrand P., Gulik A., et al. 2001. *Relationship between complement activation, cellular uptake and surface physicochemical aspects of novel PEG-modified nanocapsules.* Biomaterials. 22(22):2967-2979.

Mu Q., Jiang G., Chen L., Zhou H., Fourches D., Tropsha A., Yan B. 2014. *Chemical basis of interactions between engineered nanoparticles and biological systems*. Chem Rev. 114(15):7740-81.

Murphy K.G. and Bloom S.R. 2006. *Gut hormones and the regulation of energy homeostasis*. Nature. 444(7121):854-9.

Mutwakil M.H., Reader J.P., Holdich D.M., Smithurst P.R., Candido E.P.M., JonesD.,Stringham E. G., de Pomerai D.I. 1997. *Use of stress-inducible transgenic nematodes as biomarkers of heavy metal pollution in water samples from an English river system.* Arch. Environ Contam. Toxicol. 32:146-153

Nabeshi H., Yoshikawa T., Matsuyama K., Nakazato Y., Arimori A., Isobe M., Tochigi S., Kondoh S., Hirai T., Akase T., Yamashita T., Yamashita K., Yoshida T., Nagano K., Abe Y., Yoshioka Y., Ka-mada H., Imazawa T., Itoh N., Kondoh M., Yagi K., Mayumi T., Tsunoda S., Tsutsumi Y. 2012. *Amorphous nanosilicas induce consumptive coagulopathy after systemic exposure.* Nanotechnology. 23(4):045101.

Nabeshi H., Yoshikawa T., Matsuyama K., Nakazato Y., Arimori A., Isobe M., Tochigi S., Kondoh S., Hirai T., Akase T., Yamashita T., Yamashita K., Yoshida T., Nagano K., Abe Y., Yoshioka Y., Kamada H., Imazawa T., Itoh N., Tsunoda S., Tsutsumi Y. 2010. *Size-dependent cytotoxic effects of amorphous silica nanoparticles on langerhans cells.* Die Pharmazie. 65(3):199-201.

Nabeshi H., Yoshikawa T., Matsuyama K., Nakazato Y., Matsuo K., Arimori A., Isobe M., Tochigi S., Kondoh S., Hirai T., Akase T., Yamashita T., Yamashita K., Yoshida T., Nagano K., Abe Y., Yoshioka Y., Kamada H., Imazawa T., Itoh N., Nakagawa S., Mayumi T., Tsunoda S., Tsutsumi Y. 2011. *Systemic distribution, nuclear entry and cytotoxicity of amorphous nanosilica following topical application.* Biomaterials. 32(11):2713-24.

Nabiev I., Mitchell S., Davies A., Williams Y., Kelleher D., Moore R., Gun'ko Y.K., Byrne S., Rakovich Y.P., Donegan J.F., Sukhanova A., Conroy J., Cottell D., Gaponik N., Rogach A., Volkov Y. 2007. *Nonfunctionalized nanocrystals can exploit a cell's active transport machinery delivering them to specific nuclear and cytoplasmic compartments*. Nano. Lett. 7:3452-3461.

Nagayama S., Ogawara K-I., Fukuoka Y., Higaki K., Kimura T. 2007a. *Time-dependent changes in opsonin amount associated on nanoparticles alter their hepatic uptake characteristics.* Int. J. Pharm. 342(1):215-221.

Nagayama S., Ogawara K-I., Minato K., et al. 2007b. *Fetuin mediates hepatic uptake of negatively charged nanoparticles via scavenger receptor.* Int. J. Pharm. 329(1-2):192-198.

Nair P.M.G., Park S.Y., Lee S.W., Choi J. 2011. *Differential expression of ribosomal protein gene, gonadotrophin releasing hormone gene and Balbiani ring protein gene in silver nanoparticles exposed chironomus riparius.* Aquat. Toxicol. 101(1):31-7.

Napierska D., Thomassen L.C., Lison D., Martens J.A., Hoet P.H. 2010. *The nanosilica hazard: another variable entity.* Part. fibre toxicol. 7(1):39.

Napierska D., Thomassen L.C., Rabolli V., Lison D., Gonzalez L., Kirsch-Volders M., Martens J. A., Hoet P.H. 2009. *Size-dependent cytotoxicity of monodisperse silica nanoparticles in human endothelial cells*. Small. 5(7):846-53.

National Nanomaterial Initiative. 2010.

Navarro D.A., Bisson M.A., Aga D.S. 2012. *Investigating uptake of water-dispersible CdSe/ZnS quantum dot nanoparticles by Arabidopsis thaliana plants*. J. Hazard Mater. 211-212:427-435.

Needleman P. and Greenwald J.E. 1986. *Atriopeptin: a cardiac hormone intimately involved in fluid, electrolyte, and blood-pressure homeostasis*. N. Engl. J. Med. 314(13):828-34.

Nel A., Xia T., Madler L., Li N. 2006. *Toxic potential of materials at the nanolevel.* Science. 311:622-627.

Nel A.E., Mädler L., Velegol D., Xia T., Hoek E.M., Somasundaran P., et al. 2009. *Understanding biophysicochemical interactions at the nano-bio interface.* Nat. Mater. 8(7):543-557.

Nemmar A., Hoet P.H., Vanquickenborne B., Din-sdale D., Thomeer M., Hoylaerts M. F., Vanbilloen H., Mortelmans L., Nemery B. 2002 a. *Passage of inhaled particles into the blood circulation in humans*. Circulation. 105:411-414.

Nemmar A., Hoylaerts M.F., Hoet P.H.M., Dins dale D., Smith T., Xu H., Vermylen J., Nemery B. 2002b. *Ultrafine particles affect experimental thrombosis in an vivo hamster model* Am. J. Respir. Cri.t Care. Med. 166:998-1004

Nienhaus G.U. 2005. Ed. Protein-ligand interactions*; Methods in Molecular Biology*. Vol. 305 Humana Press: New York, USA.

Niidome T., Yamagata M., Okamoto Y., Akiyama Y., Takahashi H., Kawano T., Katayama Y., Niidome Y. 2006. *PEG-modified gold nanorods with a stealth character for in vivo applications*. J. Control. Release. 114:343-347.

Nishimori H., Kondoh M., Isoda K., Tsunoda S.I., Tsutsumi Y., Yagi K. 2009. *Silica nanoparticles as hepatotoxicants.* Eur. J. Pharm. Biopharm. 72(3):496-501.

Noguera C. 1996. *Physics and chemistry at oxide surfaces*. Cambridge University Press: Cambridge, UK.

Nordgard C.T., Nonstad U., Olderoy M.O., Espevik T., Draget K.I. 2014. *Alterations in mucus barrier function and matrix structure induced by guluronate oligomers.* Biomacromolecules. 15(6):2294-300.

Nurkiewicz T.R., Porter D.W., Barger M., Millecchia L., Rao K.M., Marvar P.J., Hubbs A. F., Castranova V., Boegehold M. A. 2006. *Systemic microvascular dysfunction and inflammation after pulmonary particulate matter exposure.* Environ Health Perspect. 114(3):412-9.

Oberdorster G. 2001. *Pulmonary effects of inhaled ultrafine particles.* Int. Arch. Occup. Environ. Health 74:1-8.

Oberdörster G. 2002. *Toxicokinetics and effects of fibrous and nonfibrous particles inhalation.* Toxicol. 14:29-56.

Oberdörster G., Ferin J., Lehnert B.E. 1994. *Correlation between particle size, in vivo particle persistence, and lung injury.* Environ. Health Persp. 102(5):173-179.

Oberdörster G., Maynard A., Donaldson K., Castranova V., Fitzpatrick J., Ausman K., Carter J., Karn B., Kreyling W., Lai D., Olin S., Monteiro-Riviere N., Warheit D., Yang H. 2005. *Principles for characterizing the potential human health effects from exposure to nanomaterials: elements of a screening strategy.* Part. Fibre Toxicol. 6:2-8.

Oberdörster G., Oberdörster E., Oberdörster J. 2005. *Nanotoxicology: An emerging discipline evolving from studies of ultrafine particles.* Environ. Health Perspect. 113(7):823-39.

Oberdörster G., Sharp Z., Atudorei V., Elder A., Gelein R., Lunts A. 2002. *Extrapulmonary translocation of ultrafine carbon particles following whole-body inhalation exposure of rats.* J. Toxicol. Environ. Health A. 65:1531-1543.

Ogawara K., Furumoto K., Nagayama S., Minato K., Higaki K., Kai, T., Kimura T. 2004. *Pre-coating with serum albumin reduces receptor-mediated hepaticdisposition of polystyrene nanosphere: implications for rational design ofnanoparticles.* Journal of Controlled Release: Official Journal of the Controlled Release Society. 100:451-455.

Oh W.K., Kim S., Choi M., et al. 2010. *Cellular uptake, cytotoxicity, and innate immune response of silica-titania hollow nanoparticles based on size and surface functionality.* ACS Nano. 4(9):5301-13.

Okpala C. 2014. *The beneficts and applications of nano composites.* International Journal of Advanced Engineering Technology. 5(4):E-ISSN 0976-3945.

Oldfield C.J., Cheng Y., Cortese M.S., Brown C.J., Uversky V.N., Dunker A.K. 2005. *Comparing and combining predictors of mostly disordered proteins.* Biochemistry. 44 (6): 1989-2000.

Oldfield C.J., Meng J., Yang J.Y., Yang M.Q., Uversky V.N., Dunker A.K. 2008. *Flexible nets: disorder and induced fit in the associations of p53 and 14-3-3 with their partners*. Bmc Genomics. 9, (1), S1.

Oldfors A. and Fardeau M. 1983. *The permeability of the basal lamina at the neuromuscular junction. An ultrastructural study of rat skeletal muscle using particulate tracers.* Neuropathol Appl. Neurobiol. 9:419-432.

Otero-González L., García-Saucedo C., Field J.A., Sierra-Álvarez R. 2013. *Toxicity of TiO_2, ZrO_2, Fe0, Fe_2O_3, and Mn_2O_3 nanoparticles to the yeast Saccharomyces cerevisiae.* Chemosphere. 93:1201-1206.

Owens D.E. 3rd, Peppas N.A. 2006. *Opsonization, biodistribution, and pharmacokinetics of polymeric nanoparticles.* Int. J. Pharm. 307(1):93-102.

Oztug Durer Z.A., Cohlberg J.A., Dinh P., Padua S., Ehrenclou K., Downes S., Tan J.K., Nakano Y., Bowman C.J., Hoskins J.L., Kwon C., Mason A.Z., Rodriguez J.A., Doucette P.A., Shaw B. F., Valentine J.S. 2009. *Loss of metal ions, disulfide reduction and mutations related to familial ALS promote formation of amyloid-like aggregates from superoxide dismutase.* PLoS One. 4(3):e5004.

Pal A.K., Aalaei I., Gadde S., Gaines P., Schmidt D., Demokritou P., Bello D. 2014. *High resolution characterization of engineered nanomaterial dispersions in complex media using tunable resistive pulse sensing technology.* ACS Nano. 8(9):9003-15.

Palmgren J.J., Mönkkönen J., Jukkola E., Niva S., Auriola S. 2004. *Characterization of Caco-2 cell monolayer drug transport properties by cassette dosing using UV/fluorescence HPLC.* Eur. J. Pharm. Biopharm. 57:319-328.

Palomaki J., Karisola P., Pylkkanen L., Savolainen K., Alenius H. 2010. *Engineered nanomaterials cause cytotoxicity and activation on mouse antigen presenting cells.* Toxicology. 267(1-3):125-31.

Pan Y., Neuss S., Leifert A., Fischler M., Wen F., Simon U., Schmid G., Brandau W., Jahnen-Dechent W. 2007. *Size-dependent cytotoxicity of gold nanoparticles.* Small. 3:1941-1949.

Parak W.J., Boudreau R., Le Gros M., Gerion D., Zanchet D., Micheel C.M., Williams S.C., Alivisatos A.P., Larabell C. 2002. *Cell motility and metastatic potential studies based on quantum dot imaging of phagokinetic tracks.* Adv. Mater. 14(12):882-885.

Pardridge W.M. 2012. *Drug transport across the blood–brain barrier.* J. Cereb Blood Flow Metab. 32(11): 1959–1972.

Park E.J. and Park K. 2009. *Oxidative stress and pro-inflammatory responses induced by silica nanoparticles in vitro and in vitro.* Toxicol. Lett. 184(1):18-25.

Park J.H., Gu L., von Maltzahn G., Ruoslahti E., Bhatia S.N., Sailor M.J. 2009. *Biodegradable luminescent porous silicon nanoparticles for in vivo applications.* Nat. Mater. 8(4):331-336.

Park K.H., Chhowalla M., Iqbal Z., Sesti F. 2003. *Single-walled carbon nanotubes are a new class of ion channel blockers.* J. Biol. Chem. 278(50):50212-6.

Park M.V.D.Z., Verharen H.W., Zwart E., Hernandez L.G., van Benthem J., Elsaesser A., Barnes C., McKerr G., Howard C.V., Salvati A., Lynch I., Dawson K.A., de Jong W.H. 2011. *Genotoxicity evaluation of amorphous silica nanoparticles of different sizes using the micronucleus and the plasmid lacZ gene mutation assay.* Nanotoxicology. 5(2):168-81.

Pathania D., Millard M., Neamati N. 2009. *Opportunities in discovery and delivery of anticancer drugs targeting mitochondria and cancer cell metabolism.* Adv. Drug Deliv. Rev. 61(14):1250-75.

Patra H.K., Banerjee S., Chaudhuri U., Lahiri P., Dasgupta A.K. 2007. *Cell selective response to gold nanoparticles.* Nanomed.-Nanotechnol. Biol. Med. 3:111-119.

Pavan C., Tomatis M., Ghiazza M., Rabolli V., Bolis V., Lison D., Fubini B. 2013. *In search of the chemical basis of the hemolytic potential of silicas.* Chemical. research in toxicology. 26:1188-1198.

Peer D., Karp J.M., Hong S., FaroKhzad O.C., Margalit R., Langer R. 2007. *Nanocarriers as an emerging platform for cancer therapy.* Nat. Nanotechnol. 2:751-760.

Pelaz B., Charron G., Pfeiffer C., Zhao Y., de la Fuente J.M., Liang X.J., Parak W.J., Del Pino P. 2013. *Interfacing engineered nanoparticles with biological systems: anticipating adverse nano-bio interactions.* Small. 9:1573-1584.

Peng X., Schlamp M.C., Kadavanich A.V., Alivisatos A.P. 1997. *Epitaxial growth of highly luminescent CdSe/CdS Core/Shell nanocrystals with photostability and electronic accessibility.* J. Am. Chem. Soc. 119(30):7019-7029.

Pernodet N., Fang X.H., Sun Y., Bakhtina A., Ramakrishnan A., Sokolov J., Ulman A., Rafailovich M. 2006. *Adverse effects of citrate/gold nanoparticles on human dermal fibroblasts.* Small. 2:766-773.

Persson H., Kobler C., Molhave K., Samuelson L., Tegenfeld J.O., Oredsson S., Prinz C.N. 2013. *Fibroblasts cultured on nanowires exhibit low motility, impaired cell division, and DNA damage.* Small. 9(23):4006-16.

Peters A., Veronesi B., Calderon-Garciduenas L., Gehr P., Chen L.C., Geiser M., Reed W., Rothen-Rutishauer B., Schurch S., Schultz H. 2006. *Translocation and potential neurological effects of fine and ultrafine particles. A critical update.* Part. Fibre. Toxicol. 8:3-13.

Petros R. and DeSimone J. 2010. *Strategies in the design of nanoparticles for therapeutic applications.* Nat. Rev. Drug. Discovery. 9:615-627.

Philbrook N.A., Winn L.M., Afrooz A.R., Saleh N.B., Walker V.K. 2011. *The effect of TiO2 and Ag nanoparticles on reproduction and development of Drosophila melanogaster and CD-1 mice.* Toxicol. Appl. Pharmacol. 257(3):429-36.

Piccinno F., Gottschalk F., Seeger S., Nowack B. 2012. *Industrial production quantities and uses of ten engineered nanomaterials in Europe and the world.* Journal of Nanoparticle Research. 14 (9), 1109.

Pierobon P. and Cappello G. 2012. *Quantum dots to tail single bio-molecules inside living cells.* Adv. Drug. Deliv. Rev. 64(2):167-178.

Pinto M., Robine-Leon S., Appay M.D., Kedinger M., Triadou N., Dussaulx E., Lacroix B., Simon-Assmann P., Haffen K., Fogh J., Zweibaum A. 1983. *Enterocyte-like differentiation and polarization of the human colon carcinoma cell line Caco-2 in culture.* Biol. Cell. 47:323-330.

Ploger R., Zhang J., Bassett D., Reeves R., Hieter P., Boguski M., Spencer F. 2000. *XREFdb: cross-referencing the genetics and genes of mammals and model organisms.* Nucleic. Acids. Res. 28(1):120-2.

Poderys V., Matulionyte M., Selskis A., Rotomskis R. 2011. *Interaction of Water-Soluble CdTe Quantum Dots with Bovine Serum Albumin.* Nanoscale Res. Lett. 6(1):9.

Podolski I.Y., Podlubnaya Z.A., Kosenko E.A., Mugantseva E.A., Makarova E.G., Marsagishvili L.G., Shpagina M.D., Kaminsky Y.G., Andrievsky G.V., Klochkov V.K. 2007. *Effects of hydrated forms of C60 fullerene on amyloid 1-peptide fibrillization in vitro and performance of the cognitive task.* J. Nanosci. Nanotechnol. 7(4-5):1479-85.

Poljak-Blaži M., Jaganjac M., Žarković N. 2010. *Cell Oxidative Stress: Risk of Metal Nanoparticles.* CRC Press Taylor: London, UK. New York USA

Polli J.W., Wring S.A., Humphreys J.E., Huang L., Morgan J.B., Webster L.O. Serabjit-Singh C.S. 2001. *Rational use of in vitro P-glycoprotein assays in drug discovery.* J. Pharmacol. Exp. Ther. 299:620-628.

Pontier C., Pachot J., Botham R., Lenfant B., Arnaud P. 2001. *HT29-MXT and Caco-2/TC7 monolayers as predictive models for human intestinal absorption: role of the mucus layer.* J. Pharm. Sci. 90:1608-1619.

Power K.W., Palazuelos M., Moudgil B.M., Roberts S.M. 2007. *Characterization of the size, shape and state of dispersion of nanoparticles for toxicological studies.* Nanotoxicology. 1(1):42-51.

Pozzi D., Caracciolo G., Capriotti A.L., Cavaliere C., La Barbera G., Anchordoquy T.J., Laganà A. 2015. *Surface chemistry and serum type both determine the nanoparticle-protein corona.* J. Proteomics. 119:209-217.

Prapainop K., Witter D.P., Wentworth P. 2012. *A chemical approach for cell-specific targeting of nanomaterials: small-molecule-initiated misfolding of nanoparticle corona proteins*. J. Am. Chem. Soc. 134(9):4100-4103.

Putnam F.W. 1975-1987. *In the plasma proteins structure, function, and genetic control.* (Putnam F. W., ed). Academic Press. New York. pp. 1-55.

Qiu Y., Liu Y., Wang L., Xu L., Bai R., Ji Y., Wu X., Zhao Y., Li Y., Chen C. 2010. *Surface chemistry and aspect ratio mediated cellular uptake of Au nanorods*. Biomaterials. 31(30):7606-19.

Qu C., Wang L., He J., Tan J., Liu W., Zhang S., Zhang C., Wang Z., Jiao S., Liu S., et al. 2012. *Carbon nanotubes provoke inflammation by inducing the pro-inflammatory genes IL-1β and IL-6.* Gene. 493(1):9-12.

Quirion F. and St-Pierre S. 1991. *Reduction of the in vitro hemolytic activity of soybean lecithin liposomes by treatment with a block copolymer.* Biophys. Chem. 40(2):129-34.
Radivojac P., Iakoucheva L.M., Oldfield C.J., Obradovic Z., Uversky V.N., Dunker A.K. 2007. *Intrinsic disorder and functional proteomics.* Biophysical Journal. 92, 1439-1456.

Rae C.S., Khor I.W., Wang Q., Destito G., Gonzalez M.J., Singh P., Thomas D.M., Estrada M.N., Powell E., Finn M.G., Manchester M. 2005. *Systemic trafficking of plant virus nanoparticles in mice via the oral route.* Virology. 343(2):224-35.

Ragnaill M., Brown M., Ye D., Bramini M., Callanan S., Lynch I., Dawson K. 2011. *Internal benchmarking of a human blood-brain barrier cell model for screening of nanoparticle uptake and transcytosis*. Eur. J. Pharm. Biopharm. 77(3):360-367.

Rasmussen K., Mech A., Mast J., De Temmerman P.J., Van Steen F., Pizzolon J.C., De Temmerman L., Van Doren E., Jensen K.A. 2013. *Synthetic Amorphous Silicon Dioxide (NM- 200, NM-201, NM-202, NM-203, NM-204): Characterisation and Physico-Chemical Properties. JRC Repository: NM-series of Representative Manufactured Nanomaterials.* JRC Scientific and Policy Reports.

Ray M., Basu N., Ray S. 1997. *Inactivation of glyceraldehyde-3-phosphate dehydrogenase of human malignant cells by methylglyoxal.* Mol. Cell. Biochem. 177(1-2):21-6.

Ray S. 2011. *Emerging nanoproteomics approaches for disease biomarker detection: A current perspective.* J Proteomics. 74(12):2660-2681.

Révillion F., Pawlowski V., Hornez L., Peyrat J.P. 2000. *Glyceraldehyde-3-phosphate dehydrogenase gene expression in human breast cancer.* Eur. J. Cancer. 36(8):1038-42.

Riek R., Hornemann S., Wider G., Billeter M., Glockshuber R., Wuthrich K. 1996. *NMR structure of the mouse prion protein domain PrP.* Nature. 382,(121-231):180-182.

Rikans L.E. and Yamano T. 2000. *Mechanisms of cadmium-mediated acute hepatotoxicity.* J. Biochem. Mol. Toxicol. 14(2):110-117.

Risom L., Møller P., Loft S. 2005. *Oxidative stress-induced DNA damage by particulate air pollution.* Mutat. Res. 592(1-2)119-137.

Rivera Gil P., Huhn D., del Mercato L.L., Sasse D., Parak W.J. 2010. *Nanopharmacy: Inorganic nanoscale devices as vectors and active compounds.* Pharmacol. Res. 62:115-125.

Roach P., Farrar D., Perry C.C. 2006. *Surface tailoring for controlled protein adsorption: effect of topography at the nanometer scale and chemistry.* J. Am. Chem. Soc. 128:3939-3945.

Robbie K., Yang J., Elliott C., Dariani R., Buzea C. 2007. *Nanomaterials and nanoparticles: Sources and toxicity.* Biointerphases. 2(4):17-172.

Röcker C., Pötzl M., Zhang F., Parak W.J., Nienhaus G.U. 2009. *A quantitative fluorescence study of protein monolayer formation on colloidal nanoparticles.* Nat. Nanotechnol. 4:577-580.

Rodríguez J.A., Fernández-García M. 2007. *Synthesis, properties and applications of oxide nanoparticles*. Whiley: New Jersey.

Rodriguez J.A., Liu G., Jirsak T., Hrbek J., Chang Z., Dvorak J., Maiti A. 2002. *Activation of gold on titania: adsorption and reaction of SO(2) on Au/TiO*. J. Am. Chem. Soc. 124(18):5242-5250.

Roduner E. 2006. *Size matters: why nanomaterials are different.* Chem. Soc. Rev. 35:583-592.
Romero P., Obradovic Z., Li X., Garner E.C., Brown C.J., Dunker A.K. 2001. *Sequence complexity of disordered protein.* Proteins. 42(1):38-48.

Rossetti R., Ellison J.L., Gibson J.M., Brus L.E. 1984. *Size effects in the excited electronic states of small colloidal CdS crystallites*. J. Chem. Phys. 80(9):4464-4469.

Rothen-Rutishauser B.M., Schurch S., Haenni B., Kapp N., Gehr P. 2006. *Interaction of fine particles and nanoparticles with red blood cells visualized with advanced microscopic techniques.* Environ. Sci. Technol. 40,4353-4359

Rouhana L.L., Jaber J.A., Schlenoff J.B. 2007. *Aggregation-resistant water-soluble gold nanoparticles*. Langmuir. 23(26):12799-801.

Rouse J.G., Yang J., Ryman-Rasmussen J.P., Barron A.R., Monteiro-Riviere N.A. 2007. *Effects of mechanical flexion on the penetration of fullerene amino acidderivatized peptide nanoparticles through skin.* Nano Lett. 7, 155–160.

Rual J.F., Venkatesan K., Hao T., Hirozane-Kishikawa T., Dricot A., Li N., Berriz G.F., Gibbons F.D., Dreze M., Ayivi-Guedehoussou N., Klitgord N., Simon C., Boxem M., Milstein S., Rosenberg J., Goldberg D.S., Zhang L.V., Wong S.L., Franklin G., Li S.M., Albala J.S., Lim J.H., Fraughton C., Llamosas E., Cevik S., Bex C., Lamesch P., Sikorski R.S., Vandenhaute J., Zoghbi H.Y., Smolyar A., Bosak S., Sequerra R., Doucette-Stamm L., Cusick M.E., Hill D.E., Roth F.P., Vidal M. 2005. *Towards a proteome-scale map of the human protein-protein interaction network.* Nature. 437, 1173-1178.

Ruge C., Kirch J., Canadas O., Schneider M., Perez-Gil J., Schaefer U., Casals C., Lehr C. 2011. *Uptake of nanoparticles by alveolar macrophages is triggered by surfactant protein A.* Nanomedicine. 7(6):690-693.

Ryman-Rasmussen J.P., Riviere J.E., Monteiro-Riviere N.A. 2006. *Penetration of intact skin by quantum dots with diverse physicochemical properties.* Toxicol. Science. 91(1):159-165.

Sadauskas E., Danscher G., Stoltenberg M., Vogel U., Larsen A., Wallin H. 2009. *Protracted elimination of gold nanoparticles from mouse liver.* Nanomedicine. 5(2):162-169.

Saha K., Moyano D.F., Rotello V.M. 2014. *Protein coronas suppress the hemolytic activity of hydrophilic and hydrophobic nanoparticles.* Mater. Horiz. 2014(1):102-105.

Saito R., Dresselhaus G., Dresselhaus M.S. 1998. *Physical properties of carbon nanotubes.* Imperial College Press. London. pp. 1-259

Sakulkhu U., Maurizi L., Mahmoudi M., Motazacker M., Vries M., Gramoun A., Ollivier Beuzelin M. G., Vallée J.P., Rezaee F., Hofmann H. 2014. *Ex situ evaluation of the composition of protein corona ofintravenously injected superparamagnetic nanoparticles in rats.* Nanoscale. 6(19):11439-11450.

Salata O.V. 2004. *Application of nanoparticles in biology and medicine.* Journal of Nanobiotechnology. 2:3.

Salvati A., Aberg C., dos Santos T., Gehr P., Nelle M., Yan B., Wick P. 2011. *Experimental and theoretical comparison of intracellular import of polymeric nanoparticles and small molecules: toward models of uptake kinetics.* Nanomedicine. 7(6): 818–826.

Salvati A., Pitek A.S., Monopoli M.P. Prapainop K., Bombelli F.B., Hristov D.R., Kelly P.M., Åberg C., Mahon E., Dawson K.A. 2013. *Transferrin-functionalized nanoparticles lose their targeting capabilities when a biomolecule corona adsorbs on the surface.* Nat. Nanotechnol. 8, 137–143.

Salvatore F., Corbo C., Gemei M., Del Vecchio L. 2015. *Oncoproteomic approaches to cancer marker discovery: the case of colorectal cancer.* Biomark. Cancer. 53–71.

Sambuy Y., De Angelis I., Ranaldi G. et al. 2005. *The Caco-2 cell line as a model of the intestinal barrier: infl uence of cell and culture-related factors on Caco-2 cell functional characteristics.* Cell Biol. Toxicol. 21:1–26.

Saptarshi S.R., Duschl A., Lopata A.L. 2013. *Interaction of nanoparticles with proteins: relation to bio-reactivity of the nanoparticle.* J. Nanobiotechnol. 11(1), 26.

Sayes C.M., Fortner J.D., Guo W., Lyon D., Colvin V.L. 2004. *The differential cytotoxicity of water-soluble fullerenes.* Nano Letters. 4:1881-1887.

Sayes C.M., Reed K.L., Warheit D.B. 2007. *Assessing toxicity of fine and nanoparticles: comparing in vitro measurements to in vivo pulmonary toxicity profiles*. Toxicol. Sci. 97:163-180.

Schaeublin N.M., Braydich-Stolle L.K., Schrand A.M., Miller J.M., Hutchison J., Schlager J.J., Hussain S.M. 2011. *Surface charge of gold nanoparticles mediates mechanism of toxicity.* Nanoscale. 3(2):410-20.

Schinazi R.F., Sijbesma R., Srdanov G., Hill C.L., Wudl F. 1993. *Synthesis and virucidal activity of a water-soluble, configurationally stable, derivatized C60 fullerene.* Antimicrob. Agents Chem. 37(8):1707-1710.

Schleh C., Rothen-Rutishauser B., Kreyling W.G. 2011. *The influence of pulmonary surfactant on nanoparticulate drug delivery systems*. Eur. J. Pharm. Biopharm. 77, 350–352.

Schmitt M., Gellert G., Ludwig J., Lichtenberg-Fraté H. 2004. *Phenotypic yeast growth analysis for chronic toxicity testing*. Ecotoxicology and Environmental Safety. 59, 142–150.

Schnedl W.J., Ferber S., Johnson J.H., Newgard C.B. 1994. *STZ transport and cytotoxicity. Specific enhancement in GLUT2-expressing cells*. Diabetes. 43(11):1326-33.

Schroeder J.E., Shweky I., Shmeeda H., Banin U., Gabizon A. 2007. *Folate-mediated tumor cell uptake of quantum dots entrapped in lipid nanoparticles.* J. Control. Release. 124(1-2):28-34.

Schrurs F. and Lison D. 2012. *Focusing the research efforts*. Nature Nanotechnology. 7(9):546-548.

Schubert D., Dargusch R., Raitano J., Chan S.W. 2006. *Cerium and yttrium oxide nanoparticles are neuroprotective.* Biochem. Biophys. Res. Commun. 342, 86-91

Schwegmann H., Feitz A.J., Frimmel F.H. 2010. *Influence of the zeta potential on the sorption and toxicity of iron oxide nanoparticles on S. cerevisiae and E. coli.* J. Colloid Interface Sci. 347, 43−48.

Semmler M., Seitz J., Mayer P., Heyder J., Oberdörster G., Kreyling W.G. 2004. *Long-term clearance kinetics of inhaled ultrafine insoluble iridium particles from the rat lung, including transient translocation into secondary organs.* Inhalation Toxicol. 16,453-459

Serpone N., Salinaro A., Emeline A. 2001. *Deleterious effects of sunscreen titanium dioxide nanoparticles on DNA: efforts to limit DNA damage by particle surface modification.* Proc. SPIE. 4258, 86-98

Shang L., Nienhaus K., Nienhaus G. 2014. *Engineered nanoparticles interacting with cells: size matters*. J Nanobiotechnol. 12(1):5.

Shang L., Wang Y., Jiang J., Dong S. 2007. *pH-dependent protein conformational changes in albumin:gold nanoparticle bioconjugates: a spectroscopic study.* Langmuir. 23, 2714–2721.

Shang W., Nuffer J.H., Dordick J.S. and Siegel R.W., 2007. *Unfolding of Ribonuclease A on Silica Nanoparticle Surfaces*. Nano Letters. 7(7): 1991–1995.

Shang W., Nuffer J.H., Muniz-Papandrea V.A., Colon W., Siegel R.W., Dordick J.S. 2009. *Cytochrome c on silica nanoparticles: influence of nanoparticle size on protein structure, stability, and activity.* Small. 5:470–476.

Shannahan J.H., Podila R., Aldossari A.A., Emerson H., Powell B.A., Ke P.C., Rao A.M., Brown J.M. 2014. *Formation of a protein corona on silver nanoparticles mediates cellular toxicity via scavenger receptors*. Toxicol. Sci. 143(1), 136–146.

Shao M., Lu L., Wang H., Luo S., Duo Duo Ma D. 2009. *Microfabrication of a new sensor based on silver and silicon nanomaterials, and its application to the enrichment and detection of bovine serum albumin via surface-enhanced Raman scattering*. Microchim. Acta. 164, 157–160.

Sharifi S., Behzadi S., Laurent S., Forrest M.L., Stroeve P., Mahmoudi M. 2012. *Toxicity of nanomaterials*. Chem. Soc. Rev. 41(6):2323–2343.

Shaw C.P., Middleton D.A., Volk M., Levy R. 2012. *Amyloid-derived peptide forms self-assembled monolayers on gold nanoparticle with a curvature-dependent beta-sheet structure*. ACS Nano. 6:1416-1426.

Shen X.-C., Liou X-Y., Ye L-P., Wang Z-Y. 2007. *Spectroscopic studies on the interaction between human hemoglobin and CdS quantum dots*. Journal of Colloid and Interface Science. 311:400–406.

Shen H., Wang H., Liu Q., Liu H., Teng M., Li X. 2014. *Structural insights into RNA recognition properties of glyceraldehyde-3-phosphate dehydrogenase 3 from Saccharomyces cerevisiae*. IUBMB Life. 66(9):631-8.

Shi H., Hudson L.G., Liu K.J. 2004. *Oxidative stress and apoptosis in metal ion-induced carcinogenesis*. Free Radic. Biol. Med. 37:582-93.

Shi M., Kwon H.S., Peng Z., Elder A., Yang H. 2012. *Effects of surface chemistry on the generation of reactive oxygen species by copper nanoparticles.* ACS Nano. 6:2157-64.

Shi Y., Zhang J-H., Jiang M., Zhu L-H., Tan H-Q., Lu B. 2010. *Synergistic genotoxicity caused by low concentration of titanium dioxide nanoparticles and p,p'-DDT in human hepatocytes*. Environmental and Molecular Mutagenesis. 51(3):192–204.

Shinohara N., Matsumoto K., Endoh S., Maru J., Nakanishi J. 2009. *In vitro and in vivo genotoxicity tests on fullerene C60 nanoparticles.* Toxicology Letters. 191(2-3):289–296.

Shintani H., Kurosu S., Miki A., Hayashi F., Kato S. 2006. *Sterilization efficiency of the photocatalyst against environmental microorganisms in a health care facility.* Biocontrol Sci. 11, 17-26

Shvedova A.A., Kisin E.R., Mercer R., Murray A.R., Johnson V.J., Potapovich A.I., Tyurina Y.Y., Gorelik, Arepalli S.O., Schwegler-Berry D., Hubs A.F., Antonini J., Evans D.E., Ku B.K., Ramsey D., Maynard A., Kagan V.E., Castranova V., Baron P. 2005. *Unusual inflammatory and fibrogenic pulmonary responses to single walled carbon nanotubes in mice.* Am. J. Physiol. Cell Mol. Physiol. 289(5):L698-708

Shwe T.T.W., Yamamoto S., Kakeyama M., Kobayashi T., Fujimaki H. 2005. *Effect of intratracheally instillation of untrafine carbon black on proinflammatory cytokine and chemokine release and mRNA expression in lung and lymph nodes of mice Toxicol.* Appl. Pharmacol. 209 51-61

Sies H. and De Groot H. 1992. *Role of reactive oxygen species in cell toxicity*. Toxicol. Lett. 64, 547–551.

Simberg D., Park J.H., Karmali P.P., Zhang W.M., Merkulov S., McCrae K., et al. 2009. *Differential proteomics analysis of the surface heterogeneity of dextran iron oxide nanoparticles and the implications for their in vivo clearance.* Biomaterials. 30(23):3926–33

Singh N., Manshian B., Jenkins G.J.S., Griffiths S.M., Williams P.M., Maffeis T.G., Wright C.J., Doak S.H. 2009. *NanoGenotoxicology: the DNA damaging potential of engineered nanomaterials*. Biomaterials.30(23-24):3891–3914.

Sirover M.A. 1997. *Role of the glycolytic protein, glyceraldehyde-3-phosphate dehydrogenase, in normal cell function and in cell pathology*. J Cell Biochem. 1;66(2):133-40.

Sirover M.A. 2005. *New nuclear functions of the glycolytic protein, glyceraldehyde-3-phosphate dehydrogenase, in mammalian cells*. J. Cell Biochem. 95:45-52.

Sisco P.N., Wilson C.G., Chernak D., Clark J.C., Grzincic E.M., Ako-Asare K., Goldsmith E.C., Murphy C.J. 2014. *Adsorption of cellular proteins to polyelectrolyte-functionalized gold nanorods: a mechanism for nanoparticle regulation of cell phenotype?* PLoS One. 9(2):e86670.

Slowing I.I., Wu C-W., Vivero-Escoto J.L., Lin V.S.Y. 2009. *Mesoporous silica nanoparticles for reducing hemolytic activity towards mammalian red blood cells.* Small. 5(1):57–62.

Smith R.E., MacQuarrie R. 1979. *The role of cysteine residues in the catalytic activity of glycerol-3-phosphate dehydrogenase.* Biochim. Biophys. Acta. 567(2):269-77.

Soenen S.J.H., Nuytten N., De Meyer S.F., De Smedt S.C., De Cuyper M. 2010. *High intracellular iron oxide nanoparticle concentrations affect cellular cytoskeleton and focal adhesion kinase-mediated signaling.* Small. 6, 832–842.

Sohaebuddin S.K., Thevenot P.T., Baker D., et al. 2010. *Nanomaterial cytotoxicity is composition, size, and cell type dependent.* Part Fibre Toxicol. 7(22):1e17.

Soto K., Garza K.M., Murr L.E. 2007. *Cytotoxic effects of aggregated nanomaterials*. Acta Biomater. 3, 351–358.

Stadtman E.R. and Berlett B.S. 1997. *Reactive oxygen-mediated protein oxidation in aging and disease.* Chem Res Toxicol. 10(5):485-94.

Stefani D., Wardman D., Lambert T. 2005. *The implosion of the Calgary General Hospital: ambient ait quality issues* J. Air Waste Manag. Assoc. 55, 52-59

Stelzer R. and Hutz R.J. 2009. *Gold nanoparticles enter rat ovarian granulosa cells and subcellular organelles, and alter in vitro estrogen accumulation.* J. Reprod. Dev. 55(6):685-90.

Stelzl U., Worm U., Lalowski M., Haenig C., Brembeck F.H., Goehler H., Stroedicke M., Zenkner M., Schoenherr A., Koeppen S., Timm J., Mintzlaff S., Abraham C., Bock N., Kietzmann S., Goedde A., Toksoz E., Droege A., Krobitsch S., Korn B., Birchmeier W., Lehrach H., Wanker E.E. 2005. *A human protein-protein interaction network: A resource for annotating the proteome.* Cell. 122, 957-968.

Stephens D.J., Allan V.J. 2003. *Light microscopy techniques for live cell imaging*. Science. 300(5616):82-86.

Su X.L., Li Y. 2004. *Quantum dot biolabeling coupled with immunomagnetic separation for detection of Escherichia coli O157:H7.* Anal Chem. 76(16):4806-4810.

Sukhanova A., Devy J., Venteo L., Kaplan H., Artemyev M., Oleinikov V., Klinov D., Pluot M., Cohen J.H.M., Nabiev I. 2004. *Biocompatible fluorescent nanocrystals for immunolabeling of membrane proteins and cells.* Anal. Biochem. 324(1):60-67.

Sukhanova A., Venteo L., Devy J., Artemyev M., Oleinikov V., Pluot M., Nabiev I. 2002. *Highly stable fluorescent nanocrystals as a novel class of labels for immunohistochemical analysis of paraffin-embedded tissue sections.* Lab. Invest. 82(9):1259-1261.

Sun L., Li Y., Liu X., Jin M., Zhang L., Du Z., Guo C., Huang P., Sun Z. 2011. *Cytotoxicity and mitochondrial damage caused by silica nanoparticles.* Toxicology in vitro: an international journal published in association with BIBRA.

Sun M., Yu Q., Liu M., Chen X., Liu Z., Zhou H., Yuan Y., Liu L., Li M., Zhang C. 2014. *A novel toxicity mechanism of CdSe nanoparticles to Saccharomyces cerevisiae: Enhancement of vacuolar membrane permeabilization (VMP).* Chemico-Biological Interactions. 220: 208–213

Sun X., Jones W.T., Uversky V.N. 2012. *Applications of Bioinformatics and Experimental Methods to Intrinsic Disorder-Based Protein-Protein Interactions.* Protein Engineering, Chap.9. DOI: 10.5772/29246

Sund J., Alenius H., Vippola M., Savolainen K., Puustinen A. 2011. *Proteomic characterization of engineered nanomaterial–protein interactions in relation to surface reactivity.* ACS Nano. 5(6), 4300–4309.

Svenson S. and Tomalia D.A. 2005. *Dendrimers in biomedical applications-reflections on the field.* Advanced Drug Delivery Reviews. 57(15):2106-2129.

Takenaka S., Karg E., Roth C., Schulz H., Ziesenis A., Heinzmann U., Schramel P., Heyder J. 2001. *Pulmonary and systemic distribution of inhaled ultrafine silver particles in rats.* Environ. Health Perspect. 4, 547–551.

Talapin D.V., Rogach A.L., Kornowski A., Haase M., Weller H. 2001. *Highly luminescent monodisperse CdSe and CdSe/ZnS nanocrystals synthesized in a hexadecylamine-trioctylphosphine oxide-trioctylphospine mixture.* Nano Lett. 1(4):207-211.

Tang M.L., Wang M., Xing T.R., Zeng J., Wang H.L., Ruan D.Y. 2008. *Mechanisms of unmodified CdSe quantum dot-induced elevation of cytoplasmic calcium levels in primary cultures of rat hi pocampal neurons.* Biomaterials. 29, 4383–4391.

Taniguchi K., Nomura K., Hata Y., Nishimura T., Asami Y., Kuroda A. 2007. The Si-tag for immobilizing proteins on a silica surface. Biotechnol Bioeng. 96(6):1023-1029.

Tannergren C., Langguth P., Hoffmann K.J. 2001. *Compound mixtures in Caco-2 cell permeability screens as a means to increase screening capacity.* Pharmazie. 56: 337-342.

Tantra R. 2016. *Nanomaterial characterization: An introduction*. Wiley.

Tavares A.M., Louro H., Antunes S., Quarre S., Simar S., De Temmerman P.J., Verleysen E., Mast J., Jensen K.A., Norppa H., Nesslany F., Silva M.J. 2014. *Genotoxicity evaluation of nanosized titanium dioxide, synthetic amorphous silica and multi-walled carbon nanotubes in human lymphocytes.* Toxicol. In Vitro. 28, 60-69.

Tavelin S., Taipalensuu J., Hallböök F., Vellonen K.S., Moore V, Artursson P. 2003a. *An improved cell culture model based on 2/4/A1 cell monolayers for studies of intestinal drug transport: characterization of transport routes*. Pharm Res. 20(3):373-81.

Tavelin S., Taipalensuu J., Söderberg L., Morrison R., Chong S., Artursson P. 2003b. *Prediction of the oral absorption of low-permeability drugs using small intestine-like 2/4/A1 cell monolayers*. Pharm Res. 20(3):397-405.

Taylor D.A. 2002. *Dust in the wind*. Environ health perspect. 110(2):A80-A87.

Tedja R., Lim M., Amal R., Marquis C. 2012. *Effects of serum adsorption on cellular uptake profile and consequent impact of titanium dioxide nanoparticles on human lung cell lines*. ACS Nano. 6(5):4083-4093.

Teichroeb J.H., Forrest J.A., Jones L.W. 2008. *Size-dependent denaturing kinetics of bovine serum albumin adsorbed onto gold nanospheres*. The European Physical Journal E: Soft Matter. 26,411–415.

Teichroeb J.H., Forrest J.A., Ngai V., Jones L.W. 2006. *Anomalous thermal denaturing of proteins adsorbed to nanoparticles*. The European Physical Journal E: Soft Matter. 21,19–24.

Tenzer S., Docter D., Kuharev J., Musyanovych A., Fetz V., Hecht R., Schlenk F., Fischer D., Kiouptsi K., Reinhardt C., Landfester K., Schild H., Maskos M., Knauer S. K., Stauber R.H. 2013. *Rapid formation of plasma protein corona critically affects nanoparticle pathophysiology*. Nat. Nanotechnol. 8(10):772-781.

Tenzer S., Docter D., Rosfa S., Wlodarski A., Kuharev J., Rekik A., Knauer S.K., Bantz C., Nawroth T., Bier C., Sirirattanapan J., Mann W., Treuel L., Zellner R., Maskos M., Schild H., Stauber R.H. 2011. *Nanoparticle size is a critical physicochemical determinant of the human blood plasma corona: a comprehensive quantitative proteomic analysis*. ACS Nano. 5:7155–7167.

Terjesen T., Apalset K. 1988. *The influence of different degrees of stiffness of fixation plates on experimental bone healing*. J. Orthop. Res. 6(2):293-299.

Thompson E.A. 2013. *Identity by descent: variation in meiosis, across genomes, and in populations*. Genetics. 194(2):301-26.

Thompson S.E., Parthasarathy S. 2006. *Moore's law: the future of si microelectronics*. Materials Today. 9:20-25.

Thwaites D.T., Armstrong G., Hirst B.H., Simmons N.L. 1995a. *D-cycloserine transport in human intestinal epithelial (Caco-2) cells mediated by a H^+ -coupled amino acid transporter.* Brit. J. Pharmacol. 115: 761-766.

Thwaites D.T., Brown C.D.A., Hirst B.H., Simmons N.L. 1993. *Transepithelial glycylsarcosine transport in intestinal Caco-2 cells mediated by expression of H^+ -coupled carriers at both apical and basal membranes*. J. Biol. Chem. 268: 7640-7642.

Thwaites D.T., McEwan G.T.A., Hirst B.H., Simmons N.L. 1995b. *H^+-coupled α-methylaminoisobutyric acid transport in human intestinal Caco-2 cells.* Biochim. Biophys. Acta. 1234: 111-118.

Tian F.R., Cui D.X., Schwarz H., Estrada G.G., Kobayashi H. 2006. *Cytotoxicity of single-wall carbon nanotubes on human fibroblasts.* Toxicol. In Vitro. 20, 1202–1212.

Tinkle S.S., Antonini J.M., Rich B.A., Roberts J.R., Salmen R., DePree K., Adkins E.J. 2003. *Skin as a route of exposure and sensitization in chronic beryllium disease.* Environ. Health Perspect. 111 1202-1208

Toll R., Jacobi U., Richter H., Lademann J., Schaefer H., Blume-Peytavi U. 2004. *Penetration Profile of Microspheres in Follicular Targeting of Terminal Hair Follicles.* J. Invest. Dermatol. 123 168 –176

Tompa P. 2003. *Intrinsically unstructured proteins evolve by repeat expansion*. Bioessays. 25, 847-855.

Tompa P. and Csermely P. 2004. *The role of structural disorder in the function of RNA and protein chaperones.* Faseb. Journal. 18, 1169-1175.

Tosaka R., Yamamoto H., Ohdomari I., Watanabe T. 2010. *Adsorption Mechanism of Ribosomal Protein L2 onto a Silica Surface: A Molecular Dynamics Simulation Study*. Langmuir: the ACS journal of surfaces and colloids. 26 (12):9950–9955.

Tran C.D.H. Timmins P., Conway B.R., Irwin W.J. 2002. Investigation of the coordinated functional activities of Cytochrome P450 3A4 and P-glycoprotein in limiting the absorption of xenobiotics in Caco-2 cells. J. Pharm. Sci. 91:117-128.

Treuel L., Brandholt S., Maffre, P., Wiegele S., Shang L., Nienhaus G.U. 2014. *Impact of protein modification on the protein corona on nanoparticles and nanoparticle-cell interactions.* ACS Nano. 8, 503–513.

Treuel L., Jiang X., Nienhaus G.U. 2013. *New views on cellular uptake and trafficking of manufactured nanoparticles*. J. R. Soc. Interface. 10 (82):20120939.

Troutman M.D. and Thakker D.R. 2003. *Rhodamine123 requires carrier-mediated influx for its activity as a P-glycoprotein substrate in Caco-2 cells*. Pharm. Res. 20: 1192-1199.

Tsai P.J., Vincent J.H., Wahl G., Maldonado G. 1995. *Occupational exposure to inhalable and total aerosol in the primary nickel production industry.* Occup. Environ. Med. 52(12):793-9.

Tsuji J.S., Maynard A.D., Howard P.C., James J.T., Lam C.W., Warheit D.B., Santamaria A.B. 2006. *Research strategies for safety evaluation of nanomaterials, Part IV: Risk assessment of nanoparticles*. Toxicol. Sci. 89 42-50

Uhrich K.E., Cannizzaro S.M., Langer R.S., Shakeshelf K.M. 1999. *Polymeric systems for controlled drug release.* Chem. Rev. 99(11):3181-3198.

Unfried K., Albrecht C., Klotz L.O., Von Mikecz A., Grether-Beck S., Schins R.P.F. 2007. *Cellular responses to nanoparticles: Target structures and mechanisms.* Nanotoxicology. 1(1):52-71.

Unlu E.S. and Koc A. 2007. *Effects of deleting mitochondrial antioxidant genes on life span.* Annals of the New York Academy of Sciences. 1100, 505–509.

Uversky V.N., Gillespie J.R., Jink A.L. 2000. *Why are "natively unfolded" proteins unstructured under physiologic conditions?* Proteins-Structure Function and Genetics. 41, 415-427.

Uversky V.N., Kutyshenko V.P., Protasova N.Y., Rogov V.V., Vassilenko K.S., Gudkov A.T. 1996. *Circularly permuted dihydrofolate reductase possesses all the properties of the molten globule state, but can resume functional tertiary structure by interaction with its ligands*. Protein Sci. 5, 1844-1851.

Vachon P.H. and Beaulieu J.F. 1992. *Transient Mosaic Patterns of Morphological and Functional Differentiation in the Caco-2 Cell Line.* Gastroenterology. 103: 414–23.

Vacic V., Uversky V.N., Dunker A.K., Lonardi S. 2007. *Composition Profiler: a tool for discovery and visualization of amino acid composition differences.* BMC Bioinformatics. 8:211.

Valden M., Lai X., Goodman D.W. 1998. *Onset of catalytic activity of gold clusters on titania with the appearance of nonmetallic properties.* Science. 28(5383):1647-1650.

van der Zande M., Vandebriel R.J., Groot M.J., Kramer E., Herrera Rivera Z.E., Rasmussen K., Ossenkoppele J.S., Tromp P., Gremmer E.R., Peters R.J., Hendriksen P.J., Marvin H.J., Hoogenboom R.L., Peijnenburg A.A., Bouwmeester H. 2014. *Sub-chronic toxicity study in rats orally exposed to nanostructured silica.* Part. Fibre Toxicol. 11, 8.

Varela J.A., Bexiga M.G., Aberg C., Simpson J.C., Dawson K.A. 2012. *Quantifying sizedependent interactions between fluorescently labeled polystyrene nanoparticles and mammalian cells*. J. Nanobiotechnol. 10:39.

Verma A., Uzun O., Hu Y.H., Hu Y., Han H.S., Watson N., Chen S.L., Irvine D.J., Stellacci F. 2008. *Surface-structure-regulated cell-membrane penetration by monolayer-protected nanoparticles*. Nat. Mater. 7, 588–595.

Villani M., Calestani D., Lazzarini L., Zanotti L., Mosca R., Zappettini A. 2012. *Extended functionality of ZnO nanotetrapods by solution-based coupling with CdS nanoparticles*. J. Mater. Chem. 22, 5694.

Vivero-Escoto J.L., Huxford-Phillips R.C., Lin W. 2012. *Silica-based nanoprobes forbiomedical imaging and theranostic applications*. Chem. Soc. Rev. 41,2673–2685.

Vogler E.A. 2012. *Protein adsorption in three dimensions.* Biomaterials. 33:1201–37.

Voura E.B., Jaiswal J.K., Mattoussi H., Simon S.M. 2004. *Tracking Mmetastatic tumor cell extravasation with quantum dot nanocrystals and fluorescence emission-scanning microscopy.* Nature Med. 10(9):993-998.

Vroman L. 1962. *Effect of absorbed proteins on the wettability of hydrophilic and hydrophobic solids.* Nature. 196:476–7.

Wagner S., Zensi A., Wien S. L., et al. 2012. *Uptake mechanism of apoemodified nanoparticles on brain capillary endothelial cells as a blood-brain barrier model.* Plos One. 7(3):e32568.

Walczyk D., Bombelli F.B., Monopoli M.P., Lynch I., Dawson K.A. 2010.*What the cell "sees" in bionanoscience.* J. Am. Chem. Soc. 132:5761–5768

Walgren R.A. and Walle T. 1999. *The influence of plasma binding on absorption/exorption in the Caco-2 model of human intestinal absorption.* J. Pharm. Pharmacol. 51: 1037-1040.

Walkey C.D., Chan W.C. 2012. *Understanding and controlling the interaction of Nanometerials with proteins in a physiological environment.* Chem. Soc. Rev. 41(7):2780-2799.

Walkey C.D., Olsen J.B., Guo H., Emili A., Chan W.C.W. 2011. *Nanoparticle size and surface chemistry determine serum protein adsorption and macrophage uptake.* J. Am. Chem. Soc. 134(4):2139-2147.

Walkey C.D., Olsen J.B., Song F., Liu R., Guo H., Olsen D.W., Cohen Y., Emili A., Chan W.C. 2014. *Protein corona fingerprinting predicts the cellular interaction of gold and silver nanoparticles.* ACS Nano. 8(3), 2439–2455.

Walter E., Janich S., Roessler B.J., Hilfinger J.M., Amidon G.L. 1996. *HT29-MTX/Caco-2 cocultures as an in vitro model for the intestinal epithelium: in vitro - in vivo correlation with permeability data from rats and humans.* J. Pharm. Sci. 85: 1070-1076.

Walter E., Kissel T., Reers M., Dicneite G., Hofmann D, Stuber W. 1995. *Transepithelial properties of peptidomimetic thrombin inhibitors in monolayers of human intestinal cell line (Caco-2) and their correlation to in vivo data.* Pharm. Res. 12: 360-365.

Wan S., Kelly P.M., Mahon E., Stöckmann H., Rudd P.M., Caruso F., Dawson K.A., Yan Y., Monopoli M.P. 2015. *The "sweet" side of the protein corona: effects of glycosylation on nanoparticle–cell interactions.* ACS Nano. 9(2), 2157–2166.

Wang B., Feng W., Wang M., Wang T., Gu Y., Zhu M., Ouyang H., Shi J., Zhang F., Zhao Y., Chai Z., Wang H., Wang J. 2008. *Acute toxicological impact of nano- and submicroscaled zinc oxide powder on healthy adult mice.* J. Nanopart. Res. 10(2):263-276.

Wang F., Yu L., Monopoli M.P., et al. 2013. *The biomolecular corona is retained during nanoparticle uptake and protects the cells from the damage induced by cationic nanoparticles until degraded inthe lysosomes.* Nanomed. Nanotechnol. Biol. Med. 9(8):1159-1168.

Wang J., Jensen U.B., Jensen G.V., Shipovskov S., Balakrishnan V.S., Otzen D., Pedersen J.S., Besenbacher F., Sutherland D.S. 2011. *Soft interactions at nanoparticles alter protein function and conformation in a size dependent manner.* Nano Lett. 11, 4985–4991.

Wang J.J., Sanderson B.J.S., Wang H. 2007. *Cyto- and genotoxicity of ultrafine TiO2 particles in cultured human lymphoblastoid cells.* Mutation Research. 628(2):99–106.

Wang L., Li J., Pan J., Jiang X., Ji Y., Li Y., Qu Y., Zhao Y., Wu X., Chen C. 2013. *Revealing the binding structure of the protein corona on gold nanorods using synchrotronradiation-based techniques: understanding the reduced damage in cell mem-branes.* Journal of the American Chemical Society. 135,17359–17368.

Wang S.H., Lee C.W., Chiou A., Wei P.K. 2010. *Size-dependent endocytosis of gold nanoparticles studied by three-dimensional mapping of plasmonic scattering images.* J. Nanobiotechnol. 8:33.

Wang T., Bai J., Jiang X., Nienhaus G.U. 2012. *Cellular uptake of nanoparticles by membrane penetration: a study combining confocal microscopy with FTIR spectroelectrochemistry.* ACS Nano. 6:1251–1259.

Wang Y., Aker W. G., Hwang H. M., et al. 2011. *A study of the mechanism of in vitro cytotoxicity of metal oxide nanoparticles using catfish primary hepatocytes and human HepG2 cells.* Sci. Total Environ. 409(22):4753-62.

Wang Z., Li J., Zhao J., et al. 2011. *Toxicity and internalization of CuO nanoparticles to prokaryotic alga Microcystis aeruginosa as affected by dissolved organic matter.* Environ. Sci. Technol. 45(14):6032-40.

Wangoo N., Suri C.R., Shekhawat G. 2008a. *Interaction of gold nanoparticles with protein: a spectroscopic study to monitor protein conformational changes.* Appl. Phys. Lett. 92(13), 133104.

Wangoo N., Bhasin K.K., Mehta S.K., Suri C.R. 2008b *Synthesis and capping of water-dispersed gold nanoparticles by an amino acid: bioconjugation and binding studies*. J. Colloid. Interface Sci. 323(2):247-54.

Ward J.J., Sodhi J.S., McGuffin L.J., Buxton B.F., Jones D.T. 2004. *Prediction and functional analysis of native disorder in proteins from the three kingdoms of life.* Journal of Molecular Biology. 337 (3):635-645.

Waters K.M., Masiello L.M., Zangar R.C., Tarasevich B.J., Karin N.J., Quesenberry R.D., Bandyopadhyay S., Teeguarden J.G., Pounds J.G., Thrall B.D. 2009. *Macrophage responses to silica nanoparticles are highly conserved across particle sizes.* Toxicological sciences: an official journal of the Society of Toxicology. 107(2):553–69.

Webster T.J. 2013. *Interview: Nanomedicine: past, present and future.* Nanomedicine. 8(4), 525–529.

Weijer C.J. 2003. *Visualizing signals moving in cells.* Science. 300(5616):96-100.

Weller H. 1993. *Colloidal semiconductor Q-Particles: chemistry in the transition region between solid state and molecules.* Angew. Chemie. 32(1):41-53.

Wells A.F. 1987. *Synthesis of thermally spherical CuO nanoparticles.* Structural Inorganic Chemistry 6th ed Oxford University Press: New York.

Wheals A.E. 1987. *In "The Yeast"*, Vol. 1, Biology of Yeasts, second edition (A. H. Rose and J. S. Harrison, eds.), p. 283, Academic Press, New York.

White J. 1954. *"Yeast Technology",* J. Wiley and Sons Inc., New York.

WHO. 2010. *World malaria report.*

Wick P., Malek A., Manser P., Meili D., Maeder-Althaus X., Diener L., Diener P. A., Zisch A., Krug H.F., von Mandach U. 2010. *Barrier capacity of human placenta for nanosized materials.* Environ. Health Perspect. 118(3):432-6.

Wikman A., Karlsson J., Carlstedt I., Artursson P. 1993. *A drug absorption model based on the mucus layer producing human intestinal goblet cell line HT29-H.* Pharm. Res. 10: 843-852.

Wikman Larhed A. and Artursson P. 1995. *Co-cultures of human intestinal Goblet (HT29H) and absorptive (Caco-2) cells for studies of drug and peptide absorption.* Eur. J. Pharm. Sci. 3: 171-193.

Wilhelm C., Billotey C., Roger J., Pons J.N., Bacri J.C., Gazeau F. 2003. *Intracellular uptake of anionic superparamagnetic nanoparticles as a function of their surface coating.* Biomaterials. 24(6):1001-11.

Wilhelm C., Lavialle F., Pechoux C., Tatischeff I., Gazeau F. 2008. *Intracellular trafficking of magnetic nanoparticles to design multifunctional biovesicles.* Small. 4(5):577-824.

Winnik F.M. and Maysinger D. 2013. *Quantum dot cytotoxicity and ways to reduce it.* Acc Chem Res. 46(3):672-8080.

Wise Sr J.P., Goodale B.C., Wise S.S., Craig G.A., Pongan A.F., Walter R.B., Thompson W.D., Ng A.K., Aboueissa A.M., Mitani H., Spalding M.J., Mason M.D. 2010. *Silver nanospheres are cytotoxic and genotoxic to fish cells.* Aquatic Toxicology. 97(1):34–41.

Wright D.T., Cohn L.A., Li H., Fischer B., Li C.M., Adler K.B. 1994. *Interactions of oxygen radicals with airway epithelium.* Environ Health Perspect. 102(10):85-90.

Wright P.E. and Dyson H.J. 1999. *Intrinsically unstructured proteins: Re-assessing the protein structure-function paradigm.* Journal of Molecular Biology. 293, 321-331.

Wu W. 2010. *In-situ immobilization of quantum dots in polysaccharide-based nanogels for integration of optical pH-sensing, tumor cell imaging, and drug delivery.* Biomaterials. 31(11):3023-3031.

Wu X.Y., Tan Y.B., Mao H., Zhang M.M. 2010. *Toxic effects of iron oxide nanoparticles on human umbilical vein endothelial cells.* Int. J. Nanomed. 5, 385–399.

Xia T., Kovochich M., Brant J., Hotze M., Sempf J., Oberley T., Sioutas C., Yeh J.I., Wiesner M.R., Nel A.E. 2006. *Comparison of the abilities of ambient and manufactured nanoparticles to induce cellular toxicity according to an oxidative stress paradigm.* Nano Lett. 6 1794-1807

Xia T., Kovochich M., Liong M., et al. 2008. *Comparison of the mechanism of toxicity of zinc oxide and cerium oxide nanoparticles based on dissolution and oxidative stress properties.* ACS Nano. 2(10):2121-34.

Xiao Q., Huang S., Qi Z.D., Zhou B., He Z.K., Liu Y. 2008. *Conformation, thermodynamics and stoichiometry of HSA adsorbed to colloidal CdSe/ZnS quantum dots*. Biochim. Biophys. Acta 1784(7-8):1020-7.

Xiao L., Aoshima H., Saitoh Y., Miwa N. 2011. *Highly hydroxylated fullerene localizes at the cytoskeleton and inhibits oxidative stress in adipocytes and a subcutaneous adipose-tissue equivalent.* Free Radic. Biol. Med. 51(7):1376-89.

Xie G., Sun J., Zhong G., Shi L., Zhang D. 2010. *Biodistribution and toxicity of intra-venously administered silica nanoparticles in mice.* Arch. Toxicol. 84,183–190.

Xie J., Xu C., Kohler N., Hou Y., Sun S. 2007. Molecular *effects of uptake of gold nanoparticles in HeLa cells*. Chem. Biochem. 8(11):1237-40.

Xu A., Chai Y., Nohmi T., Hei T.K. 2009. *Genotoxic responses to titanium dioxide nanoparticles and fullerene in gpt delta transgenic MEF cells*. Particle and Fibre Toxicology. 6(3).

Yamamoto T., Watanabe K., Hernandez E.R., Geim A.K., Novoselov K.S. 2007. *Mechanical Properties, Thermal Stability and Heat Nanotubes: Advanced Topics in the Synthesis, Structure, Properties and Applications. Springer; The Rise of Graphene.* Nat. Mater. 6:183–191.

Yamashita K., Yoshioka Y., Higashisaka K., Mimura K., Morishita Y., Nozaki M., Yoshida T., Ogura T., Nabeshi H., Nagano K., Abe Y., Kamada H., Monobe Y., Imazawa T., Aoshima H., Shishido K., Kawai Y., Mayumi T., Tsunoda S., Itoh N., Yoshikawa T., Yanagihara I., Saito S., Tsutsumi Y. 2011. *Silica and titanium dioxide nanoparticles cause pregnancy complications in mice.* Nat. Nanotechnol. 6(5):321-8.

Yameen B., Il Choi W., Vilos C., Swami A., Shi J., Farokhzad O. C. 2014. *Insight into nanoparticle cellular uptake and intracellular targeting.* Journal of Controlled Release. 28(190):485-99.

Yan M. 2011. *An in vitro study of vascular endothelial toxicity of CdTe quantum dots.* Toxicology. 282(3):94-103.

Yang H., Fung S.Y., Liu M. 2011. *Programming the cellular uptake of physiologically stable peptide-gold nanoparticle hybrids with single amino acids.* Angew Chem. Int. Ed. 50(41):9643-9646.

Yang L. and Li Y. 2006. *Simultaneous detection of Escherichia coli O157[ratio]H7 and Salmonella Typhimurium using quantum dots as fluorescence labels*. Analyst. 131(3):394-401.

Yang L., Shang L., Nienhaus G.U. 2013. *Mechanistic aspects of fluorescent gold nanocluster internalization by live HeLa cells.* Nanoscale. 5:1537–1543.

Yang S.T., Liu Y., Wang Y.W., Cao A. 2013. *Biosafety and bioapplication of nanomateri-als by designing protein–nanoparticle interactions.* Small. 9,1635–1653.

Yang X., Liu J., He H., Zhou L., Gong C., Wang X., Yang L., Yuan J., Huang H., He L., Zhang B., Zhuang Z. 2010. *SiO_2 nanoparticles induce cytotoxicity and protein expression alteration in hacat cells.* Particle and fibre toxicology. 7:1.

Yeates D.B. and Mauderly J.L. 2001. *Inhaled environmental/occupational irritants and allergens: mechanisms of cardiovascular and systemic responses.* Introduction. Environ. Health Perspect. 4, 479–481.

Yin H., Chen R., Casey P.S., Ke P.C., Davis T.P., Chen C. 2015. *Reducing the cytotoxicity of ZnO nanoparticles by a pre-formed protein corona in a supplemented cell culture medium.* RSC Adv. 5(90), 73963–73973.

Yin H., Too H.P., Chow G.M. 2005. *The effect of particle size and surface coating on the cytotoxicity of nickel ferrite.* Biomaterials. 26, 5818-5826

Yoo S.I., Yang M., Brender J.R. *et al.* 2011 *Inhibition of amyloid peptide fibrillation by inorganic nanoparticles: functional similarities with proteins.* Angew. Chem. Int. Ed. Engl. 50(22), 5110–5115 (2011).

Yu T., Malugin A., Ghandehari H. 2011. *Impact of silica nanoparticle design on cellular toxicity and hemolytic activity.* ACS Nano. 5(7):5717–5728.

Zannis V.I., Chroni A., Krieger M. 2006. *Role of apoA-I, ABCA1, LCAT, and SR-BI in the biogenesis of HDL.* J. Mol. Med. (Berl). 84(4):276-94.

Zhang C.Y. and Johnson L.W. 2007. *Quantifying RNA-peptide interaction by single-quantum dot-based nanosensor: an approach for drug screening.* Anal. Chem. 79(20):7775-7781.

Zhang H., Burnum K.E., Luna M.L., Petritis B.O., Kim J.S., Qian W.J., Moore R.J., Heredia-Langner A., Webb-Robertson B.J., Thrall B.D., Camp D.G. 2nd, Smith R.D., Pounds J.G., Liu T. 2011. *Quantitative proteomics analysis of adsorbed plasma proteins classifies nanoparticles with different surface properties and size.* Proteomics. 11(23), 4569–4577.

Zhang H., Dunphy D.R., Jiang X., Meng H., Sun B., Tarn D., Xue M., Wang X., Lin S., Ji Z., Li R., Garcia F.L., Yang J., Kirk M.L., Xia T., Zink J.I., Nel A., Brinker C.J. 2012. *Processing pathway dependence of amorphous silica nanoparticle toxicity: colloidal vs pyrolytic.* J. Am. Chem. Soc. 134, 15790-15804.

Zhang H., Gilbert B., Huang F., Banfield J.F. 2003. *Water-driven structure transformation in nanoparticles at room temperature.* Nature. 424,1025-1029

Zhang L.W., Zeng L., Barron A.R., Monteiro-Riviere N.A. 2007. *Biological interactions of functionalized single-wall carbon nanotubes in human epidermal keratinocytes.* Int. J. Toxicol. 26, 103–113.

Zhang T., Stilwell J.L., Gerion D., Ding L., Elboudwarej O., Cooke P.A.; Gray J.W., Zhu Z-J., Yeh Y.-C., Tang R., Yan B., Tamayo J., Vachet R.W., Rotello V.M. 2011. *Stability of quantum dots in live cells.* Nature Chem. 3:963-8.

Zhang J.Y., Zhang F., Hong C.Q., Giuliano A.E., Cui X.J., Zhou G.J., Zhang G.J., Cui Y.K. 2015 *Critical protein GAPDH and its regulatory mechanisms in cancer cells*. Cancer Biol. Med. 12(1):10-22.

Zhao Y., Sun X., Zhang G., Trewyn B.G., Slowing I.I., Lin V.S. 2011. *Interaction of mesoporous silica nanoparticles with human red blood cell membranes: size and surface effects.* ACS Nano. 5:1366–1375.

Zhu X., Hondroulis E., Liu W., et al. 2013. *Biosensing approaches for rapid genotoxicity and cytotoxicity assays upon nanomaterial exposure*. Small. 9:1821-30.

Zweibaum A. 1991. *Differentiation of human colon cancer cells.* In: Wilson, G.X., Davis, S.S., Illum, G., Zweibaum, A. (Eds) Differentiation of human colon cancer cells. Plenum Press. New York: pp. 27-38.

Zweibaum A., Pinto M., Chevalier G., Dussaulx E., Triadou N., Locroix B., Haffen K., Brun J.L., Rousset M. 1985. *Enterocytic differentiation of a subpopulation of the human colon tumor cell line HT29 selected for growth in sugar-free medium and inhibition by glucose*. J. Cell Physiol. 122: 21-29.

Ringraziamenti

Al termine di questi tre anni di dottorato desidero ringraziare tutte le persone che mi hanno accompagnato in questo percorso e senza le quali questo lavoro di tesi non sarebbe stato possibile realizzare. Innanzitutto vorrei ringraziare il Professor Nelson Marmiroli, nonché coordinatore del mio dottorato di ricerca, per avermi dato la possibilità di intraprendere tale persorso e per il suo sostegno durante tutte le fasi del mio lavoro di ricerca. Un ringraziamento speciale lo dedico alla mia tutor Roberta, non solo per l'immenso contributo teorico e metodologico e la sua dedizione a seguirmi, ma anche per l'esempio che è stata per me di intelligenza, correttezza, amore per la ricerca e professionalità, e che costituirà sempre per me un modello da perseguire nella vita e nel lavoro. Vorrei inoltre ringraziare tutti i professori, i miei colleghi di laboratorio e i laureandi tesisti e tirocinanti con i quali ho condiviso impegni, lezioni, esperimenti e momenti di svago. Ringrazio Valentina Buff per la sua allegria e per le nostre chiacchierate che hanno un inizio ma che poi non si sa su cosa vanno a finire!!

Vorrei inoltre ringraziare immensamente la mia famiglia, mamma, papà, Rosaria, Clarissa, Salvo, Antonella e la dolce nonnina per non avermi mai fatto mancare il proprio sostegno morale, per le lunghe telefonate per sentirci meno lontani e per la vostra preziosa presenza, sia nei momenti tristi che in quelli felici.

Ringrazio le mie "Molecoline", Caty e Xe, per tutto l'affetto e l'amicizia che mi dimostrate, per i vostri consigli e le parole di supporto. Quanto mi mancate!!! Vi voglio bene amiche mie!

Infine, ma non perchè meno importante, ringrazio Te amore mio, per essermi stato vicino sempre, per i tuoi manicaretti prelibati e a volte fantasiosi, e per i tuoi abbracci che valgono più di mille parole. Ti amo